Dissertation

Use of Complementary Testing Technology for the Evaluation of the Characteristics of Different Systems

ausgeführt zum Zwecke der Erlangung des akademischen Grades eines Doktors der technischen Wissenschaften unter der Leitung von

Univ. Prof. Dipl.-Ing. Dr.techn. Markus Valtiner

E134

Institut für Angewandte Grenzflächenphysik

eingereicht an der Technischen Universität Wien

Fakultät für Chemie

von

DI Simon WIENER

01455244

Linz, Oktober 2023

Simon Wiener

TECHNISCHE UNIVERSITÄT WIEN

Ich habe zur Kenntnis genommen, dass ich zur Drucklegung meiner Arbeit unter der Bezeichnung

Dissertation

nur mit Bewilligung der Prüfungskommission berechtigt bin.

Ich erkläre hiermit an Eides statt, dass ich meine Dissertation nach den anerkannten Grundsätzen für wissenschaftliche Abhandlungen selbstständig ausgeführt habe und alle verwendeten Hilfsmittel, insbesondere die zugrunde gelegte Literatur, genannt habe.

Weiters erkläre ich, dass ich dieses Dissertationsthema bisher weder im In- noch Ausland (einer Beurteilerin/einem Beurteiler zur Begutachtung) in irgendeiner Form als Prüfungsarbeit vorgelegt habe und dass diese Arbeit mit der vom Begutachter beurteilten Arbeit übereinstimmt.

Linz, September 2023

Simon Wiener

=

Abstract

Corrosion is a major concern in various industries, and protective coatings play a crucial role in mitigating this challenge by creating a barrier against corrosion-causing agents. Given the myriad of parameters involved, all of which influence the properties and performance of the coatings in different ways, an extensive range of tests exist to assess these individual influences. However, since it is not feasible to carry out all tests for every coating due to time and budget limitations, it is crucial to decide which tests should be carried out in each case.

The overarching aim of this thesis was to establish standardized methods using as few lab tests as possible while at the same time maximizing the yield of data concerning the specimens under investigation. For this goal, an array of laboratory tests using various methods such as electrochemical impedance spectroscopy and salt spray testing was used to undertake a comprehensive examination of coating performance and attributes. A specific emphasis was laid on thermoset thin film primers with variations of the contained pigments, aiming to enhance corrosion resistance within industrial milieus. Furthermore, it was tried to examine the influence of substrate, layer thickness, and particle size on the performance, and to investigate how to reduce delamination, especially cathodic delamination.

The thesis presents a review of the current state of the art on the performance of primers under different conditions as well as information on the occurrence and prevention of damage to coatings. The first chapter undertook an extensive characterization of several anti-corrosion pigments, resulting in the selection of two for further investigations. The second chapter optimized thin-film primer parameters, identifying a dry film thickness of 3 µm as effective corrosion protection under specific conditions. The third chapter investigated graphene nanoparticle additives' potential, highlighting both their promise and practical limitations. The fourth chapter assessed the influence of grinding time on particle size distribution and performance, suggesting implications for coating development. The fifth chapter delves into cathodic delamination, revealing intricate electrochemical and mechanical factors driving this phenomenon. The results of selected experiments were also published in the form of two papers.

In conclusion, this thesis's multifaceted research enhances corrosion protection strategies for galvanized steel sheets. The insights gained from each chapter contribute to the development of more effective and durable corrosion protection solutions, with potential applications across various industries. Continued research in these areas promises to improve the understanding in the field and application of corrosion-resistant coatings.

Kurzfassung

Korrosion stellt in verschiedenen Branchen eine ernsthafte Herausforderung dar, und Schutzbeschichtungen sind von entscheidender Bedeutung, um diese Herausforderung zu bewältigen, indem sie eine Barriere gegen korrosionsverursachende Stoffe bieten. Aufgrund der Vielzahl an Parametern, die alle auf unterschiedliche Weise die Eigenschaften und Leistungsfähigkeit von Beschichtungen beeinflussen, gibt es eine umfangreiche Anzahl an Tests zur Beurteilung dieser einzelnen Einflüsse. Da es jedoch aus Zeit- und Kostengründen nicht möglich ist, alle Prüfungen für jede Beschichtung durchzuführen, ist es essenziell zu entscheiden, welche Prüfungen im Einzelfall durchgeführt werden sollen.

Das Ziel dieser Arbeit bestand darin, standardisierte Methoden zu etablieren, um mit möglichst wenigen Labortests die Datenausbeute der untersuchten Proben zu maximieren. Zu diesem Zweck wurde eine Reihe von unterschiedlichen Methoden wie elektrochemische Impedanzspektroskopie oder Salzsprühtests durchgeführt, um eine umfassende Untersuchung der Beschichtungsleistung und Beschichtungseigenschaften durchzuführen. Ein besonderer Schwerpunkt wurde auf duroplastische Dünnschichtprimer mit Variationen der enthaltenen Pigmente gelegt, um die Korrosionsbeständigkeit in industriellen Umgebungen zu verbessern. Darüber hinaus wurde versucht, den Einfluss von Substrat, Schichtdicke und Partikelgröße auf die Leistung zu untersuchen und festzustellen, wie Enthaftung, insbesondere kathodische Delamination, reduziert werden kann.

Die Arbeit enthält eine umfassende Übersicht über den momentanen Stand des Wissens über die Fähigkeit von Primern unter verschiedenen Bedingungen sowie Informationen über das Auftreten und die Vermeidung von Schäden an Beschichtungen. Im ersten Kapitel wurde eine ausführliche Charakterisierung mehrerer Korrosionsschutzpigmente vorgenommen, die zur Auswahl von zwei für weitere Untersuchungen führte. Im zweiten Kapitel wurden die Parameter von Dünnschichtprimern optimiert und eine Trockenschichtdicke von 3 µm als wirksamer Korrosionsschutz unter bestimmten Bedingungen identifiziert. Das dritte Kapitel untersuchte das Potenzial von Graphen-Nanopartikel-Additiven und hob sowohl deren Leistungsfähigkeiten als auch praktische Einschränkungen hervor. Im vierten Kapitel wurde der Einfluss der Partikelmahldauer auf die Partikelgrößenverteilung und -leistung untersucht und mögliche Auswirkungen auf die Beschichtungsentwicklung aufgezeigt. Das fünfte Kapitel befasst sich mit der kathodischen Delamination und deckt komplizierte elektrochemische und mechanische Faktoren auf, die dieses Phänomen antreiben. Die Ergebnisse ausgewählter Experimente wurden auch in Form von zwei Arbeiten veröffentlicht.

Zusammenfassend lässt sich sagen, dass die vielfältigen Forschungsergebnisse dieser Arbeit Korrosionsschutzstrategien für verzinkte Stahlbleche verbessern. Die in jedem Kapitel gewonnenen Erkenntnisse tragen zur Entwicklung effektiverer und langlebigerer Korrosionsschutzlösungen mit potenziellen Anwendungen in verschiedenen Branchen bei.

List of Abbreviations

Ca/Silica	calcium-exchanged silica oxide
CD	Cathodic delamination
CSP	Cross section polisher
D50	Diameter at which 50% of the particles are smaller (=mean diameter)
D90	Diameter at which 90% of the particles are smaller
EIS	Electrochemical impedance spectroscopy
EDX	Energy-dispersive X-ray spectroscopy
FTIR	Fourier-transform infrared spectroscopy
GI	Galvanized
ICP-OES	Inductively coupled plasma optical emission spectroscopy
KT70	Blister tests, conducted at 70 °C
LPR	(Linear) polarization resistance
LSV	Linear sweep voltammetry
NSST	Neutral salt spray test
OCP	Open circuit potential
PMT	Peak metal temperature
SDS	Safety data sheet
SHE	Standard hydrogen electrode
SEM	Scanning electron microscope
SMD	Sauter mean diameter
THF	Tetrahydrofuran
VMD	Volume mean diameter

wt.%	Mass fraction
XRD	X-ray crystallography
Z	Steel hot-dip galvanized with pure zinc
ZM	Steel hot-dip galvanized with a zinc/aluminum/magnesium alloy

Table of Contents

1 Introduction and Objective

Corrosion presents a formidable challenge across various industries, leading to financial setbacks, safety concerns, and a decline in operational efficiency. Sectors such as infrastructure, transportation, manufacturing, and energy are particularly susceptible to the detrimental effects of corrosion on both their structures and equipment. The safeguarding of steel, a globally renowned material for its versatile properties, holds special significance. Notably, the steel industry is a major player, contributing to about 10% of the world's CO_2 emissions [1] [2]. An extensive study conducted by the International Measures of Prevention, Application, and Economics of Corrosion Technology (IMPACT), led by NACE (National Association of Corrosion Engineers), underscores the magnitude of the issue. The IMPACT study estimates that the global cost of corrosion stands at a staggering US$2.5 trillion, equating to roughly 3.4 percent of the global Gross Domestic Product (GDP) [3]. In response to this persistent issue, protective coatings have gained widespread acceptance as an effective countermeasure. These coatings serve as a protective barrier between the metal substrate and the surrounding environment, providing a defense against corrosive agents.

The effectiveness of coating systems in providing protection relies heavily on a comprehensive understanding of their mechanisms and interactions with the substrate. Extensive research efforts have been devoted to determining the factors that influence coating performance, including adhesion strength, chemical resistance, and mechanical durability. By gaining a deep understanding of these factors, researchers and engineers can develop coating systems that exhibit enhanced resistance to corrosion, prolonged service life, and reduced maintenance costs.

The objectives of this study are therefore:

- gathering comprehensive information about coating systems while minimizing the number of required tests
- identifying the key factors influencing the performance of coating systems in corrosion protection, encompassing critical parameters such as substrate selection, composition of the coating – especially the contained anti-corrosion pigments – and layer thickness
- examining the mechanisms involved in coating disbondment, especially the mechanism of cathodic delamination

By achieving these objectives, it is possible to enhance the understanding of corrosion mechanisms and their interactions with different types of coatings. This knowledge is crucial for the development of more efficient and durable coating systems, enabling customization for

specific applications, optimizing material performance, and reducing maintenance expenses associated with corrosion-related issues.

To identify principal factors and parameters for evaluating coating performance and corrosion resistance, various analytical techniques were employed, including neutral salt spray tests (NSST), electrochemical impedance spectroscopy (EIS), and blistering tests at 70 °C (KT70).

This thesis is structured into several sections to ensure a coherent reading experience. The introduction and objective part provides an overview of the importance of corrosion protection across various industries. It outlines the research objectives and questions to be addressed throughout the study.

Following this section, the current state of the art review critically reviews existing research and knowledge related to coating systems, corrosion and disbondment mechanisms, and factors influencing coating performance. This review identifies gaps in current understanding and sets the stage for the research conducted in this thesis.

The subsequent section provides a comprehensive overview of the materials and methods used in the study, including the experimental setup, sample preparation, and testing protocols employed for evaluating coating performance and corrosion resistance.

The main body of the thesis comprises five chapters, each focusing on a specific corrosion-related topic and addressing a unique research question.

Chapter 1, titled "Analyses of typical commercially available anti-corrosion pigments," investigates the properties and structure of common anti-corrosion pigments used within coating systems. This comprehensive investigation led to the identification of two promising candidates for further research, Shieldex and ASP600, both selected based on their distinctive properties that exhibit potential to enhance corrosion protection.

Chapter 2, named "Thermoset thin film primers: Influence of Substrate, Layer Thickness, and Wettability of Additives in Laboratory Testing", presents the results and interpretations of several experiments in which different parameters were varied to determine their influence on the performance of the samples. A dry film thickness of 3 µm was identified as sufficient in providing effective corrosion protection under specific circumstances. The examination included a broad spectrum of factors encompassing coating thickness, composition, and substrate material. The content of this chapter was also published in an article [4].

In chapter 3 entitled "Evaluation of a Commercial Graphene Additive for Boosting the Corrosion Performance of a Thermal Curing Primer" the effect of adding a commercially available graphene additive on the properties of a commercial primer system was tested. Although the outcomes across various test protocols are found to be mixed, the improvements in performance in some of the tests underscore the crucial role of graphene as a possible additive. These results were also published in a paper [5].

Chapter 4, bearing the title "The Influence of Pigment Milling Time and Primer Layer Thickness on Anti-Corrosion Coatings for Galvanized Steel Strip Samples," delves into the influence that pigment milling time and primer layer thickness exert on the efficacy of anti-corrosion coatings for samples of galvanized steel strips. The chapter's analysis unveils a crucial relationship, demonstrating that extended pigment milling times contribute to enhanced particle distribution and heightened anti-corrosion protection. This revelation holds significant implications for the development and optimization of coatings for safeguarding galvanized steel strip samples.

Chapter 5, named "Examining the Influence of Different Parameters on Cathodic Delamination: Assessing their Impact on Coating Integrity" delves into the range of parameters that impact cathodic delamination and analyzes how they affect the integrity of coatings. Through rigorous analysis, the chapter illuminates the connection between electrochemical and mechanical factors that affect this complex behavior.

Each chapter provides an in-depth analysis of the respective topic, supported by experimental data, interpretation of the gained results, and relevant literature.

Finally, the conclusions and outlook section summarizes the key findings of the study, highlights the contributions made to the field of corrosion protection, and suggests future research directions. By following this structured approach, the thesis aims to contribute to the knowledge base surrounding coating systems and corrosion protection. Ultimately, the findings of this research endeavor will facilitate the development of more effective and sustainable solutions for corrosion mitigation in various industries.

2 Current state of the art

2.1 Corrosion Protection

In today's economy, metals play a crucial role and find extensive application in vital sectors like construction, automotive, and aviation. However, despite their importance, metals are

susceptible to corrosion, which can lead to structural degradation, increased maintenance costs, and compromised safety. Consequently, the industry is consistently trying to discover effective strategies for reducing corrosion damage and extending the lifespan of metal components. Historically, corrosion-related challenges were tackled through the development of corrosion-resistant alloys and the application of inorganic coatings. A still commonly employed technique for steel is galvanizing, which involves the deposition of a protective zinc layer on the surface of the substrate. These zinc coatings serve as physical barriers, effectively shielding the metal from corrosive agents present in the surrounding environment [6, 7, 8].

However, in some cases these protective measures prove to be insufficient. Therefore, researchers and engineers have explored alternative approaches to enhance corrosion protection and adhesion of coatings. One such approach involves the formation of conversion layers by chemically modifying the oxide layer on the metal surface. These conversion layers, commonly composed of chromates or phosphates, not only improve corrosion resistance but can also serve as forming aids and consequently enhance the malleability of metals. In addition, they also promote better adhesion between the substrate and subsequent organic coatings, such as paints and lacquers [9, 10].

Organic coatings, which encompass a wide range of formulations, are widely used to provide enhanced corrosion protection or fulfill specific material requirements. They consist of various components, including binders, solvents, fillers, additives, and pigments. Of particular interest are the anti-corrosion pigments, which can be broadly classified into three categories based on their mode of action: barrier pigments, sacrificial pigments, and inhibitive pigments. Barrier pigments slow or prevent the diffusion of corrosive substances along with altering the polarization of the cathode and/or anode, sacrificial pigments provide cathodic protection by sacrificially corroding in place of the metal substrate, and inhibitive pigments inhibit the corrosion process by passivating the metal surface [11, 12, 13, 14].

2.2 Anti-Corrosion Pigments

For a long time, zinc chromate-based pigments served as the gold standard for corrosion protection. However, their use became highly controversial due to the implementation of the RoHS directives and REACH regulations in the European Union. As a result, companies began exploring alternative options. The pigments commonly employed today can be classified into different categories, some of which include:

- Phosphates
- Exchanged silicon oxides

- Graphene and (reduced) graphene oxides
- Silicates
- Layered Double Hydroxides (LDH)

As the demand for environmentally friendly and sustainable corrosion protection continues to rise, research in this area has expanded, leading to the development of new pigments and coating formulations. These advancements aim to meet the strict regulatory requirements while ensuring effective and long-lasting corrosion resistance. By understanding the mechanisms of action and performance of these alternative pigments, researchers and industry professionals can make informed decisions and contribute to the development of improved corrosion protection strategies. This review will focus on two types of pigments - exchanged silicon oxide and graphene.

Exchanged silicon oxide is part of a class of corrosion inhibiting pigments known as ion exchangers. These materials are formed through reactions of cations (such as calcium, cerium, etc.) or anions (such as phosphates, chromates, etc.) with suitable inorganic oxide hydrates. A generic example of an alkaline ion exchanger, with a pH of approximately 9, is calcium-exchanged silica oxide (Ca/Silica). It differs from a mere calcium silicate, constituting a chemical framework composed of silica oxide intertwined with embedded particles of calcium oxide or calcium hydroxide. The pigment is typically synthesized through an acid-base interaction between surface groups on silica and calcium ions in solution. Remarkably, it possesses distinctive characteristics, including a comparatively low specific gravity and relatively elevated oil absorption, distinguishing it from other pigments. Such properties may prove advantageous, depending on the specific requirements of the coating system. Despite its low porosity, it possesses a large surface area of 60 m^2g^{-1}, enabling various surface processes such as adsorption, desorption, and ion exchange [15, 16].

The corrosion inhibition process begins upon contact of aggressive cations with the coating. In response, calcium ions are selectively released from the pigments, which serve to impede or at least slow down the movement of the aggressive cations towards the metal surface. This can be regarded as an acid-base reaction at the interphase. Additionally, the presence of Ca/Silica lowers the cathodic current density in oxygen-depleted regions [17, 18].

Generally, there are three theories explaining the functioning of ion exchange pigments [19, 20]:

- The ion exchange theory suggests that the pigments engage in an exchange reaction with other aggressive ions (e.g., H^+), immobilizing or at least retarding them while the originally incorporated calcium ions are leached out. The pigments may also possess an overall negative charge, repelling chloride ions.
- The migration theory postulates that both silica and calcium ions can freely move within the coating, slowly forming a protective layer at the interface with the substrate. This protective layer has been confirmed through XPS measurements and electrochemical tests. Additionally, the pigment can fill the pores of the paint.
- The pigment theory proposes that the pigment influences certain properties of the coating (crosslinking, permeability, porosity, etc.), thereby positively modifying the coating's ability.

Another possible mechanism underlying the protective action of Ca/Silica is the establishment of a high pH value by the pigment. This theory is supported by the fact that in conducted experiments, steel did not corrode in a chloride-containing solution with a pH of 9.2, whereas it did corrode in a solution with a pH of 7 in the absence of chloride ions. However, the alkaline nature of the pigment can lead to undesirable side effects, as the high pH causes to reactions with acidic binders or catalysts. These effects can be mitigated through appropriate formulation of the coating. Nevertheless, the pH theory is disputed, as other publications suggest that there is no causation between pH value and protective properties. The high pH value is believed to promote the properties and solubility of the pigment and does not affect the ion exchange capacity [17, 19, 18, 21, 22].

The proper binder-to-pigment ratio is crucial when using Ca/Silica. Several publications have demonstrated that the best properties are gained at a concentration of approximately 10 wt%. Higher concentrations lead to increased permeability, resulting in reduced barrier effectiveness. While the increased permeability enhances the pigment's exchange capacity, it also promotes underfilm corrosion and blistering, which could potentially be mitigated by applying a thicker coating. In addition, surface adhesion is essential to ensure a functional coating, thus the substrate should be properly pretreated before the coating application [15, 16, 22, 23].

The correct selection of binder is also necessary to ensure sufficient effectiveness. Some publications indicate that coatings based on epoxy, in combination with Ca/Silica pigments, achieve better results compared to coatings based on polyester or alkyd. This is attributed to improved adhesion of the paint and protection against permeability [19, 24].

Ca/Silica has maintained a substantial presence in the commercial market, notably under the trademark Shieldex©, for an extended period. The pigment's individual efficacy has been substantiated across the passage of time. Nonetheless, several publications have reported instances of enhanced corrosion protection through the combined use of zinc phosphate and Ca/Silica pigments [17, 18].

Graphene, on the other hand, is not currently used on a large scale, but has received significant attention in recent years due to its unique properties. As a two-dimensional, atomically thin carbon film with a hexagonal honeycomb structure and sp^2 binding orbitals, graphene stands out among other carbon modifications such as fullerenes, carbon nanotubes, and graphite. Its notable characteristics include exceptional thermal conductivity, strength, and a theoretically projected specific surface area exceeding 2,500 m^2g^{-1}. Moreover, graphene exhibits remarkable impermeability to gases. These extraordinary characteristics have inspired extensive research efforts exploring diverse graphene-based technologies in various applications. Notably, graphene has already found utility in fuel cells, biological devices, and as an anti-corrosive coating for metallic substrates [25, 26, 27, 28, 29, 30, 31].

Extensive efforts have been made to utilize the protective capabilities of graphene coatings against corrosion, particularly through chemical vapor deposition (CVD). However, this approach is not without its challenges. While these coatings can provide formidable short-term protection, their long-term effectiveness can be compromised. Imperfections in CVD coatings are practically unavoidable, leading to microgalvanic corrosion. Corrosive fluids can infiltrate the graphene layer and progress towards the metal interface, establishing an electrochemical connection between the graphene and the metal. Additionally, the formation of corrosion products on the metal surface leads to the detachment and cracking of the graphene coating. As a result, some researchers propose that graphene's potential as a corrosion prevention material might be limited to early transient periods. Consequently, the long-term potential of graphene to prevent corrosion remains uncertain [32, 33, 34].

The corrosion mitigation offered by graphene particles predominantly stems from from their substantial surface area, leading to impressive barrier properties, as well as their inherent hydrophobicity. Acting as an almost impermeable barricade within the coating, graphene slows the propagation of cracks and prevents the diffusion of corrosive media to the substrate. Additionally, graphene serves as an electron conduit within the coating, enhancing the protective properties of sacrificial anodes by establishing connections between anodic particles and the substrate. The strong adhesion characteristics of graphene, combined with the

film-forming attributes of the coating matrix, synergize within graphene composite coatings, enhancing overall performance. Incorporating graphene as a filler material also enables the use of conventional coating formulations, avoiding the complexities and costs associated with pure graphene coatings [35].

Despite these advantages, the commercial utilization of graphene as an anti-corrosion pigment is still limited. This can be attributed primarily to the challenges associated with the compatibility of graphene dispersions with resins, leading to significant issues. The main obstacle in integrating graphene into composite coatings lies in its limited solubility in solvents due to the absence of functional groups. Furthermore, the high aspect ratio and the presence of van der Waals forces lead to a rapid agglomeration of graphene particles. Consequently, practical coating formulations require complex compositions and the usage of various additives such as leveling agents, anti-settling agents, and anti-foaming agents. Furthermore, current investigations mainly focus on the transient corrosion behavior observed in controlled laboratory settings, despite some research groups have reported promising findings in real life applications [36, 37, 38].

Nevertheless, select suppliers now offer ready-made graphene particles that can be directly applied in coating formulations. Moreover, the field of anti-corrosion coatings has witnessed significant advancements with the development of nanotechnology in recent years, resulting in notable improvements in performance. By incorporating smaller nanoparticles into coatings, nanotechnology enhances anti-corrosion properties, adhesion, and scratch resistance. Furthermore, the utilization of nanoparticles enables cost-effective measures by reducing the thickness of the coating. The efficacy of nanoparticle-based anti-corrosion coatings has been demonstrated in various applications, including marine environments and the automotive industry, through recent studies [39, 40, 41, 42, 43].

2.3 Cathodic Disbondment

Various forms of damage that can occur to coatings exist, but these can be broadly categorized into a few groups, more specifically anodic and cathodic delamination [44, 45, 46, 47], blistering [48, 49, 50, 51], water disbondment [52, 53], and filiform corrosion [54, 55].

Coating delamination or disbondment describes the separation or detachment of a protective coating from the underlying substrate or surface. This phenomenon arises when the adhesion between the coating and the substrate weakens or fails, resulting in the loss of protective and aesthetic properties provided by the coating. Disbondment can occur due to diverse factors, including inadequate surface preparation, improper coating application, mechanical stress,

chemical attacks, or environmental exposure. In addition, electrochemical disbondment is also possible and occurs when the adhesion between a coating and its substrate is compromised due to electrochemical processes.

Upon establishment of an electron flow conduit between the zinc substrate and the aqueous milieu, an electrochemical process, corrosion, is initiated. Since the presence of oxygen plays a crucial role for the cathodic part of the reaction, the diffusion of oxygen into the delimited area around the zinc substrate is an important aspect to consider. In the presence of water, molecular oxygen undergoes a reduction process, yielding hydroxide ions through the uptake of electrons, resulting in the alkalization of the reaction region. The diffusion of oxygen and the reduction to hydroxide ions are thus closely linked and influence the course of the cathodic reaction.

The cathodic reaction is accompanied by an anodic reaction, wherein the zinc substrate undergoes oxidation in the presence of sufficient hydroxide ions and forms a complex. This complex chelates the hydroxide ions and leads to a decrease in pH, causing zinc oxide and water to precipitate. The anodic reaction thus buffers the pH since a pH that is too alkaline would further increase the anodic reaction rate. Therefore, although the pH is maintained at a value above 10, it is maintained at a lower value than, for example, iron, where the pH can reach values as high as 14. Diffusion of O_2 then starts the process all over again. Since the coating would be partially destroyed by the alkaline pH, this buffer effect can stabilize pH-sensitive coatings on galvanized steel. In **Figure 1** the postulated mechanism is shown [56, 57].

In the absence of oxygen or at very negative voltages (more negative than -1,350 mV vs. SHE [58]), the reduction of oxygen is replaced by the dissociation of water, yielding hydrogen gas and hydroxide ions:

$$H_2O + 2\ e^- \rightarrow H_2 \uparrow + 2\ OH^-$$

Regardless of the specific cathodic reaction, the production of hydroxide ions transpires, consequently resulting in a pH increase [59].

Other sources postulate a two-stage cathodic mechanism:

$$2\ H^+ + O_2 + 2\ e^- \rightarrow H_2O_2$$

$$H_2O_2 + 2\ e^- \rightarrow 2\ OH^-$$

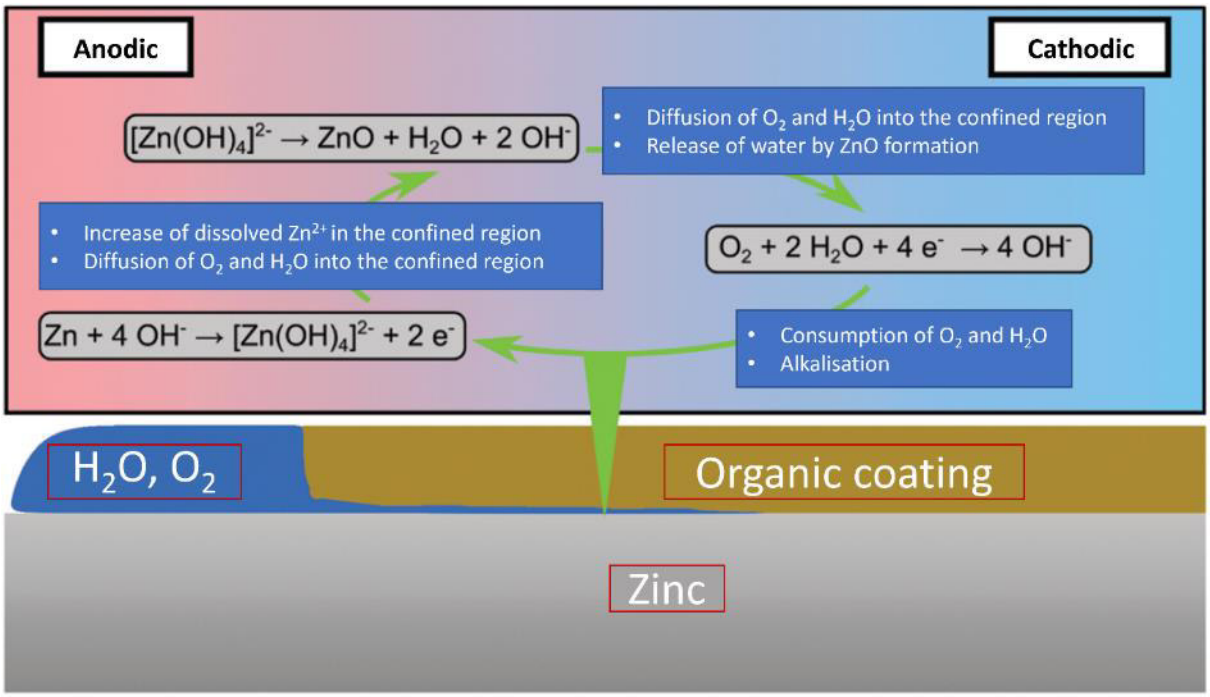

Figure 1: Postulated mechanisms of electrochemical partial reactions in corrosion. O_2 reduction in the presence of water leads to an increase in the hydroxide concentration, causing zinc to oxidize and form a complex. Binding of the hydroxide ions in the complex causes the pH to decrease and zinc oxide and water precipitate. Diffusion of O_2 starts the process all over again. Figure reproduced with permission and adapted from [57].

According to this theory, peroxide exists in solution as HO_2^- ions. There are two ways in which the oxygen reduction occurring the delamination front can lead to the propagation of the front: either through pH elevation or the generation of highly oxidizing intermediates and it would not be possible to distinguish between these two mechanisms. Supporting the notion that peroxide molecules drive delamination, among other considerations, is the observation that the delamination rate on polymer-coated zinc was strongly dependent on the presence of oxygen but not on the presence of NaOH in the electrolyte. This implies that OH^- is not the important species in the degradation reaction, although these results could also be explained by the inhibition of ion transport through the polymer layer and the metal-polymer interface [60].

Other results have demonstrated a degree of correlation between the alkali resistance of the surface layer in tested specimens and the susceptibility to cathodic delamination. An additional argument refuting the theory that the rate-limiting step involves the direct polymer oxidation by intermediates participating in the oxygen reduction reaction is the absence of delamination on phosphated surfaces. The steady increase in pH occurring at the interface of the metal and polymer can potentially attack the surface treatment layer or the polymer matrix, thereby intensifying the corrosion rate of the underlying zinc metal layer. Therefore, mechanisms encompassing pH changes are deemed to be more favorable [60].

In literature, 4 reactions are typically attributed to cathodic disbonding of coatings [61, 62]:

- Dissolution of the metal oxide, leading to the detachment of the coating from the substrate.
- Polymer hydrolysis just above the boundary layer, leaving behind a thin polymer residue.
- Alkaline degradation of metal/coating bonds.
- Mechanical delamination triggered by hydrogen formation.

If polymer hydrolysis above the boundary layer has already occurred, subsequent oxide layer dissolution becomes irrelevant to the delamination process, as delamination has already taken place. In cases of metal oxide dissolution and alkaline attack on metal/coating bonds, the rate-limiting step is the generation of hydroxide ions, for polymer hydrolysis, it is instead the rate of water diffusion into the coating, influenced by factors including the size of hydrated ions present [61]. A graphical overview of the delamination mechanisms is presented in **Figure 2**.

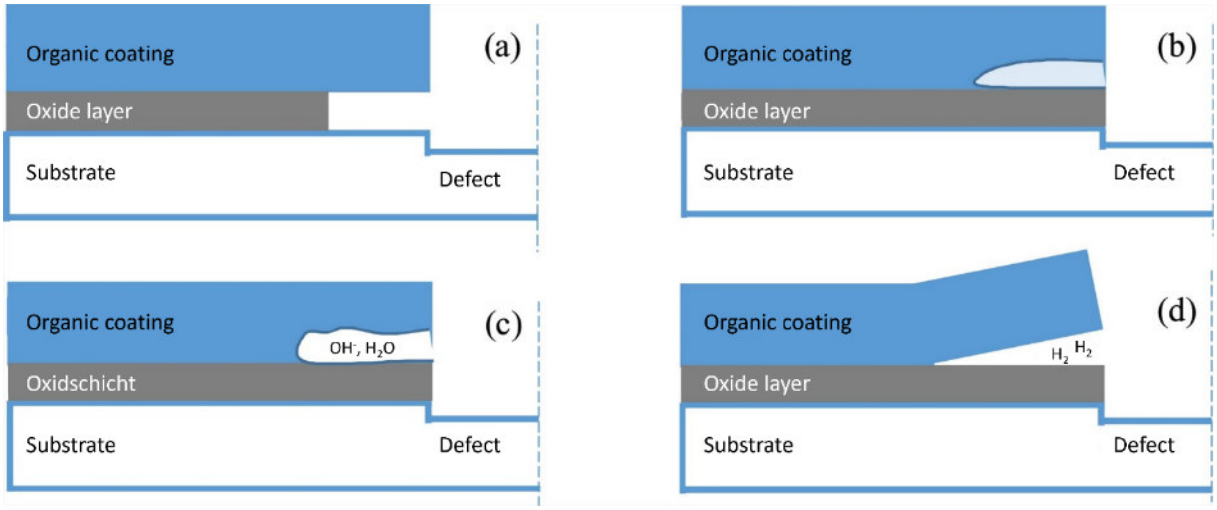

Figure 2: Overview of the 4 possible delamination mechanisms. a) dissolution of the metal oxide, b) hydrolysis of the polymer, c) alkaline attack on the metal/coating bonds, d) mechanical delamination by hydrogen. Figure reproduced with permission and adapted from [63].

Determining the responsible mechanism for delamination in each scenario involves the consideration of different parameters: For oxide reduction, the potential must be very high (noble), while polymer failure at the interface exhibits kinetics dependent on migration path length, yielding a directly proportional relationship between delamination area and test time. Polymer hydrolysis manifests observable diffusion through the polymer, resulting in failure across the entirety of the polymer area exposed to the aqueous phase [61].

Diverse mechanisms can be the driving force for delamination under varying conditions, with potential coupling between mechanisms. A pH increase leads to surface treatment dissolution

and increased available metallic surface area for oxygen reduction. This intensifies oxygen reduction beneath the coating, thereby further elevating pH within the interfacial region. Even when the anode and cathode are in close proximity, acidification due to hydrolysis of Zn^{2+} remains minimal, as localized corrosion of zinc leads to a net pH increase [60].

The distinction between anodic and cathodic regions often poses challenges. Initial stages of delamination allow a clear differentiation, but as the delamination front progresses, both anode and cathode can coexist beneath the coating. In addition, voluminous corrosion products can form, exerting considerable mechanical force on the coating from below. Fürbeth and Stratmann reported that under a high CO_2 partial pressure, the formation of $ZnCO_3$ inhibits the electron transfer of oxygen reduction, resulting in pure anodic delamination for coated electrolytically galvanized steel. Experimental observations have therefore shown that the explanation of delamination becomes complicated when passive films or corrosion products form under the coating [60, 64].

During accelerated testing, most of the area beneath coatings exhibits anodic behavior, yet the delamination front remains cathodic. It has been shown that the anodic mechanism is dominant for complete automotive coating systems, as these coatings form significant barriers to oxygen diffusion. However, thin polymer layers, such as cathodically deposited primer systems in the automotive sector, permit oxygen diffusion, consequently favoring the cathodic delamination mechanism [60].

Furthermore, cathodic disbonding frequently occurs in coated metal structures submerged in seawater or soil and protected by sacrificial anodes. The failure of organic coatings can often be attributed to the formation of local cathodes. As soon as a defect occurs in the coating, anodic corrosion reactions transpire directly, accompanied by cathodic reductions beneath the coating near the defect. Primarily, these involve the reduction of oxygen in the presence of water to yield hydroxide ions. A prerequisite for this reaction to occur is that sufficient water and oxygen have diffused through the coating to the substrate below. This reaction increases the pH, which eventually leads to the destruction of the metal/primer bonds and thus to delamination. The released metal surface can then serve as an anode, continuing the process of delamination. Thicker coatings inhibit diffusion, which can reduce or even completely inhibit the extent of cathodic delamination [65].

As per Stratmann et al., cathodic delamination systems encompass three zones: a defect, for example a scribe, exposing bare metal to the atmosphere, a delaminated zone where the bonds are partially damaged, and an intact zone where no reactions have taken place so far.

Delamination generally originates at the defect and propagates from there. The deposition of $Zn(OH)_2$ or ZnO on the exposed zinc substrate prevents corrosion of the uncoated area, therefore, on coated zinc samples, the cathodic reaction on the scratch becomes dominant. Under these conditions, on zinc and steel, the delaminated region spreads laterally away from the defect with a well-defined delamination front. Exposure of the metal surface to the atmosphere thereby promotes metal dissolution at the defect. Along the delaminated zone, where the anodic reactions are inhibited by the presence of the coating, O_2 and water penetrate the coating and react at the interface. During the delamination process, the coating is transformed into a gel-like medium, weakening the adhesive bond at the metal-coating interface. [60, 64].

However, there are other studies, according to which the extent of delamination of coatings is controlled by other factors. Huang et al. showed that the overall delamination process is mainly determined by the transport of cations from the defect to the front region. The rate of delamination depends on the mobility, ionic strength, and concentration of cations. The presence of large, hydrated cations can slow down the process of delamination because they are preferentially attracted by the potential field of the substrate to the regions of the coating where the cross-links are weaker, and their presence stops the migration of water molecules. Large molecules take longer to migrate through the coating, thus, it takes longer for water molecules to use the subsequently vacated paths through the coating for migration. Watts and Sørensen came to similar conclusions. [64, 61, 66].

Sørensen et al. demonstrated in several studies that an increased concentration of secondary OH groups within the coating correlates with reduced cathodic delamination This relationship is attributed to a greater number of coating adhesion sites, thereby enhancing adhesion strength. The authors also suggest that factors diminishing adhesion forces, such as the occurrence of high internal stresses, heighten cathodic delamination. Pigments hinder air and oxygen diffusion into the coating layer, further mitigating delamination. At the same filling level, diffusion is particularly well avoided by platelet-shaped pigments, such as graphene. Glover et al. suggest that the addition of graphene as a flat pigment in coatings reduces the diffusion of oxygen and thus slows down cathodic delamination particularly well [66, 67, 68].

In conclusion, the phenomenon of cathodic delamination, encompasses a complex interplay of electrochemical and chemical processes. The various theories proposed to explain cathodic delamination mechanisms, such as those focusing on oxygen reduction, peroxide generation, pH elevation, and polymer hydrolysis emphasize the challenges in determining a single

dominant mechanism. Additionally, the interplay of factors such as coating adhesion strength, pigment characteristics, and diffusion pathways further complicates the overall picture. As illustrated by the diverse experimental observations and studies, no single mechanism is exclusively responsible for cathodic delamination across all scenarios.

It is, therefore, evident that a comprehensive investigation into cathodic delamination necessitates a thorough assessment of these competing mechanisms. In the following section, the methodologies and insights gained through various corrosion testing techniques are delved into, with the aim of shedding light on the underlying factors driving cathodic delamination and its associated mechanisms.

2.4 Corrosion Testing

To assess the effectiveness and durability of coating systems, corrosion testing is crucial. These tests aim to simulate real-world conditions and provide insights into the performance of coatings under various environmental factors. Commonly employed corrosion tests include accelerated tests conducted in laboratory settings, in which the coated specimens are subjected to fastened deterioration by exposing them to aggressive environments such as salt spray or high humidity [69, 70].

Another useful tool, which has emerged and proved to be a valuable tool in corrosion testing due to its ability to provide detailed information about corrosion mechanisms and material performance, is electrochemical testing. Techniques such as potentiodynamic or cyclic polarization tests enable researchers to evaluate the electrochemical behavior of coated systems and identify factors that influence their corrosion resistance. Another significant milestone in this field was the development of electrochemical impedance spectroscopy (EIS), enabling researchers to characterize the electrical response of coatings and gain insights into their protective properties [71].

While a wide array of corrosion tests and techniques is available, it is crucial to select appropriate tests that effectively capture the key corrosion mechanisms. Understanding the specific mechanisms involved in coating degradation is essential for developing reliable predictions of performance under actual operating conditions.

However, the complexity of corrosion processes and the interplay of numerous parameters pose significant challenges. Factors such as coating thickness, applied potential, substrate properties, and environmental conditions can influence the corrosion behavior of coatings. The interdependencies among these parameters further complicate the prediction of coating

performance. Therefore, extensive research efforts are dedicated to comprehensively elucidate the individual factors influencing different corrosion mechanisms and develop predictive models that enable accurate assessment of coating performance in real-world scenarios [72, 73, 74].

Although considerable progress has been made in corrosion research, there is still much to learn about the complex factors influencing corrosion behavior. Ongoing research efforts are focused on refining corrosion testing methodologies, exploring innovative approaches to testing, and expanding our knowledge of coating performance under diverse conditions. These endeavors are crucial for the advancement of cutting-edge coating technologies and for mitigating the economic and environmental impacts of corrosion in various industrial sectors.

The research objective of this study was therefore to gather comprehensive information about coating systems while minimizing the number of required tests. By achieving this objective, researchers and engineers aim to enhance their understanding of corrosion mechanisms and their interactions with different types of coatings. This knowledge is essential for developing more efficient and long-lasting coating systems. Additionally, it helps in customizing coatings for specific applications, optimizing material performance, and reducing maintenance costs associated with corrosion-related problems.

3 Material and Methods

3.1 Materials

In this work, two types of steel strips were used as substrates, depending on the specific requirements of the respective test program. The first type, hereinafter referred to as Z, consisted of hot-dip galvanized steel with an alloy coating composed of zinc and aluminum. The second type, hereinafter referred to as ZM, was hot-dip galvanized steel with a Zn-Al-Mg alloy coating. All used samples were technological steel samples, which were produced on a large-scale industrial plant of voestalpine Stahl GmbH in Linz. The specimens used were skin-pass rolled, oiled, and had a total thickness of 0.52 mm and 0.75 mm respectively. The Z specimens had a coating density of 275 g/m², and the ZM had a coating of 120 g/m² (half on each side). The exact material designation was DX52D + Z275MB for Z and DX52D + ZM120MB for ZM, where DX52D describes the steel substrate and Z275MB or ZM120MB describes the galvanized coating (Z = Zn/Al coating; ZM = Zn/Al/Mg coating; 120 and 275 = coating density in g/m²; MB = surface finish).

The steel substrates were designated according to their chemical composition in accordance with DIN EN 10346:2015; the exact parameters of the specimens are listed in **Table 1**.

Table 1: Composition and thickness of the metallic coatings on the used steel substrates.

Label	Zn (%)	Al (%)	Mg (%)	Coating thickness (µm)	Total thickness (µm)
Z	99,8	0,2	-	20	520
ZM	96,0	2,5	1,5	9	750

In this study, two types of primers were employed. Firstly, commercially available primers based on polyester polyol binders were utilized, incorporating blocked trimeric isocyanate crosslinkers. These primers were occasionally modified to align with specific test requirements,, for example by adding graphene nanoparticles. Additionally, custom-made model primers were also employed to systematically assess the impact of diverse factors, such as pigment hydrophobization, and to establish comparisons between various pigment types. All primers possessed a peak metal temperature (PMT; temperature needed to completely crosslink the coating) between 231 °C and 236 °C and an approximate dwell time of 25 s. A total of 10 different primer formulations were the subject of this study. The formulations of the model primers used in chapter 4.2 to study various parameters are given in **Table 2** and **Table 3**. Two commercially available topcoats based on polyester polyol binders were additionally used for some tests.

Table 2: Primer formulations used for comparison between barrier pigments and inhibitive pigments.

	Formula 1 with barrier pigments (P1B)	Formula 1 with inhibitive pigments (P1I)	Formula 2 with barrier pigments (P2B)	Formula 2 with inhibitive pigments (P2I)
Polyester resin (linear; MW 15,000)	14,00	14,00	10,00	10,00
Epoxy resin (MW 20,000)	-	-	4,10	4,10
Soft resin (linear; MW 7,000)	4,70	4,70	4,70	4,70
Isocyanate	4,70	4,70	4,70	4,70

Shieldex C303	-	5,75	-	5,75
Titanium dioxide TR 81	10,45	10,45	10,45	10,45
ASP 600	5,75	-	5,75	-
Aerosil R 972	0,30	0,30	0,30	0,30
Methoxy propyl acetate (MPA)	39,85	39,85	52,375	52,375
Butyl acetate	20,00	20,00	-	-
Cyclohexanone	-	-	12,375	12,375
Defoamer	0,25	0,25	0,25	0,25
Sum in wt.-%	**100,00**	**100,00**	**105,00**	**105,00**

Table 3: Primer formulations used to determine the influence of hydrophobization and addition of barrier pigments.

	S	**HS**	**SM**	**SK**	**HSM**	**HSK**
Polyester resin	21.5	21.5	21.5	21.5	21.5	21.5
Epoxy resin	1.8	1.8	1.8	1.8	1.8	1.8
Soft resin	4.0	4.0	4.0	4.0	4.0	4.0
Isocyanate	5.0	5.0	5.0	5.0	5.0	5.0
Defoamer	0.3	0.3	0.3	0.3	0.3	0.3
Silane	-	2.5	-	-	2.5	2.5
Shieldex C303	7.9	7.9	7.9	7.9	7.9	7.9
Titanium dioxide TR 81	10.2	10.2	10.2	10.2	10.2	10.2
ASP 600	-	-	-	4.5	-	4.5
Plastorit micro	-	-	4.5	-	4.5	-
Aerosil R 972	0.3	0.3	0.3	0.3	0.3	0.3

Methoxy propyl acetate	29.0	26.5	30.0	30.0	27.0	27.0
Solvesso 150	10.0	10.0	10.0	10.0	10.0	10.0
Sum in wt.%	**90.0**	**90.0**	**95.5**	**95.5**	**95.0**	**95.0**

chapter 4.1 of this thesis deals with the characterization of various anti-corrosion pigments, which were obtained directly from the manufacturers. A list of the characterized pigments is depicted in **Table 4**.

Table 4: Trade name, manufacturer and composition of the pigments examined.

Tradename	Manufacturer	Composition according to Manufacturer
Novinox XCA02	SNCZ	Calcium ion-exchanged amorphous silica
Novinox PAT30	SNCZ	$MgHPO_4 \cdot 3\ H_2O$
Novinox PAT15	SNCZ	$MgHPO_4 \cdot 3\ H_2O$
Novinox PAM	SNCZ	$AlH_2P_3O_{10} \cdot 2\ H_2O + MgO$
Novinox PC01	SNCZ	$CaHPO_4 \cdot x\ H_2O$
Shieldex C303	Grace	Calcium ion-exchanged amorphous silica
Heucophos CMP	Heubach GmbH	$CaMg(HPO_4)_2 \cdot x\ H_2O$
Heucophos SRPP	Heubach GmbH	Strontium aluminum polyphosphate hydrate
Zinkweiss Harzsiegel CF	Norzinco GmbH	ZnO
ASP 600	BASF SE	$Al_4[(OH)_8\|Si_4O_{10}]$
K-White G730	Tayca Corp	Modified aluminum triphosphate; $Al_2P_6O_{20} \cdot 4\ H_2O$
K-White TC 720	Tayca Corp	Magnesium ion-exchanged amorphous silica

3.2 Coating Application

The substrates were cleaned applying a strong alkaline cleaning solution in a cleaning machine to remove dirt and traces of oil. Bonderite C-AK C 72 (Henkel AG & Co. KGaA) was used as the cleaning agent in a concentration of 10 g/L and the cleaning solution was heated to 40 °C during the process. The samples went through a cleaning zone and a washing zone twice each, with a throughput speed of 3 m/min.

Subsequently, a chromium-free pretreatment solution (Bonderite 1455; Henkel AG Co. KGaA) was applied to the clean substrates to form a conversion layer that served as both an adhesion promoter for the organic coating and provided additional protection against corrosion. Depending on the requirements, the specimens were then coated with primer with a layer thickness of 3 to 9 µm using spiral wire bar coaters (RD Specialties, Inc.) and then dried at the PMT of the appropriate material in an air-circulating oven (Hofmann Wärmetechnik GmbH). Typically, a primer layer of 6 µm thickness was employed unless stated otherwise, which aligns with the standard thickness for industrial samples. However, certain scientific tests incorporated varying layer thicknesses. In order to simulate the curing behavior of a primer topcoat system, samples that were only coated with primer underwent a second cure at the PMT of the primer. For primer-topcoat systems, the primer was first applied to the substrate and cured at its PMT. Then, a topcoat with a thickness of approximately 20 µm was applied on top of the primer, followed by curing of the entire coating at the appropriate topcoat PMT. The dry film thicknesses of the topcoats and primers were measured using the magneto-inductive method (Deltascope FMP30, Fischer) and the beta backscatter method (Fischerscope MMS, Fischer), respectively. The measurements revealed thickness variations of ±1 µm.

As part of some experimental programs, free films were generated. For this purpose, polytetrafluoroethylene (PTFE) films were affixed to degreased steel sheets, on top of which primer coatings were created through the use of spiral bar coaters and subsequently heated to their PMT in an air-circulated oven. The free films were then peeled off once the coatings had cooled down. The PTFE foil substrate enabled a convenient peel-off process, yielding films with an approximate dry film thickness of 12 µm.

3.3 Characterization

Cross-sectional images were obtained using scanning electron microscopy (SEM; Zeiss/Ultra 55) to identify the surface morphologies and particle distribution of the composite

coatings. For this purpose, the coated samples were sputtered with gold and embedded in an epoxy matrix. The components were identified using an energy dispersion X-ray analyzer (EDX; Tescan Clara, Tescan Orsay Holding) at an accelerating voltage of 15 keV and quantitative compositional data was acquired. The samples were prepared using cross-section polishing (CSP) with an argon ion beam. This technique is commonly used in materials science and microscopy to prepare samples for analysis by creating a smooth and flat surface perpendicular to the cross-section of the material. It involves bombarding the sample surface with a focused beam of argon ions, which removes material through sputtering. A typical cross-section demonstrating the composition and distribution of the primer's components is depicted in **Figure 1a.**

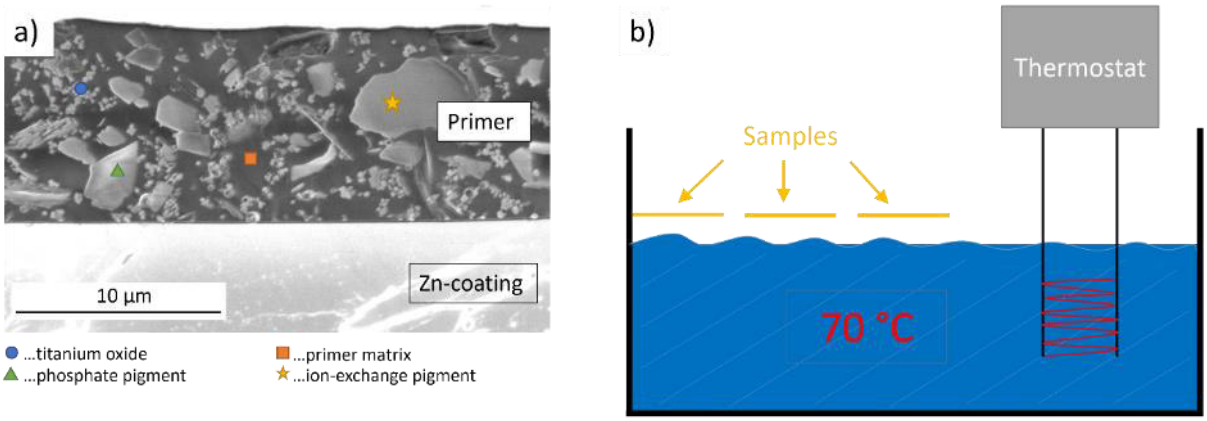

Figure 1: a) A cross-section polisher (CSP) cross-section of a primer-coated sample on a hot-dip galvanized steel substrate with a zinc coating of approximately 20 µm per side (Z) before exposure to a NSST. A commercially available primer with a layer thickness of approximately 9 µm was applied on top of the zinc coating. To identify the primer components, they were labeled with symbols. The square denotes the primer matrix, the circle titanium oxide, the triangle, a phosphate pigment, and the star an ion-exchange pigment. b) Schematic set-up of the blister tester used.

Anti-corrosion pigments were either purchased directly from the manufacturer or gained by separating them from commercially available primers using repeated centrifugation and subsequent decanting using THF. To determine the particle size of the anti-corrosion pigments that were obtained from the liquid primer, two methods were employed. Firstly, a laser diffraction analysis (HELOS/BR & QUIXEL; Sympatec GmbH) was used to evaluate the particle size distribution and secondly, a grindometer (Grindometer nach Hegman, Modell 232; Erichsen GmbH & Co. KG) was utilized to determine the maximum particle size for particles dispersed in primer. The particle size of pigments, which were received directly from the manufacturer, were only analyzed using laser diffraction analysis.

X-ray diffraction (XRD, PANalytcal X'Pert PRO MPD) measurements of all pigments were performed at a glancing angle of 3° using a Cobalt Kα radiation (λ = 1.78 Å) at a scanning rate

of 1.5°/min in the 2θ range of 10−115°. Characterizations of the pigments and some coatings were also carried out using FTIR (Transit Platinum ATR, Bruker) and Raman (DXR SmartRaman Spectrometer, Thermo Fisher Scientific).

3.4 Physical/Mechanical Tests

Depending on the requirements of the test program, various mechanical tests were performed. Color measurements in the CIELAB color space (MA68II, X-Rite) were taken to determine the changes in color. Tribological measurements (Pin-On-Disk Tribometer: TRB^3, Anton Paar) were performed to estimate the different friction coefficients. The wettability was determined by calculating the surface energy by measuring the corresponding contact angles of the applied liquids (Mobile Surface Analyzer - MSA One-Click SFE; Krüss), and the dry adhesion was determined by pull-off tests in accordance with DIN EN ISO 4624. Thermomechanical analysis (TMA; Q400, TA Instruments) was used to determine the glass transition temperatures (Tg) of the primer.

Thermal analysis (TGA/DSC) was conducted on all pigments, which were analyzed in the form of pellets. The samples were placed in Al_2O_3 crucibles with a capacity of 85 µl and were analyzed without a lid under a nitrogen atmosphere. The thermal analysis procedure followed a temperature protocol commencing at 30 °C and subsequently ramping up at a rate of 10 K/min until reaching 800 °C, at which point it was maintained for a duration of 30 minutes.

3.5 Corrosion Tests

Neutral salt spray tests (NSST) were performed in accordance with DIN EN ISO 9227. The specimens were cut to dimensions of 150 mm × 100 mm using plate shears. Tests were conducted on both, the barrier properties of the specimens, for which undamaged samples were used, and protection against anodic delamination, for which two scribes were applied to the sample surface. A scribe extending to the zinc coating was administered on the left-hand side, while another scribe extending to the steel substrate underneath was applied on the right-hand side. To mitigate ambiguous corrosion occurrences at the specimen edges, adhesive tape was employed to cover them entirely. The samples were photographed daily during the initial weeks, transitioning to a weekly schedule thereafter, in order to monitor the progression of corrosion. Following a predetermined duration, ranging between 600 to 3,000 hours based on specific requirements and experimental setups, all samples were taken out of the chamber, and in the case of samples with scribes, the delaminated region was removed using a blunt scalpel. Each sample was examined using SMART, a commercial image analysis program, to quantify the extent of corrosion or delamination (accessible at http://www.quantiz.tech/). Via

identification of any color changes on the surface, it was possible to distinguish between intact and delaminated portions in taken images.

In addition, a homemade blister tester applying 100% condensing humidity was used to replicate and accelerate the effects of rain and dew on the coated materials. Primer and top coat samples measuring 90 mm x 90 mm were used. Because of the ambient temperature of approximately 23 °C and the constant water bath temperature of 70 °C, the backsides of the samples had a thermal gradient and a surface temperature of approximately 55 °C. A schematic of the used set-up is depicted in **Figure 1b.** The coatings were examined for defects, and the extent of blistering was visually evaluated once a week, in accordance with ISO 4628-2. A bubble assessment matrix was used to convert bubble quantity (q) and size (s) into numerical values, as shown in **Table 5**. Reference photographs were employed to rate the samples on a scale of 0 to 5, with 0 indicating no bubble formation and 5 indicating significant bubble formation.

Table 5: A blister assessment matrix in accordance with ISO 4628-2. Using reference photos, the bubble quantity (m) and bubble size (g) were rated and consequently converted into numerical values. 0 denotes no bubble formation and 5 denotes extensive bubble production.

Numerical Evaluation	**Blister image rating according to ISO 4628-2**									
0	q0s0									
1	q1s1									
2	q1s2	q2s1	q1s3							
3	q2s2	q1s4	q1s5	q3s1						
4	q3s2	q4s2	q4s3	q2s3	q3s3	q2s4	q1s5	q4s1	q5s1	
5	q5s2	q4s3	q5s3	q3s4	q4s4	q5s4	q2s5	q3s5	q4s5	q5s5

3.6 Electrochemical Tests

All electrochemical measurements were performed with a 2-electrode setup using homemade measuring cells. PMMA tubes were affixed to the sample surfaces, using a two-component glue (UHU 2-Komponentenkleber Plus, UHU GmbH & Co KG) creating an exposed area of about 12.5 cm^2. The working electrode was the steel substrate, which was in contact with the electrolyte solution (1 M NaCl solution), a platinum mesh was used as the counter/reference

electrode and the sample was connected to a potentiostat (Gamry Reference 600; Gamry Instruments Inc.). The parameters of the measurements were changed in accordance with the experiments. A representation of the setup is depicted in **Figure 2.**

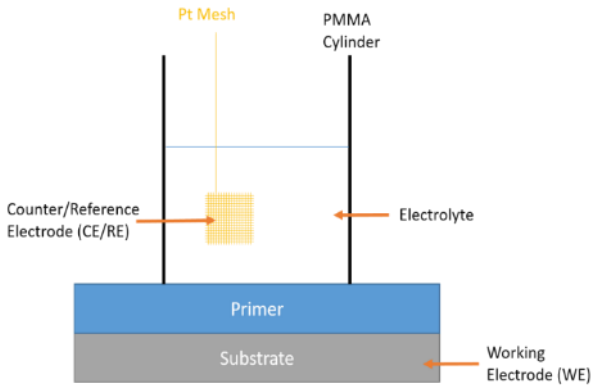

Figure 2: A Schematic illustration of the two-electrode setup used for the electrochemical measurements. Figure from *[4]*.

The equilibrium OCP value was recorded after the sample had been in contact with the electrolyte solution (1 M NaCl solution) for 24 h, and this value served as the starting point for further electrochemical measurements. In each experiment, the measured value had adjusted to the value of the substrate after 24 hours, regardless of the coating. For the Z-samples, the OCP value was -750 ± 10mV vs SHE, while for the ZM-samples, it was -783 ± 10mV vs SHE. Visual examination with the naked eye did not reveal any noticeable disparities on the sample surface after exposure to the electrolyte. Although there were no discernible chemical differences detected by EDX analyses, SEM images indicated minor visual differences after electrolyte exposure, with the surface appearing somewhat rougher.

For the impedance measurements, the excitation amplitude was 10 mV, and the recorded frequency range was 10^{-2}-10^{5} Hz. The measurements were performed every 30 min for 24 h to track the changes in the impedances of the coatings. Echem AnalystTM software was used for the analysis (Gamry Instruments Inc.). To measure the linear polarization resistance (LPR), electrolyte solution was added to the tube, and polarization curves in the range of ±10 mV vs the OCP were recorded every 30 minutes for 24 hours. The slope of the polarization curves in the range of ±5 mV vs the OCP was used to calculate the resistance.

Two devices were used to measure the cathodic delamination (CD), both of which were self-made or consisted of an adaption of an existing electrochemical cell. On the one hand, a cathodic delamination apparatus, which had been constructed for verifying whether specimens were pretreated before coating, was used. In this device up to 8 samples can be exposed in parallel to a specified current intensity. Test duration, temperature, and current intensity are

freely selectable, but only a galvanostatic mode of operation is possible. The specimens were cut to a size of 30 mm x 150 mm for use in this test and, in the case of full coating build-up specimens, a 50 mm long and 1 mm wide scribe was applied in the center down to the zinc coating (scribe according to van Laar). The edges of the specimens were masked and after exposure, the detached paint was removed with a blunt scalpel, and the distance of the detached paint from the scribe is determined either visually or using the SMART program. In this test, a potassium hydroxide solution was used as electrolyte.

On the other hand, an electrochemical cell from Gamry was adapted by 3D printing a replacement for one part of the cell, therefore creating a sample test area of approximately 38.5 cm² for the experiments. This modified cell configuration enabled the variation of multiple parameters, including changes in the electrolyte composition and gassing conditions. Moreover, the setup allowed for the versatility to operate in either galvanostatic or potentiostatic modes. **Figure 3** illustrates the two experimental setups.

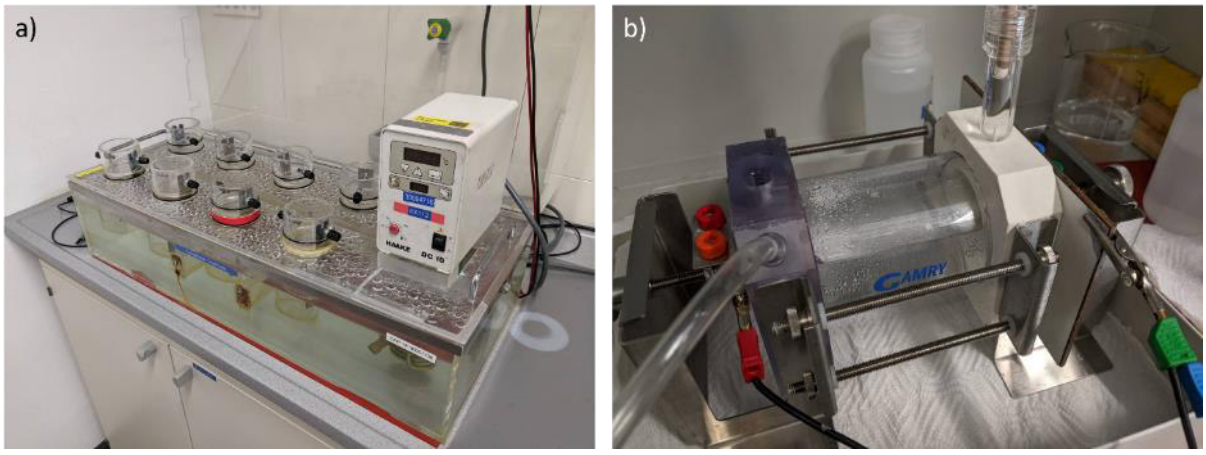

Figure 3: a) Self-built delamination apparatus used by voestalpine to check whether samples have been pretreated. b) Electrochemical cell adapted by means of 3D printing.

Upon the completion of the tests, for samples that were additionally coated with a topcoat, the detached coating was carefully removed using a blunt scalpel. The extent of detachment, measured from the point of origin at the scribe, was subsequently determined either through visual inspection or by utilizing the SMART image analysis software.

3.7 Elution Tests

Free coating films were used to carry out elution tests. Approximately 550 mg of the coating film was immersed in 400 mL of deionized water at 50 °C for 10 days. Flame atomic absorption spectrometry (F-AAS, Analytic ContrAA 300; Analytic Jena GmbH), inductively coupled plasma-mass spectrometry (ICP-MS, Thermo Scientific ICAP-RQ, Thermo Scientific Inc.), and anion chromatography (Thermo Science AS9-HC 4 mm Ion Pac, Thermo Fisher Scientific Inc.)

were used to measure the ion concentration in the eluate. Furthermore, daily measurements of the conductivities of all eluates were conducted to monitor all changes.

3.8 Water Uptake

The water absorption of the primer samples was determined using two different methods. On the one hand, it was calculated by evaluating Nyquist plots derived from impedance measurements using the Brasher-Kingsbury equation. On the other hand, it was calculated gravimetrically using a sorption balance (Aquadyne DVS™, Quantachrome Instruments). For the sorption balance measurements, free coating films were utilized as described in section 3.2, and a program was used in which the temperature was kept at 30 °C and the relative humidity was increased over a period of 24 h in increments of 10% per hour from 0 to 100% and then decreased again to 0%. During the first 3 hours of the measurements, the samples were each dried at 80 °C in the sorption balance in order to reset aging effects The change in mass of the sample material with subsequent humidity variations at 30 °C was continuously measured.

4 Results and Discussion

4.1 Analyses of Typical Commercially Available Anti-Corrosion Pigments

4.1.1 Objective of the Study and Implementation

There is a whole range of commercially available pigments, which can be divided into different categories. The aim of this part of the thesis was to analyze and categorize 12 commercially available pigments as comprehensively as possible using a variety of methods, including infrared spectroscopy (IR), Raman spectroscopy, scanning electron microscopy (SEM), energy-dispersive X-ray spectroscopy (EDX), X-ray diffraction analysis (XRD), inductively coupled plasma optical emission spectroscopy (ICP-OES), and particle size distribution analysis using laser diffraction. This comprehensive characterization was carried out in order to identify the different corrosion protection mechanisms of the pigments.

The results showed that the 12 pigments can be classified into one of three categories: barrier pigments, sacrificial pigments, and inhibitive pigments. The barrier pigments act as a physical barrier to prevent the corrosive species from coming into contact with the metal surface. The sacrificial pigments corrode preferentially to the metal, thereby protecting it and the inhibitive pigments function by forming a protective layer on the metal surface, which slows down the corrosion process.

The use of different characterization techniques allowed for a comprehensive understanding of the morphology, composition, and distribution of the pigments. IR and Raman spectroscopy were used to determine the functional groups present in the pigments. SEM and EDX were used to study the morphology and elemental composition of the pigments. For SEM analysis, the pigments were each embedded in Araldite© DBF epoxy resin 2,2'-bis[4-(2,3-epoxypropoxy)phenyl]propane in combination with Aradur HY 956 / REN HY 956© (triethylenetriamine) hardener. ICP-OES was used to determine the concentration of various metals in the pigments. Particle size distribution analysis using laser diffraction was employed to study the size distribution of the pigments.

In conclusion, this study provides a comprehensive analysis and characterization of 12 different anti-corrosion pigments, allowing for a better understanding of their mechanism of corrosion inhibition. The classification of the pigments into three categories provides insights into their unique properties and potential applications in various industries.

4.1.2 Results

An overview of the mechanical properties of all the pigments provided by the companies' data sheets is displayed in **Table 6**.

Table 6: Properties of all pigments according to their data sheet.

Pigment	Density / g cm^{-3}	Oil Count / mL 100 g^{-1}	pH	Solubility / g L^{-1}	D50 / µm	Hazards
Novinox XCA02	2,1	75	7,0	1,0	5	None
Novinox PAT30	2,2	26	7,8	0,5	-	H400, H410
Novinox PAT15	2,2	45	8,2	0,3	-	H412
Novinox PAM	2,6	50	9,5	0,6	4	H319
Novinox PC01	2,7	35	6,0	0,1	4	None
Shieldex C303	1,8	80	9,0	-	2,5-3,8	None
Heucophos CMP	2,8	45	6,5	1,7	< 3	None

Heucophos SRPP	2,8	40	5,0	-	2,5-3,5	H319
Zinkweiss Hazsiegel CF	5,6	14	7,5-8	0,0016	-	H410
ASP 600	0,03-0,48	35-45	3,5-5	-	0,6	H319
K-White G730	4,5	41	9,5	1,4	-	H319
K-White TC720	-	-	-	-	-	-

Table 7 shows the grain size distribution of the particles, measured via laser diffraction, carried out in the laboratory for environmental and operational analysis at voestalpine Stahl GmbH. The D50 value, the D90 value, the Sauter mean diameter (SMD) and the volume mean diameter (VMD) are listed.

Table 7: Particle size distribution of all Pigments, measured via laser diffraction.

Pigment	D50 / µm	D100 / µm	SMD / µm	VMD / µm
Novinox XCA02	4,89	15,00	3,94	5,04
Novinox PAT30	7,86	30,50	4,68	8,52
Novinox PAT15	5,78	33,37	3,85	7,29
Novinox PAM	4,06	30,5	4,68	8,52
Novinox PC01	4,98	25,50	2,89	6,06
Shieldex C303	3,80	10,50	3,18	3,93
Heucophos CMP	3,71	21,50	2,54	4,22

Heucophos SRPP	2,73	30,50	2,11	3,27
Zinkweiss Hazsiegel CF	2,08	30,50	1,44	3,56
ASP 600	3,79	30,50	2,67	5,13
K-White G730	5,58	39,85	3,87	7,64
K-White TC720	13,14	47,33	4,53	14,19

SEM images were taken of all samples, which are provided in the appendix. Individual results for all pigments are as follows:

4.1.2.1 Novinox XCA02

According to the manufacturer, the pigment is an amorphous calcium-exchanged silica. "NOVINOX XCA02 is a corrosion inhibiting pigment designed for coil coatings. It is a stable and easily dispersed white powder with a low tinting strength. NOVINOX XCA02 has been developed as a non-toxic and Eco-Friendly alternative to Strontium chromate in Coil Coatings. Compatible with PU and PE/Melamine systems, NOVINOX XCA02 gives excellent anticorrosive performance in Coil Coatings applied to HDGS, Galfan, Galvalume and CRS. NOVINOX XCA02 may be used alone or in association with a phosphate-based pigment." [75].

The EDX analysis revealed the predominant presence of nearly pure calcium oxide (CaO) and silicon dioxide (SiO_2) particles within the sample. This outcome is potentially attributable to the combination of pure CaO and SiO_2 particles during the manufacturing process of the pigment. The compositional profile exhibited high purity, as confirmed by ICP-OES analysis, which detected only a minor trace of magnesium (Mg) impurity alongside the anticipated elemental constituents, namely calcium (Ca), silicon (Si), and oxygen (O). In addition, the EDX analysis on a carbon tape exhibited an absence of detectable impurities. It is therefore worth noting that the EDX technique has a lower sensitivity compared to ICP-OES. Quantification of carbon content was not feasible using either analytical method due to their limitations for carbon detection. Detailed ICP-OES and EDX compositions are listed in **Table 8**.

Table 8: Chemical composition of Novinox XCA02 according to ICP-OES and area EDX. Impurities are underlined and bold.

Analysis Method	Fusion	Ca / w%	Mg / w%	Si / w%	O / w%
ICP-OES	$NaHSO_4$	3,80	**0,07**	36,60	59,53
EDX	-	3,2	-	38,0	58,7

The XRD analyzes posed challenges because of the amorphous nature of the material. However, calcium carbonate and hatrurite could be detected (see **Table 9**). Unfortunately, a large proportion of pure silicon oxide is still missing for a realistic depiction of the element ratios. **Figure 3** shows the XRD spectrogram of the pigment.

Table 9: List of phases found in the XRD of Novinox XCA02.

Mineral	Molecular formula
Calciumcarbonat	$CaCO_3$
Hatrurit	Ca_3SiO_5

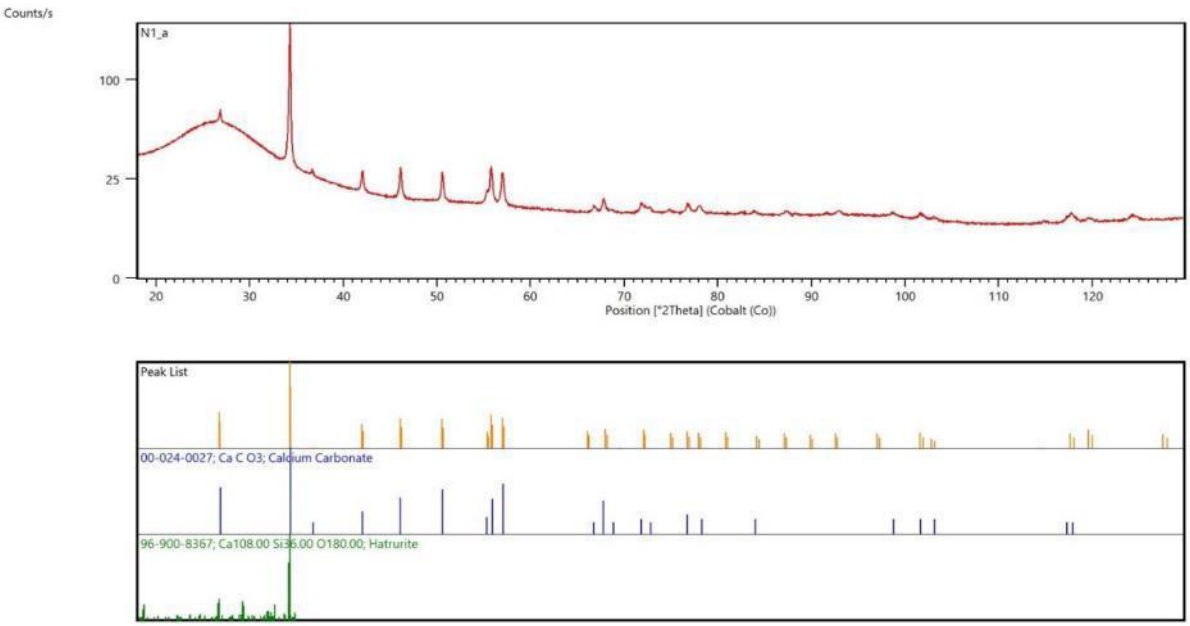

Figure 3: XRD spectrogram of Novinox XCA02.

Characterization using infrared and Raman spectroscopy was only possible to a limited extent due to the amorphous nature of the material. However, characteristic bands could be found

which indicate amorphous SiO_2 (FTIR) and carbonates (Raman). In **Figure 4**, the wave number is plotted against the transmission (FTIR) and the intensity (Raman).

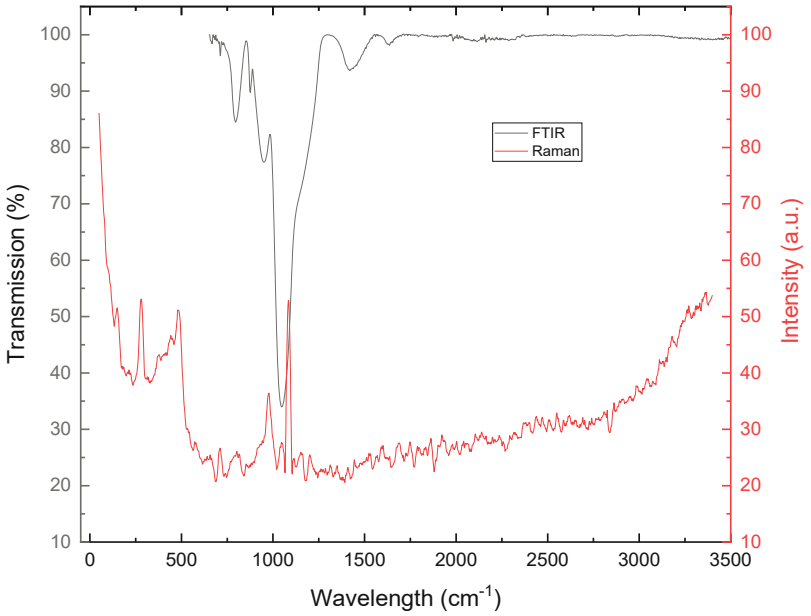

Figure 4: FT-IR and Raman spectra of Novinox XCA02.

4.1.2.2 Novinox PAT30

According to the manufacturer, the pigment is a magnesium hydrogen phosphate trihydrate ($MgHPO_4$ $3H_2O$) with a low impurity of zinc phosphate (<5%).

"NOVINOX PAT30 is a corrosion inhibiting pigment that allows the formulation of environmentally friendly paints. It is a stable and non-hygroscopic white powder, which is easily dispersed. NOVINOX PAT30 is compatible with solvent and water-based resins. It shows the best performance in solvent borne alkyd systems. NOVINOX PAT30 is also used in coil coating in association with ion exchanged silica." [76].

Contamination with zinc were detected in both elemental analyses, a result which is in accordance with the manufacturer's documented information, accessible on the official website of the product. In addition, a small amount of calcium contamination was detected. The carbon content of the sample could not be determined because both analytical methods are unsuitable for measuring carbon. **Table 10** lists the ICP-OES and EDX compositions on carbon tape.

Table 10: Chemical composition of Novinox PAT30 according to ICP-OES and area EDX. Impurities are underlined and bold.

Analysis Method	Fusion	Ca / w%	Mg / w%	P / w%	Zn / w%	O / w%
ICP-OES	HCl	**0,15**	14,80	17,60	**0,47**	66,98
EDX	-	**0,2**	16,1	18,2	**0,9**	64,6

The peaks could be well assigned to the expected substances: magnesium hydrogen phosphate trihydrate and zinc phosphate tetrahydrate, with only magnesium hydrogen phosphate being desirable from the two substances and zinc phosphate being an impurity, which was announced by the manufacturer. **Figure 5** shows the spectrogram of the pigment, **Table 11** shows the phases found.

Table 11: List of phases found in the XRD of Novinox PAT30.

Mineral	Molecular formula
Magnesium hydrogen phosphate trihydrate	$MgHPO_4 \cdot (H_2O)_3$
Zinc phosphate tetrahydrate	$Zn_3(PO_4)_2 \cdot (H_2O)_4$

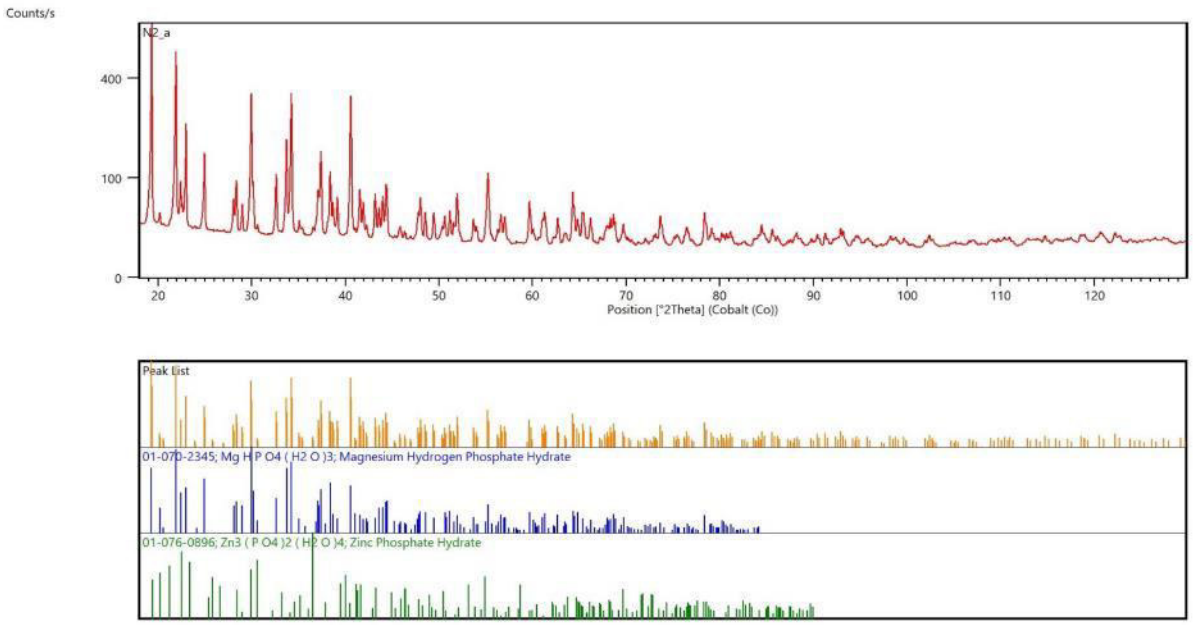

Figure 5: XRD spectrogram of Novinox PAT30.

When characterizing the pigment using FTIR and Raman spectroscopy, characteristic bands for magnesium phosphate trihydrate (FTIR) and magnesium hydrogen phosphate (Raman) were

found. In **Figure 6**, the wave number is plotted against the transmission (FTIR) and the intensity (Raman).

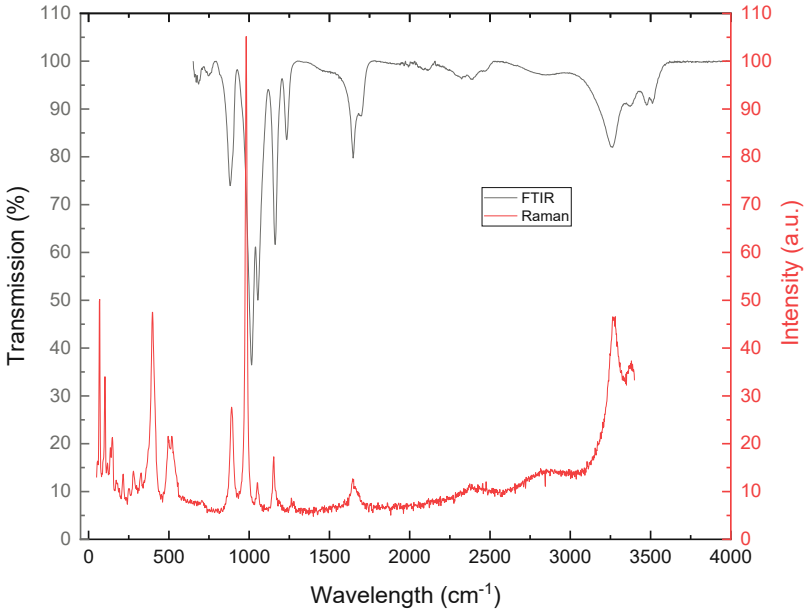

Figure 6: FT-IR and Raman spectra of Novinox PAT30.

4.1.2.3 Novinox PAT15

According to the manufacturer, the pigment is a magnesium hydrogen phosphate trihydrate ($MgHPO_4 \cdot 3H_2O$) with a small impurity of zinc phosphate (0-2.5%).

"NOVINOX PAT15 is a corrosion inhibiting pigment developed to formulate Chrome free coil coatings. It is a stable and non-hygroscopic white powder, which can be easily dispersed. NOVINOX PAT15 is compatible with PU and PE/melamine systems designed for coil coatings. NOVINOX PAT15 is usually used in association with Novinox XCA02." [77].

Based on ICP OES data, the pigment contains no impurities, with solely magnesium and phosphorus detected (oxygen and hydrogen being beyond detection limits). The particle analysis using EDX revealed a heterogeneity in magnesium concentrations among different particles. As indicated by the manufacturer, the pigments do contain minor zinc impurities and the EDX analyzes also found small amounts of calcium impurities, similar to the Novinox PAT30 sample. This outcome is consistent with the expectations as Novinox PAT30 and Novinox PAT15 share their chemical compositions. Interestingly, these impurities remained undetected in ICP-OES analyses. The carbon content of the sample could not be determined due to the unsuitability of EDX analyses on carbon tape for carbon measurement. **Table 12** lists the EDX compositions.

Table 12: Chemical composition of Novinox PAT15 according to surfaces EDX. Impurities are underlined and bold.

Analysis Method	Fusion	Ca / w%	Mg / w%	P / w%	Zn / w%	O / w%
ICP-OES	$NaHSO_4$	-	17,79	15,28	-	66,93
EDX	-	**0,3**	21,6	14,6	**0,4**	63,1

Magnesium phosphates were present in their modifications as phosphate and hydrogen phosphate. The zinc phosphate impurity appears to be present as diphosphate. **Figure 7** shows the spectrogram of the pigment, **Table 13** shows the phases found.

Table 13: List of phases found in the XRD of Novinox PAT15.

Mineral	Summenformel
Magnesium Hydrogen Phosphate Hydrate	$MgHPO_4 \cdot (H_2O)_3$
Magnesium Phosphate Hydrate	$Mg_3(PO_4)_2 \cdot (H_2O)_8$
Zinc phosphate	$Zn_2P_2O_7$

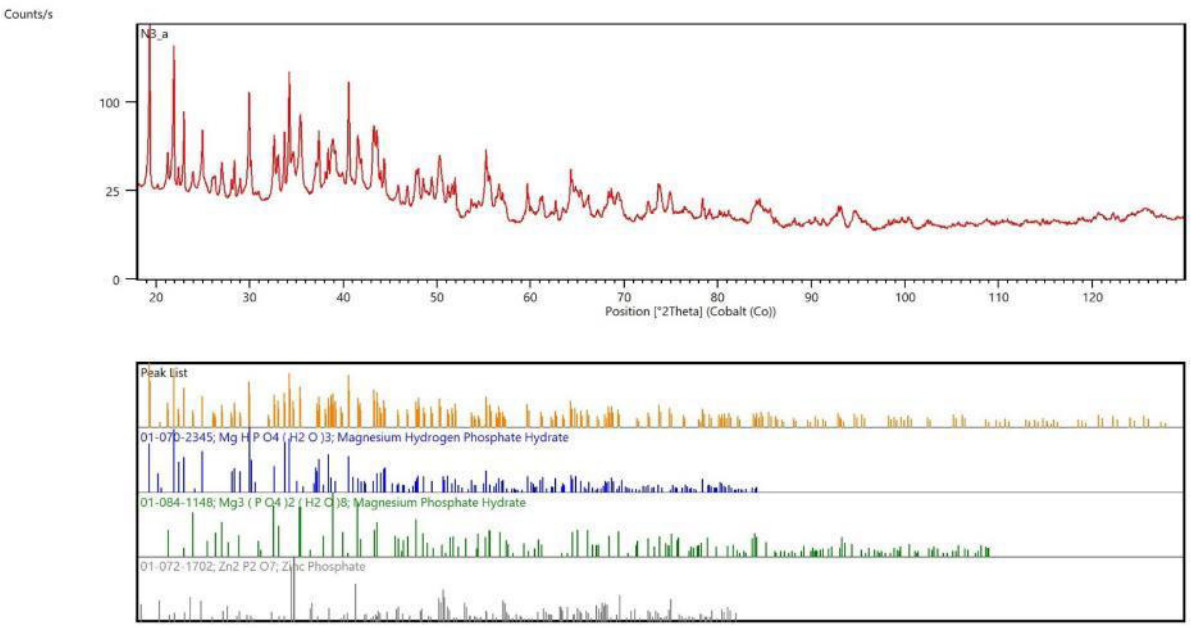

Figure 7: XRD spectrogram of Novinox PAT15.

The FT-IR and Raman spectra indicate (magnesium) phosphates, like Bobierrite ($Mg_3(PO4)_2 \cdot 8\ H_2O$). In **Figure 8** the wave number is plotted against the transmission (FTIR) and the intensity (Raman).

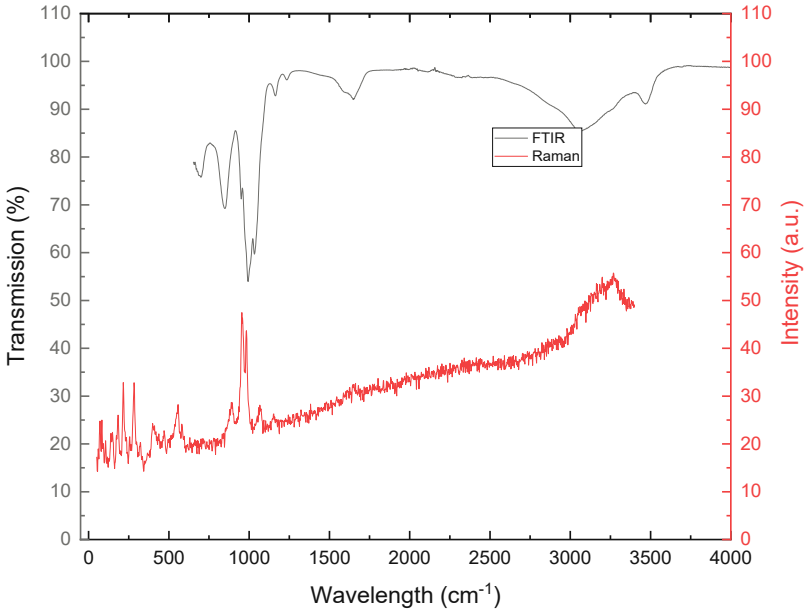

Figure 8: FT-IR and Raman spectra of Novinox PAT15.

4.1.2.4 Novinox PAM

According to the manufacturer, the pigment is a magnesium aluminum triphosphate ($AlH_2P_3O_{10} \cdot 2\ H_2O + MgO$) (impurity: zinc oxide (<0.25%)).

"NOVINOX PAM is a corrosion inhibiting pigment suitable for coil coatings. It is a stable and non-hygroscopic white powder with a low tinting strength, it is easily dispersed. NOVINOX PAM has been developed to be an alternative to Strontium chromate in Coil Coatings. It is compatible with PU and PE/melamine systems. It gives excellent anti-corrosive performance in Coil Coatings applied to Galvalume." [78].

The particles measured with EDX all consist almost exclusively of either aluminum phosphate or magnesium oxide. The pigment appears to have either originally existed as a double salt or simply two different salts were mixed together. The ICP OES analysis also found very small amounts of iron and zinc oxide. The carbon content of the sample could not be determined due to the unsuitability of EDX analyzes on a carbon tape for measuring carbon. **Table 14** lists the compositions according to ICP OES and EDX.

Table 14: Chemical composition of Novinox PAM according to ICP-OES and area EDX. Impurities are underlined and bold.

Analysis Method	Fusion	Mg / w%	P / w%	Zn / w%	Al / w%	Fe / w%	O / w%
ICP-OES	H_2SO_4	17,90	20,30	**0,04**	6,60	**0,04**	55,12
EDX	-	19,7	20,1	-	7,3	-	52,9

The XRD measurements detected aluminum triphosphate (as dihydrate and anhydrous) and magnesium oxide in the form of periclase. **Figure 9** shows the spectrogram of the pigment and **Table 15** shows the phases found.

Table 15: List of phases found in the XRD of Novinox PAM.

Mineral	Molecular formula
Aluminum dihydrogen triphosphate dihydrate	$Al[H_2P_3O_{10}]\cdot(H_2O)_2$
Aluminum dihydrogen triphosphate	$Al[H_2P_3O_{10}]$
Periclase	MgO

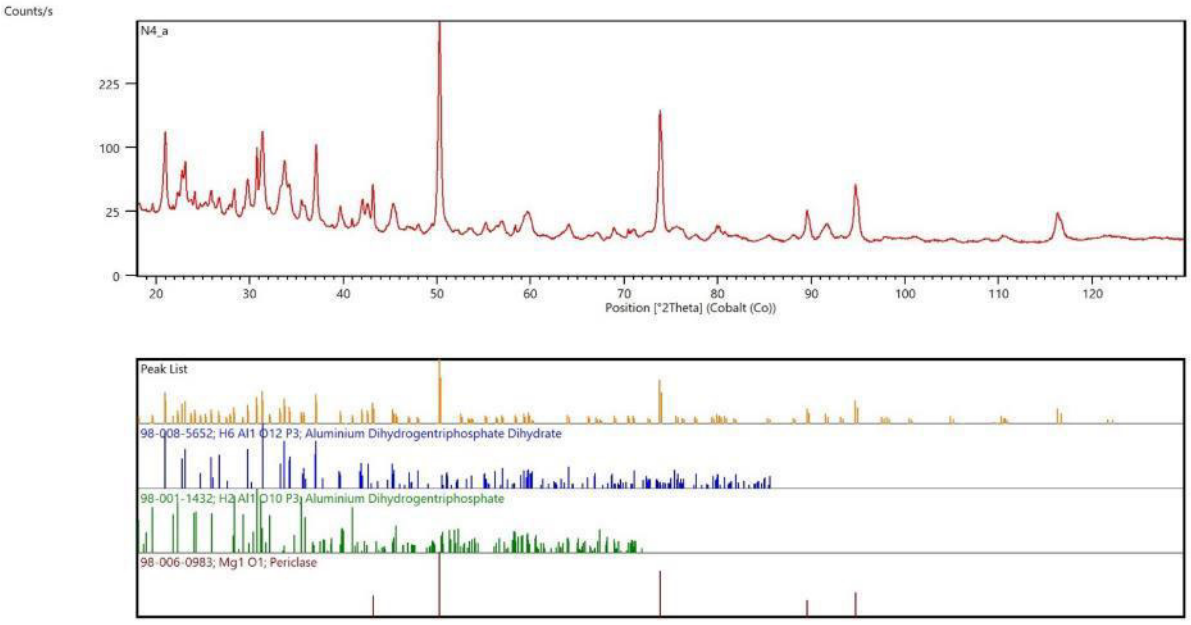

Figure 9: XRD spectrogram from Novinox PAM.

Despite clear bands, no assignment using the database was possible. There are, however, indications of phosphates. In **Figure 10**, the wave number is plotted against the transmission (FTIR) and the intensity (Raman).

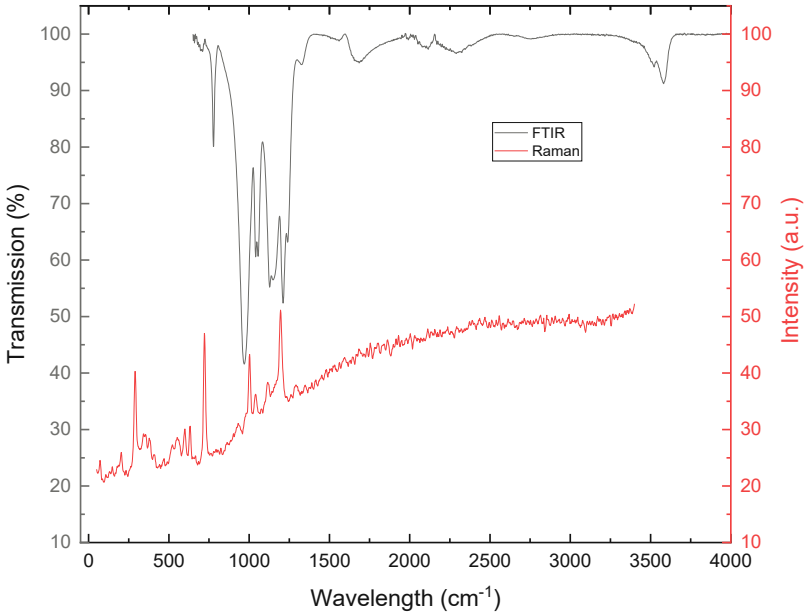

Figure 10: FT-IR and Raman spectra of Novinox PAM.

4.1.2.5 Novinox PC01

According to the manufacturer, the pigment is a calcium hydrogen phosphate (in the form of mono- and dihydrate). "NOVINOX PC01 is a calcium phosphate used as an anticorrosion inhibiting pigment in DYI coatings. It is a stable and non-hygroscopic white powder, it is easily dispersed. NOVINOX PC01 may be used in formulations for environmentally friendly coatings." [79].

The measured elements almost perfectly reproduce the expected, theoretical composition, with the exception of iron (0.4% and 0.2%, respectively) and magnesium (0.8%) impurities. The carbon content of the sample could not be determined because EDX analyzes on a carbon tape are unsuitable for measuring carbon. **Table 16** lists the compositions according to ICP OES and EDX.

Table 16: Chemical composition of Novinox PC01 according to ICP-OES and area EDX. Impurities are underlined and bold.

Analysis method	Fusion	Ca / w%	P / w%	Fe / w%	O / w%	Mg / w%
ICP-OES	HCl	27,00	20,80	**0,40**	51,80	-
EDX	-	27,9	19,7	**0,2**	51,4	**0,8**

XRD measurements revealed the presence of calcium phosphate in the modifications hydrogen phosphate and hydroxyapatite. In addition, a proportion of calcium carbonate was detected,

which should not actually be present. **Figure 11Figure *47*** shows the spectrogram of the pigment and **Table 17** shows the phases found.

Table 17: List of phases found in the XRD of Novinox PC01.

Mineral	Molecular formula
Calcium hydrogen phosphate	$CaHPO_4$
Hydroxyapatite	$Ca_5[OH(PO_4)_3]$
Calcite	$CaCO_3$

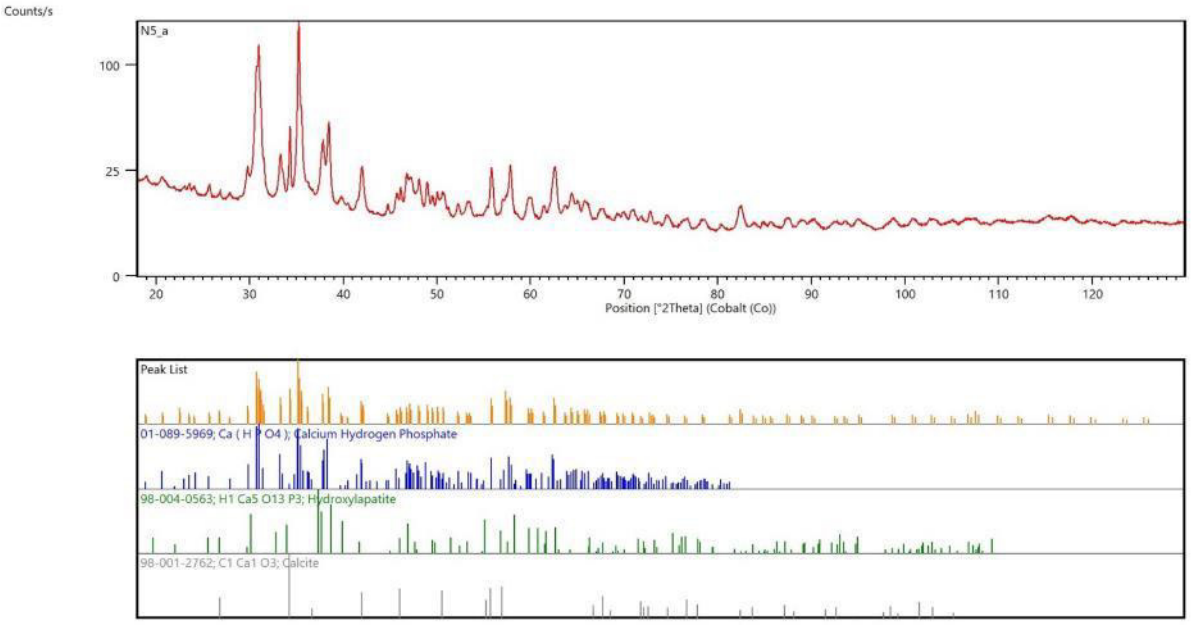

Figure 11: XRD spectrogram from Novinox PC01.

Characteristic bands for calcium phosphate (FTIR) and calcite, $CaCO_3$ (Raman) were found when characterizing the pigment using FTIR and Raman spectroscopy. Since $CaCO_3$ was detected in both the XRD measurement and the Raman measurement, it can be assumed that carbonate is present in the pigment. In **Figure 12**, the wave number is plotted against the transmission (FTIR) and the intensity (Raman).

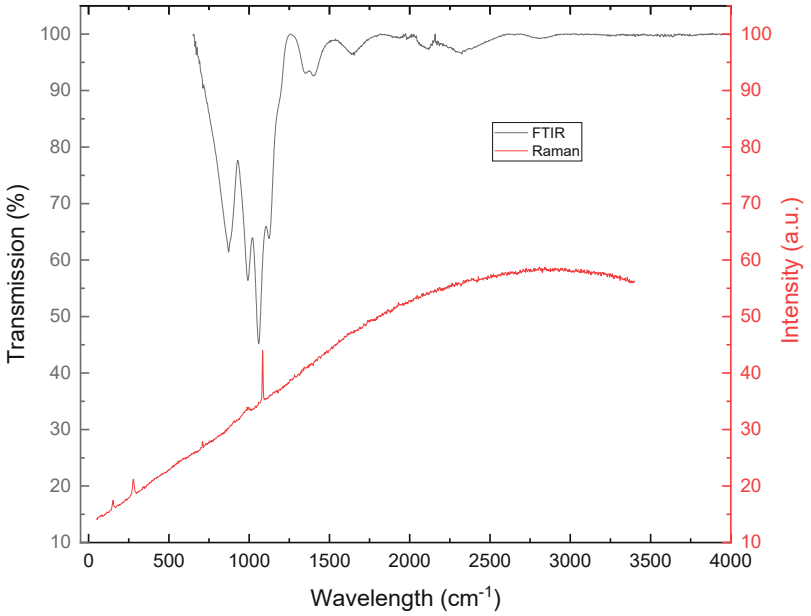

Figure 12: FT-IR and Raman spectra of Novinox PC01.

4.1.2.6 Shieldex C303

Shieldex C303 is a well-established pigment with a history of use and numerous existing publications exploring potential reaction mechanisms. As stated by the manufacturer, the pigment is composed of amorphous calcium-exchanged silica [80].

The measured elements are very similar to the expected values with a small impurity of magnesium measured using ICP OES (0.04%). The carbon content of the sample could not be determined because EDX analyzes on a carbon tape are unsuitable for measuring carbon. **Table *18*** lists the compositions according to ICP OES and EDX.

Table 18: Chemical composition of Shieldex C 303 according to ICP-OES and area EDX. Impurities are underlined and bold.

Analysis method	Fusion	Ca / w%	Mg / w%	Si / w%	O / w%
ICP-OES	$NaHSO_4$	2,73	**0,04**	39,29	57,94
EDX	-	2,9	-	41,7	55,4

Since the pigment is highly amorphous, phases could not really be detected. Only mutinaite, a modification of silicon dioxide, can be assumed. **Figure 13** shows the spectrogram of the pigment and **Table 19** shows the phases found.

Table 19: List of phases found in the XRD of Shieldex C 303.

Mineral	Molecular formula
Mutinaite	SiO_2

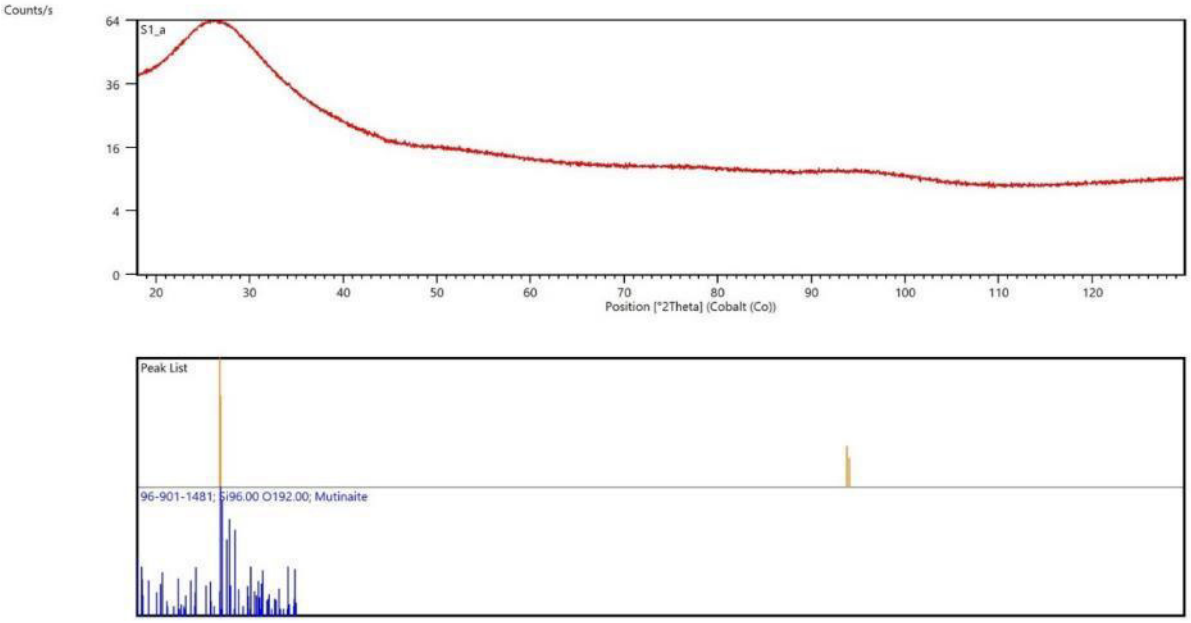

Figure 13: XRD spectrogram of Shieldex C 303.

When characterizing the pigment using FTIR, characteristic bands for amorphous silicon dioxide were found. It was not possible to gain a Raman spectrum. In **Figure 14** the wave number is plotted against the transmission (FTIR).

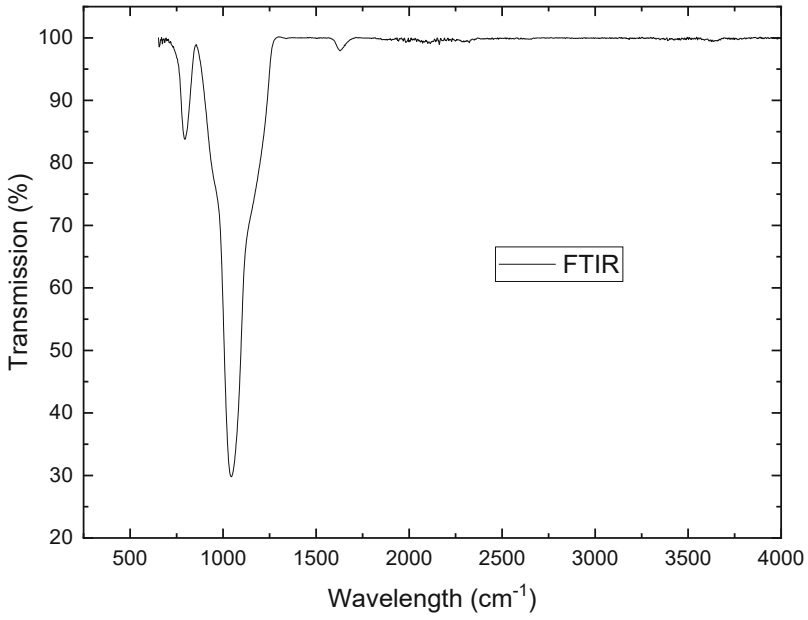

Figure 14: FT-IR spectrum of Shieldex C 303.

4.1.2.7 Heucophos CMP

According to the manufacturer's specifications, the pigment consists of calcium magnesium orthophosphate a compound that has a well-established history in the market, supported by relevant literature. The particle properties were found on the manufacturer's website [81].

Upon elemental analysis, the pigment exhibited traces of contamination, including zinc, aluminum, and iron. It is worth noting that the concentrations of aluminum and iron were exclusively quantifiable using the more sensitive ICP OES analysis method. The proportion of calcium is many times higher than that of magnesium. **Table 20** lists the compositions according to ICP OES and EDX.

Table 20: Chemical composition of Heucophos CMP according to ICP-OES and area EDX. Impurities are underlined and bold.

Analysis method	Fusion	Ca / w%	Mg / w%	P / w%	Zn / w%	Al / w%	Fe / w%	O / w%
ICP-OES	HCl	30,60	1,82	18,90	**0,83**	**0,09**	**0,02**	47,74
EDX	-	31,9	1,9	18,2	**3,1**	-	-	45,0

The measurements encompass a mixture of different calcium phosphate and magnesium phosphate modifications, as well as a composite of both. A spectrogram of the pigment is depicted in **Figure 15**, while **Table 21** details the identified phases.

Table 21: List of phases found in the XRD of Heucophos CMP.

Mineral	Molecular formula
Monetite	$CaHPO_4$
Hydroxyapatite	$Ca_5[OH(PO_4)_3]$
Magnesium hydrogen phosphate trihydrate	$MgHPO_4 \cdot (H_2O)_3$
Whitlockite	$Ca_9Fe_{0.2}Mg_{0.8}[PO_3OH(PO_4)_6]$

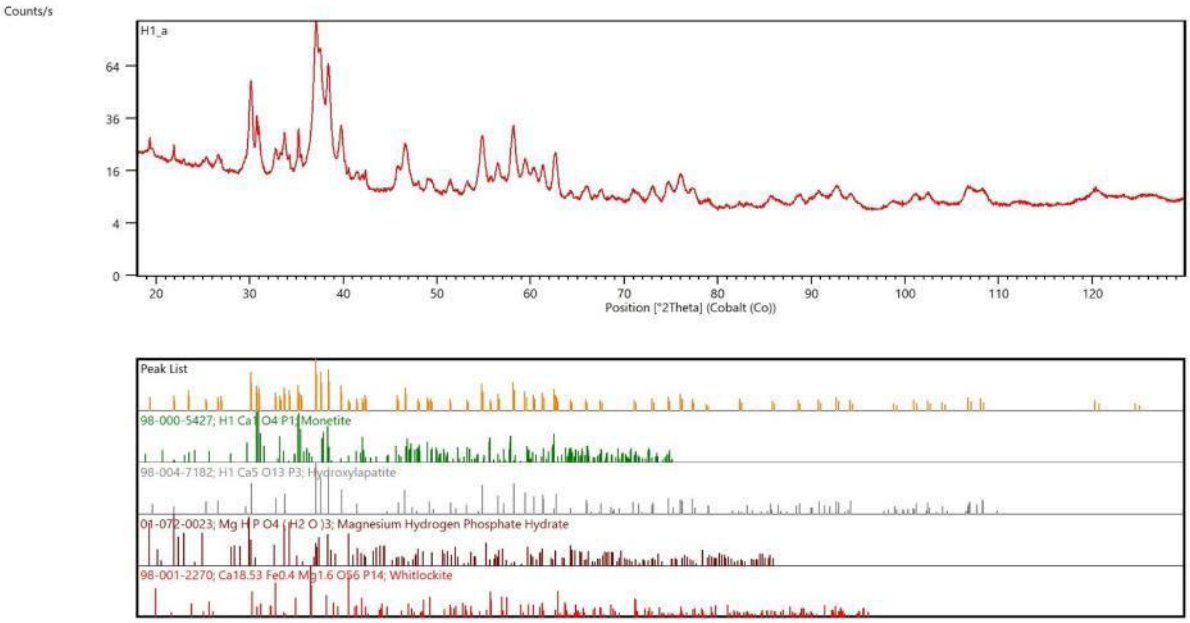

Figure 15: XRD spectrogram of Heucophos CMP.

When characterizing the pigment using FTIR and Raman spectroscopy, characteristic bands for hydroxyapatite, $Ca_5(PO_4)_3(OH)$ (FTIR) and apatite, $Ca_5[(F,Cl,OH)|(PO_4)_3]$ (Raman) were found. In **Figure 16**, the wave number is plotted against the transmission (FTIR) and the intensity (Raman).

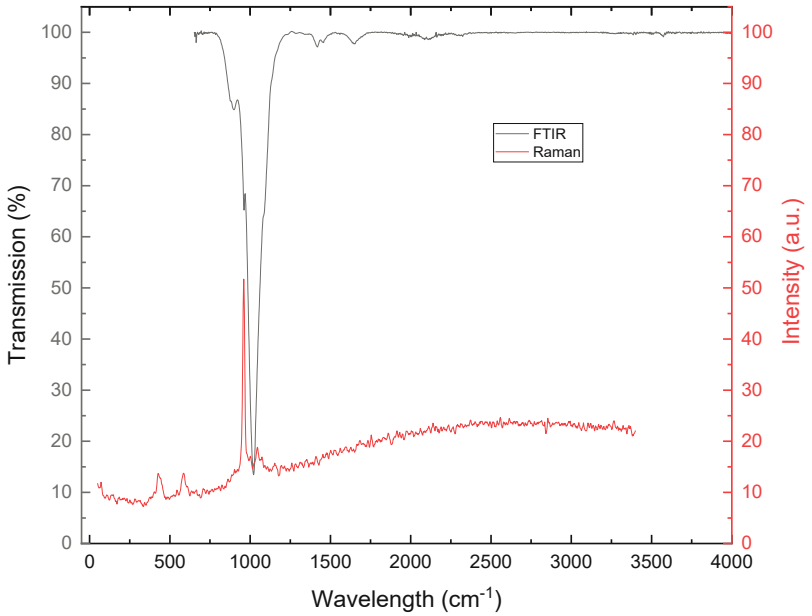

Figure 16: FT-IR and Raman spectra of Heucophos CMP.

4.1.2.8 Heucophos SRPP

According to the manufacturer, the pigment consists of strontium aluminum polyphosphate hydrate [82].

ICP-OES analysis was unfeasible due to the pigment's insolubility, resisting dissolution via traditional methods—neither through $NaHSO_4$, nor when subjected to HCl or H_2SO_4. In the EDX analysis, the expected elements were identified, with a higher proportion of aluminum than strontium. Both composite particles, comprising aluminum and strontium, and particles comprising only one of those were quantifiable. **Table 22** lists the EDX compositions on carbon tape.

Table 22: Chemical composition of Heucophos SRPP according to area EDX.

Analysis method	Fusion	Sr / w%	P / w%	Al / w%	O / w%
EDX	-	18,8	19,7	7,2	54,3

During the XRD analysis, unexpected findings emerged, including aluminum phosphate, aluminum triphosphate, and a variant of strontium carbonate – contrary to anticipated outcomes. According to the manufacturer, strontium phosphate should be present instead. **Figure 17** shows the spectrogram of the pigment and **Table 23** depicts the phases found.

Table 23: List of phases found in the XRD of Heucophos SRPP.

Mineral	Molecular formular
Berlinit	$AlPO_4$
Aluminum dihydrogen triphosphate dihydrate	$Al[H_2P_3O_{10}]\cdot(H_2O)_2$
Strontianite	$SrCO_3$

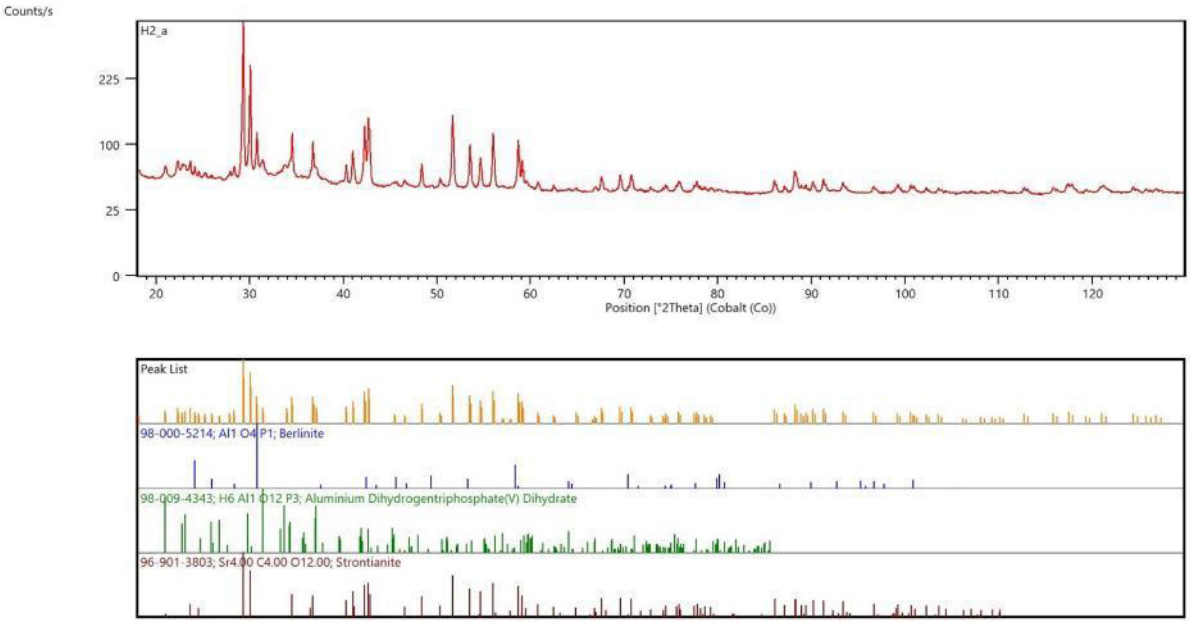

Figure 17: XRD spectrogram of Heucophos SRPP.

With pigment characterization through FTIR and Raman spectroscopy, characteristic bands for carbonates were found in both analyses. Since carbonates were also detected in the XRD measurement, it is reasonable to assume the presence of carbonate within the pigment. In **Figure 18**, the wave number is plotted against the transmission (FTIR) and the intensity (Raman).

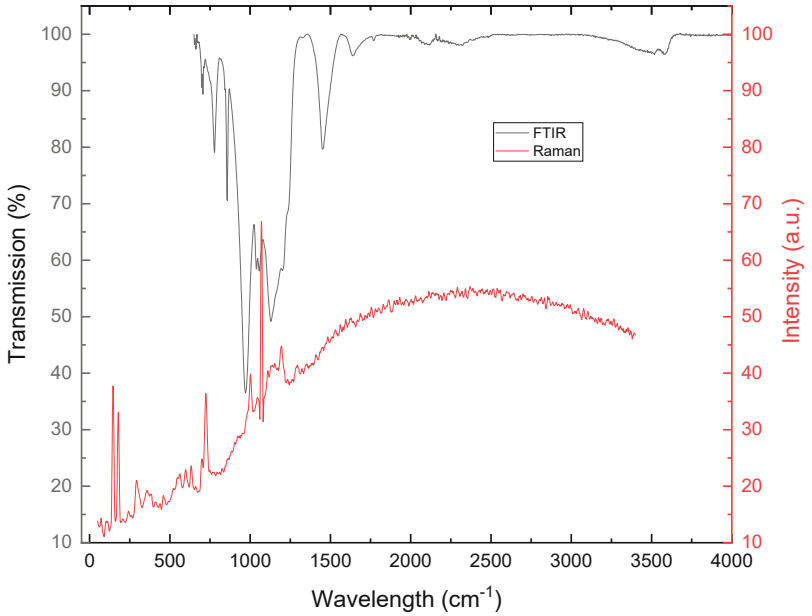

Figure 18: FT-IR and Raman spectra of Heucophos SRPP.

4.1.2.9 Zinkweiss Harzsiegel CF

The pigment is composed exclusively of zinc oxide, a very old pigment predominantly used for cold rolled coil coatings. Numerous publications discussing its properties and applications are available, the safety data sheet contains the following information [83].

Both ICP-OES and EDX analyses exclusively revealed the presence of zinc oxide, suggesting that the pigment likely exists in a pure form. **Table 24** lists the results of the EDX analysis and the ICP OES analysis.

Table 24: Chemical composition of Zinkweiss Harzsiegel CF according to ICP-OES and surfaces EDX.

Analysis method	Fusion	Zn / w%	O / w%
ICP-OES	HCl	80,60	19,40
EDX	-	81,0	19,0

Only one modification of zinc oxide was detected in the XRD measurement. This is listed in **Table 25**. The XRD spectrogram is shown in **Figure 51**.

Table 25: List of the phases found in the XRD of Zinkweiss Harzsiegel CF.

Mineral	Molecular formular
Zincite	ZnO

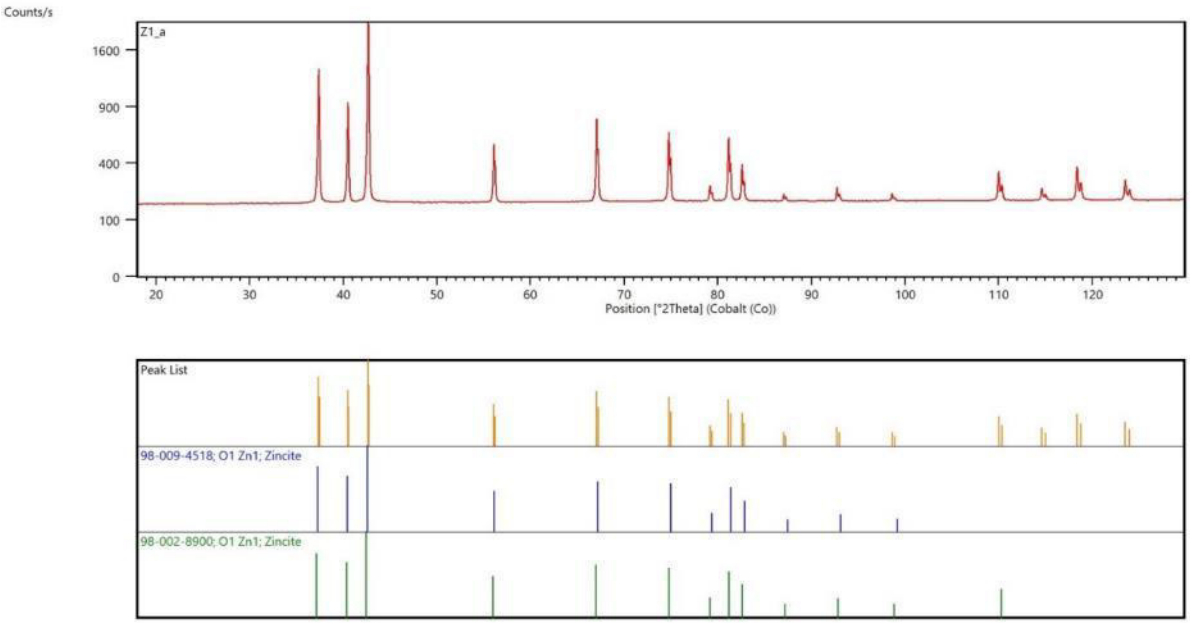

Figure 19: XRD spectrogram of Zinkweiss Harzsiegel CF.

When characterizing the pigment using FTIR and Raman spectroscopy, characteristic bands for zincite and ZnO were found in both analyses, which is consistent with the XRD analysis. In **Figure 20** the wave number is plotted against the transmission (FTIR) and the intensity (Raman).

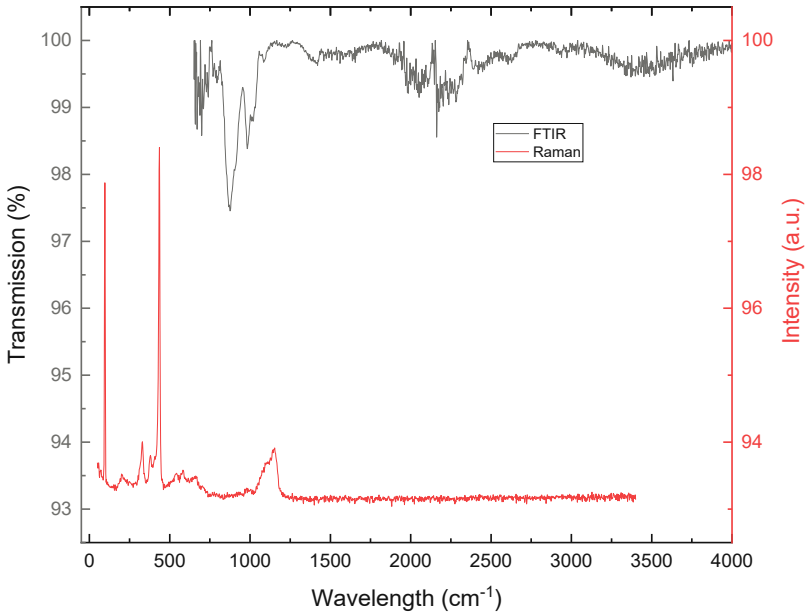

Figure 20: FT-IR and Raman spectra of Zinkweiss Harzsiegel CF.

4.1.2.10 ASP 600

ASP600 is a filler which, according to the manufacturer, consists largely of kaolinite [84]. "ASP® 600 is a good extender when used in primers. ASP® 600 kaolin is highly recommended for polyester pultrusion profiles and is generally used in solvent-borne adhesives and rubber compounds where color is not of primary importance. Typical applications: OEM primers, phenolics, solvent-borne gravure inks, BMC / SMC, solvent-borne adhesives and sealants, pultrusion profiles" [85].

In addition to the expected elements, the elemental analysis also detected impurities of calcium, titanium and iron. **Table 26** lists the compositions according to ICP OES and EDX.

Table 26: Chemical composition of ASP 600 according to ICP-OES and area EDX. Impurities are underlined and bold.

Analysis method	Fusion	Ca / w%	Si / w%	Al / w%	Ti / w%	Fe / w%	O / w%
ICP-OES	$NaHSO_4$	**0,14**	20,76	19,70	**0,75**	-	58,65
EDX	-	-	19,6	20,0	**0,8**	**0,6**	59,1

In addition to the expected modification kaolinite, a modification of alumina and two modifications of silica were found, which could be present due to decomposition of kaolinite. Notably absent are the identified phases for the measured impurities – calcium, titanium, and iron – likely due to their possibly low concentrations. **Figure 21** shows the spectrogram of the pigment, **Table 27** shows the phases found.

Table 27: List of phases found in the XRD of ASP 600.

Mineral	Molecular formular
Silicon oxide hydride	$H_3SiOSiH_3$
Kaolinite	$Al_4[(OH)_8\|Si_4O_{10}]$
Zeolite	SiO_2
Aluminum oxide	Al_2O_3

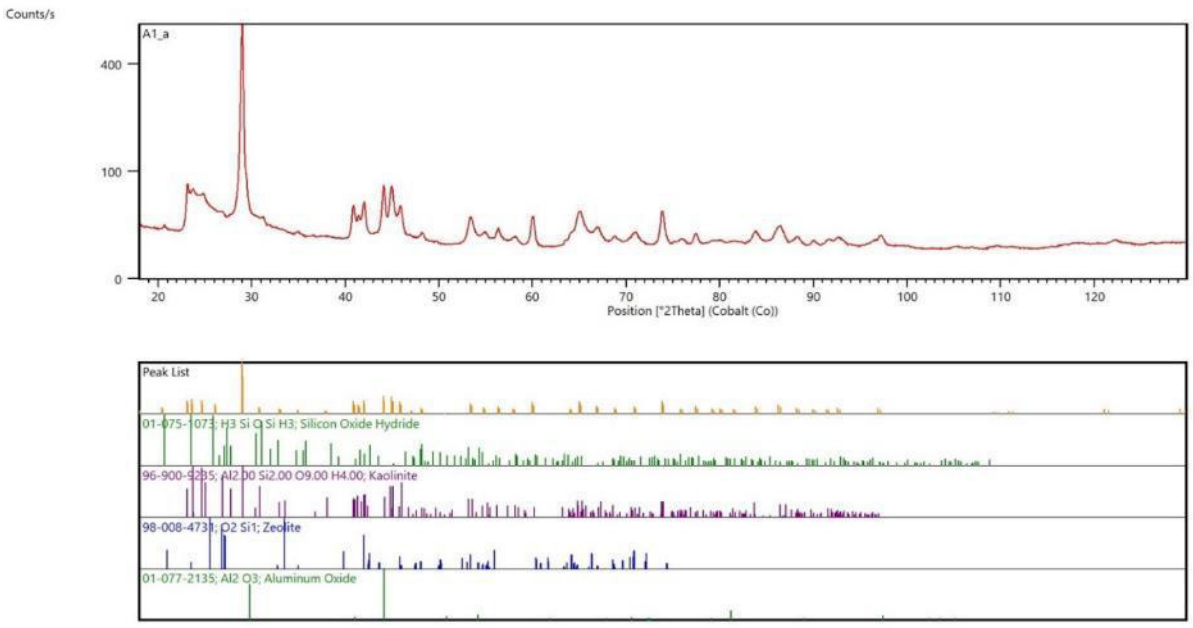

Figure 21: XRD spectrogram of ASP 600.

During the pigment's characterization through FTIR and Raman spectroscopy, characteristic bands corresponding to aluminum silicate were discernible within the FTIR spectrogram, which aligns with findings from other analyses. Furthermore, the Raman spectrogram revealed the presence of titanium oxide. Thus, the detected titanium exists in an oxide form, commonly employed as an industry-grade filler. In **Figure 22**, the wave number is plotted against the transmission (FTIR) and the intensity (Raman).

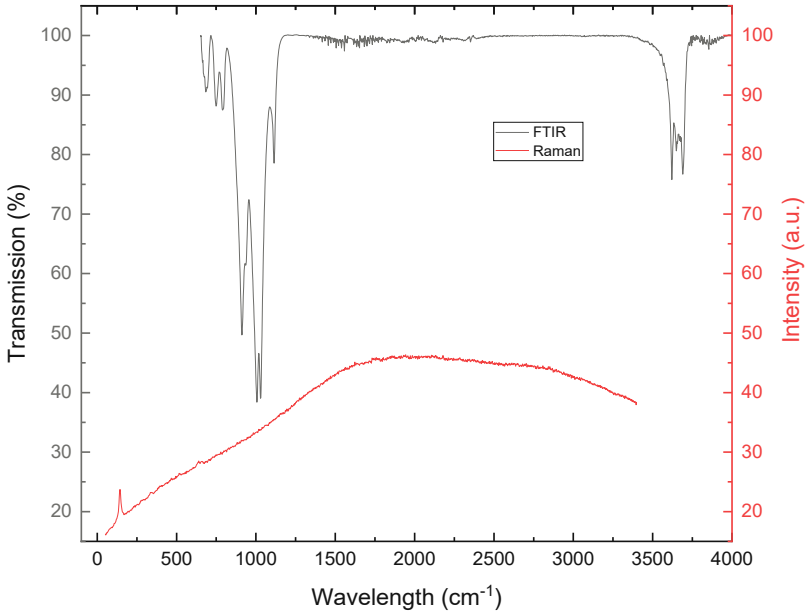

Figure 22: FT-IR and Raman spectra of ASP 600.

4.1.2.11 K-White G730

According to the manufacturer, K-White G 730 is an anti-corrosion pigment based on modified aluminum triphosphate [86, 87].

In the elemental analysis, in addition to the expected elements, the ICP-OES revealed an unexpected presence of calcium, while the EDX analysis detected zinc and silicon. The proportion of magnesium is greater than that of aluminum, contradicting the fact that the pigment is advertised as modified aluminum phosphate and not modified magnesium oxide. **Table 28** lists the compositions according to ICP OES and EDX.

Table 28: Chemical composition of K-White G730 according to ICP-OES and area EDX. Impurities are underlined and bold.

Analysis method	Fusion	Si / w%	Al / w%	Ca / w%	Mg / w%	Zn / w%	P / w%	O / w%
ICP-OES	$NaHSO_4$	-	4,24	**0,12**	12,86	-	14,24	68,5
EDX	-	**5,2**	7,8	**0,1**	10,7	**1,2**	24,5	50,4

As stated by the manufacturer, aluminum phosphate, which is present in its dimeric form, could be detected in the XRD analysis. In addition, magnesium oxide in the modification periclase and silicon dioxide were found. In the case of the latter, it is uncertain whether the compound was not contaminated with silicon oxide particles during sample preparation, since no silicon

could be detected in the analysis using ICP OES. The spectrogram of the pigment is listed in **Figure 23**, and the phases found in **Table 29**.

Table 29: List of phases found in the XRD of K-White G 730.

Mineral	Molecular formular
Periclase	MgO
Aluminum triphosphate dihydrate	$Al_2P_6O_{20} \cdot 4\ H_2O$
Silica	SiO_2

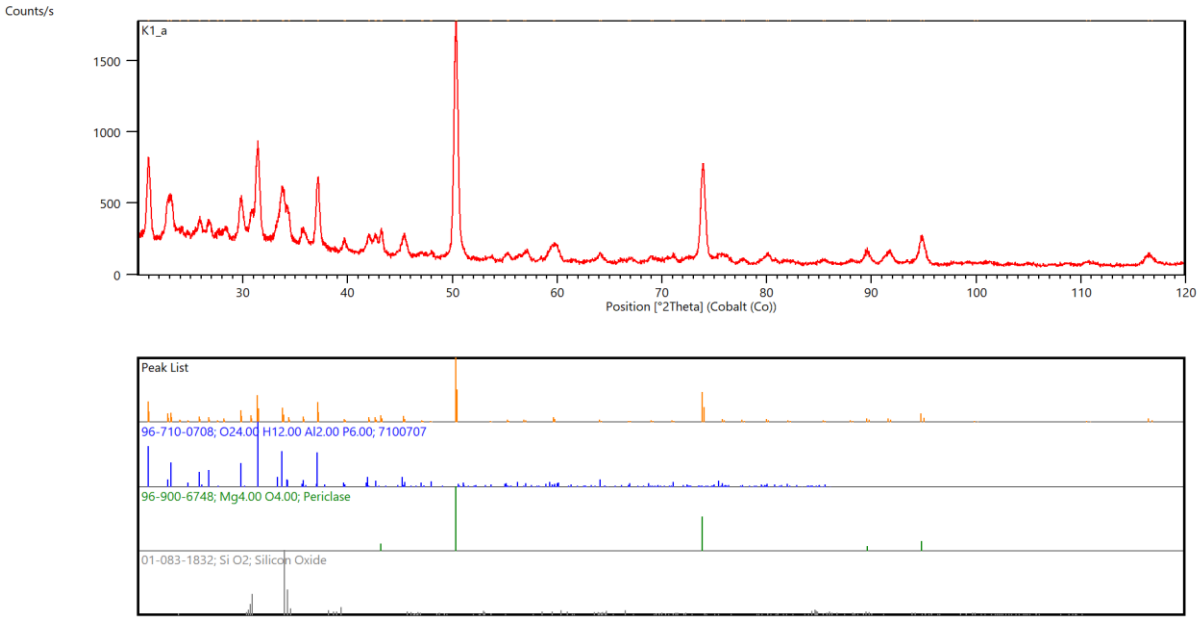

Figure 23: XRD spectrogram of K-White G 730.

Although both Raman and infrared spectra could be displayed, a clear assignment of compounds was not possible. However, there is evidence of the presence of phosphates in the pigments. In **Figure 24** the wave number is plotted against the transmission (FTIR) and the intensity (Raman).

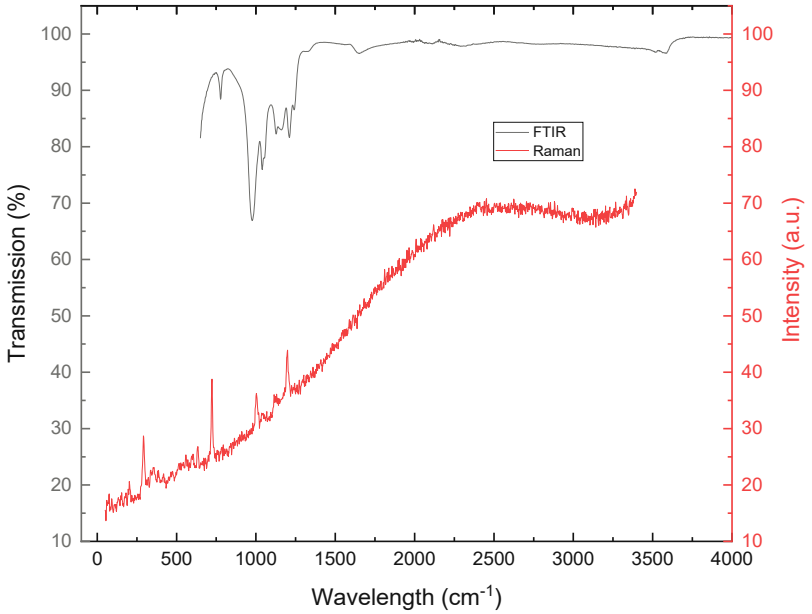

Figure 24: FT-IR and Raman spectra of K-White G730.

4.1.2.12 K-White TC720

Information regarding the anti-corrosion pigment K-White TC 720 is generally scant, however, the consensus among various online sources is that it constitutes a magnesium-modified silicon oxide [87].

During the elemental analysis, a substantial quantity of titanium was identified through both methods, which was probably added as a filler in the form of titanium dioxide. In addition to the expected elements, contamination with aluminum and zinc could also be detected during the analysis using EDX on carbon tape. **Table 30** lists the compositions according to ICP OES and EDX.

Table 30: Chemical composition of K-White TC 720 according to ICP-OES and area EDX. Impurities are underlined and bold.

Analysis method	Fusion	Si / w%	Al / w%	Mg / w%	Zn / w%	Ti / w%	O / w%
ICP-OES	$NaHSO_4$	19,75	-	1,57	-	26,08	52,6
EDX	-	19,4	**0,6**	1,4	**0,6**	32,2	45,7

In the XRD analyses, the measured signals could be assigned to the minerals dodecasil 1H and rutile. The pigment consists to a large extent of silicon oxide to which a large amount of titanium dioxide has been added as a filler. No modification of magnesium oxide could be detected,

possibly the proportion was too low, or the signals were superimposed. The spectrogram of the pigment is listed in **Figure 25**, and the phases found in **Table 31**.

Table 31: List of phases found in the XRD of K-White TC 720.

Mineral	Molecular Formular
Dodecasil 1H	SiO_2
Rutile	TiO_2

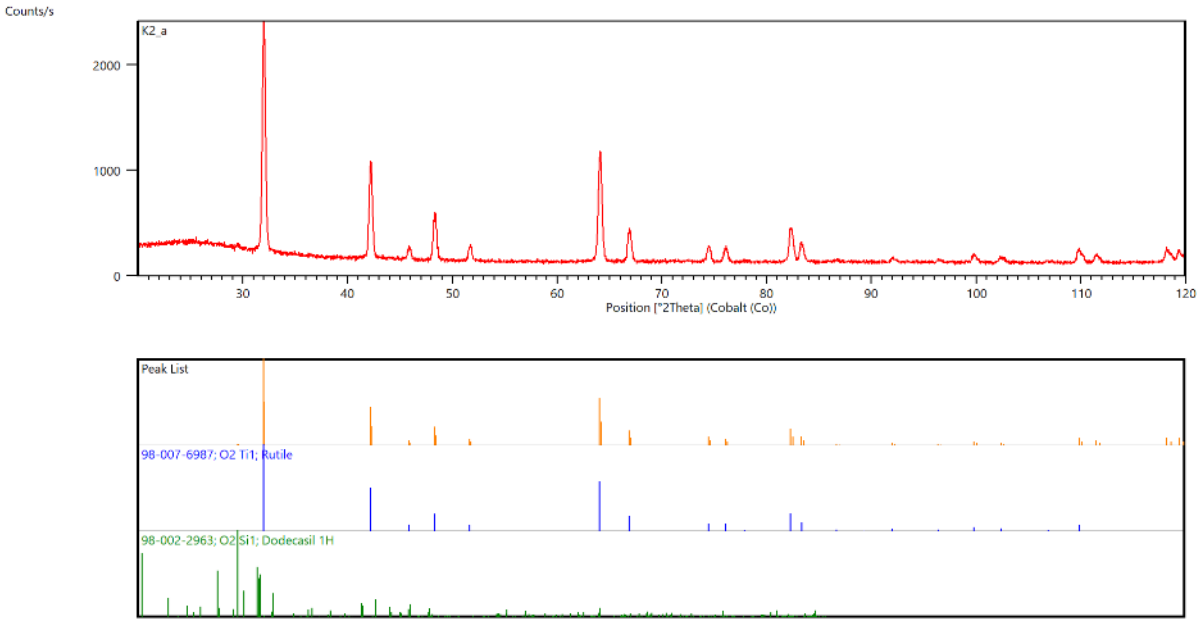

Figure 25: XRD spectrogram of K-White TC 720.

The signals detected in the infrared spectrum could be assigned to amorphous silicon dioxide and the signals in the Raman spectrum to titanium dioxide (anatase). In **Figure 26**, the wave number is plotted against the transmission (FTIR) and the intensity (Raman).

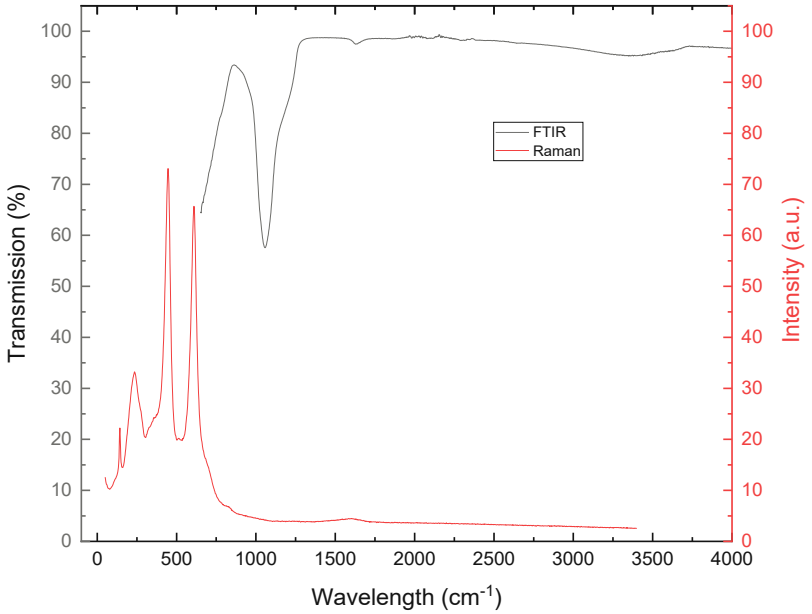

Figure 26: FT-IR and Raman spectra of K-White TC720.

4.1.3 Final Conclusion and Selection of Pigments

The first chapter of this thesis delved into an extensive characterization of various anti-corrosion pigments through a diverse range of analytical methods. From this comprehensive analysis, two pigments, Shieldex and ASP600, were selected for further investigation in the following chapters. The decision to focus on those two pigments was driven by several reasons that highlighted their potential as effective corrosion inhibitors.

Firstly, Shieldex, a calcium-exchanged silica, showed immense promise due to its ability to form a robust and protective barrier on metal surfaces. This barrier formation is crucial in preventing corrosive agents from reaching the underlying substrate, thus acting as an efficient shield against degradation. Shieldex has earned a reputation as a dependable additive for coatings, thus prompting our decision to thoroughly evaluate its potential.

Similarly, ASP has demonstrated impressive anti-corrosion properties and is a well-established industrial material. Its effectiveness has been well-documented, and it seamlessly integrates with existing coating systems, making it a strong candidate for further exploration. Moreover, ASP's abundance and cost-effectiveness make it an appealing option for corrosion protection strategies.

Additionally, both Shieldex and ASP demonstrated properties that complemented each other in a corrosion protection system. Shieldex's ability to form a robust barrier, combined with ASP's

unique interactions and compatibility with other components, suggested a synergistic potential that could enhance the overall anti-corrosive performance of the thin film primers.

By focusing on Shieldex and ASP, we aimed to shed light on their individual contributions to the overall corrosion protection system while exploring potential synergies when combined. The meticulous evaluation of these pigments through a battery of corrosion tests and analysis of key engineering parameters sought to provide valuable insights into their efficacy, thereby contributing to the development of more effective and durable corrosion protection strategies for galvanized steel sheets.

4.2 Thermoset thin film primers: Influence of Substrate, Layer Thickness and Wettability of Additives in Laboratory Testing

The results shown in this section were in large part published in [4]. The publication is available at https://onlinelibrary.wiley.com/doi/full/10.1002/maco.202313786. The copyright agreement is attached in **Appendix 8**.

4.2.1 Objective of the Study and Implementation

Typically, a combination of a thermoset thin film primer and a top coat is used for corrosion protection of galvanized steel sheets. However, the corrosion resistance of thin film primers alone has not been thoroughly studied. In this part of the thesis, it was tried to assess the performance of thin film primers using a variety of corrosion tests across a range of engineering parameters, including thickness, wettability, and substrate. 13 primer formulations were tested without a top coat on GI and ZM-coated steel, with primer layer thicknesses ranging from 3 to 9 µm using five established, complementary tests. Those tests cover all predominant mechanisms that may occur and include cathodic and anodic delamination as well as barrier protection. In order to be able to better interpret the results, they were grouped into two sections. In section 4.2.2, the variation in the composition of the primers was interpreted, in section 4.2.3 a variation in the layer thickness.

4.2.2 Results Primer Composition and Substrate Variations

In this part of the study, the performance of primers of different compositions was evaluated and a comparison was made between coated Z and ZM substrates.

Table 3 in section 3.1 provides a list of the model primer components employed to distinguish different aspects of the formulations, including hydrophobizing and the incorporation of barrier pigments. Furthermore, a comparison was made between the performance of primers containing

only barrier pigments and primers containing only inhibitive pigments. **Table 2** gives an overview of the compositions of these primers. Moreover, three commercially available primers, designated as P1 to P3, were used. These primers were based on polyester polyol binders and blocked trimeric isocyanate crosslinkers, and they contained inhibitive pigments, that is, calcium-exchanged silica. The PMT required for complete crosslinking of the coatings was approximately 235 °C, with a dwell time in the oven of 25 s. In total, 13 distinct primer formulations were evaluated in this study.

4.2.2.1 Sample Characterization

The samples underwent various characterization methods before their performance was evaluated through several tests. Specifics on the characterization can be found in section 3.3. EDX was used to examine the components of the samples, and cross-sectional images were taken to visualize the arrangement of the primer system components. Microstructural characterization was possible by combining these images with EDX. **Figure 27** displays the elemental analyses of various model primer samples, which contained either classical or hydrophobized Shieldex pigments and were supplemented with either mica or kaolin as barrier pigments to selected samples. The low layer thickness may have contributed to the fact that no differences in pigment distribution were observed in the coating among the samples, despite the utilization of various pigments. All pigments had an average particle diameter of ≤ 3.8 µm.

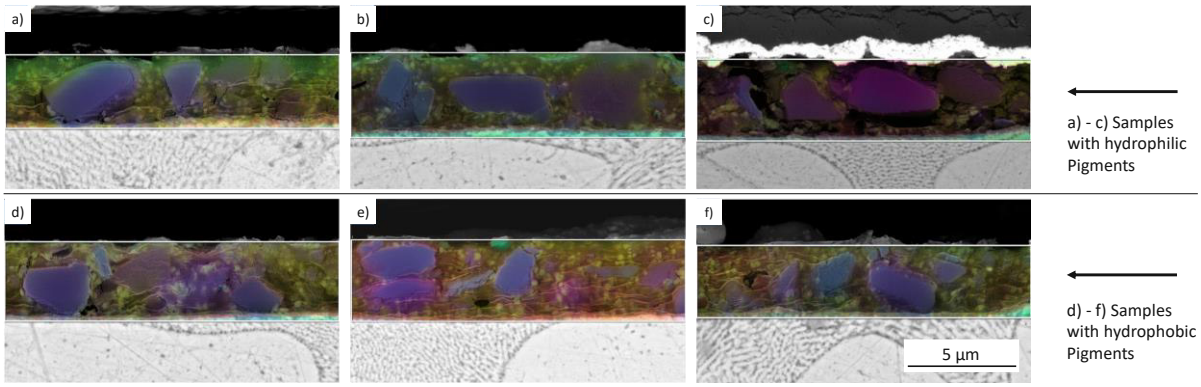

Figure 27: Cross-sectional SEM images were taken of six model primer samples: a) containing only Shieldex, b) containing Shieldex and mica, c) containing Shieldex and kaolin, d) containing only hydrophobized Shieldex, e) containing hydrophobized Shieldex and mica, and f) containing hydrophobized Shieldex and kaolin. In addition to these pigments, all samples also contained titanium dioxide. The elements in the images were color-coded for easy identification: titanium was highlighted in yellow, silicon in purple, oxygen in blue, carbon in red, and calcium in green. Despite the use of different pigments, no variations in pigment distribution were observed among the samples. The thickness of the primer layer in all samples was roughly 3 µm.

4.2.2.2 Salt Spray Tests

After undergoing 1,000 hours of salt exposure in the NSST, all specimens which had been put in the chamber with intact surfaces demonstrated remarkable resistance to corrosion (data not

shown). Nearly all specimens remained visually unscathed, suggesting that a 3 µm thickness is sufficient to safeguard the underlying substrate against corrosion for a few weeks in the NSST. Even at a lower film thickness, the primer coating's barrier protection appears to be given regardless of the composition of the primer.

To further investigate the impact of substrate and pigments on anodic delamination protection, NSSTs were conducted with specimens with coating defects. Two scribes were applied to each specimen, one on the left-hand side down to the zinc coating and the other on the right-hand side reaching the underlying steel substrate, following ISO 17872:2007 guidelines.

In a first experiment, the performance of samples coated solely with a clearcoat was compared to samples coated with primers containing either barrier pigments (kaolin; ASP 600) or inhibitive pigments (calcium exchanged silica; Shieldex) in the NSST. The purpose of this experiment was to evaluate the protective abilities of these different coatings against corrosion.

As anticipated, the samples coated with a primer that did not contain any pigments were completely corroded after 672 hours of exposure in the NSST. This outcome aligns with expectations, as the absence of pigments leaves the substrate vulnerable to direct contact with corrosive agents – in this case NaCl – present in the test environment. The corrosion observed on these samples served as a control, highlighting the importance of incorporating protective pigments in coating formulations.

Interestingly, when comparing the performance of primers containing barrier pigments to those containing inhibitive pigments, the latter demonstrated superior corrosion protection capabilities. This disparity in performance can be attributed to the specific mechanisms of action employed by these two types of pigments. Barrier pigments primarily act by establishing physical barriers by forming a dense and impermeable layer, thereby preventing corrosive species from reaching the substrate. However, they may not provide effective long-term protection if the coating is compromised or if corrosion-inducing species manage to permeate the barrier layer.

On the other hand, inhibitive pigments possess inherent chemical properties that enable them to actively inhibit the corrosion process. These pigments release inhibiting compounds or form a passivating layer when exposed to corrosive environments, thus impeding the electrochemical reactions that lead to corrosion. This active corrosion inhibition mechanism exhibited by inhibitive pigments makes them more effective at preventing the onset and progression of corrosion, especially in scenarios where the coating may be compromised to some extent, which

is not unlikely, as primer coatings are comparatively thin. **Figure 28** shows all samples after 672 hours (4 weeks) in the salt spray test with scribes.

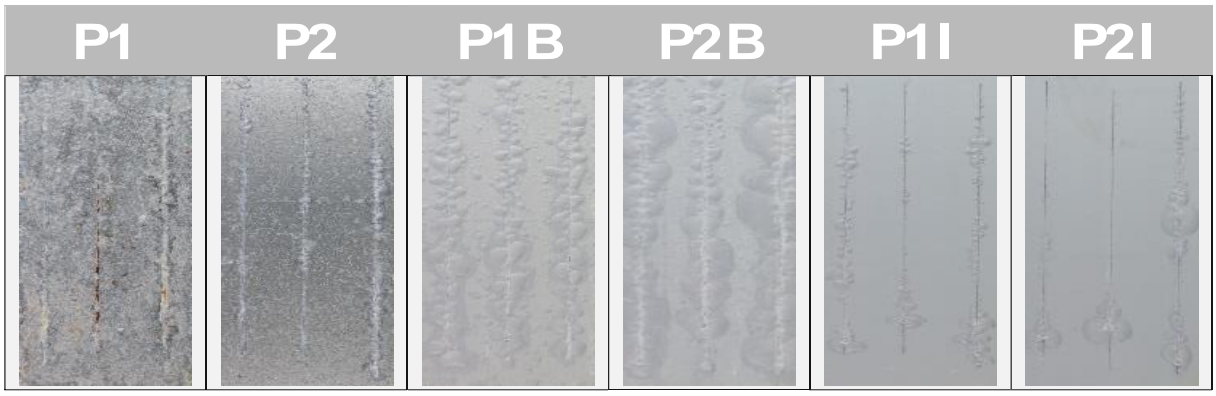

Figure 28: Delamination initiated at the scribes of two polyester model primers (P1 and P2), each with barrier pigment (P1B and P2B respectively) and inhibitive pigment (P1I and P2I respectively) after 672 hours (4 weeks) in the salt spray test.

In a more comprehensive experiment, various pigment combinations were evaluated, including the use of an inhibitive pigment (calcium-exchanged silica; Shieldex) in its original (S) and hydrophobized (HS) form, alone and in combination with two different barrier pigments: mica (M) and kaolin (K). Z and ZM steel were used to assess the influence of the substrate (see section 3.1 for details). **Figure 29a** presents the outcomes of this experiment after 672 hours (for Z) and 2,000 hours (for ZM) in the salt spray test. Because steel specimens with a ZM coating have better salt spray test resistance than those with a Z coating, a longer test duration was required for meaningful differentiation and evaluation [88, 89]. Blisters were only discernible on the Z samples, while the ZM-coated specimens exhibited only corrosion at the scribes, likely due to the influence of the substrate.

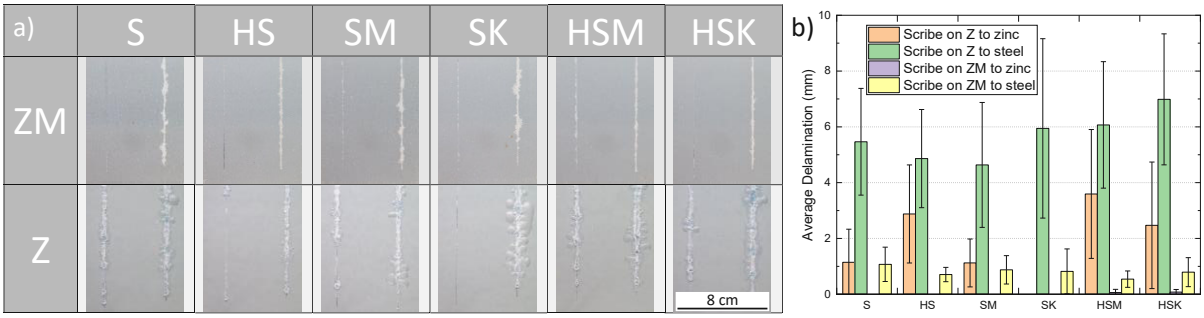

Figure 29: a) The corrosion and delamination of model primers were observed starting from the scribes on substrates with either a pure zinc coating (Z) or a zinc-magnesium-aluminum coating (ZM) after exposure for 672 h (for Z) and 2,000 h (for ZM). The primer formulations included S with only Shieldex, HS with hydrophobized Shieldex, SM and SK with Shieldex and mica or kaolin, respectively, and HSM and HSK with hydrophobized Shieldex and mica or kaolin, respectively. The sample panels had dimensions of 100 mm x 150 mm, and the primer film thickness was uniform at 3 µm across all samples. b) The scribe delamination of the model primers was evaluated on both Z and ZM substrates.

In order to quantitatively determine the extent of primer delamination, the detached primer was removed using a blunt scalpel and the distance of detachment was measured from the scribes using the SMART software. The average delamination length for Z-coated and ZM-coated samples is shown in **Figure 29b**. To verify the results, the samples were also analyzed with a white light interferometer to measure height differences between the primer surface and detached areas. **Figure 30a** shows a typical evaluation of a Z-coated sample, with the height profile indicating that the delamination was anodic due to the dissolution of the zinc coating. This phenomenon is also visible in the cross section recorded using a light microscope, as shown in **Figure 30b**.

The experiments demonstrated that when artificial coating defects, such as scribes, are present on the zinc coating or underlying steel substrate, delamination occurs. The galvanic effects within the scribe play a role, as delamination proceeding from scribes down to the steel substrate are more pronounced than from those down to the zinc coating. Under these conditions, anodic contributions were mainly observed, with complete dissolution of the metallic coating under the delaminated coating, as can be seen in **Figure 30b**.

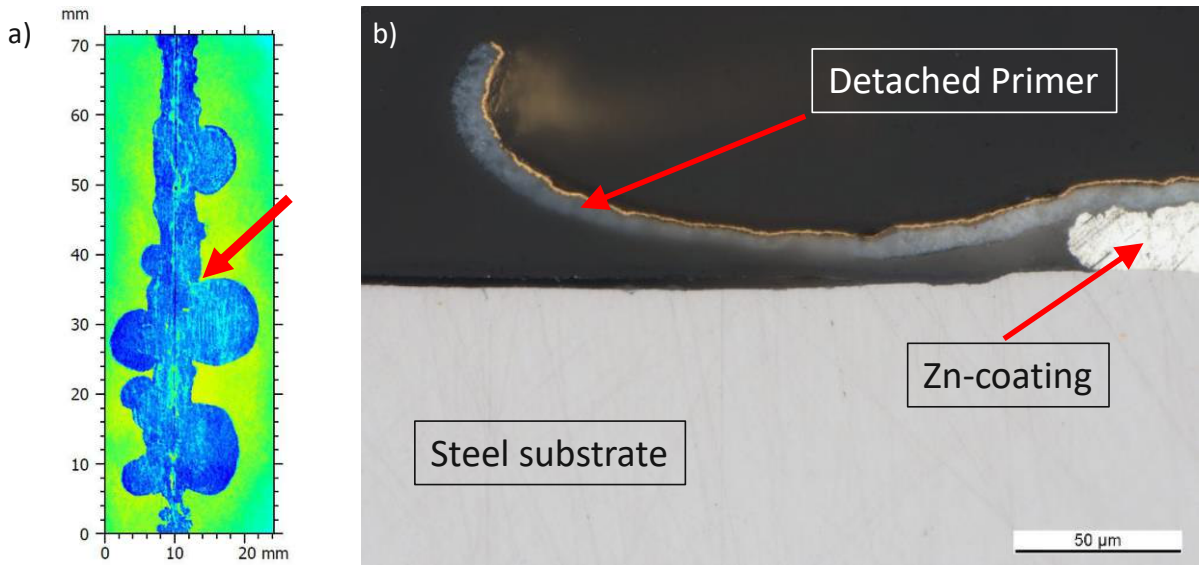

Figure 30: a) Using a white-light interferometer, a height profile of the samples subjected to the salt-spray test was generated to determine the type of delamination. The arrow points to the location where the cross-section was taken. b) An optical microscope image of the transition region between the delaminated and still-adhering primer confirms the prevalence of the anodic delamination mechanism.

In addition, variations were observed in the behavior of different substrates. On coated Z samples, spherical irregularities were observed around the scribe, indicating the occurrence of local cathodic delamination in the form of blistering at an earlier stage of the NSST. In contrast, delamination on coated ZM substrates happened due to the formation and spread of corrosion products around the scribes. This occurs because coated ZM substrates generate corrosion

products that hinder oxygen reduction on the sample surface, in contrast to Z substrates [88, 90]. Consequently, due to the potential gradient between the defect and the undamaged interface, cathodic delamination is not possible with ZM. Instead, delamination occurs through an anodic mode triggered by ion migration at the metal oxide/polymer interface. Although the rate of delamination under prolonged exposure to the NSST is slower for coated ZM than for coated Z, it is not insignificant [91]. However, the corrosion of the ZM samples was similarly severe regardless of the primer formulation.

In this test setup, the hydrophobic treatment of the pigments hardly had any effect on delamination starting from the scribes down to the steel substrate. Nevertheless, it led to a deterioration on delamination starting from the scribes down to the zinc coating on average. We believe that the hydrophobic treatment slowed the dissolution kinetics of the pigments, thereby reducing their protective effect, as part of the protective mechanism is the dissolution of the pigment [92]. It was not possible to provide a definitive statement regarding the addition of the barrier pigments, mica, and kaolin on the protection of the coatings.

4.2.2.3 Cathodic Delamination Tests

In another experiment, CD tests were conducted with test durations optimized for the best possible differentiation among sample setups (see section 3.6 for specifics). After the completion of each test, the delaminated primer was removed using a blunt scalpel and adhesive tape in compliance with ISO 2409:2013. **Figure 31a** illustrates the outcomes of primer composition variations on GI steel and steel with ZM coating, respectively, with a primer layer thickness of 3 µm. S denotes Shieldex only, HS hydrophobized Shieldex, SM and SK contain mica and kaolin in addition to Shieldex, while HSM and HSK contain hydrophobized Shieldex and mica and kaolin, respectively. The percentage of detached primers was calculated using the commercially available image analysis software SMART, as shown in **Figure 31b**.

The addition of barrier pigments (mica and kaolin) was found to worsen the protection against cathodic delamination in these experiments, possibly due to the formulation of the primers not being optimized, resulting in the creation of additional diffusion pathways. However, hydrophobizing the inhibition pigments significantly increased the resistance to delamination, particularly when comparing primer samples containing only Shieldex (S) with those containing hydrophobic Shieldex (HS) on ZM. Hydrophobicity appeared to be crucial for the performance in this test. This improvement can be attributed to the enhanced adhesion of the primer resulting from the silanization of the pigments, a phenomenon described in the literature [92].

However, when analyzing the average performance among all tests, also including the NSST and the electrochemical tests described in following sections, primer formulations incorporating hydrophobic pigments showed lower effectiveness compared to their non-hydrophobic counterparts overall. It is suspected that this discrepancy arises from the slower kinetics of pigment dissolution caused by the hydrophobic treatment. This treatment may create a barrier on the pigment surface, leading to reduced leaching and hindering subsequent exchange processes. Consequently, the corrosion inhibition mechanism becomes less efficient.

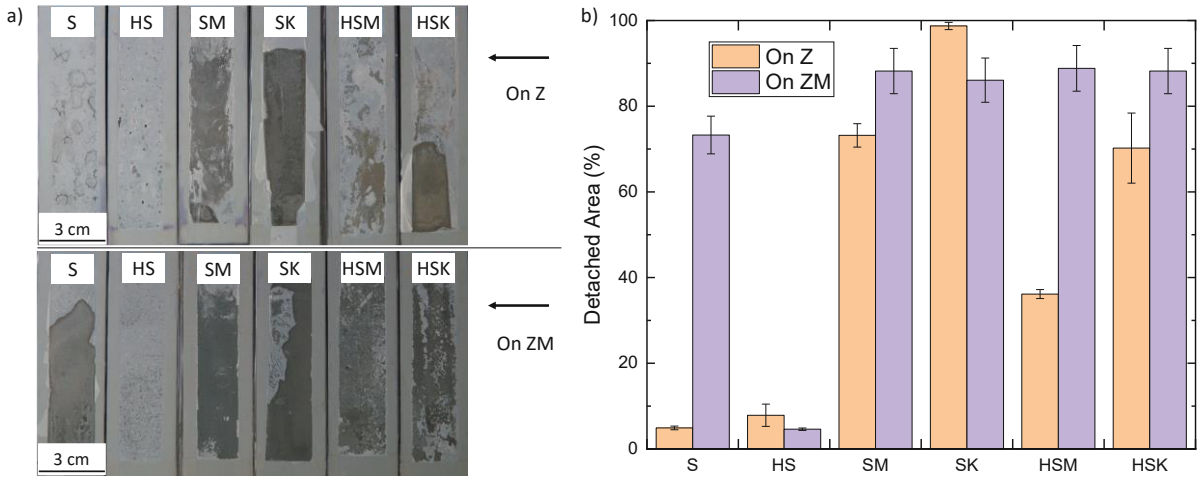

Figure 31: a) The cathodic delamination of the model primers was compared after a 5-minute test on hot-dip galvanized steel with Z coating (upper half) and hot-dip galvanized steel with ZM coating (lower half). The primers used were S, which contained only Shieldex, HS, which contained hydrophobized Shieldex, SM, which included Shieldex and mica, SK, which included Shieldex and kaolin, and HSM and HSK, which included hydrophobized Shieldex along with mica and kaolin, respectively. All samples had a primer film thickness of 3 µm, and the delaminated primer was removed using adhesive tape in accordance with ISO 2409:2013. b) An overview of the percentages of detached primers using the image evaluation software.

4.2.2.4 EIS measurements

The EIS measurements aimed to determine the barrier properties of the primers, and the impact of the pigments was more noticeable in this test compared to the others. Hydrophobization of the inhibition pigments led to an increase in impedance value, which was similar to the effect of switching from a Z substrate to a ZM substrate. Coated ZM substrates have a tendency to corrode faster, which leads to the formation of protective corrosion products that increase the measured impedance value. Moreover, the addition of barrier pigments, such as mica and kaolin, did not show a significant impact on the measured impedance value. This could potentially be attributed to suboptimal formulation conditions, where the concentration or dispersion of these pigments may not have been optimized for enhancing barrier properties. **Figure 32a** depicts the measured impedance values at 100 mHz for the various primer compositions on both substrates.

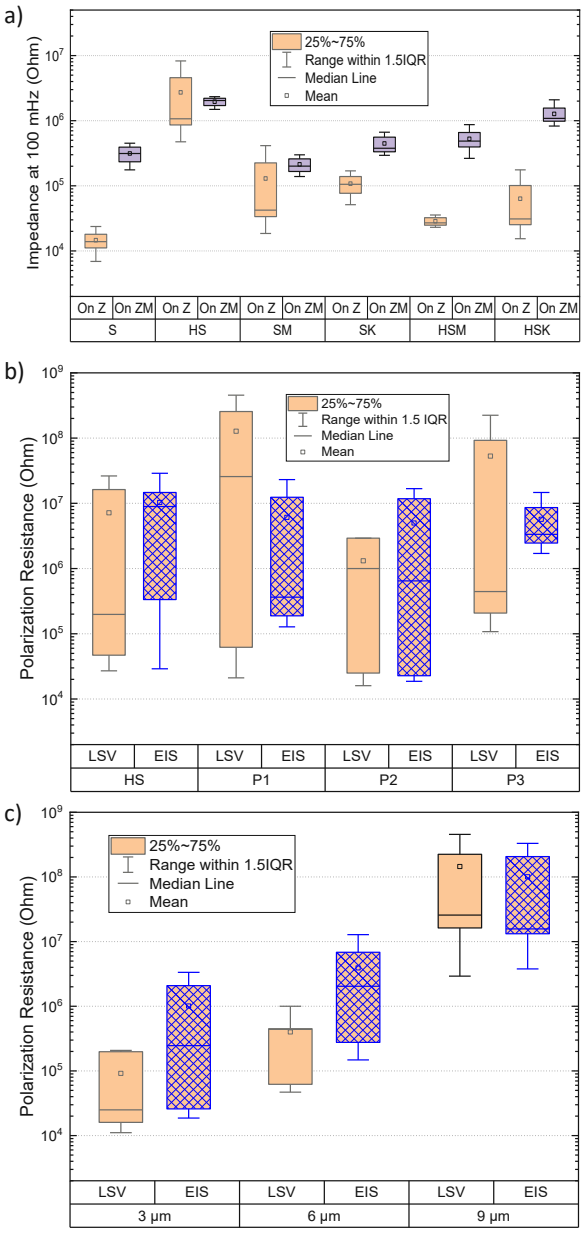

Figure 32: a) The impedance values at 100 mHz were measured after exposing 3 µm thick model primer coatings on substrates with pure zinc coating and Zn-Al-Mg coating to a 1 M NaCl solution for 24 hours. The primer formulations used were S containing only Shieldex, HS containing hydrophobized Shieldex, SM and SK containing Shieldex and mica/kaolin, respectively, and HSM and HSK containing hydrophobized Shieldex and mica/kaolin, respectively. b) The polarization resistances measured using linear sweep voltammetry (LSV) and the impedance values at 100 mHz measured using electrochemical impedance spectroscopy (EIS) were compared for different commercial primers (P1-P3) sorted by primer type in a black frame and blue frame, respectively. c) The same measurements were sorted by primer thickness.

4.2.3 Results Primer Thickness Variations

After identifying the influence of the primer composition and the substrate in previous tests, additional tests were conducted to evaluate the impact of the primer layer thicknesses on the performance of the samples.

4.2.3.1 Salt Spray Tests

In order to find out the influence in salt spray tests, undamaged samples with layer thicknesses of 3 µm, 6 µm and 9 µm on Z were placed in the NSST chamber. Four different primers were used, which included a model primer containing hydrophobized inhibitive pigments (HS), two commercially available thin-film primers with classical inhibitive pigments (P1 and P2), and a commercially available thick-film primer containing classical inhibitive pigments (P3). Because these primers did not contain hydrophobic pigments, they exhibited similarity to the model primers S, SM, or SK.Similar to the first part of the test program, described in section 4.2.2, the samples were largely intact after 1,000 hours NSST, even with a layer thickness of only 3 µm. In the absence of any damage to the primer surface, it appears that there is adequate protection against salt exposure for several weeks, even given this thin film thickness.

In a subsequent step, two artificial defects in the form of scribes were applied to the samples, on the left-hand side down to the zinc coating, on the right-hand side down to the steel substrate underneath. A duration of 840 hours was selected for this test in order to ensure the best possible differentiation between the samples. An overview matrix of all specimen setups after 840 h of exposure in the salt spray test is displayed in **Figure 33a**. The detached primer was removed with a blunt scalpel.

The SMART software was utilized to assess the delamination, as shown in **Figure 33b**, for both delamination starting from the scribe to the zinc coating and that starting from the scribe to the underlying steel. **Figure 33c** groups together different formulations with the same layer thickness to highlight their impact on corrosion protection. This not only facilitates differentiation among various primer combinations but also highlights distinctions between film thicknesses. As a result, a relationship was established between the thickness of the applied primer coating and its capacity to guard against delamination. This relationship indicates that a thicker coating corresponds to reduced delamination. None of the used primers demonstrated superiority over the others, and there was no correlation in the delamination outcomes between scribes down to the zinc coating and those down to the steel substrate. The increase in delamination is more significant when the primer layer thickness is increased from 3 µm to 6 µm than when it is increased from 6 µm to 9 µm. It is likely that a minimum layer thickness is required to provide stable protection against water diffusion, which is necessary for the electrochemical processes. This phenomenon can be attributed to the dimensions of the pigment particles within the coating, as well as less efficient diffusion pathways along the coating as the coating becomes much thicker than the pigment dimensions.

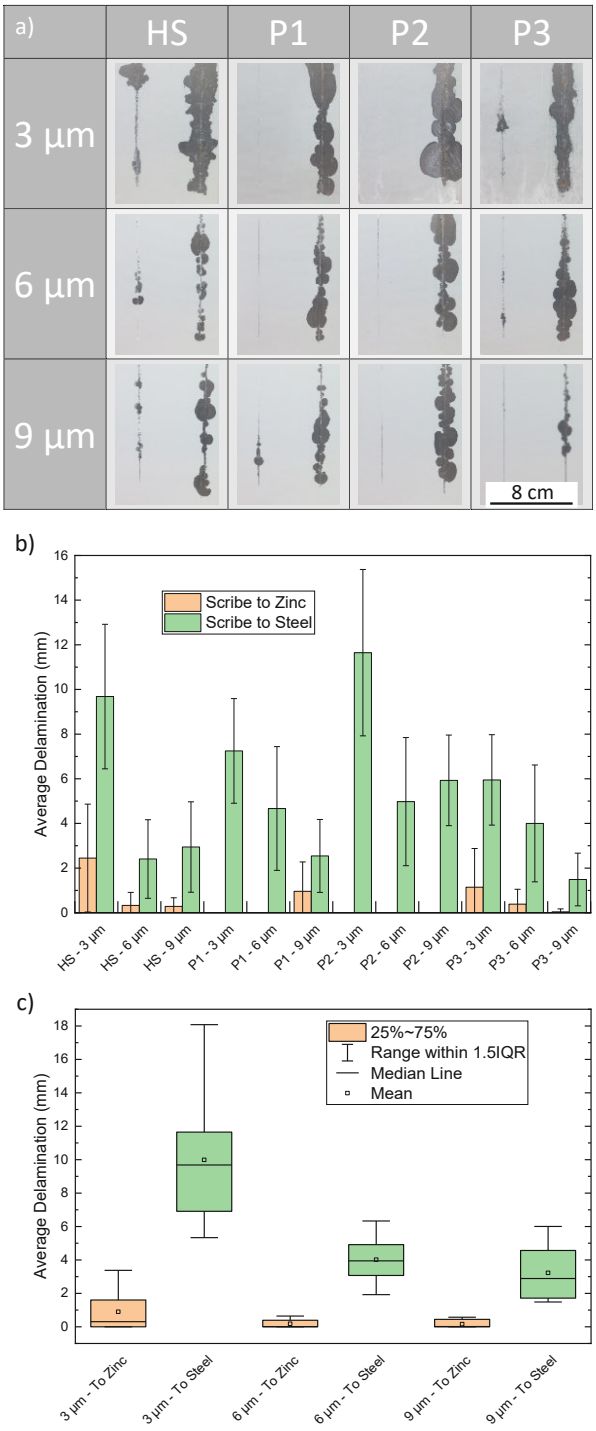

Figure 33: a) The result matrix displays the delamination of primers starting from the scribes (with the left scribe down to the zinc coating and the right scribe down to the steel substrate below) after exposure for 840 hours in the salt spray test. The primers tested were HS, a model primer, P1 and P2, commercially available thin-film primers, and P3, a commercially available thick-film primer. The primers were applied in different layer thicknesses (3, 6, and 9 µm) on hot-dip galvanized steel substrates (Z) of size 100 mm x 150 mm. b) The image evaluation software SMART was used to evaluate the delamination of the four primers with different layer thicknesses after exposure for 840 hours in a single image. c) The delamination of the four primers at different layer thicknesses was compared.

4.2.3.2 Cathodic Delamination Tests

The results of the cathodic delamination test for the same set of samples are depicted in **Figure *34***. The percentage of detached primers was determined using the software SMART. **Figure *34*a** presents the results sorted by primer and layer thickness, while in **Figure 34b** the results are sorted by layer thickness of different primers and displayed as a box plot. This type of visualization provides a clearer understanding of the range and distribution of delamination percentages for each thickness category across different primers.

In general, an increasing film thickness shows a correlation with improved protection against delamination. This observation suggests that thicker primer layers provide better resistance to detachment during the cathodic delamination test. However, it is important to note that even a primer thickness of 9 µm is insufficient to offer complete protection against delamination over extended periods of testing.

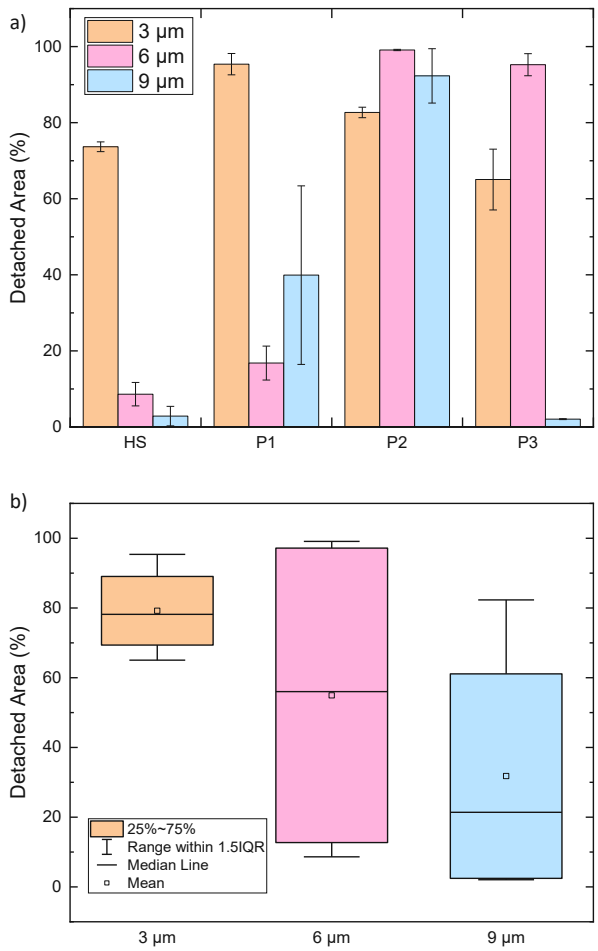

Figure 34: The percentage of detached primer from different specimen setups after cathodic delamination testing for a duration of 10 minutes is presented. The detachment of the primer was performed with adhesive tape following ISO 2409:2013. The primers used in the experiment include HS, a model primer containing hydrophobized Shieldex pigments, commercially available thin-film primers P1 and P2, and a commercially available thick-film primer, P3. Each primer was

applied with film thicknesses of 3 µm, 6 µm, and 9 µm. The data is presented in two ways: a) sorted by primer and b) sorted by film thickness.

4.2.3.3 Electrochemical Tests

To gain a more comprehensive understanding of the primer performance, additional electrochemical measurements were conducted to complement the earlier findings. These measurements involved the use of two techniques: Electrochemical Impedance Spectroscopy (EIS) and Linear Sweep Voltammetry (LSV). The purpose was to evaluate the polarization resistance of the samples, which is a key parameter to evaluate their corrosion resistance.

The EIS analysis focused on investigating the dominant influence of polarization resistance at a frequency of 100 mHz. By measuring the impedance response of the samples, the polarization resistance could be assessed, providing insights into the samples' ability to withstand corrosion. On the other hand, LSV was employed as an alternative electrochemical method to evaluate polarization resistance. This method involved analyzing the slope of the linear region of ±5 mV of the open circuit potential (OCP). By comparing the results obtained from both techniques, a comprehensive understanding of the polarization resistance behavior was obtained.

Figure 32b and **32c** present the data from both, the EIS and the LSV measurements for different primer layer thicknesses, arranged in two different manners. In **Figure 32b**, the measurement data are sorted based on the type of primer, allowing for a comparison of the polarization resistance values among different primer compositions. In **Figure 32c**, the data are organized according to layer thickness, enabling an assessment of the influence of layer thickness on polarization resistance.

The results revealed a direct relationship between the measured resistance value and the layer thickness, regardless of the technique used to determine polarization resistance. As the layer thickness increased, the measured resistance value also increased, indicating improved corrosion protection. This correlation highlights the importance of considering layer thickness as a critical factor influencing polarization resistance in the tested samples.

However, it is worth noting that significant variations were observed in the measurements of samples with the same layer thickness. This suggests that factors other than layer thickness, such as primer composition or specific formulation characteristics, may contribute to the observed variations in polarization resistance. Nonetheless, the impact of layer thickness on the measured polarization resistance appeared to be more pronounced than that of the primer composition, as demonstrated in **Figure 32**.

In summary, the electrochemical measurements performed using EIS and LSV techniques provided further insights into the corrosion resistance of the samples. The results highlighted the direct relationship between layer thickness and polarization resistance, emphasizing the importance of considering layer thickness as a crucial parameter in designing effective corrosion protection systems.

4.2.4 Conclusions

This part of the thesis aimed to comprehensively investigate the impact of various factors, including coating thickness, composition, and substrate, on the corrosion resistance of galvanically protected steel sheets coated solely with thin film primers. Through the experimental programs conducted, several key findings emerged, which contribute to the optimization of thin-film primers:

- A dry film thickness of 3 µm was found to provide complete corrosion protection for 1,000 hours in the NSST (Neutral Salt Spray Test) as long as the coating film remained intact. However, once damage had occurred, the thickness of the coatings played a significant role in determining the performance of the primers.
- Increasing the film thickness had a positive impact on performance across all tests, regardless of the primer composition, except in NSST tests without scribes. In those specific tests, a 3 µm thickness was sufficient for achieving full protection, and further increasing the film thickness did not yield additional benefits.
- The hydrophobization of Shieldex, a component used in the primer formulation, demonstrated a positive effect on the cathodic delamination test by enhancing pigment efficiency. However, it had a negative impact on protection against white rust formation. It is suspected that the hydrophobic treatment slowed down pigment leaching and ion exchange, thereby reducing the protective function in the NSST. On the other hand, the silanization process improved adhesion and provided protection against cathodic delamination.

These findings contribute to the ongoing optimization of thin-film primers. However, further research is necessary to fully comprehend their potential in practical applications. Future studies should evaluate the performance of these coatings in real-world environments, such as marine or industrial settings, while considering additional factors like UV radiation, humidity, and long-term corrosion resistance monitoring. Additionally, it is recommended to investigate the effect of hydrophobization on corrosion resistance, as it had divergent effects on cathodic delamination and protection against white rust formation.

Overall, this study demonstrates that the suggested combination of five corrosion tests effectively reveals competing effects and enables targeted engineering of thin film primers. Practitioners and researchers in the field of corrosion protection are encouraged to consider these findings when developing improved thin-film primers for diverse applications.

4.3 Evaluation of a Commercial Graphene-Additive for Boosting the Corrosion Performance of a Thermal Curing Primer

The results shown in this section were in large part published in [5]. The publication is available at https://onlinelibrary.wiley.com/doi/full/10.1002/maco.202313914. The copyright agreement is attached in **Appendix 8**.

4.3.1 Objective of the Study and Implementation

The unique planar structure and low permeability of graphene make it an attractive additive for enhancing the corrosion resistance of organic coatings. While several publications have reported positive outcomes attributed to its barrier properties, detailed investigations of incorporating commercial-grade graphene into coatings have been limited due to its restricted availability, hindering widespread utilization. This part of the thesis addresses this gap by comprehensively evaluating the impact of the addition of a commercially available graphene additive on the performance of a commercial primer. Industry-standard corrosion tests and advanced characterization techniques were employed to assess the coating's behavior.

4.3.2 Results and Discussion

4.3.2.1 Rheology preliminary tests

As graphene particles were supplied suspended in xylene by AGM, the direct addition of the suspension to the primer base was deemed to be the most suitable method to incorporate the nanoparticles to the existing primer base. However, to determine the concentration of xylene required to achieve the desired flow behavior, viscosity measurements were conducted using a rheometer. Dilutions of 0, 5, 10, 15, and 20 wt.% xylene were used, and a technical primer sample from a plant was used as a reference. The viscosity was measured while varying the shear rate.

The results showed that the addition of xylene to the primer base decreased the viscosity of the primer, and the viscosity decreased with increasing shear rate. Based on the results of the rheology tests, it was decided to use an addition of 20 wt.% of xylene for the addition of graphene particles to the primer base to achieve the desired concentration of 0.1 wt.% graphene.

It is worth noting that although the flowing behavior of the primer at this concentration is not optimal, it was considered as the best option to achieve the desired graphene concentration. **Figure 35** shows the measured viscosity at varying shear rates for the addition of different xylene-graphene suspension concentrations and the viscosity of the reference sample from the plant.

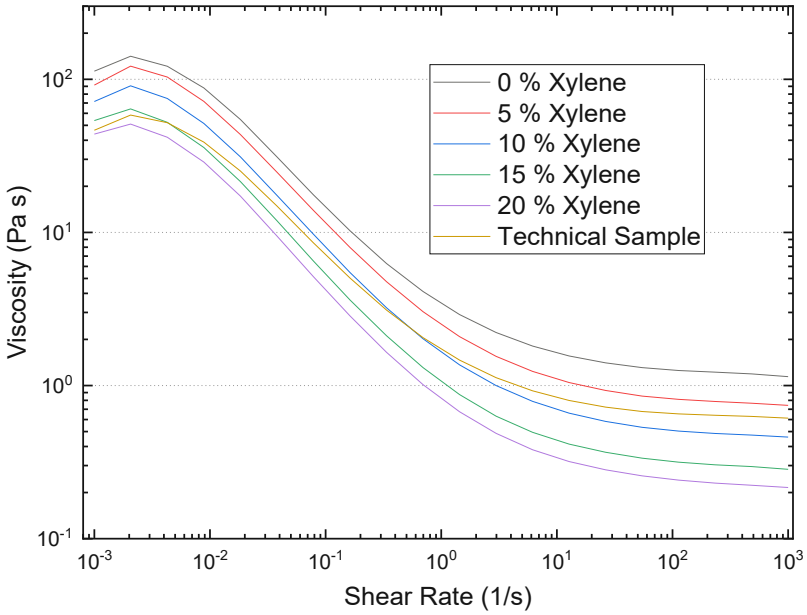

Figure 35: Viscosity measured at varying shear rate for the addition of different xylene-graphene suspension concentrations.

4.3.2.2 Characterization

According to the SDS, the graphene particles possessed a particle size distribution with a D50 value of 5-6 µm and a D90 value of 6-28 µm. Both, the primer samples with and without graphene nanoparticles, exhibited a comparable microstructure and a similar distribution as observed in crosscut SEM images. Therefore, the incorporation of graphene did not have an impact on the orientation or distribution of the primer constituents. **Figure 36a** and **Figure 36b** depict crosscut images of the primer applied on Z substrates. The higher quantity of pigments visible in **Figure 36a** is a coincidence.

Furthermore, the graphene particles obtained from the graphene-xylene suspension were characterized. **Figure 37** depicts a joint FTIR and Raman spectrum. FTIR spectroscopy was utilized to investigate the modification of the graphene particles and identify the presence of graphene oxide (GO). One of the indicators for the presence of GO is the peak observed at 3000 cm^{-1}, representing hydroxyl groups. Other supporting evidence for the existence of GO includes the bands at 1055 cm^{-1} and 1150 cm^{-1}, which correspond to C-O stretching vibrations of alkoxy and epoxy groups, as well as the bands at 1370 cm^{-1} (stretching of tertiary C-OH groups) and 1730 cm^{-1} (C=OH stretching of COOH groups). Furthermore, two more bands are

visible in the FTIR spectrum: one at 1220 cm^{-1} due to C=C skeletal vibration and the other at 1640 cm^{-1} owing to a stretch of C=C groups [93, 94].

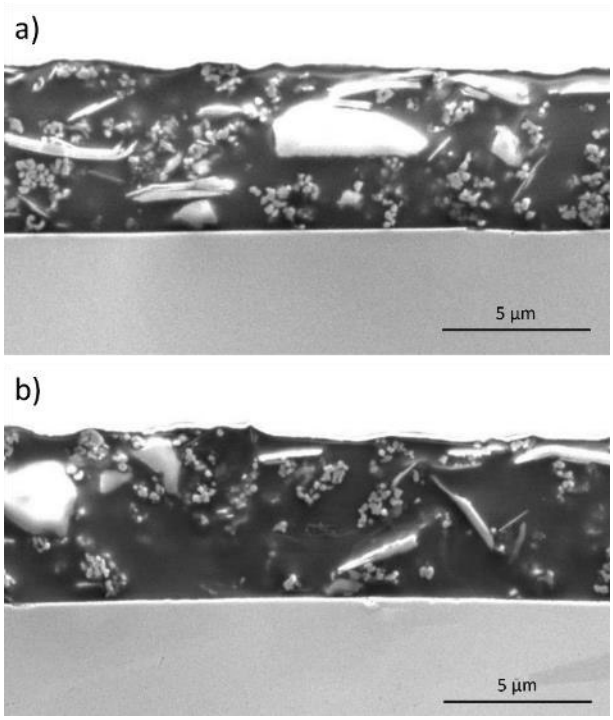

Figure 36: a) The CSP cross-section of a primer to which xylene has been added, and b) the CSP cross-section of a primer to which both xylene and graphene nanoparticles have been added, were analyzed. The dry-film coating thickness was consistently around 6 µm on average.

Figure 37 also displays the Raman spectrum of the graphene particles. The D band was observed at 1360 cm^{-1}, the G band at 1560 cm^{-1}, the D' band at 1580 cm^{-1}, and the 2D band at 2840 cm^{-1} in the spectrum. The G band appears due to the first-order dispersion of the E2g mode, while the D band arises from defects in the material, such as bond-angle disorder, bond-length disorder, vacancies, and edge defects. The 2D band is employed to evaluate the structural parameters of the orientation of the c-axis. Both, graphene and graphite exhibit G and 2D peaks, however, the 2D peak in graphene is sharp and intense, whereas in graphite, it is broad, less intense, and it splits. Therefore, it can be deduced that graphite was present in the suspension, in addition to graphene oxide [95, 96].

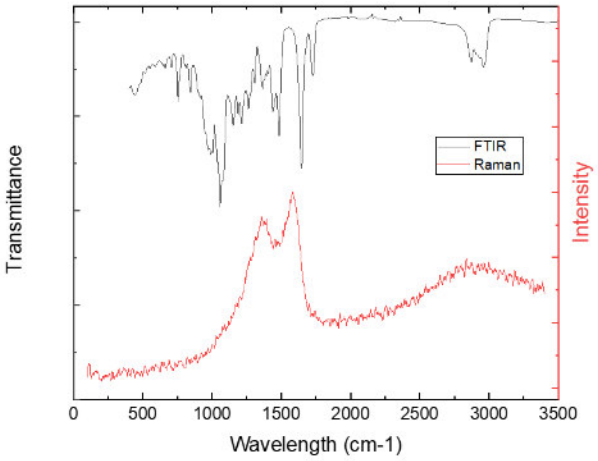

Figure 37: A combined FTIR and Raman spectrum of the graphene nanoplatelets.

Additionally, color measurements were conducted on primer samples with and without graphene nanoparticles. The CIELAB color space, which characterizes colors based on their lightness (L*), red-greenness (a*), and yellow-blueness (b*), was used to evaluate the results. The findings proved that the addition of graphene nanoparticles significantly impacted the color of the primer. Specifically, the L* value decreased, indicating that the color became darker, and the a* and b* values increased, suggesting that the primer's green and blue hues became more red and yellow, respectively. These changes were quantified by calculating the color difference (ΔE) between the samples with and without graphene particles. **Table 32** summarizes the average L*, a*, b*, and ΔE values obtained from the samples. **Figure 45** visually represents the color changes by displaying images of the primer samples with and without graphene nanoparticles, showcasing the effects of graphene on the primer's appearance. Higher concentrations of graphene would result in even more pronounced effects, thereby restricting its suitability for industrial applications.

Table 32: Measured values in the cielab color space and the dE value calculated from them.

	L*	a*	b*
Without Graphene	75,02	-2,78	-2,41
With Graphene	58,23	-1,04	-0,95
ΔE		16,95	

4.3.2.3 Physical/Mechanical Tests

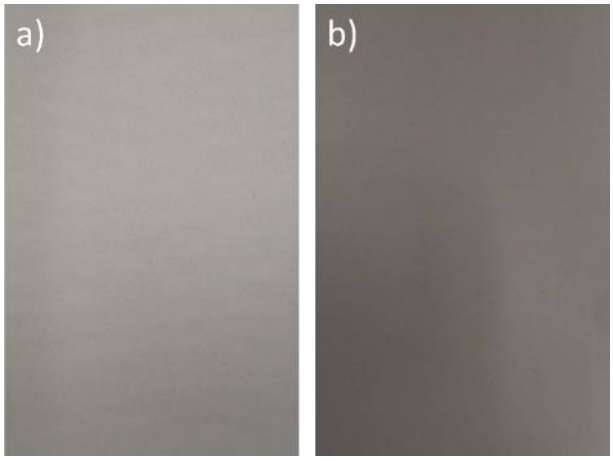

Figure 38: Coated samples a) primer without graphene b) primer with graphene.

Incorporation of graphene particles into the primer resulted in a decline in the pull-off adhesion as evidenced in **Figure 39a**. This decrease may be attributed to the presence of graphene particles at the interface which permits only non-chemical bonds or van der Waals forces to form. Besides, the high surface energy of graphene particles and their propensity to agglomerate often lead to poor adhesion and a rough surface finish.

In addition, the inclusion of graphene particles in the primer led to an increase in the maximum coefficient of friction, as demonstrated in **Figure 39b**. Graphene is known for its superior lubrication properties, and its incorporation into a primer can result in a reduction in surface friction, making it smoother and less susceptible to damage. However, if the graphene pigments agglomerate, it can result in uneven dispersion and coverage, leading to variations in the concentration of graphene and negatively affecting the performance of the coating. Agglomeration may also result in an irregular or rough coating surface, which can cause an increase in the coefficient of friction.

The coefficient of friction can also be influenced by the orientation and distribution of graphene nanoparticles in the primer matrix. Graphene is a highly anisotropic material, meaning its characteristics can differ significantly based on the orientation of the flakes. Thus, the observed increase in the coefficient of friction upon addition of graphene pigments to the primer can be attributed to both agglomeration and the anisotropic nature of graphene. The choice of polymer and its interaction with graphene may also play a significant role, since while the majority of research has reported a reduction in the coefficient of friction, some publications have reported an increase [97, 98].

The surface tension of the coated samples was assessed by analyzing the contact angle of two different liquids, water and formamide, on primers with and without graphene nanoparticles. Contact angle values were utilized to determine surface energies, the results are shown in **Table *33***. The surface tension values were similar, but the primer with graphene particles exhibited a marginally higher percentage of disperse energy. This increase may be attributed to changes in the surface energy of the primer caused by altering the interactions between the primer and the test liquids. It is worth noting that the addition of graphene particles to the primer was only 0.1%, which may explain why the influence on surface tension was minimal. The measured contact angle values and the calculated surface energies obtained using them are shown in **Figure 39c**.

Table 33: Measured contact angles for primers with (+G) and without (-G) graphene nanoplatelets.

	Contact angle – water / °	**Contact angle – formamide / °**
-G	81,4 ± 0,9	66,1 ± 0,6
+G	83,1 ± 0,6	66,0 ± 1,0

According to TMA measurements, the addition of graphene nanoparticles did not have any significant effect on the glass transition temperature (Tg) of the primer system. Both systems exhibited a Tg value of 68±1 °C. The Tg is a crucial parameter in coating technology and polymer processing, and it can be influenced by various factors such as the molecular weight of the polymer chains, spatial structure, and the addition of additives [99, 100]. This finding is important for potential applications of the primer system, as it suggests that although graphene has been reported to increase the Tg, this may not be the case at such low concentrations. Additionally, poor dispersion of graphene in the primer system may also hinder its ability to interact with the polymer matrix and modify its properties.

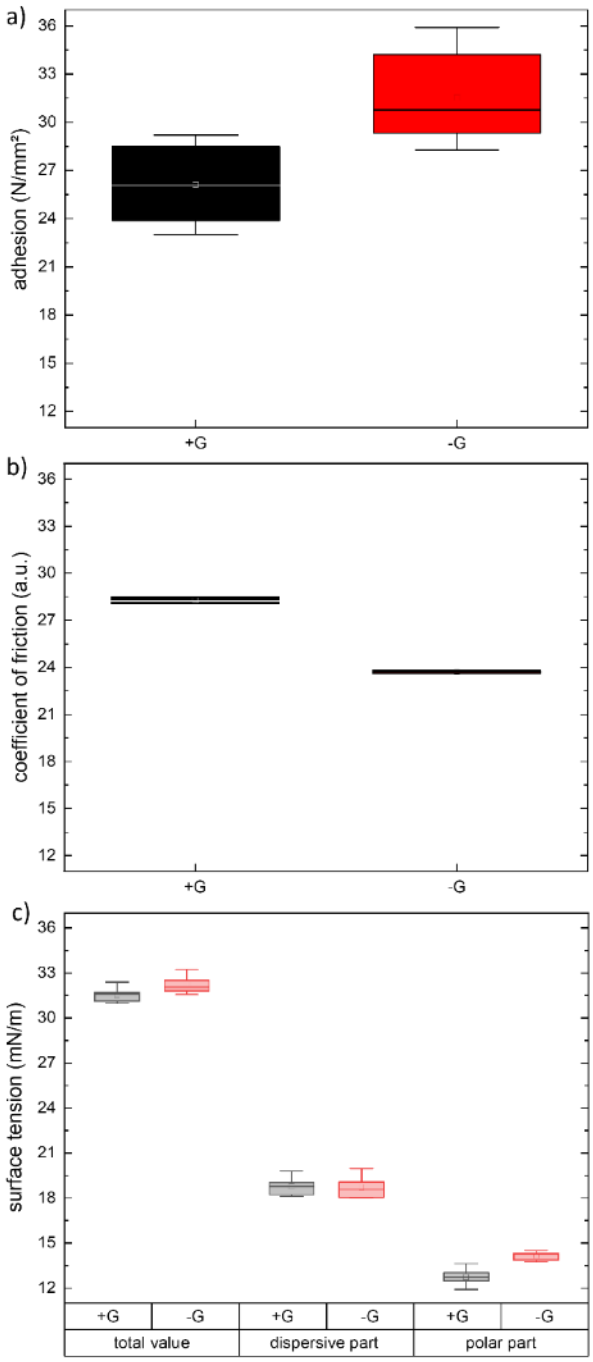

Figure 39: a) adhesion, determined by means of pull-off tests b) the maximum measured coefficient of friction, measured with a tribometer c) surface energies, calculated from contact angle measurements with formamide and water. All measurements were conducted for primed samples with (+G) and without (-G) graphene.

4.3.2.4 Salt Spray Tests

Salt spray tests were performed to evaluate the long-term corrosion resistance of undamaged primer samples with and without graphene particles for 3,000 hours. Images of the samples were captured periodically to evaluate the surface conditions as displayed in **Figure 40a**. Even after 1,500 hours, no visible changes were observed on the sample surface. However, corrosion phenomena gradually migrated from the taped edges towards the center of the specimen center.

After 3,000 hours, all samples exhibited a considerable amount of corrosion products on the surface, which had moved there from the edges. Although the addition of graphene particles could potentially improve the barrier protection, the protective effect of the coating without graphene was already sufficient to withstand the entire test period. Therefore, this test could not be used to confirm the influence of graphene platelets on the barrier properties, as suggested in the literature [35, 101].

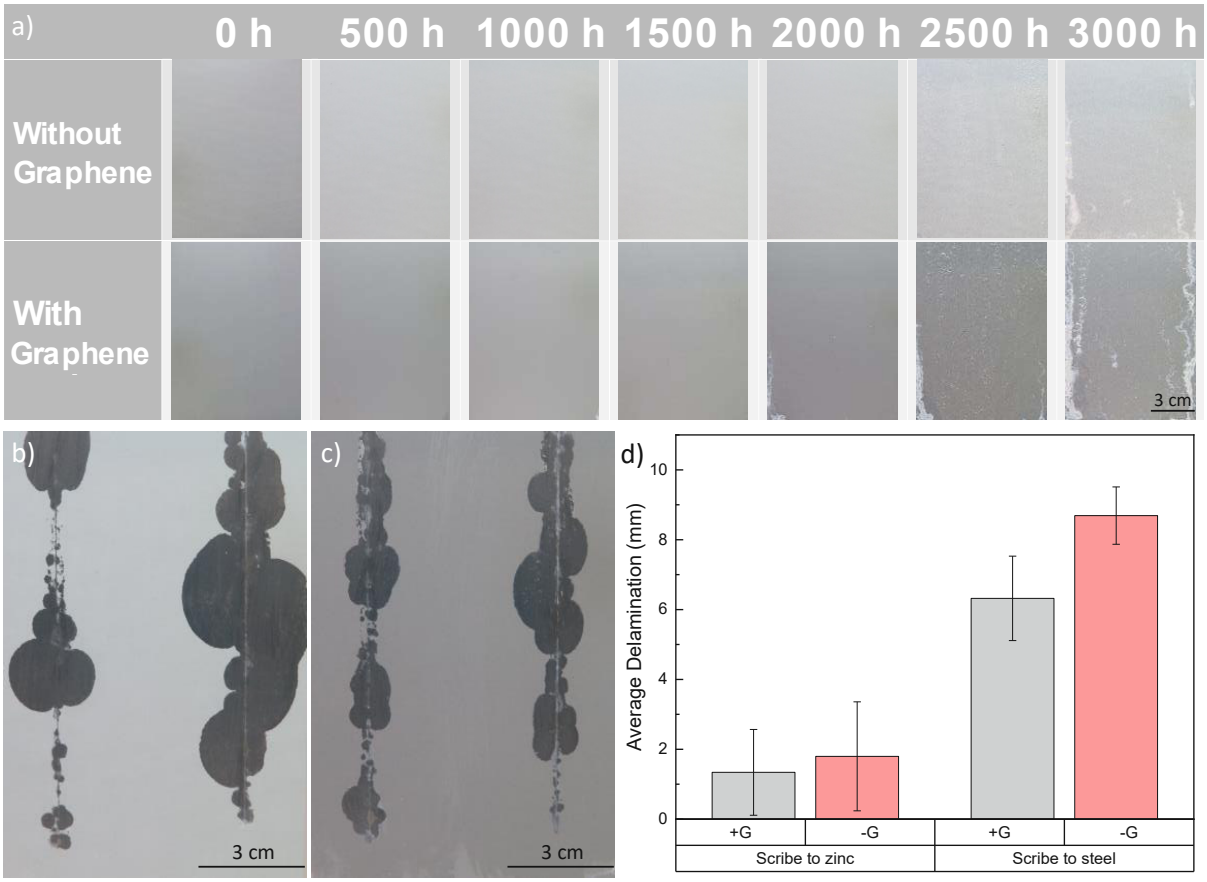

Figure 40: a) Comparison of the conditions of the primer samples without scribes with and without graphene in the salt spray chamber over the course of 3,000 h. b) Image of a sample without graphene with a scribe to the zinc coating on the left and on the right down to the steel substrate below after 1,000 h in the salt spray chamber. c) Image of a primer with graphene nanoparticles. The delaminated primer was removed using a blunt scalpel. d) The evaluation of delamination using the commercial software SMART is presented.

In addition to the specimens with intact surfaces, protection against anodic delamination was tested by using specimens in the NSST that had been scribed twice, on the left-hand side down to the zinc coating, on the right-hand side down to the steel substrate below. After undergoing 1,000 hours of exposure to the salt spray, the samples were examined and analyzed using the SMART image analysis software. **Figure 40b** and **Figure 40c** depict typical images of the samples after the delaminated primer had been removed, while the SMART software evaluation of the delamination is presented in **Figure 40d**. The primer samples that contained graphene

particles showed a decrease in delamination in both the scribes down to the zinc coating and the scribes down to the underlying steel substrate. One explanation for this is the high potential of the graphene particles, which shifts the potential of the entire system to a more noble region. Additionally, the enhanced barrier protection of the coating reduces the diffusion of oxygen and other ions through it to the interface, thereby inhibiting redox reactions. Consequently, the delamination reactions are reduced [35, 102].

4.3.2.5 Blistering Tests

A homemade blister testing apparatus was used to evaluate samples coated with primer and topcoat, and the samples were monitored for 14 weeks. During the first 7 weeks, no changes were observable on any of the samples, whether graphene was present in the primer or not. However, during the 8th week, small bubbles emerged on the primer-coated samples containing graphene, while the primer-only samples without graphene continued to exhibit no changes. The number and size of blisters on the graphene-containing samples increased progressively and reached a plateau at week 12, after which no significant changes were observed. The experiment was concluded after 14 weeks, at which point the surfaces of the non-graphene primer samples had still remained entirely intact. The evaluation of bubble formation according to **Table 5** is shown in **Figure 41b**. The findings indicate a noticeable decrease in blistering resistance, which may be due to several factors, such as oxygen reduction on graphene or accelerated diffusion pathways. The test involved exposing the coating system to high humidity conditions, which can cause moisture to infiltrate the coating layers, creating blisters and bubbles. Given that the adhesion of the graphene-containing primer is weaker than that of its non-graphene counterpart, moisture infiltration may have been more pronounced, resulting in more severe blistering. The findings differ from the salt spray test outcomes due to variations in the delamination processes. This highlights the importance of using different tests to determine the overall performance of graphene coatings.

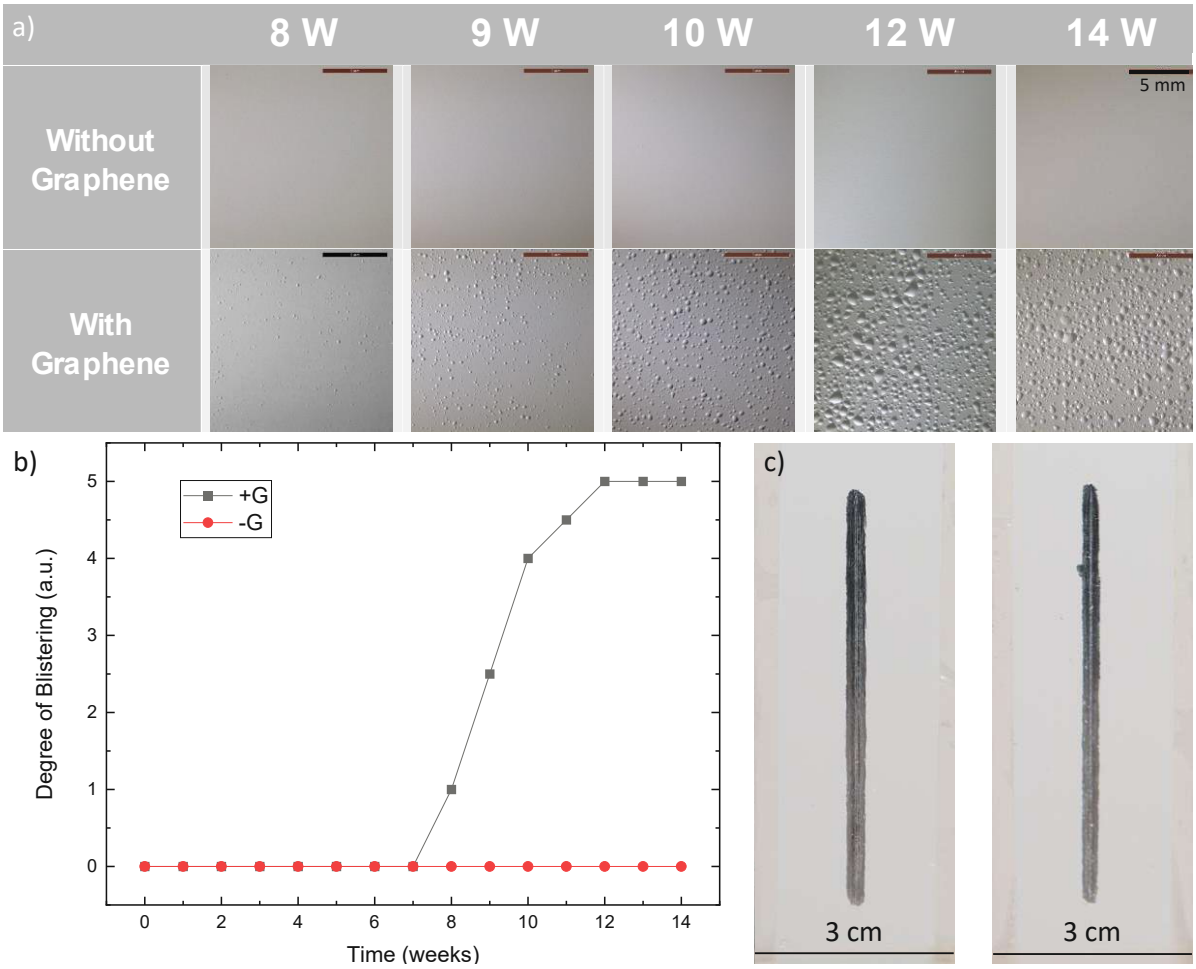

Figure 41: a) The surface of the samples in the blister tester was monitored for several weeks, and blisters began to appear on the graphene-containing samples at week 8. b) The formation of blisters was evaluated according to **Table 5** for 14 weeks, and samples with graphene in the primer (G+) and without graphene (G-) were tested, both of which had a topcoat. c) The samples with primer and topcoat underwent a 30-minute cathodic delamination test. One sample had graphene nanoparticles in the primer (on the left-hand side), while the other did not contain graphene (on the right-hand side). The test was performed in a 0.5 M KOH solution at 36°C with a current of 0.5 A.

4.3.2.6 Cathodic Delamination Tests

During the cathodic delamination tests, samples coated with both, primer and topcoat were assessed. The inclusion of graphene particles in some primer samples did not yield any enhancement in contrast to those lacking graphene. On the contrary, a slight rise in cathodic delamination was observed, suggesting that the introduction of particles did not have a favorable effect on sample performance. Nonetheless, this change was of negligible magnitude. **Figure 41c** illustrates the average cathodic delamination. Subsequent analysis of delamination using the SMART image analysis software produced the following outcomes: 1.08±0.06 mm delamination for primer samples with graphene and 0.98±0.06 mm delamination for primer samples without graphene.

4.3.2.7 Electrochemical Tests

Electrochemical measurements were executed following the guidelines outlined in section 3.6. The incorporation of graphene into the coatings resulted in a shift of the open circuit potential (OCP) towards more positive levels, signifying improved corrosion protection [103]. For primer samples containing graphene, impedance measurements displayed slightly elevated |Z| values, indicating fortified barrier protection. Nevertheless, all recorded |Z| values remained under 10^6 Ohm cm², indicating insufficient barrier protection [104]. The phase angles of all samples showed a similar progression, but the primer samples containing graphene exhibited a leftward shift, resulting in slightly better performance. The breakthrough frequency, which is the frequency at which capacitive behavior transitions to ohmic behavior (phase angle = 45 °), occurred at lower frequencies in samples containing graphene. A breakpoint frequency exceeding 10 Hz indicates the failure of a protective function in an organic coating [105]. Nevertheless, it is important to note that this threshold serves only as a general rule of thumb, as it may vary depending on the specific characteristics of the coating system. The averaged measured Bode plots of primer samples with and without graphene in **Figure 42** showed slightly better performance in electrochemical tests for graphene-containing samples. The fluctuations at the beginning of the impedance measurements were due to water absorption, and the values stabilized later. These results agree with those of the salt spray test with a scribe, in which slightly better barrier properties were observed in coatings containing graphene. However, it should be noted that the threshold for the breakdown of a coating's protective function varies depending on the coating system.

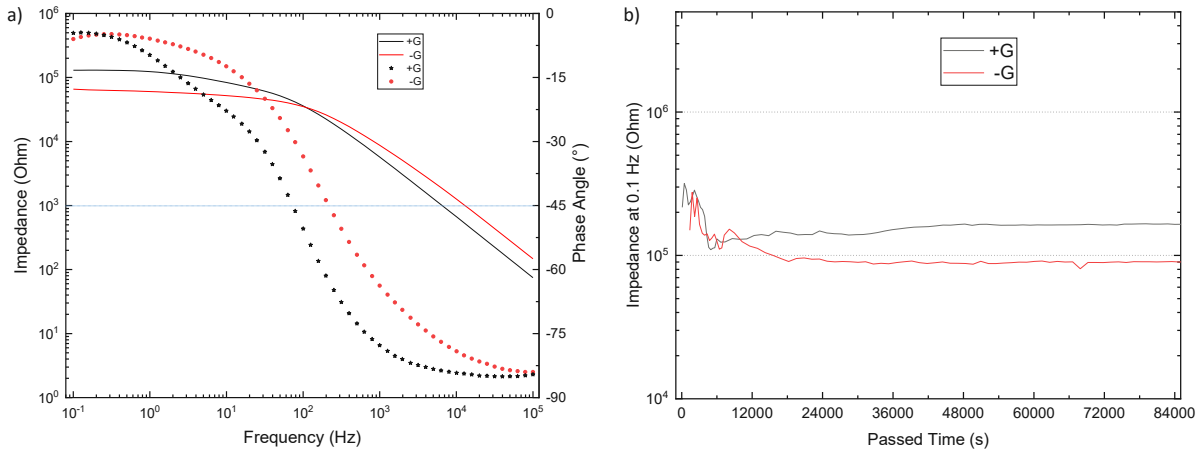

Figure 42: a) EIS measurements were conducted on primer samples with (+G) and without (-G) graphene pigments after 24 h in a 1 M NaCl solution, over a frequency range of 10^{-1}-10^5 Hz, and were plotted on Bode diagrams. The impedance values were represented by lines, while the phase angle was denoted by dots. b) The EIS measurements were conducted for 24 hours, and the magnitude of impedance at 0.1 Hz was monitored over time.

4.3.2.8 Water Uptake

Two methods were used to investigate the impact of graphene addition on the water sorption behavior of the coating: sorption balance measurements and analysis of electrochemical impedance spectroscopy (EIS) data using the Brasher-Kingsbury equation. **Figure 43** presents the results obtained from both methods. The outcomes indicate that the incorporation of graphene pigment has only a minimal effect on the water vapor sorption behavior of the coating, which is mainly influenced by the ion exchange pigments in the coating. The water absorption variation resulting from the addition of graphene was less than 0.2 percentage points in the sorption balance measurements, suggesting that the water sorption behavior of the coating is not significantly altered by the graphene pigment. However, caution is required when interpreting the results since the Brasher-Kingsbury equation is based on various assumptions, including low water content in the coating and a uniform distribution of it throughout the whole coating. While the first assumption limits the validity of the equation to the initial stages of absorption, the second assumption is seldom met during transient mass transfer processes [106]. These findings suggest that coating systems containing graphene could be utilized in moisture-sensitive applications without compromising their water sorption properties. Further research could explore the coating's other properties to assess its suitability for practical applications.

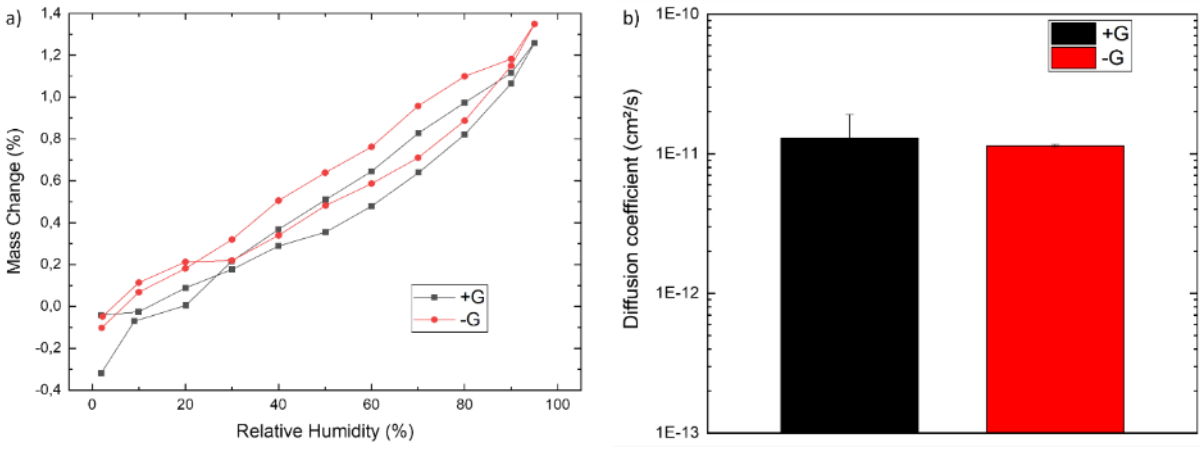

Figure 43: a) Change in the mass of primers with (+G) and without (-G) graphene pigments with changes in relative humidity. The measurements were carried out using a sorption balance at a constant temperature of 30 °C. The relative humidity was increased in increments of 10% from 0 to 100% and then stepwise decreased back to 0%. b) Diffusion coefficients calculated from EIS measurements using the Brasher-Kingsbury equation.

4.3.3 Conclusions

The aim of this part of the thesis was to investigate whether the addition of graphene nanoparticles to a commercial primer base could enhance its anti-corrosion properties without affecting the overall performance of the coating. Both, the graphene suspension and the primer,

are commercially available, and they were tested as additives at a concentration of 0.1 w%. The graphene particles were extensively characterized using Raman and FTIR, which revealed the presence of both graphene oxide and graphite. The results of industrial tests were mixed, with some indicating only minor improvements in performance, while others showed significant decreases, as summarized in **Table 34**. A particular decrease was detected in blistering resistance, which could be due to oxygen reduction on graphene or accelerated diffusion pathways. Additionally, the presence of graphene at the surface was found to lower adhesion, likely due to weaker binding of the coatings to the base material, as graphene cannot bond specifically or via any acid/base mechanism. However, the addition of graphene did improve NSST performance, possibly due to an increased barrier effect or electrochemical modification of the surface. The inconsistent results from the tests indicate that further research and optimization are necessary before considering graphene as a viable additive for industrial corrosion-resistant coatings. For instance, reducing interfacial graphene adsorption could improve performance for all test protocols. Furthermore, the limited beneficial properties of graphene and its cost suggest that its incorporation into commercial coatings may not be justified at this time.

Table 34: Overview table summarizing the influences of Graphene on the individual tests.

Analysis	Effect of the addition of graphene on the primer
Color change	Darker surface
Adhesion	Decrease
Surface tension	Almost the same
Coefficient of friction	Increase
Glass transition temperature	Stayed the same
Blistering test	Decreased performance
Cathodic delamination test	A slight decrease in performance
Impedance measurement	Slight improvement in performance
NSST without scribes	Almost the same
NSST with scribes	Slight improvement in performance

4.4 The Influence of Pigment Milling Time and Primer Layer Thickness on Anti-Corrosion Coatings for Galvanized Steel Strip Samples

4.4.1 Objective of the Study and Implementation

Organic coatings containing anti-corrosion pigments are widely used to protect substrates against corrosion. Nevertheless, the impact of varying the milling time of these pigments remains poorly understood. To address this knowledge gap, the effect of milling time variation (100%, 75%, 50%, and 25%) of an ion-exchanged silica pigment commonly utilized in a commercially available primer system on Z samples as substrates was investigated. Additionally, the influence of primer layer thickness on the performance of coatings was examined. Samples of all four grinding times were prepared with three different layer thicknesses: 3 µm, 6 µm and 9 µm.

This investigation provided valuable insights into optimizing anti-corrosion coatings for hot dip galvanized steel strip samples, with the potential for practical implications in industries such as automotive and construction.

4.4.2 Results and Discussion

4.4.2.1 Characterization

The particle size distribution analysis of the gained anti-corrosion pigments was conducted for all grinding times using laser diffraction analysis. The obtained results indicate that the median particle size did not significantly change, even when the milling time was reduced by 75%. However, the number of particles larger than 10 µm changed with varying grinding times. A longer grinding time led to a decrease in the number of oversized particles, as confirmed by grindometer testing. Furthermore, an increase in grinding time resulted in a reduction of the average maximum particle size.

Several possible explanations exist for why an increased milling time resulted in a decrease in the number of oversized particles without affecting the median particle size. One possibility lies within the physical properties of the pigment, as calcium-exchanged silica is a hard and abrasive material, which can cause bigger particles to break or fracture during grinding. This could reduce the number of oversized particles but may not necessarily affect the median particle size. Another explanation is that the particle size distribution of the calcium-exchanged silica pigments is relatively narrow, meaning that most particles are already close to the desired average size before grinding. Therefore, increasing the grinding time may not significantly affect the average particle size but can still reduce the number of oversized particles. It is

essential to note that other factors such as the properties of the primer and other components in the formulation could also impact the final particle size distribution of the pigment in the paint system. Therefore, any changes in these components could potentially impact the milling process and the resulting particle size distribution.

To visualize the particle size distribution, **Figure 44a** shows the probability density function of particle sizes for different milling times using laser diffraction analysis, while **Figure 44b** shows the average maximum particle size as determined using a grindometer.

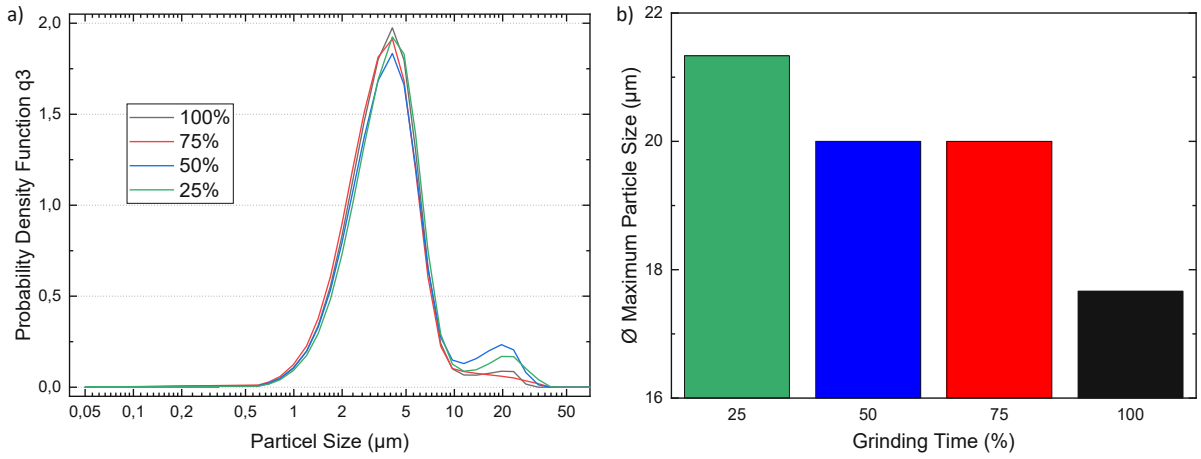

Figure 44: a) Probability density function of the particle sizes at different grinding times determined using laser diffraction analysis. b) Determined maximum particle sizes at different grinding times using a grindometer.

Cross-sectional images of the coated Z275 samples were obtained to visually assess the distribution of the primer components. **Figure 45** shows images of samples from all grinding durations with a layer thickness of approximately 9 µm. No differences were found between samples with different grinding times. A reason for that might be that the coating process could have caused the oversized particles to break down or disperse more evenly throughout the coating layer. Moreover, the oversized particles may have been present in the coating layer but were not visible in the SEM images due to their distribution or orientation. SEM images are limited by their two-dimensional nature, and particles that are oriented perpendicular to the surface or that are buried within the coating layer may not be visible.

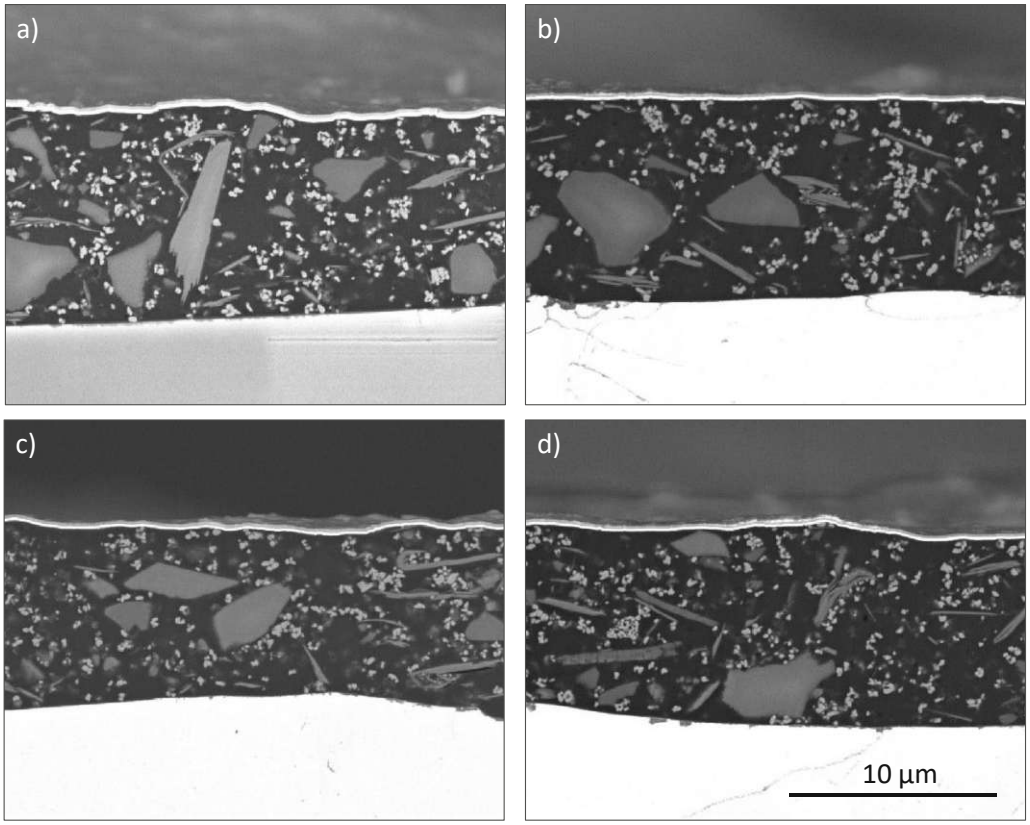

Figure 45: SEM images of the cross sections of primer samples with different milling times of the anti-corrosion pigments. a) 100% grinding time, b) 75% grinding time, c) 50% grinding time, and d) 25% grinding time.

4.4.2.2 *Samples in Salt Spray Test*

Salt spray tests were conducted with scribed and unscribed samples. The surfaces of all samples without a scribe, even those with a layer thickness of only 3 µm, were still intact after 1,000 h in the salt spray chamber. After 1,500 h, all samples with a layer thickness of 3 µm began to show signs of white rust, regardless of the milling time of the contained anti-corrosion pigments, which increased further over the course of an additional 500 h. At 2,000 hours, corrosion began to migrate from the taped edges to the exposed surface on all samples, leading to the termination of the test. Samples with layer thicknesses of 6 µm and 9 µm showed intact surfaces up to this point. **Figure 46a** shows the result matrix of the samples with a milling time of 100% over the course of 2,000 h. The study found no differences between samples with the same layer thickness but different milling times. However, 3 µm thick samples performed worse than those with higher thicknesses.

In the case of the surfaces of the scribed samples, no clear differences were recognizable with different milling times of the anti-corrosion pigments, but there were discernible differences with variations in the layer thickness. The thicker the coating, the lower the delamination. This observation was further confirmed by determining the delaminated area using the SMART software. **Figure 46b** shows the primer samples after 1,000 h of neutral salt spray testing after

the delaminated primer was carefully removed with a blunt scalpel. **Figure 46c** shows the evaluation of the average delamination of all the samples using the evaluation software SMART.

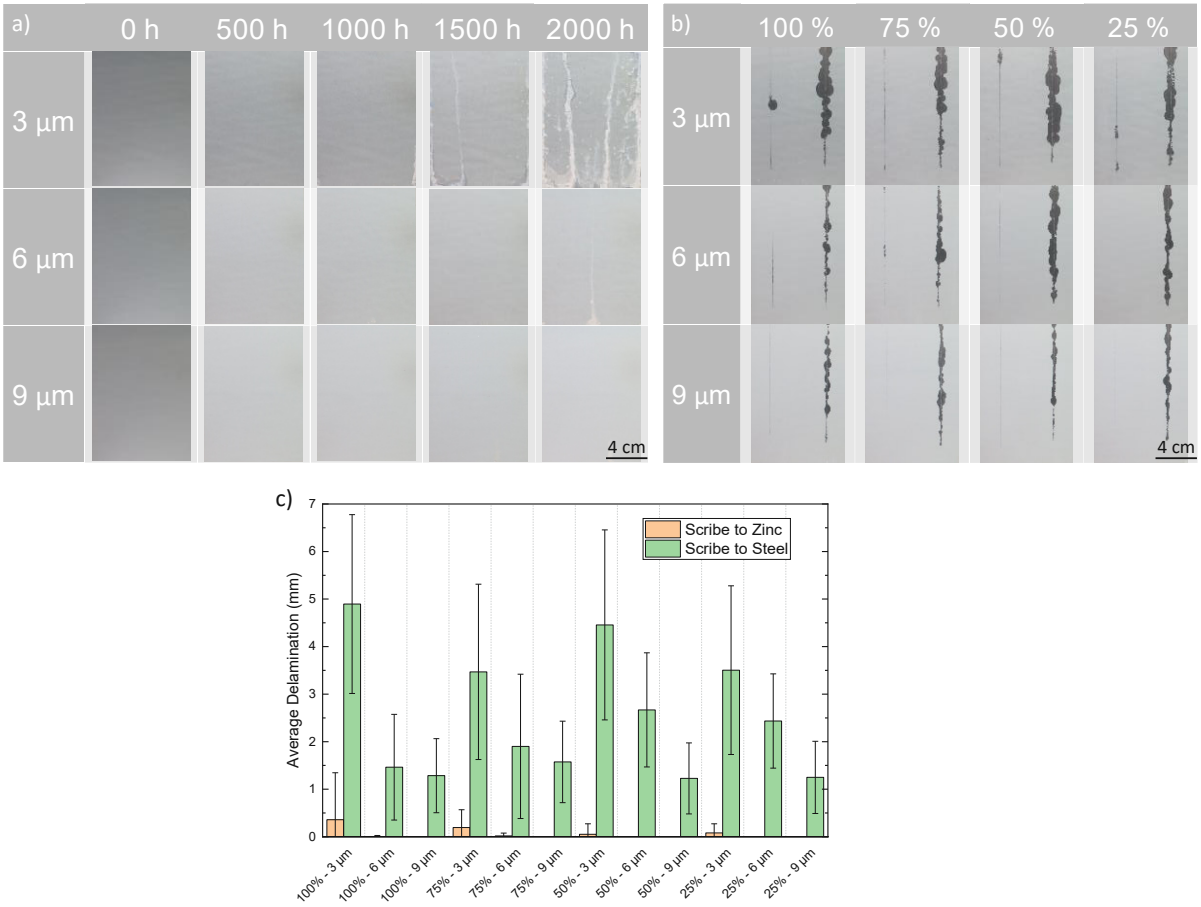

Figure 46: a) Sample matrix of primer samples of primers with a grinding time of 100% without scribes over the course of 2,000 h in the salt spray chamber. b) Sample matrix of the primer samples with scribes after 1,000 h in the salt spray chamber with different degrees of grinding (25-100%) and different layer thicknesses (3-9 µm). The scribe on the left is down to the zinc coating, and that on the right is down to the underlying steel substrate. c) Evaluation of the average delamination using the SMART software.

The findings of this experiments are consistent with previous research, which suggests that a thicker coating layer is generally more effective in providing protection against corrosion [107]. This is because a thicker coating layer can decrease the rate of penetration of corrosive agents and oxygen through the coating, thereby decreasing their concentration at the interface between the substrate and the coating layer. As a result, the corrosion rate slows down. In the presence of a scribe, a thicker coating layer can further decrease the likelihood of corrosion occurring at the scratch site by decreasing the rate of penetration of corrosive agents and oxygen. If corrosion does initiate at the scratch site, a thicker coating layer can limit its spread by confining it to the immediate vicinity of the scratch site. In summary, a thicker coating layer can effectively reduce

the occurrence and severity of delamination in a salt spray test by decreasing the corrosion rate and confining it to the scratch site.

4.4.2.3 *Blistering Tests*

Samples with primer and top coat were exposed to a blister tester for 20 weeks. Upon weekly examination, the surfaces of the samples remained intact under a light microscope for the first 9 weeks. However, blister formation began to occur slowly thereafter. The longer the grinding time, the longer it took for the first bubbles to appear, and the subsequent propagation and enlargement kinetics were decelerated. In **Figure 47a**, images taken with a light microscope at 16x magnification after 10-20 weeks in the blister tester show the sample surfaces. **Figure 47b** displays a plot of bubble size and count against time after being converted to numerical values according to **Table 5**. The results indicate that samples with a grinding time of 50% and 25% exhibited significantly poorer performance compared to those with 75% and 100% grinding time, which showed only a minimal difference.

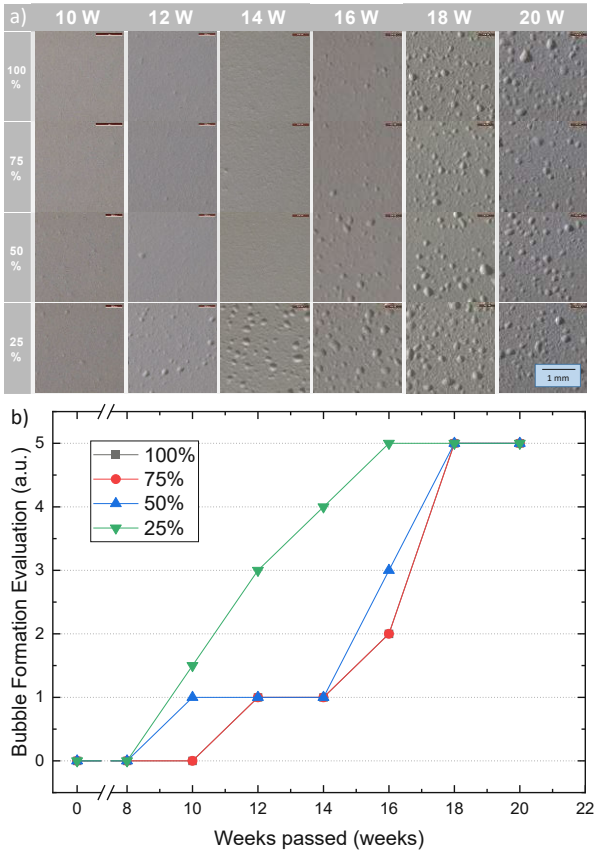

Figure 47: a) Development of blisters from weeks 10 to 20 in the blistering test for grinding times of 25-100%. b) Bubble size and bubble count on the sample surfaces were converted to numerical values according to **Table 5** and plotted against the weeks passed.

The observed results may be attributed to the reduction of the number of oversized particles and a more uniform dispersion in the primer resulting from a longer grinding time. This

contributes to the formation of a compact and homogeneous primer layer with fewer defects and pores, thereby offering superior protection against corrosive agents. A shorter grinding time, on the other hand, can result in a higher number of oversize particles remaining in the primer, which may result in voids and weak spots that allow corrosive agents to penetrate more easily, leading to blister formation.

Furthermore, the oversized particles in the primer layer may impede the adhesion of the topcoat, creating bumps or roughness on the surface, thereby weakening the bond between the topcoat and the primer. This may eventually cause premature failure of the coating system.

4.4.2.4 *Cathodic Delamination Tests*

For this test, samples coated with only primer as well as samples coated with primer and top coat were used. Samples coated with only primer performed similarly well at the same coating thickness, regardless of the grinding time of the contained anti-corrosion pigments. For samples that were additionally coated with a top coat, it was found that the grinding time had a strong influence on the performance in the test. Similar to the blistering test, a longer milling time correlated with less pronounced delamination starting from the scribe. The delamination itself increased steadily with increasing testing duration. The results indicate that the grinding time of the anti-corrosion pigments used in the coating of the hot-dip galvanized steel samples only has a strong influence on the performance in the cathodic delamination test when a top coat is used. It appears that the effectiveness of the top coat is influenced by the quality of the underlying primer, as oversized particles in the primer layer may impede the adhesion of the topcoat, creating bumps or roughness on the surface, thereby weakening the bond between the topcoat and the primer. This may eventually cause premature failure of the coating system. **Figure 48a** shows surfaces of samples coated with primer and topcoat after 30 min cathodic delamination test at 0.5 A in a 0.5 M KOH solution at 36 °C. **Figure 48b** shows the evaluation of the average delamination at different degrees of grinding and test durations using the SMART image analysis software, confirming the correlation between longer grinding time and reduced delamination.

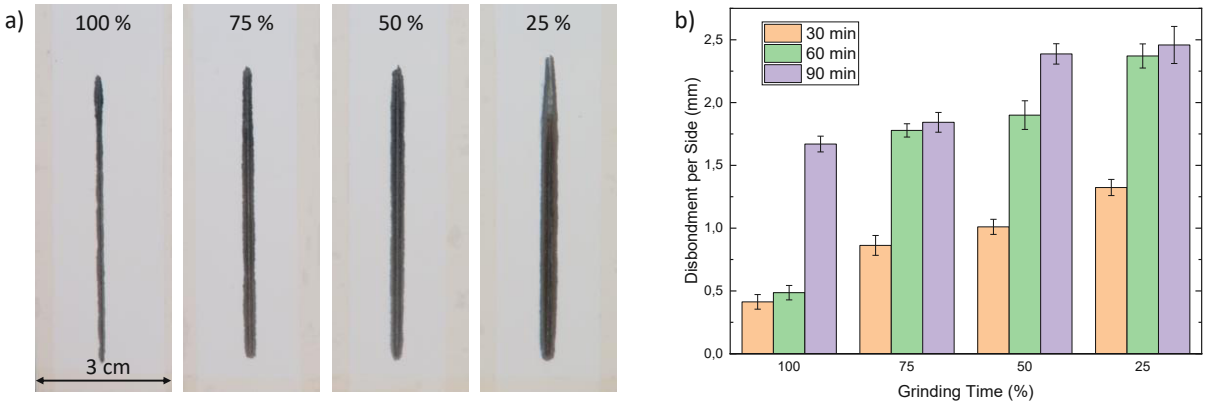

Figure 48: a) Samples after 30 min cathodic delamination testing with a 0.5 A current using a custom-built tester. A 0.5 M KOH electrolyte was used, and the temperature was maintained at 36 °C. The delaminated primer was removed with a blunt scalpel. b) The samples were evaluated using the SMART image software.

4.4.2.5 *Electrochemical Tests*

The comparison of impedance values gained at 100 mHz revealed a clear trend with respect to dry film thickness, wherein thicker coatings exhibited higher values. This is attributed to the superior barrier properties provided by thicker coatings, which restrict the flow of ions and electrons through the coating, thereby resulting in increased impedance and indicating stronger corrosion resistance. Additionally, the breakdown frequencies, which indicate the transition from capacitive to ohmic behavior, were evaluated. Typically, the initial reference point for analysis is defined as the absolute value of the frequency at which the phase angle falls below 45°. The lower the frequency value, the better the barrier properties. Breakpoint frequencies greater than 10 Hz suggest a failure of the barrier function, but this value should only be used as a general reference due to coating system variability [105]. A similar correlation was observed between the thickness of the layer and both the impedance value and the breakdown frequency.

Linear sweep voltammetry (LSV) was employed to measure the polarization resistance (LPR), which also exhibited a strong dependence on the dry film thickness of the coating. Thicker coatings resulted in higher polarization resistance values, indicating better protection against corrosion. Notably, no clear correlation was observed between milling time and the measured impedance or polarization resistance values, indicating that the milling process has a negligible impact on the barrier properties of the coating.

Figure 49 depicts the measured impedance magnitudes at 100 mHz and the polarization resistance values determined using LSV measurements, which are in good agreement with each other. **Table 35** displays the breakdown frequencies determined using EIS measurements. Overall, the results emphasize the crucial role of dry film thickness in determining the barrier

properties of organic coatings. Thicker coatings offer superior corrosion resistance, resulting in higher impedance and polarization resistance values.

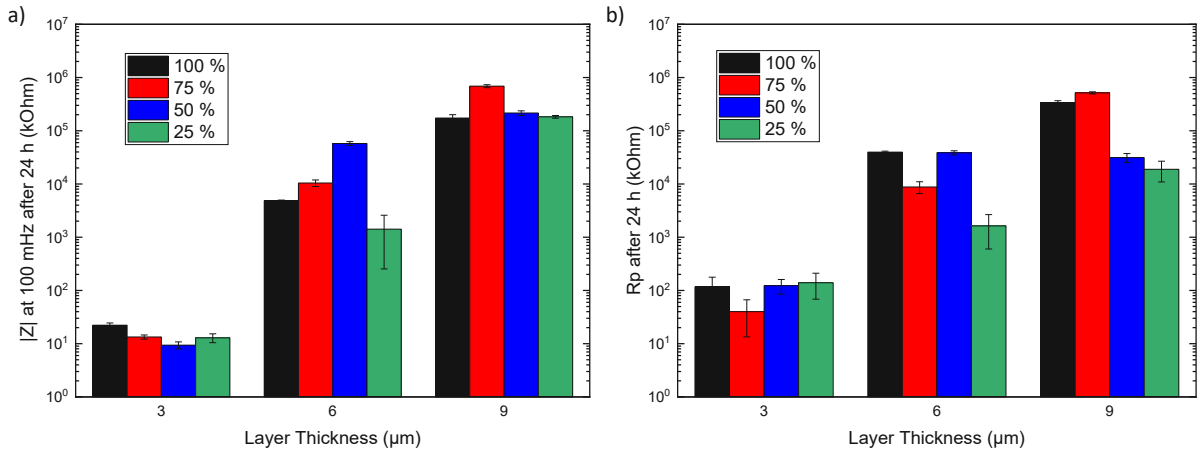

Figure 49: The results of a) EIS measurements at 100 mHz of samples with different primer layer thicknesses and grinding times of the anticorrosion pigments. b) Polarization resistance values determined using LSV measurements. All measurements were conducted after the sample surface had been in contact with a 1 M NaCl electrolyte for 24 h.

Table 35: Average breakthrough frequencies of primer samples with different layer thicknesses and grinding times determined using EIS measurements.

Grinding Time / %	Average breakthrough frequency after 24 h / Hz		
	3 µm	6 µm	9 µm
100	166	124	70
75	150	126	83
50	127	136	91
25	162	142	66
Average	151	132	81

4.4.2.6 *Elution Tests*

The release of ions over time from free coating films, which were produced as described in materials and methods, was investigated through elution tests. The conductivity of the eluents was measured, and an initial increase was observed for all grinding times, followed by a plateau after approximately 8 days, with only slight changes thereafter. A correlation was noted between pigment grinding time and solution conductivity, indicating that a longer pigment grinding time results in a higher number of dissolved ions. However, an exception was found

for the 25% grinding time. **Figure 50a** shows the progression of the conductivity over the course of the first 10 days.

To determine the ions responsible for the increase in conductivity, the composition of the eluate was analyzed. The concentration of all ions in the eluate was found to be nearly equal, except for calcium and silicon, which had higher concentrations on average in primer samples with longer pigment grinding times. The findings indicate that the enhanced conductivity observed can be attributed to the depletion of calcium and silicon ions from the coating films. **Figure *50*b** shows the measured concentration of calcium and silicon after 10 days of leaching for all grinding times.

In summary, the elution tests suggest that the release of ions from free coating films, which is a time-dependent process, is influenced by pigment grinding time. The differences in conductivity are believed to be due to the different concentrations of dissolved silicon and calcium, with their concentration increasing with longer pigment milling times.

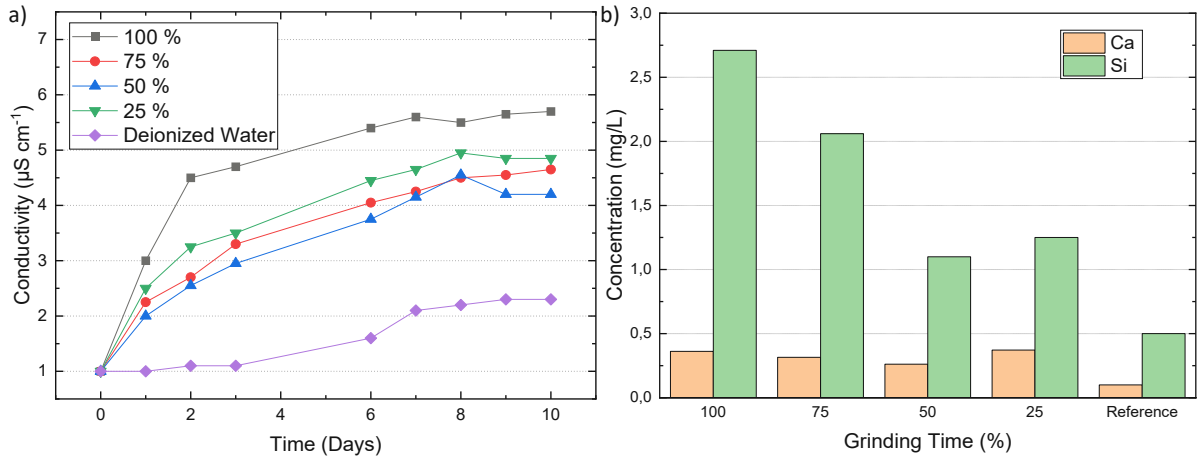

Figure 50: The results of the elution tests using free films of primers with different grinding times of their contained anticorrosion pigments. Each time, 550 mg of the sample was leached in 400 mL of deionized water at 50 °C for 10 days and conductivity and ion content were determined. a) The evolution of conductivity over 10 days for different pigment grinding times. b) The dissolved calcium and silicon concentration at the end of the 10-day leach.

In addition, attempts were made to find a relationship between the conductivity of the eluate and the mass loss of the pigments separated by TGA. It was found that the higher the conductivity was after 10 days, the higher the proportion of the sample that remained at a temperature of 700 °C in the TGA. **Figure 51a** shows the TGA curves of the separated anti-corrosion pigments. **Figure 51b** shows the Correlation between the conductivity of the leached free coating films and mass loss in TGA. Further investigation would be necessary to determine the specific mechanism behind this correlation.

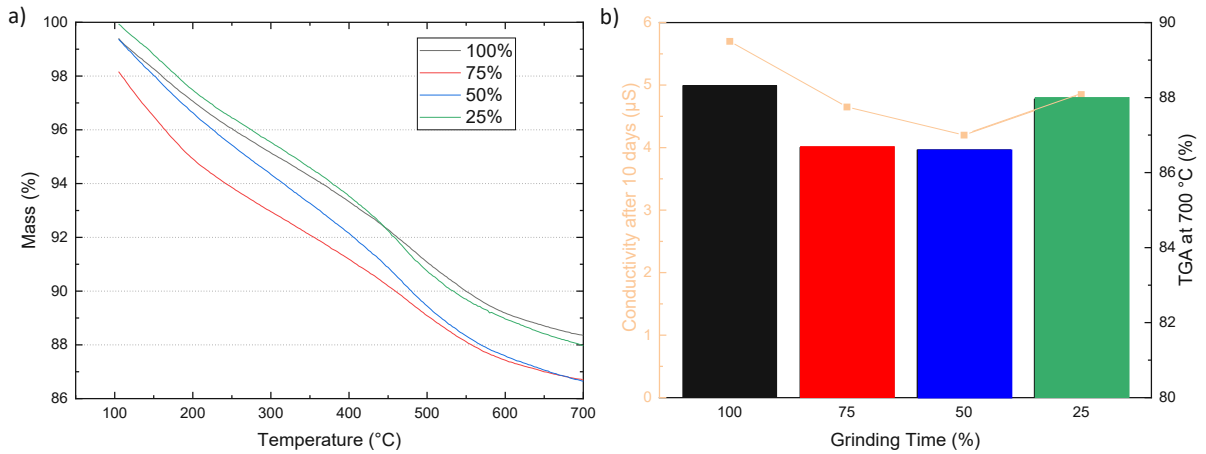

Figure 51: a) Mass loss of the anti-corrosion pigments separated from the primers with different grinding times at TGA in the temperature range of 100 to 700 °C. b) Correlation between the conductivity of the leached free coating films and mass loss in TGA.

4.4.2.7 *Water Uptake*

The water absorption of the coatings was assessed using two different techniques: sorption balance measurements and evaluation of electrochemical impedance spectroscopy (EIS) data using the Brasher-Kingsbury equation. The sorption balance measurements indicated minimal differences in water uptake between free coating films with varying grinding times, with a deviation of less than 0.2 percentage points between the specimens. All samples showed a similar hysteresis, suggesting comparable water absorption.

When using the Brasher-Kingsbury equation to evaluate EIS measurements of steel samples coated with primer, only slight differences were observed for different grinding times, but significant differences were found for variations in layer thickness. This is because thicker coatings can absorb more water, resulting in lower capacitance values and a higher diffusion coefficient, which are inversely related in the Brasher-Kingsbury equation [108]. Therefore, only samples with the same layer thickness should be compared. However, the results should be interpreted with caution, as the Brasher-Kingsbury equation depends on certain assumptions, including low water content in the coating and uniform distribution of water throughout it. While the first assumption often limits the applicability of the equation to the early stages of absorption, the second assumption is rarely met during the transient mass transfer process [106].

In conclusion, there was no clear trend between the grinding time of the anti-corrosion pigments and the diffusion coefficient. The results of the sorption balance measurements are presented in **Figure 52a**, the calculated diffusion coefficients from EIS measurements using the Brasher-Kingsbury equation in **Figure 52b**.

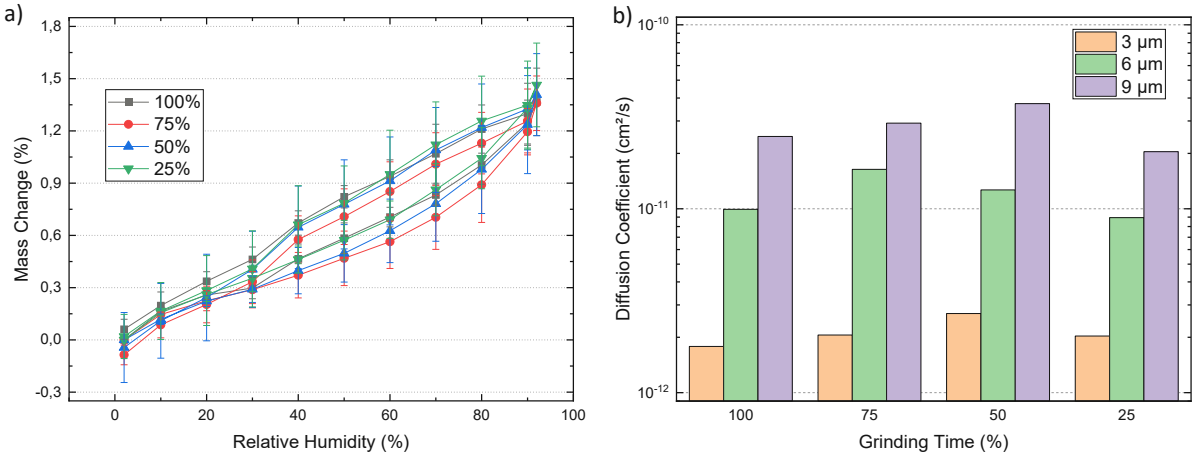

Figure 52: a) The change in mass of a free film sample measured using a sorption balance. The relative humidity was increased in increments of 10 % from 0 to 100 % and then decreased again in increments to 0 % while the temperature was held constant at 30°C. b) Diffusion coefficients calculated from EIS measurements using the Brasher-Kingsbury equation.

4.4.3 Conclusions

The aim of this part of the thesis was to investigate the effect of grinding time on the particle size distribution and performance of calcium-exchanged silica anti-corrosion pigments in a paint system. Laser diffraction analysis was used to determine the particle size distribution of the pigment, while SEM images were used to evaluate the distribution of the primer components, and salt spray and blister tests were conducted to assess the performance of the coated samples.

The results of the particle size distribution analysis indicate that the median particle size remained relatively constant, even when the milling time was reduced by 75%. However, the distribution of particles larger than 10 µm varied with different grinding times. Longer grinding times were found to reduce the number of oversized particles, and the average maximum particle size also decreased with increased grinding time, as confirmed by grindometer testing. Possible explanations for this result include the physical properties of the pigment and the influence of other components in the formulation.

The cross-sectional images of the coated samples revealed no significant differences between samples with different grinding times. A reason for this might be that the coating process could have caused the oversized particles to break down or disperse more evenly throughout the coating layer. Moreover, oversized particles may have been present in the coating layer but were not visible in the SEM images due to their distribution or orientation.

The salt spray tests revealed that all samples with a layer thickness of 3 µm began to show signs of white rust after 1,500 hours, regardless of the milling time of the anti-corrosion pigments. At 2,000 hours, corrosion began to migrate from under the taped edges to the exposed surface on

all samples, leading to the termination of the test. Samples with layer thicknesses of 6 and 9 µm showed intact surfaces up to this point. The test could not differentiate between 6 µm and 9 µm samples as the experiment was terminated at 2,000 hours, with all sample surfaces still intact at that time. In the case of the surfaces of the scribed samples, no clear differences were recognizable with different milling times of the anti-corrosion pigments, but there were discernible differences with variations in the layer thickness.

The blister tests revealed that the longer the grinding time, the longer it took for the first bubbles to appear, and the subsequent propagation and enlargement kinetics were decelerated.

In conclusion, the results of this study suggest that longer grinding times can reduce the number of oversized particles and decrease the average maximum particle size of calcium-exchanged silica anti-corrosion pigments but may not necessarily affect the median particle size. The properties of the primer and other components in the formulation may also influence the final particle size distribution of the pigment in the paint system. A thicker coating layer is generally more effective in providing protection against corrosion as it reduces the rate of penetration of corrosive media and oxygen through the coating layer. This reduces the concentration of corrosive agents at the interface between the substrate and the coating layer, thus slowing down the corrosion rate. The longer the grinding time of the pigment, the longer it takes for blister formation to occur, and the subsequent propagation and enlargement kinetics are decelerated. Overall, the findings of the study have important implications for the development and optimization of anti-corrosion coatings for steel products. By providing insights into the influence of various factors on the corrosion resistance of coated samples, the study can help improve the durability, reliability, and safety of steel products in a range of applications.

4.5 Examining the Influence of Different Parameters on Cathodic Delamination: Assessing their Impact on Coating Integrity

4.5.1 Objective of the Study and Implementation

The evaluation of the resistance of coatings to cathodic delamination plays an essential role in determining their performance in the protection of metallic surfaces against corrosion. There are various test methods used to evaluate their resistance, which differ both in the procedures used and in their test duration. The range of test periods extends from several weeks to just a few minutes.

A representative standard in this context is DIN EN ISO 15711, which is used to determine the resistance to cathodic disbonding of coatings in seawater. This standard requires a minimum test period of 26 weeks, which is equivalent to about 6.5 months. Another significant standard is the VGB/BAW standard "Corrosion Protection of Offshore Structures for the Utilization of Wind Energy", Part 2, which describes the compatibility testing of coating materials with corrosion protection systems and stipulates a test duration of 15 months.

Although test periods of this length allow detailed observation of the behavior of the coatings under realistic conditions, such an extended test duration is often impractical and economically demanding for companies in practice. Especially in dynamic industries, where rapid responses to product innovations and market demands are required, waiting for results over several months proves unfeasible.

However, there are also test methods that aim to significantly shorten the test duration. An example of this is the Volkswagen Group standard for cathodic polarization on coated metallic materials, which prescribes a test duration of only 24 hours. Similarly, the BMW Group standard for a galvanostatic cathodic polarization test on painted steel substrates also specifies a test duration of this length. Such short-term tests offer the advantage of faster results and can be used as a screening method for rapid evaluation of coatings. However, these galvanostatic tests use more unrealistic test media and employ extreme cathodic polarizations in the range of -1,600 to -3,000 mV vs. Ag/AgCl. In contrast, the two previously mentioned standardized tests use test media that are closer to reality, and the coatings are tested in realistic polarization ranges of -800 to -1,100 mV vs. Ag/AgCl. These tests are performed potentiostatically.

Given the wide variety of test methods and the widely varying test durations, it is of great importance to understand the respective advantages and disadvantages and to select the most appropriate method according to the specific requirements of the coatings and the intended application. This is particularly relevant since cathodic disbondment test methods, which have been developed to shorten test cycles, face some criticisms. First of all, it is criticized that in order to reduce the test times, the test parameters were excessively tightened, which leads to a distortion of the real conditions and questions the transferability of the results to practical applications.

Another point of criticism concerns the comparability of the test results with other established methods. The validity of the test depends heavily on whether it provides results that are comparable with those of other recognized tests. A lack of comparability could affect the acceptance and use of the procedure in industry, as concerns have been expressed about

potential competition with already established VGB/BAW procedures and DIN standards. The introduction of new test methods needs to prove itself in order to be accepted as a reliable alternative and to obtain industry accreditation.

Another critical aspect concerns the mechanism leading to cathodic delamination. In particular, it is criticized that the present test procedure has a strong focus on mechanical delamination by hydrogen. There is a possibility that other important mechanisms that can also lead to delamination are not sufficiently considered, which limits the validity of the test results. Furthermore, the derivation of meaningful electrochemical parameters is challenging, which calls into question the validity and added value of the method for the evaluation of cathodic delamination.

In this study, the influence of the test parameters on the delamination behavior was investigated. For this purpose, hot-dip galvanized steel specimens were used as substrate, which were first pretreated and then coated with primer and topcoat. In the subsequent experiments, the parameters were systematically varied to determine the respective effects on the progress of delamination. Variations included test duration, which ranged from a few minutes to several hours, to evaluate the resistance of the coating to delamination at longer exposure times, temperature, ranging from 30 to 60 °C, and current density in the mA/cm² range, to determine thresholds at which delamination onset and propagation were more likely to occur. Furthermore, additional variations such as a change of electrolyte, the presence of oxygen or a change from galvanostatic to potentiostatic mode of operation were tested.

A comprehensive analysis and evaluation of the experimental results obtained with home-built experimental setups should contribute to a better understanding of the factors affecting cathodic delamination.

4.5.1.1 Samples With Only Primer

In a first step, samples coated solely with a commercially available primer, having a layer thickness of 6 µm, were tested. The self-constructed setup, as described in section 3.6, was employed for this purpose. The standard conditions for performing the test were the usage of a 0.5 M KOH solution as electrolyte, a temperature of 35 °C, a duration of 30 minutes, and a continuous current flow set at 0.5 A. Subsequently, these parameters were systematically varied to achieve a more comprehensive study.

It is worth noting that the standard test duration of 30 minutes is tailored to samples with a complete system setup, including both a primer and a topcoat, resulting in an overall layer

thickness of approximately 25 µm. However, to assess the standalone performance of the primer, the test duration for pure primer samples was substantially reduced, and each test was conducted for only a few minutes. This adjustment allowed us to examine the initial resistance and early failure mechanisms of the primer layer in isolation. **Figure 53c** showcases the results obtained from a series of tests where the test duration was systematically varied, captured at a 4-fold magnification. The images were then evaluated using the SMART image evaluation software and the proportion of the detached primer was plotted against the test duration, as displayed in **Figure 53a**.

Within the first 3 minutes of the test, no changes were visually detectable. This indicates that during the initial period, the primer layer remains relatively stable and has sufficient adhesion to the substrate. It takes some time for the electrolyte to fully diffuse into the primer and allow current flow to the substrate. However, as the test progresses beyond the critical time frame, the coating begins to delaminate at existing defects. The observed phenomenon of delamination in the primer samples can be attributed to hydrogen evolution at the surface of the samples. It is known that the electrochemical reactions that take place during accelerated testing at voltages below -1.35 V vs. SHE can lead to the formation of hydrogen gas at the cathodic sites [58]. In this case, the strong negative potential during the test allows a strong evolution of H_2, which in combination with the strong alkaline pH can cause detachment of the coating. In **Figure 53b**, the strong gas bubble formation during the performance of the test in the delamination apparatus can be seen.

The observed delamination phenomenon become more pronounced with increasing test duration, ultimately leading to complete detachment after 12 minutes. This significant deterioration highlights the limited barrier effect provided by the pure primer samples, even within the short testing period.

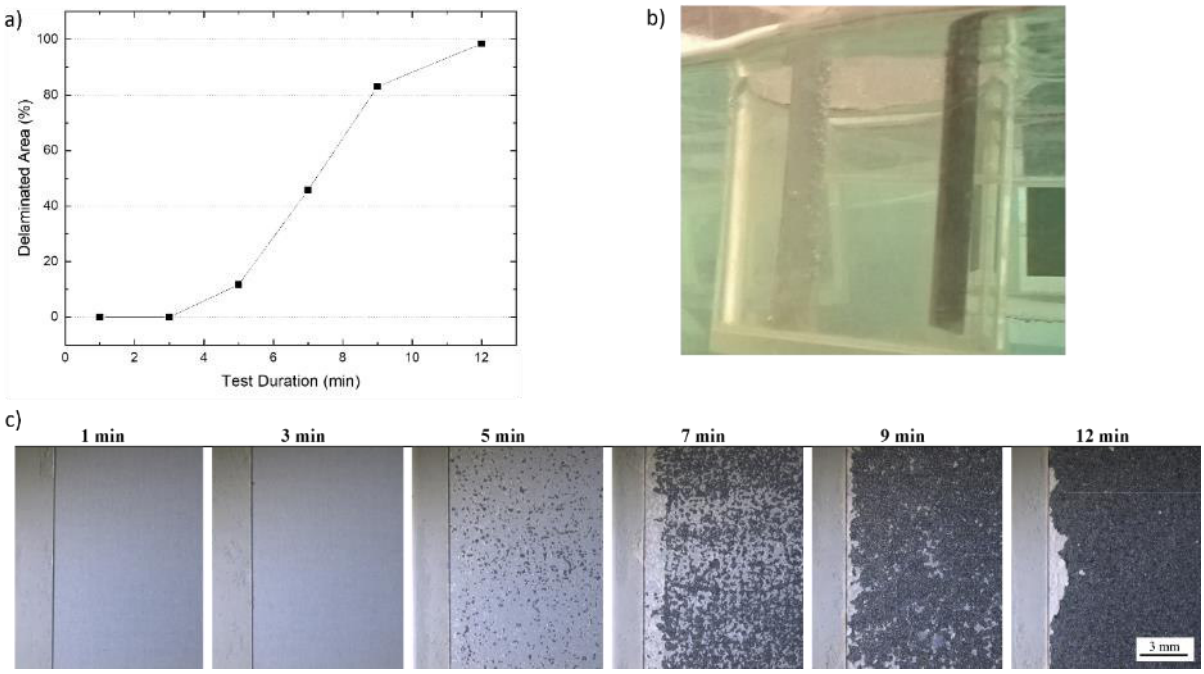

Figure 53: a) The proportion of primer detached plotted against the test duration. b) Hydrogen formation in the delamination apparatus while performing the cathodic delamination test. c) Surface of samples coated only with primer with varying test duration.

The results indicate that the protective effect of the coating, which is completely maintained for the standard duration of 30 minutes with a full coating build-up, appears to fail within a few minutes when the primer is tested independently. In order to ascertain whether the triggering factor for delamination is the current flow and its consequent hydrogen evolution, or if it is the elevated pH of the KOH solution, undamaged primer samples were immersed in the KOH solution for several hours, followed by surface observations. Even after an extensive period of 168 hours (1 week), the surfaces maintained their integrity under optical microscopy, exhibiting sustained primer adhesion that withstood peel tests using adhesive tape. Delamination, therefore, only occurs with simultaneous formation of hydrogen gas. However, discerning whether delamination could also result solely from gas formation remains uncertain, as such gas generation is accompanied by a simultaneous rise in pH into the alkaline range. In **Figure *54*** optical images taken at 5- and 50-times magnification of samples before and after contact with KOH for 168 hours are shown.

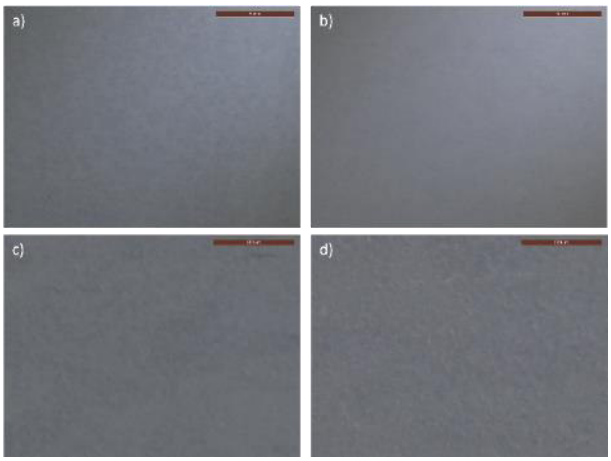

Figure 54: a) Surface of a pretreated and primer-coated sample before contact with KOH. Image taken with an optical microscope at 5x magnification. b) Image taken with 50x magnification. c) Surface of a sample after contact with 0.5 M KOH for 168 hours. Image taken with 50x magnification.

4.5.1.2 Samples With Primer and Topcoat

In the next step, samples with a full coating buildup, consisting of primer and top coat were tested. For this, both the self-made test apparatus, as described in section 3.6, and the 3D-printed cell were used. Since no change on the surface of undamaged samples was detectable even after several hours when a high voltage or current was applied, provided the coating did not have any defects, the samples were scribed with a 50 mm long and 1 mm wide scribe down to the zinc coating. The conditions originally used (30 minutes, 35 °C, 0.5 A) were systematically varied in different experiments. In **Figure 56** the varied parameters were plotted against the delamination. The test duration was varied in a), the temperature in b) and the current intensity in c). When varying those parameters, it can be seen that an increase in the respective value leads to greater delamination, with the effect being most pronounced when the temperature is increased. In all the tests performed, it was also seen that when the parameter under investigation was aggravated, delamination starting at the scribes increased. In **Figure 55** an overview of the effects of varying the parameters is shown. The greater occurrence of bubble formation with an increase in temperature, test duration or current intensity can be seen as well.

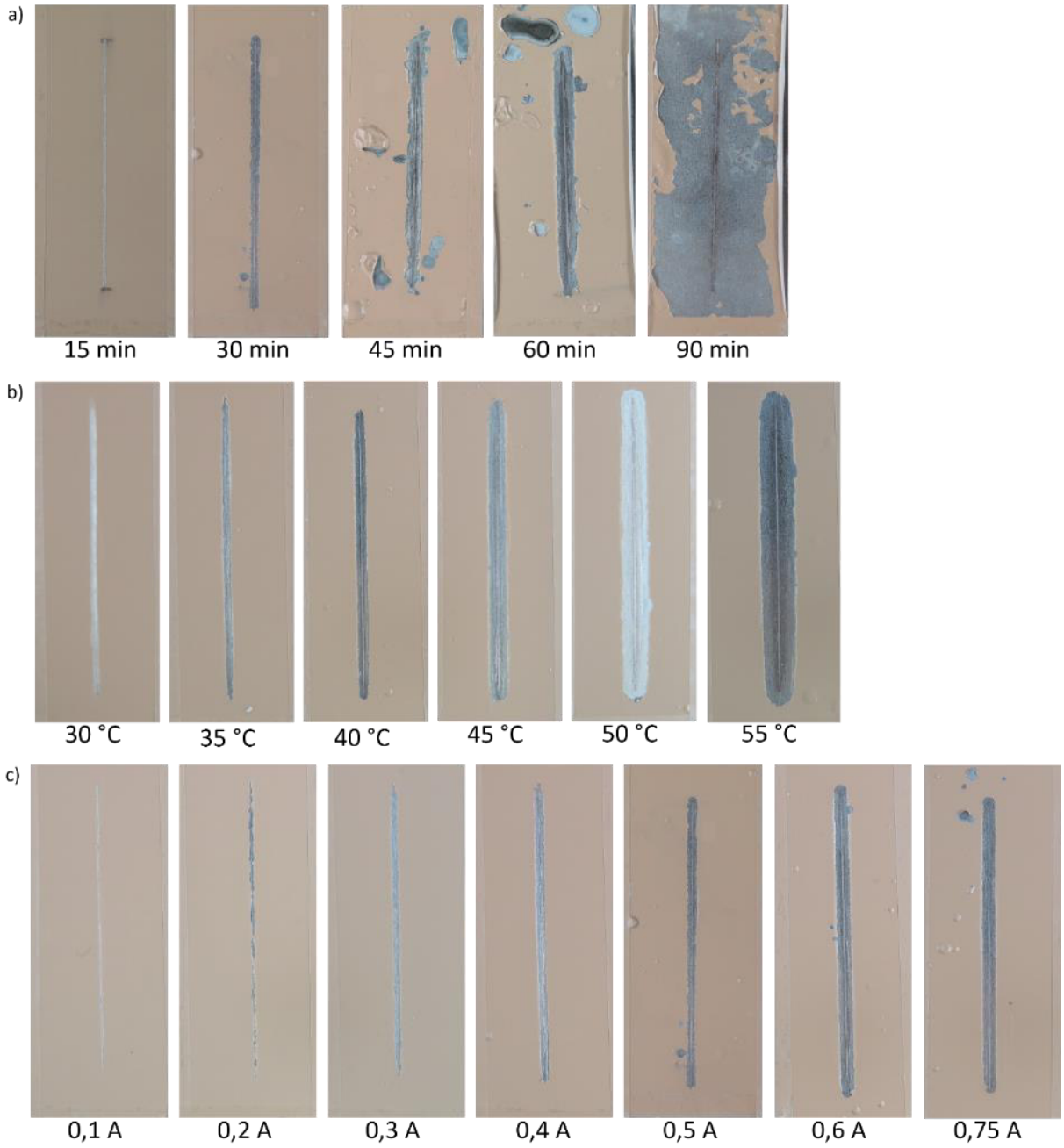

Figure 55: Effect of varying the investigated parameters in cathodic delamination tests of specimens with full coating buildup with a scribe. In a) the test duration was varied, in b) the electrolyte temperature and in c) the current flow. It can be seen that the delamination distance increases as the value of the investigated parameter is increased. The occurrence of bubble formation is increased as well.

The observed tendency of increased delamination at elevated temperature can be attributed to several underlying factors. First, higher temperatures tend to enhance the mobility and diffusion of molecules within the coating system. Increased mobility generally accelerates the rate at which reactions occur, which could also increase the rate of delamination. Additionally, increased mobility can lead to a change in interfacial interactions such as adhesion, which can subsequently promote delamination.

Additionally, elevated temperatures can induce thermal expansion effects, causing differential expansion coefficients between the layers of the coating system. This discrepancy in expansion rates can create significant stress at the interface, potentially surpassing the adhesion strength and contributing to delamination.

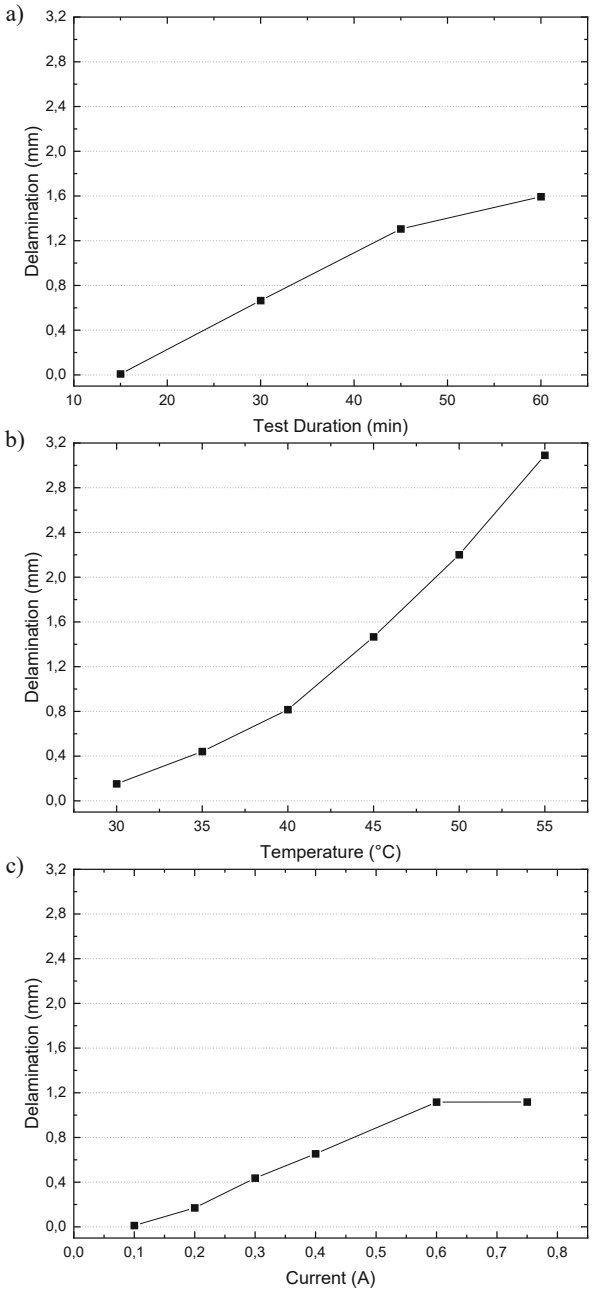

Figure 56: The parameters of the cathodic delamination test were varied systematically, and the respective parameter was plotted against delamination, starting from the scribe. In a) the test duration was varied, in b) the temperature and in c) the current flow.

Moreover, increased temperature can accelerate the degradation or breakdown of chemical bonds within the coating layers, particularly in cases where the polymer or binder materials are

susceptible to thermal degradation. This degradation can weaken the structural integrity of the coating, making it more susceptible to delamination under applied stress.

In some tests, the temperature was increased above the glass transition temperature Tg of approximately 40 °C, which is the temperature at which an amorphous material (such as certain polymers or coatings) transitions from a rigid, glassy state to a softer and more rubbery state. Above this temperature, the polymer chains of the paint or coating material may exhibit more mobility and flexibility, resulting in a decrease in stiffness and an increase in elasticity. It is important to note that the specific mechanisms governing delamination under elevated temperature conditions may vary depending on the composition, structure, and properties of the coating system.

When the test duration was varied, an almost linear relationship was found, since the delamination increased continuously with increasing test duration. After about 90 minutes, almost complete delamination had occurred. One possible reason for this delamination rate is the increase in the delamination area. The delamination reaction leads to a progressive increase in the delaminated area and thus in the interface between the coating and the substrate. This causes a continuously increasing reaction area, which accelerates the delamination process. At the same time, delamination results in increased defects in the coating, which increases its permeability. This favors easier access of the delamination medium to the interface between coating and substrate and further contributes to the acceleration of the delamination process.

Due to the fact that the current flow is synonymous with the reaction rate, an increase in the current intensity results in an increased formation of hydrogen gas. At the same time, this increased current intensity causes an accelerated and more pronounced increase in pH at the interface due to the increased formation of hydroxide ions. As a result, delamination also increases with an increase in current intensity. However, plateau formation can be observed at a value above 0.6 A, since delamination is the same for 0.6 A and 0.75 A. This behavior could indicate that neither the hydrogen gas formation nor the increase in the number of hydroxide ions in this range are the rate-limiting steps, and at this threshold value and above, neither more hydrogen gas nor a higher pH value can further increase the delamination rate.

Since the possibilities of varying the parameters in our home-made apparatus were limited, a with a 3D printed part modified cell as described in section 3.6 was used for further experiments. Here, the KOH electrolyte (0.5 M; pH 13.7; 98.7 mS/cm) was replaced with a sodium sulfate electrolyte (0.1 M; pH 5.8; 16.4 mS/cm), as predefined by the standards considered for these experiments. Some other standards recommend the use of KOH solutions,

but the reasons for choosing these specific electrolytes are not clear. Besides typical reasons such as high conductivity, chemical stability and easy availability of the substances, two possible hypotheses for the choice are, on the one hand, that these electrolytes were chosen because they are chloride-free. In the case of strong cathodic polarization in a chloride-containing electrolyte, the formation of toxic chlorine gas is a significant health risk. On the other hand, sodium sulfate solution in particular provides a good source of hydrogen, which is advantageous in this experimental setup. The use of sodium sulfate as an electrolyte thus meets the goal of ensuring both safety and efficient hydrogen release.

Among other variations, the influence of changing from a galvanostatic to a potentiostatic mode of operation was also tested. With polarizations, the ohmic voltage drop in the electrolyte leads to measured potentials that are subject to a measurement error. This measurement error is also called "iR drop", which stands for "internal resistance drop" (or "internal voltage drop"). The occurrence is evident because the further the reference electrode is from the sample surface, the more negative the measured potential becomes. However, since the iR drop is merely a measurement error, it has no influence on the result of the delamination in the case of galvanostatic polarizations. In **Figure 57** the delamination for two different paint systems at different applied voltages (potentiostatic mode of operation) or different current flows (galvanostatic mode of operation) for various times is shown. The delaminated paint was removed with a blunt scalpel and the distance of the delaminated area starting from the cracks was evaluated using the image evaluation software SMART. In **Figure 58** the evaluation of the delamination is plotted against time.

The series of tests carried out showed an almost linear increase in delamination with increasing test duration. This indicates an attack on the metal-polymer bonds, which is additionally supported and accelerated by the simultaneous generation of hydrogen gas. Furthermore, the investigation revealed that increased delamination occurs when a more negative voltage is applied or an increased current flow is used, which is consistent with the results of the tests with the delamination apparatus.

These observations can be attributed to the fact that, on the one hand, fewer hydroxide ions were formed at a lower reaction rate, which means that the postulated delamination mechanisms can proceed more slowly. This can be seen, among other things, in pH value measurements of the sample surface after completion of 24-hour tests, which are more negative at more negative voltages or higher current flows. The higher pH value at a higher current flow, whether directly by adjustment in a galvanostatic mode of operation or indirectly by adjusting a lower voltage,

which also results in a higher current flow, is the consequence, since a higher current flow corresponds to a higher reaction rate and all possible reactions taking place (reduction of oxygen, hydrogen ions or water) are accompanied by an increase in the pH value.

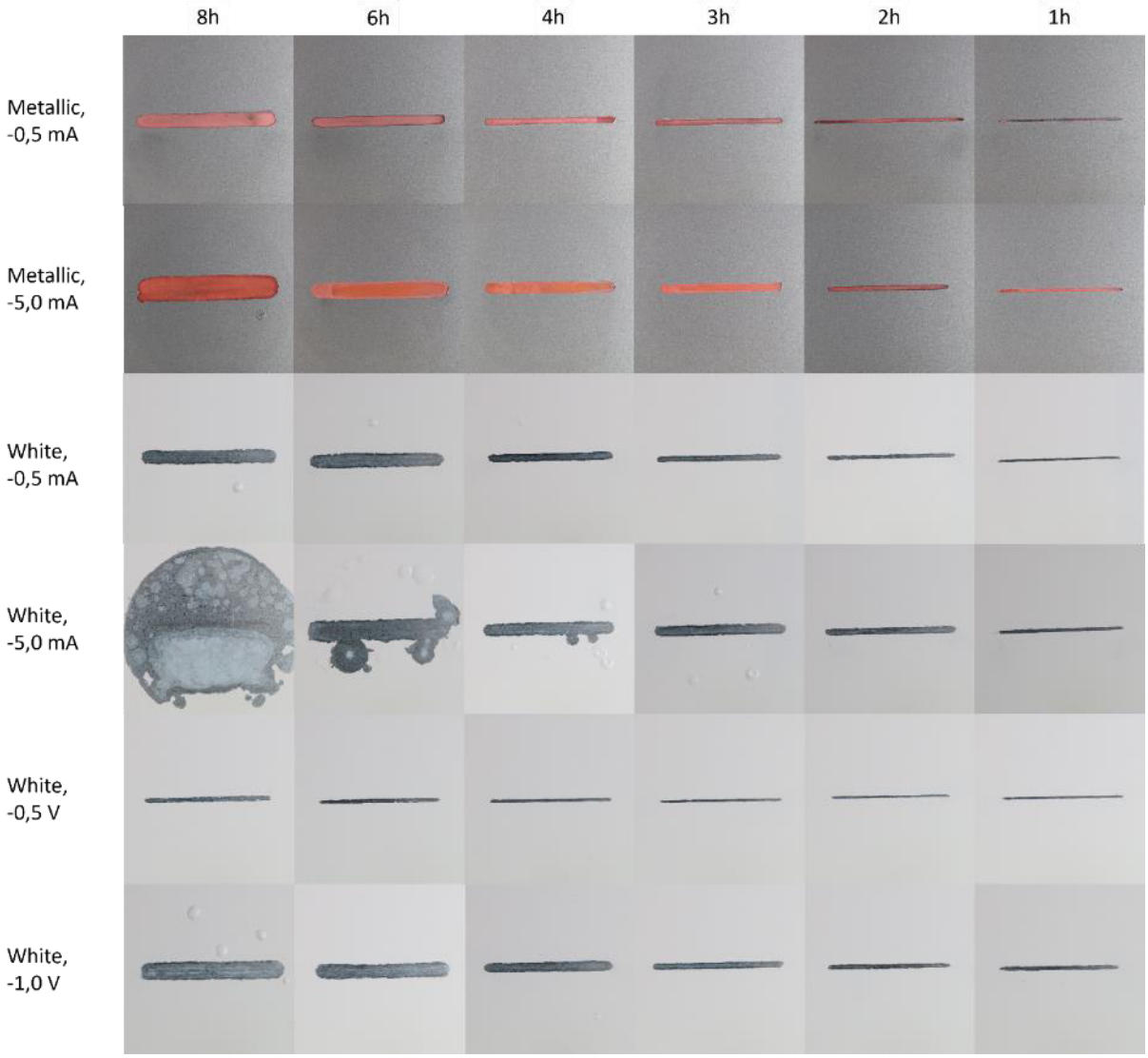

Figure 57: Delamination for different paints at different voltages or currents for different times. The delaminated paint was removed with a blunt scalpel in each case. In the case of the samples with metallic paint, the exposed zinc surface was copper-plated after removal of the delaminated paint to enable evaluation using the SMART software.

Additionally, no visual formation of hydrogen gas could be observed when more positive voltages or a lesser current flow were applied, resulting in reduced bubble formation.

In another variation of the experimental parameters, the influence of oxygen exclusion was tested. For this purpose, the electrolyte solution was thoroughly rinsed with nitrogen before the test was carried out and the test was performed under nitrogen flow. It was observed that the pH was slightly lower compared to previous experiments and at the same time the delamination was reduced. A plausible explanation for this lies in the altered cathodic reaction during the

test. Due to the exclusion of oxygen, the reduction of oxygen no longer occurred as the predominant process. Instead, reduction of hydrogen ions or of water took place. In **Figure 59** the pH values of the electrolyte and below the delaminated primer are shown. In a) for an experiment where a voltage of -1.0 V vs. OCP (=-2.0 V vs. SHE) was applied for 24 hours at room conditions, in b) the same conditions under oxygen exclusion.

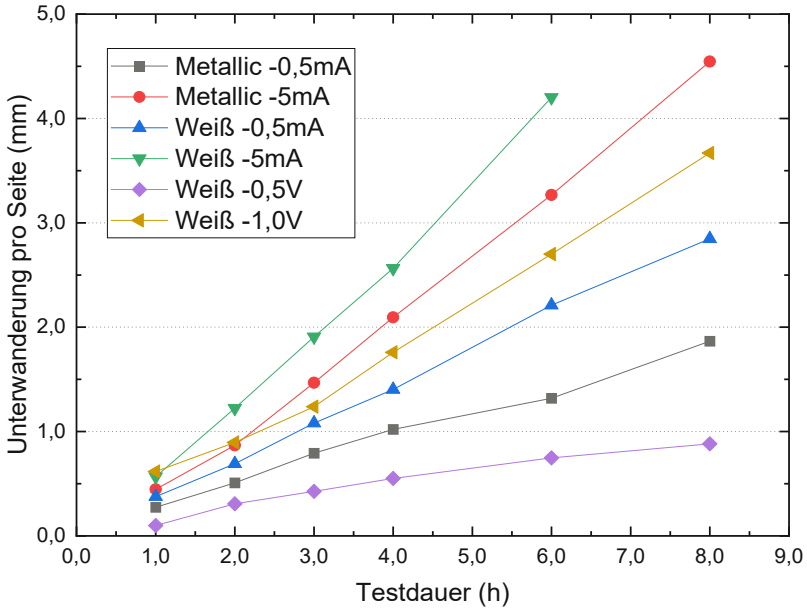

Figure 58: Variation of the applied voltage and current flow for different test durations. The distance of the delaminated area starting from the applied scribe was performed using the SMART software.

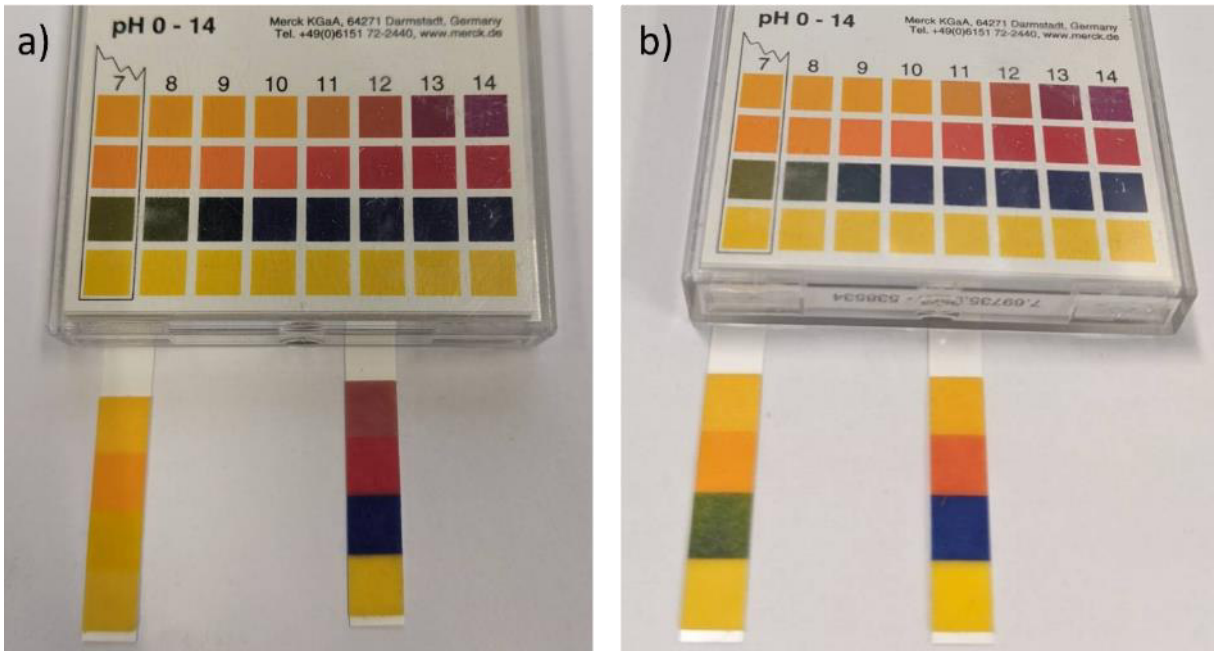

Figure 59: a) pH value after 24 hours of current flow when -1 V vs. OCP (=-2 V vs. SHE) is applied under room atmosphere: left pH value of -the electrolyte, right pH value under the delaminated paint**.** b) pH value after 24 hours of current flow when -1 V vs. OCP (=-2 V vs. SHE) is applied under oxygen exclusion: left pH value of -the electrolyte, right pH value under the delaminated paint.

4.5.2 Conclusions

In this part of the thesis, an in-depth investigation into the phenomenon of cathodic delamination of coatings was conducted. The goal was to understand the influence of various test parameters on the delamination behavior and to shed light on the underlying mechanisms that drive this process. The experiments were carried out using hot-dip galvanized steel specimens (Z) coated with primer and topcoat layers, and a range of parameters including test duration, temperature, current density, electrolyte composition, and mode of operation were systematically varied.

The findings from the experiments provide valuable insights into the complex interplay of factors affecting cathodic delamination. For samples coated only with a 6 µm primer layer, it was observed that the initial stability of the primer layer vanishes rapidly when subjected to cathodic polarization in an alkaline electrolyte. The observed delamination phenomenon was attributed to hydrogen evolution at the sample surface, resulting from electrochemical reactions under negative potentials. Moreover, the relationship between test duration and delamination showed an exponential trend, indicating that the expansion of the delamination area accelerates the process.

Samples with both primer and topcoat displayed similar trends but demonstrated in additionally conducted experiments that elevated temperature had the most significant impact on promoting delamination. This effect could be attributed to increased mobility and diffusion of molecules within the coating, thermal expansion effects, and potential degradation of chemical bonds. The current intensity was also shown to contribute to delamination, particularly through enhanced hydrogen gas evolution and increased alkalinity. Furthermore, switching from a galvanostatic to a potentiostatic mode of operation or excluding oxygen from the system resulted in observable changes in the delamination behavior, indicating the complexity of the underlying mechanisms.

The results presented here emphasize the intricate balance between electrochemical and mechanical factors governing cathodic delamination. While short-duration tests offer rapid screening capabilities, longer-term tests under more realistic conditions yield insights into the behavior of coatings over time. The study also raises important questions about the validity and transferability of results from accelerated tests to practical applications. The selection of appropriate test methods must be carefully considered to ensure reliable and meaningful evaluations of coatings' performance against cathodic delamination.

Ultimately, this research contributes to the broader understanding of cathodic delamination mechanisms and provides valuable guidance for choosing appropriate testing methodologies that align with industry needs and real-world scenarios. As the field of corrosion protection continues to evolve, further research will undoubtedly refine our understanding of this intricate phenomenon and drive advancements in protective coating technologies.

5 Conclusions and Outlook

This doctoral thesis has addressed key aspects of corrosion protection, focusing on the characterization of anti-corrosion pigments, the optimization of thin-film primers, the potential of graphene nanoparticle additives, the influence of grinding time on pigment performance, and the investigation of cathodic delamination behavior in coatings. Each chapter has provided valuable insights and contributed to the development of more effective corrosion protection strategies for galvanized steel sheets.

In the first chapter, an extensive characterization of 10 anti-corrosion pigments was performed, leading to the selection of Shieldex and ASP600 for further investigation. Shieldex, a calcium-exchanged silica, exhibited immense promise due to its ability to form a robust and protective barrier on metal surfaces. This attribute is critical in preventing corrosive agents from reaching the underlying substrate, making it a valuable corrosion inhibitor. Shieldex's reputation as a reliable additive for coatings underscored its potential, leading to its selection for thorough evaluation. Similarly, ASP600 demonstrated noteworthy anti-corrosion properties and established industrial use. Its effectiveness had been well-documented, and its compatibility with existing coating systems positioned it as a strong candidate for deeper investigation. Furthermore, the cost-effectiveness and widespread availability of ASP600 enhanced its appeal as a corrosion protection solution. Moreover, the combination of Shieldex and ASP600 showcased properties that complemented each other in a corrosion protection system. The barrier-forming ability of Shieldex, combined with ASP600's interactions and compatibility, suggested a synergistic potential that could elevate the overall anti-corrosive performance of thin-film primers.

The second chapter delved into optimizing thin-film primers, exploring factors such as coating thickness, composition, and substrate The research unveiled important insights, including the fact that a dry film thickness of 3 µm provided complete corrosion protection for 1,000 hours in the Neutral Salt Spray Test (NSST), as long as the coating remained intact. Furthermore, the study showed that increasing film thickness generally improved performance across various

tests, except in NSST tests without scribes, where a 3 µm thickness was sufficient. The hydrophobization of Shieldex showed mixed effects, enhancing cathodic delamination resistance but negatively affecting protection against white rust formation. These findings offer valuable guidance for optimizing thin-film primers and point toward further research in real-world conditions. In addition, the need for real-world testing and assessment of additional factors like UV radiation and humidity were emphasized.

In the third part, the potential of graphene nanoparticles as additives for enhancing anti-corrosion properties in commercial primers was explored. The outcomes were mixed, with varying effects observed across different test protocols. While some tests indicated minor improvements in performance, others revealed significant decreases, particularly in blistering resistance. The presence of graphene at the surface was also found to lower adhesion due to weak binding mechanisms. However, the addition of graphene did improve NSST performance, possibly due to an increased barrier effect or electrochemical surface modification. The chapter emphasizes the need for further research and optimization before considering graphene as a viable additive for industrial corrosion-resistant coatings. The currently still high price in combination with the limited benefit from the addition of graphene makes its use unattractive at the moment.

The fourth chapter investigated the influence of grinding time on the particle size distribution and performance of calcium-exchanged silica anti-corrosion pigments within paint systems. The analysis revealed that while the median particle size remained relatively constant, grinding time affected the distribution of particles larger than 10 µm. Longer grinding times reduced the number of oversized particles and decreased the average maximum particle size. The properties of the primer and other formulation components may also have influenced the final particle size distribution. The cross-sectional images of coated samples indicated no significant differences between different grinding times, possibly due to coating processes influencing particle distribution. Salt spray tests showed that thicker coating layers were more effective in providing corrosion protection, corroborating with reduced corrosive media penetration and slower corrosion rates. Furthermore, longer grinding times correlated with delayed blister formation, indicating decelerated kinetics. These findings hold implications for anti-corrosion coating development, offering insights into the impact of various factors on coating performance and corrosion resistance.

Lastly, the fifth chapter delved into the complex phenomenon of cathodic delamination in coatings. Using hot-dip galvanized steel specimens coated with primer and topcoat layers, the

study systematically varied test parameters to unravel the complex factors influencing delamination behavior. The results highlighted the interplay of electrochemical and mechanical factors driving cathodic delamination. For samples with only a 6 µm primer layer, the primer's initial stability vanished rapidly under cathodic polarization in an alkaline electrolyte. This delamination was attributed to hydrogen evolution from electrochemical reactions under negative potentials. Moreover, the relationship between test duration and delamination exhibited an exponential trend, suggesting that delamination area expansion accelerated the process. For samples with both primer and topcoat, elevated temperature emerged as a prominent promoter of delamination. The impact of current intensity, mode of operation, and electrolyte composition further emphasized the complex mechanisms at play. The study underscored the intricate balance between various factors contributing to cathodic delamination behavior and highlighted the importance of careful test method selection for meaningful coating performance evaluations.

While this thesis has made notable contributions to the field of corrosion protection, it also unveils various potential directions for future research. Real-world testing of optimized thin-film primers is essential to validate laboratory findings and assess the coatings' performance under diverse environmental conditions. Further investigation into the potential synergistic effects of Shieldex and ASP600 in practical applications is warranted.

Incorporating graphene nanoparticles as anti-corrosion additives requires continued research to overcome challenges related to adsorption and cost. Efforts should focus on developing strategies to improve graphene's compatibility with coating systems while maximizing its beneficial properties. The findings related to grinding time and particle size distribution highlight the need for more comprehensive studies involving different pigment systems and coating formulations. Understanding the impact of particle size distribution on coating performance can lead to more tailored corrosion protection solutions. Regarding cathodic delamination, future research should focus on bridging the gap between accelerated testing and real-world applications. Developing standardized protocols that provide reliable and transferable results will be crucial. Furthermore, exploring alternative mechanisms contributing to delamination and validating their significance will enhance the understanding of this complex phenomenon.

In conclusion, this doctoral thesis has made significant strides in advancing the knowledge of corrosion protection strategies. The insights gained from characterizing pigments, optimizing primers, exploring new additives, understanding particle size effects, and investigating

delamination mechanisms collectively contribute to the development of more robust and reliable corrosion protection solutions for diverse industrial applications. Continued research in these directions will play a pivotal role in enhancing the durability and longevity of materials in corrosive environments.

6 References

[1] H. Zeisel. [Online]. Available: https://energieforschung.at/projekt/neostahl-neue-energieoptimierungsverfahren-und-modelle-in-der-prozessautomation-zur-co2-reduktion-in-der-stahlindustrie. [Accessed 03 10 2023].

[2] A. Hasanbeigi, "Global Steel Industry's GHG Emissions," 07 04 2021. [Online]. Available: https://www.globalefficiencyintel.com/new-blog/2021/global-steel-industrys-ghg-emissions. [Accessed 03 10 2023].

[3] P. Crevolin, R. Francis, K. Garrity, S. Hall, R. Kinzie, D. Kroon, L. Lee, F. Rampton, D. Riddle, H. Tanabe and D. Webster, "International Measures of Prevention, Application, and Economics of Corrosion Technologies Study," NACE International, Houston, TX 77084, 2016.

[4] S. Wiener, B. Strauß, G. Luckeneder, J. Hagler and M. Valtiner, "Thermoset thin film primers: Influence of substrate, layer," *Materials and Corrosion,* vol. 74, no. 8, p. 1183–1195, 2023.

[5] S. Wiener, B. Strauß, G. Luckeneder, J.-F. Hagler and M. Valtiner, "Evaluation of a commercial graphene-additive for boosting the corrosion performance of a thermal curing primer," *Materials and Corrosion,* vol. 74, no. 10, pp. 1416-1428, 2023.

[6] F. Presuel-Moreno, M. A. Jakab, N. R. Tailleart, M. E. Goldman and J. R. Scully, "Corrosion-resistant metallic coatings," *Materials Today,* vol. 11, no. 10, pp. 14-23, 2008.

[7] N. Priyantha, P. Jayaweera, A. Sanjuro, K. Lau, F. Lu and K. Krist, "Corrosion-resistant metallic coatings for applications in highly aggressive environments," *Surface and Coatings Technology,* vol. 163, pp. 31-36, 2003.

[8] Y. Shi, B. Yang and P. K. Liaw, "Corrosion-Resistant High-Entropy Alloys: A Review," *Metals,* vol. 7, no. 43, 2017.

[9] A. E. Hughes, "Conversion Coatings," in *Encyclopedia of Interfacial Chemistry*, 2018, pp. 108-114.

[10] A. Zaki, "Coatings," in *Principles of Corrosion Engineering and Corrosion Control*, Butterworth-Heinemann, 2006, pp. 382-437.

[11] O. Ø. Knudsen and A. Forsgren, Corrosion Control Through Organic Coatings, Boca Raton: CRC Press, 2017.

[12] S. B. Lyon, R. V. Bingham and D. J. Mills, "Advances in corrosion protection by organic coatings: What we know and what we would like to know," *Progress in Organic Coatings,* vol. 102, no. Part A, pp. 2-7, 2017.

[13] P. A. Sørensen, S. Kiil, K. Dam-Johansen and C. E. Weinell, "Anticorrosive Coatings: a review," *Journal of Coatings Technology and Research,* vol. 6, no. 2, pp. 135-176, 2009.

[14] C. G. Dariva and A. F. Galio, "Corrosion Inhibitors – Principles, Mechanisms and," *IntechOpen,* pp. 365-379, 2014.

[15] L. W. Vasconcelos, I. C. Margarit, O. R. Mattos, F. L. Fragata and A. F. Sombra, "Inhibitory Properties of Calcium Exchanged Silica Epoxy Paintings," *Corrosion Science,* pp. 2291-2303, 2001.

[16] N. Granizo , J. M. Vega, I. Díaz, B. Chico, D. de la Fuente and M. Morcillo, "Paint systems formulated with ion-exchange pigments applied on carbon steel:," *Progress in Organic Coatings,* pp. 394-400, 2011.

[17] F. Deflorian, S. Rossi, M. Fedel, L. G. Ecco, R. Paganica and M. Bastarolo, "Study of the effect of corrosion inhibitors on powder coatings appliedon steel," *Progress in Organic Coatings,* pp. 2133-2139, 2014.

[18] K. Przywecka, K. Kowalczyk and B. Grzmil, "Sequential co-precipitation as a convenient preparation method of anticorrosive hybrid calcium phosphate/calcium silicate powder pigments," *Powder Technology,* p. 660–670, 2020.

[19] R. Romagnoli, C. Deyá and B. del Amo, "The mechanism of the anticorrosive action of calcium exchanged silica," *Surface Coatings International,* pp. 135-141, 2003.

[20] B. Chico, J. Simancas, J. M. Vega, N. Granizo, I. Díaz, D. de la Fuente and M. Morcillo, "Anticorrosive behaviour of alkyd paints formulated with ion-exchange pigments," *Progress in Organic Coatings,* p. 283–290, 2008.

[21] C. Deyá, B. Guillermo, B. del Amo and R. Romagnoli, "Evaluation of eco-friendly anticorrosive pigments for paints in service conditions," *Progress in Organic Coatings,* pp. 1-6, 2010.

[22] N. Granizo, J. M. Vega, D. de la Fuente, J. Simancas and M. Morcillo, "Ion-exchange pigments in primer paints for anticorrosive protection of steel in atmospheric service: Cation-exchange pigments," *Progress in Organic Coatings,* vol. 75, p. 147– 161, 2012.

[23] J. M. Vega, N. Granizo, J. Simancas, D. de la Fuente, I. Díaz and M. Morcillo, "Corrosion inhibition of aluminum by organic coatings formulated with calcium exchange silica pigment," *Journal of Coatings Technology and Research,* vol. 10, p. 209–217, 2012.

[24] F. Deflorian, I. Felhosi, S. Rossi, L. Fedrizzi and P. L. Bonora, "Performance of Primers Containing Polyphosphate-Based Ion-Exchange Pigments for the protection of Galvanised Stee," *Macromolecular Symposia,* vol. 187, pp. 87-96, 2002.

[25] A. K. Geim and K. S. Novoselov, "The rise of graphene," *Nature Materials,* vol. 6, pp. 183-191, 2007.

[26] A. Geim, "Graphene: Status and Prospects," *Science,* vol. 324, pp. 1530-1534, 2009.

[27] N. Dey, S. Vickram, S. Thanigaivel, C. Kamatchi, R. Subbaiya, N. Karmegam and M. Govarthanan, "Graphene materials: Armor against nosocomial infections and biofilm formation – A review," *Environmental Research,* vol. 214, p. 113867, 2022.

[28] A. Janković , S. Eraković , M. Vukašinović-Sekulić , V. Mišković-Stanković, S.-J. Park and K. Y. Rhee, "Graphene-based antibacterial composite coatings electrodeposited on titanium for biomedical applications," *Progress in Organic Coatings,* vol. 83, pp. 1-10, 2015.

[29] R. K. Yadav, J.-O. Lee, A. Kumar, N.-J. Park, D. Yadav, J. Y. Kim and J.-O. Baeg, "Highly Improved Solar Energy Harvesting for Fuel Production from CO2 by a Newly Designed Graphene Film Photocatalyst," *Scientific Reports,* vol. 8, p. 16741, 2018.

[30] J. S. George, P. Vijayan P, J. K. Paduvilan, S. Nisa, J. Sunarso, N. Kalarikkal, N. Hameed and S. Thomas, "Advances and future outlook in epoxy/graphene composites for anticorrosive applications," *Progress in Organic Coatings,* vol. 162, p. 106571, 2022.

[31] J. Mu, F. Gao, G. Cui, S. Wang, S. Tang and Z. Li, "A comprehensive review of anticorrosive graphene-composite coatings," *Progress in Organic Coatings,* vol. 157, p. 106321, 2021.

[32] Y.-P. Hsieh, M. Hofmann, K.-W. Chang, J. G. Jhu, Y.-Y. Li, K. Y. Chen, C. C. Yang, W.-S. Chang and L.-C. Chen, "Complete Corrosion Inhibition through Graphene Defect Passivation," *ACS Nano,* vol. 8, no. 1, pp. 443-448, 2014.

[33] R. Ding, W. Li, X. Wang, T. Gui, B. Li, P. Han, H. Tian, A. Liu, X. Wang, X. Liu, X. Gao, W. Wang and L. Song, "A brief review of corrosion protective films and coatings based on graphene and graphene oxide," *Journal of Alloys and Compounds,* vol. 764, pp. 1039-1055, 2018.

[34] Y. Wu, X. Zhu, W. Zhao, Y. Wang, C. Wang and Q. Xue, "Corrosion mechanism of graphene coating with different defect levels," *Journal of Alloys and Compounds,* vol. 777, pp. 135-144, 2019.

[35] G. Cui, Z. Bi, R. Zhang, J. Liu, X. Yu and Z. Li, "A comprehensive review on graphene-based anti-corrosive coatings," *Chemical Engineering Journal,* vol. 373, pp. 104-121, 2019.

[36] Y. He, C. Chen, G. Xiao, F. Zhong, Y. Wu and Z. He, "Improved corrosion protection of waterborne epoxy/graphene coating by combining non-covalent and covalent bonds," *Reactive and Functional Polymers,* vol. 137, pp. 104-115, 2019.

[37] X. Cao, F. Huang, C. Huang, J. Liu and F. Y. Cheng, "Preparation of graphene nanoplate added zinc-rich epoxy coatings for enhanced sacrificial anode-based corrosion protection," *Corrosion Science,* vol. 159, p. 108120, 2019.

[38] S. Peretz-Damari, L. Cullari, D. Laredo, R. Nadiv, E. Ruse, R. Sripada and O. Regev, "Graphene and boron nitride nanoplatelets for improving vapor barrier properties in epoxy nanocomposites," *Progress in Organic Coatings,* vol. 136, p. 105207, 2019.

[39] J. Vidales-Herrera and I. López, "Nanomaterials in coatings: an industrial point of view," *Handbook of Nanomaterials for Manufacturing Applications,* pp. 51-77, 2020.

[40] E. Alibakhshi, E. Ghasemi, M. Mahdavian, B. Ramezanzadeh and A. Askari, "Active corrosion protection of Mg-Al-PO43− LDH nanoparticle in silane primer coated with epoxy on mild steel," *Journal of the Taiwan Institute of Chemical Engineers,* vol. 75, pp. 248-262, 2017.

[41] M. Rostami, S. Rasouli, B. Ramezanzadeh and A. Askari, "Electrochemical investigation of the properties of Co doped ZnO nanoparticle as a corrosion inhibitive pigment for modifying corrosion resistance of the epoxy coating," *Corrosion Science,* vol. 88, pp. 387-399, 2017.

[42] J.-W. Cheon, I.-J. Kim, J.-H. Kim, J.-W. Jang, D.-J. Lee, S. Y. Mun, J.-W. Park, J. H. Lee and S. Yu, "Silica-polyethersulfone core–shell nanoparticles as multifunctional filler for marine applications," *Composites Part A: Applied Science and Manufacturing,* vol. 152, p. 106721, 2022.

[43] H. Ge, J. Zhang, Y. Yuan, J. Liu and X. Liu, "Preparation of organic–inorganic hybrid silica nanoparticles with contact antibacterial properties and their application in UV-curable coatings," *Progress in Organic Coatings,* vol. 106, pp. 20-26, 2017.

[44] R. Montoya, F. R. García-Galván, A. Jiménez-Morales and J. C. Galván, "A cathodic delamination study of coatings with and without mechanical defects," *Corrosion Science,* vol. 82, pp. 432-436, 2014.

[45] K. Ogle, S. Morel and N. Meddahi, "An electrochemical study of the delamination of polymer coatings on galvanized steel," *Corrosion Science,* vol. 47, no. 8, pp. 2034-2052, 2005.

[46] W. Fürbeth and M. Stratmann, "The delamination of polymeric coatings from electrogalvanised steel – a mechanistic approach.: Part 1: delamination from a defect with intact zinc layer," *Corrosion Science,* vol. 43, no. 2, pp. 207-227, 2001.

[47] P. A. Sørensen, S. Kiil, K. Dam-Johansen and C. E. Weinell, "Influence of substrate topography on cathodic delamination of anticorrosive coatings," *Progress in Organic Coatings,* vol. 64, no. 2-3, pp. 142-149, 2009.

[48] J. M. Pommersheim and T. Nguyen, "Prediction of Blistering in Coating Systems," in *Organic Coatings for Corrosion Control*, Washington, DC, American Chemical Society, 1998, pp. 137-150.

[49] R. P. Berkelaar, P. Bampoulis, E. Dietrich, H. P. Jansen, X. Zhang, E. S. Kooij, D. Lohse and H. J. W. Zandvliet, "Water-Induced Blister Formation in a Thin Film Polymer," *Langmuir,* vol. 31, pp. 1017-1025, 2015.

[50] A. S. Kuznetsov, M. A. Gleeson and F. Bijkerk, "Hydrogen-induced blistering mechanisms in thin film coatings," *Journal of Physics: Condensed Matter,* vol. 24, p. 052203, 2012.

[51] J. W. Martin, E. Embree and W. Tsao, "Non-Osmotic, Defect-Controlled Cathodic Disbondment Of a Coating from a Steel Substrate," *Journal of Coating Technology,* vol. 62, no. 790, pp. 25-, 1990.

[52] S. J. Spadafora and H. Leidheister, "Water Disbondment Characterisation of Polymer Coating/Metal Substrate Systems," in *RS5C*, Gothenburg, 1988.

[53] H. Leidheiser and W. Funke, "Water disbondment and wet adhesion of organic coatings on metals: A review and interpretation," *Journal of The Oil And Colour Chemists' Association,* vol. 70, no. 5, pp. 121-132, 1987.

[54] M. Van Loo, D. D. Laiderman and R. R. Bruhn, "Filiform Corrosion," *Corrosion,* vol. 9, no. 8, pp. 277-283, 1953.

[55] R. T. Ruggeri and T. R. Beck, "An Analysis of Mass Transfer in Filiform Corrosion," *Corrosion,* vol. 39, no. 11, pp. 452-465, 1983.

[56] W. Fürbeth and M. Stratmann, "The delamination of polymeric coatings from electrogalvanised steel - a mechanistic approach. Part 1: delamination from a defect with intact zinc layer," *Corrosion Science,* vol. 43, pp. 207-227, 2001.

[57] D. Iqbal, A. Sarfraz, M. Stratmann and A. Erbe, "Solvent-starved conditions in confinement cause chemical oscillations excited by a passage of a cathodic delamination front," *Chem. Commun.,* vol. 51, pp. 16041-16044, 2015.

[58] R. N. Parkins, A. J. Markworth and J. H. Holbrook, "Hydrogen Gas Evolution from Cathodically Protected Pipeline Steel Surfaces Exposed to Chloride-Sulfate Solutions," *Corrosion,* vol. 44, no. 8, pp. 572-580, 1988.

[59] M. Haji-Ghassemi, R. A. Cottis and J. D. Scantlebury, "Hydrogenpermeation measurements on lacquer-coated mild steel under cathodicpolarization in sodium chloride solution," *Journal of the Oil & Colour Chemists' Association,* vol. 75, no. 7, p. 277–280, 1992.

[60] K. Ogle, S. Morel and N. Meddahi, "An electrochemical study of the delamination of polymer coatings on galvanized steel," *Corrosion Science,* vol. 47, pp. 2034-2052, 2005.

[61] J. F. Watts, "Mechanistic Aspects of the Cathodic Delamination of Organic Coatings," *The Journal of Adhesion,* vol. 31, pp. 73-85, 1989.

[62] M. Babutzka and A. Burkert, "Prüfverfahren zur Bewertung der kathodischen Enthaftung bei organischen Beschichtungen - Eine kritische Betrachtung," in *ZVO Oberflächentage Berlin 2019 Kongress für Galvano- und Oberflächentechnik*, Berlin, 2019.

[63] M. Xu, C. C. Lam, D. Wong and A. Asselin, "Evaluation of the cathodic disbondment resistance of pipeline coatings – A review," *Progress in Organic Coatings,* vol. 146, p. 105728, 2020.

[64] M.-W. Huang, C. Allely, K. Ogle and M. E. Orazem, "A Mathematical Model for Cathodic Delamination of Coated Metal Including a Kinetic pH–Porosity Relationship," *Journal of The Electrochemical Society,* vol. 155, no. 5, pp. C279-C292, 2008.

[65] H. Leidheiser, W. Wang and L. Igetoft, "The Mechanism for the Cathodic Delamination of Organic Coatings from a Metal Surface," *Progress in Organic Coatings,* vol. 11, pp. 19-40, 1983.

[66] P. A. Sørensen, K. Dam-Johansen, C. E. Weinell and S. Kiil, "Cathodic delamination of seawater-immersed anticorrosive coatings: Mapping of parameters affecting the rate," *Progress in Organic Coatings,* vol. 68, pp. 283-292, 2010.

[67] P. Sørensen, S. Kiil, K. Dam-Johansen and C. Weinell, "Influence of substrate topography on cathodic delamination of anticorrosive," *Progress in Organic Coatings,* vol. 64, pp. 142-149, 2009.

[68] C. Glover, C. Richards, J. Baker, G. Williams and H. McMurray, "In-coating graphene nano-platelets for environmentally-friendly corrosion protection of iron," *Corrosion science,* vol. 114, pp. 169-172, 2017.

[69] M. Ström, "A century with salt spray testing: Time for a final phasing-out by a replacement based on newly developed more capable test regimes," in *Proceedings of the EUROCORR 2014*, Pisa, 2014.

[70] H. S. Gardner, Cyclic Cabinet Corrosion Testing, ASTM International, 1995.

[71] I. C. P. Margarit-Mattos, "EIS and organic coatings performance: Revisiting some key points," *Electrochimica Acta,* vol. 354, p. 136725, 2020.

[72] F. Deflorian, S. Rossi and M. Fedel, "Organic coatings degradation: Comparison between natural and artificial weathering," *Corrosion Science,* vol. 50, no. 8, pp. 2360-2366, 2008.

[73] F. Deflorian, S. Rossi, L. Fedrizzi and C. Zanella, "Comparison of organic coating accelerated tests and natural weathering considering meteorological data," *Progress in Organic Coatings,* vol. 59, no. 3, pp. 244-250, 2007.

[74] X. Yong, H. Ji, Z. Chen and X. Ruan, "Comparison between Accelerated Tests and Natural Exposures for Organic Coating Protective Systems Based on EIS Parameters," *Journal of The Electrochemical Society,* vol. 168, no. 12, 2021.

[75] SNCZ, "SNCZ S.A.S.," SNCZ, 2021. [Online]. Available: https://www.sncz.com/en/pigment/novinox-xca02/. [Accessed März 2021].

[76] SNCZ, "SNCZ S.A.S.," SNCZ, 2021. [Online]. Available: https://www.sncz.com/en/pigment/novinox-pat30/. [Accessed März 2021].

[77] SNCZ, "SNCZ S.A.S.," SNCZ, 2021. [Online]. Available: https://www.sncz.com/en/pigment/novinox-pat15/. [Accessed März 2021].

[78] SNCZ, "SNCZ S.A.S.," SNCZ, 2021. [Online]. Available: https://www.sncz.com/en/pigment/novinox-pam/. [Accessed März 2021].

[79] SNCZ, "SNCZ S.A.S.," SNCZ, 2021. [Online]. Available: https://www.sncz.com/en/pigment/novinox-pc01/. [Accessed März 2021].

[80] SpecialChem, "SpecialChem S.A.," SpecialChem, 2021. [Online]. Available: https://coatings.specialchem.com/product/p-grace-shieldex-c-303. [Accessed März 2021].

[81] Heubach GmbH, "Heubachcolor," 2020. [Online]. Available: https://www.heubachcolor.com/fileadmin/downloads/technical_datasheets/phcmp_gb_001.pdf. [Accessed März 2021].

[82] Heubach GmbH, "Heubachcolor," 2020. [Online]. Available: https://www.heubachcolor.com/fileadmin/downloads/technical_datasheets/phsrpp_gb_001.pdf. [Accessed März 2021].

[83] Norzinco GmbH, "b2bcomposites," 2021. [Online]. Available: https://www.b2bcomposites.com/msds/ted/78630.pdf. [Accessed März 2021].

[84] BASF, "BASF," 2021. [Online]. Available: https://kaolin.basf.com/files/pdf/ASP%20400P%20and%20600%20Pultrusion%20Brochure%2012-08.pdf. [Accessed März 2021].

[85] BASF, "kaolin.basf.com," BASF, 2021. [Online]. Available: https://kaolin.basf.com/products/application/asp/asp600. [Accessed 20 April 2021].

[86] TAYCA, "http://www.tayca.co.jp/," 2009. [Online]. Available: http://www.tayca.co.jp/english/products/pdf/20100629h.pdf. [Accessed März 2021].

[87] Lehmann&Voss&Co, "Lehmann&Voss&Co," 2021. [Online]. Available: https://www.lehvoss-surfacetec.de/en/products/additives/id/anticorrosive-pigments-1.pdf. [Accessed März 2021].

[88] M. S. Azevedo, "Corrosion mechanisms of ZnMgAl coated steel in," Université Pierre et Marie Curie, Paris, 2014.

[89] T. A. Keppert, G. Luckeneder, K.-H. Stellnberger, C. Commenda, G. Mori and H. Antrekowitsch, "The effect of magnesium on the corrosion of hot-dip galvanized steel in chloride containing environments," *Materials and Corrosion,* vol. 65, no. 9, pp. 871-880, 2014.

[90] T. A. Keppert, G. Luckeneder, K.-H. Stellnberger, G. Mori and H. Antrekowitsch, "The effect of sulphate, phosphate, nitrate and acetate on the corrosion behaviour of Zn–Al–Mg hot-dip galvanised steel," *Materials and Corrosion,* vol. 65, no. 6, pp. 560-568, 2014.

[91] R. Hausbrand, M. Stratmann and M. Rohwerder, "Corrosion of zinc–magnesium coatings: Mechanism of paint delamination," *Corrosion Science,* vol. 51, no. 9, pp. 2107-2114, 2009.

[92] T. Fletcher , "Ion-Exchanged Silica Anticorrosive Pigments: A Review and recent developments," *JCT CoatingsTech,* vol. 10, pp. 28-39, 2013.

[93] M. B. Moraes, L. Cividanes and G. Thim, "Synthesis of Graphene Oxide and Functionalized CNT Nanocomposites Based on Epoxy Resin," *Journal of Aerospace Technology and Management,* vol. 10, 2018.

[94] N. Sharma, V. Sharma, Y. Jain, M. Kumari, R. Gupta, S. K. Sharma and K. Sachdev, "Synthesis and Characterization of Graphene Oxide (GO) and Reduced Graphene Oxide (rGO) for Gas Sensing Application," *Macromolecular Symposia,* vol. 376, no. 1, p. 1700006, 2017.

[95] F. C. Andrea, "Raman spectroscopy of graphene and graphite: Disorder, electron–phonon coupling, doping and nonadiabatic effects," *Solid State Communications,* vol. 143, no. 1-2, pp. 47-57, 2007.

[96] K. Krishnamoorthy, M. Veerapandian, K. Yun and S.-J. Kim, "The chemical and structural analysis of graphene oxide with different degrees of oxidation," *Carbon,* vol. 53, pp. 38-49, 2013.

[97] M. Kalin, M. Zalaznik and S. Novak, "Wear and friction behaviour of poly-ether-ether-ketone (PEEK) filled with graphene, WS2 and CNT nanoparticles," *Wear,* Vols. 332-333, pp. 855-862, 2014.

[98] A. Chij, A. Ansón-Casaos and J. Puértolas, "Frictional and mechanical behavior of graphene/UHMWPE composite coatings," *Tribology International,* vol. 116, pp. 295-302, 2017.

[99] K.-L. Tung and K.-T. Lu, "Effect of tacticity of PMMA on gas transport through membranes: MD and MC simulation studies," *Journal of Membrane Science,* vol. 272, no. 1-2, pp. 37-49, 2006.

[100] C. Wei, D. Srivastava and K. Cho, "Thermal Expansion and Diffusion Coefficients of Carbon Nanotube-Polymer Composites," *Nano Letters,* vol. 2, no. 6, pp. 647-650, 2002.

[101] A. K. Hussain, I. Sudin, U. M. Basheer and M. Z. M. Yusop, "A review on graphene-based polymer composite coatings for the corrosion protection of metals," *Corrosion Reviews,* vol. 37, no. 4, pp. 343-363, 2019.

[102] H. N. Othman, C. M. Ismail, M. Mustapha, N. Sallih, K. E. Kee and R. A. Jaal, "Graphene-based polymer nanocomposites as barrier coatings for corrosion protection," *Progress in Organic Coatings,* vol. 135, pp. 82-99, 2019.

[103] S. Liu, L. Gu, H. Zhao, J. Chen and H. Yu, "Corrosion Resistance of Graphene-Reinforced Waterborne Epoxy," *Journal of Materials Science & Technology,* vol. 32, pp. 425-431, 2016.

[104] Y. González-García, S. González and R. M. Souto, "Electrochemical and structural properties of a polyurethane coating on steel substrates for corrosion protection," *Corrosion Science,* vol. 49, no. 9, pp. 3514-3526, 2007.

[105] R. M. Souto, L. Fernández-Mérida, S. Gonzáles and J. D. Scantlebury, "Comparative EIS study of different Zn-based intermediate metallic layers in coil-coated steels," *Corrosion Science,* vol. 48, no. 5, pp. 1182-1192, 2006.

[106] A. S. Castela, A. M. Simões and M. G. Ferreira, "E.I.S. evaluation of attached and free polymer films," *Progress in Organic Coatings,* vol. 38, pp. 1-7, 2000.

[107] G. P. Bierwagen, "Corrosion and Its Control by Coatings," in *Organic Coatings for Corrosion Control*, Washington, DC, American Chemical Society, 1998, pp. 1-8.

[108] C. Moreno, S. Hernández, J. J. Santana, J. González-Guzmán, R. M. Souto and S. González, "Characterization of Water Uptake by Organic Coatings Used for the Corrosion Protection of Steel as Determined from Capacitance Measurements," *International Journal of Electrochemical Science,* vol. 7, pp. 7390-7403, 2012.

7 Appendix 1 – SEM Images of the Pigments

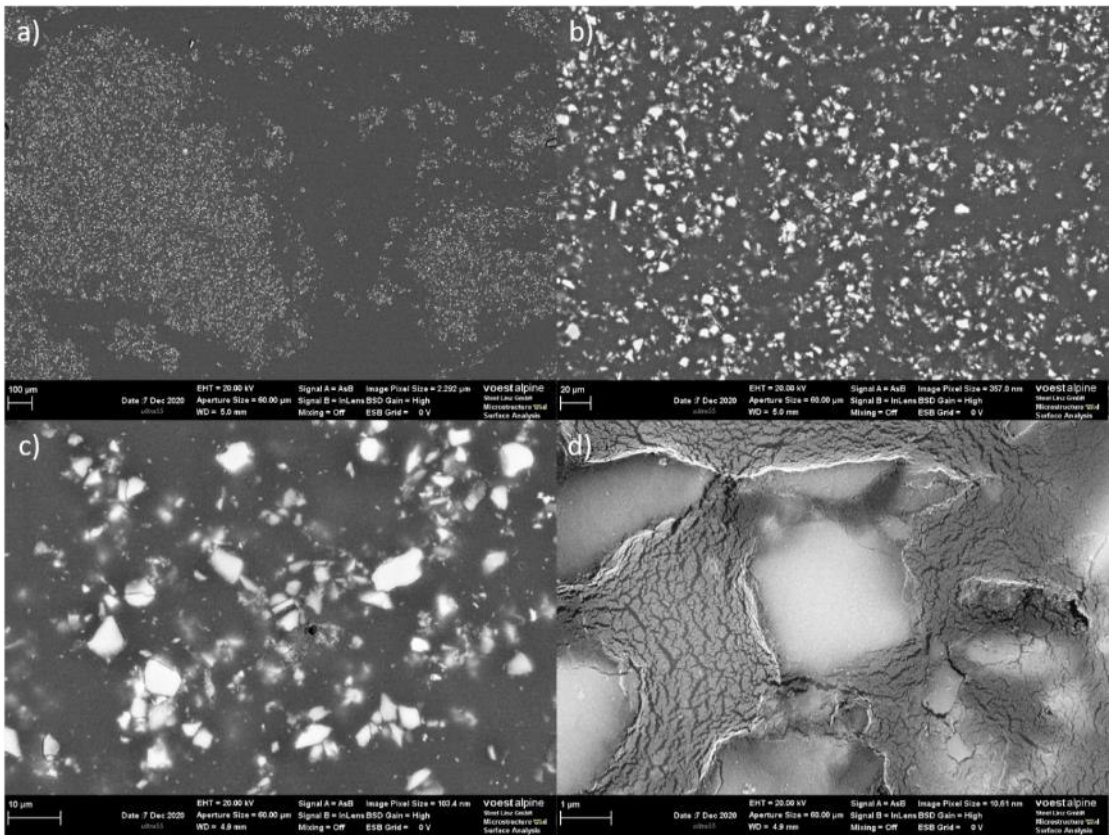

Figure 60: SEM images of Novinox XCA02 at different magnifications: a) 50, b) 1,000, c) 3,000, d) 30,000.

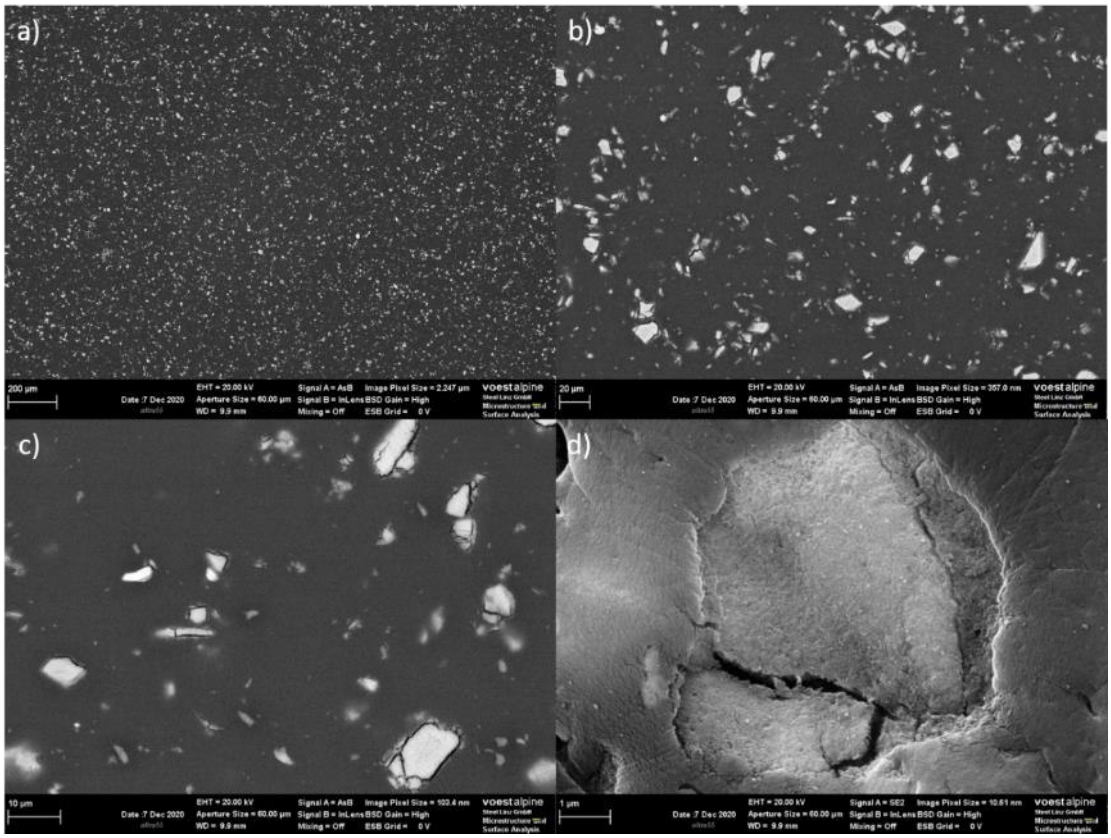

Figure 61: SEM images of Novinox PAT30 at different magnifications: a) 50, b) 1,000, c) 3,000, d) 30,000.

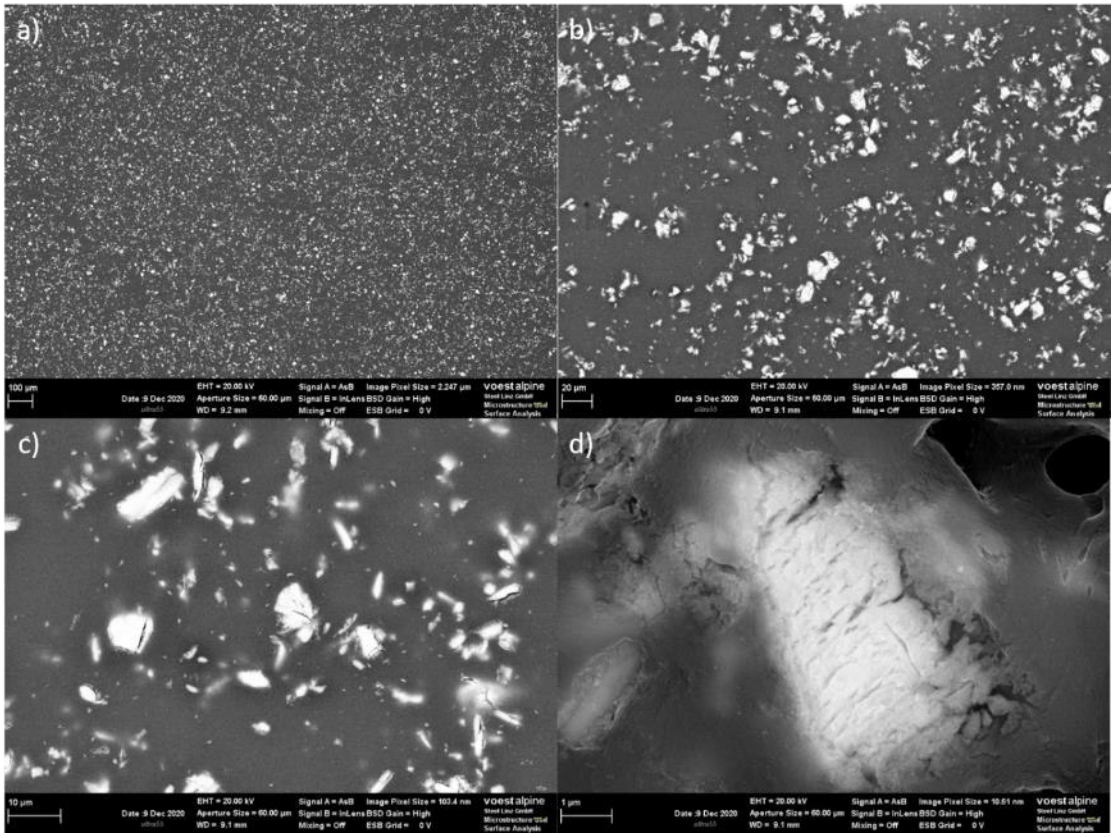

Figure 62: SEM images of Novinox PAT15 at different magnifications: a) 50, b) 1,000, c) 3,000, d) 30,000.

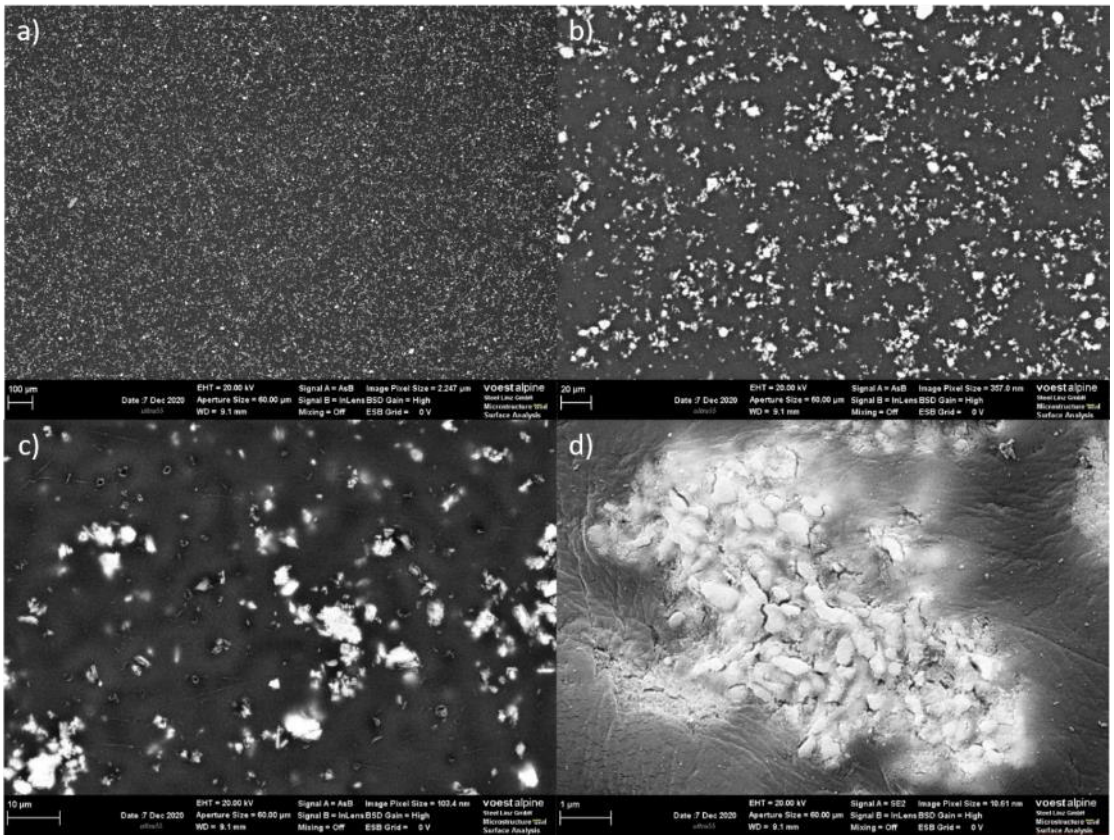

Figure 63: SEM images of Novinox PAM at different magnifications: a) 50, b) 1,000, c) 3,000, d) 30,000.

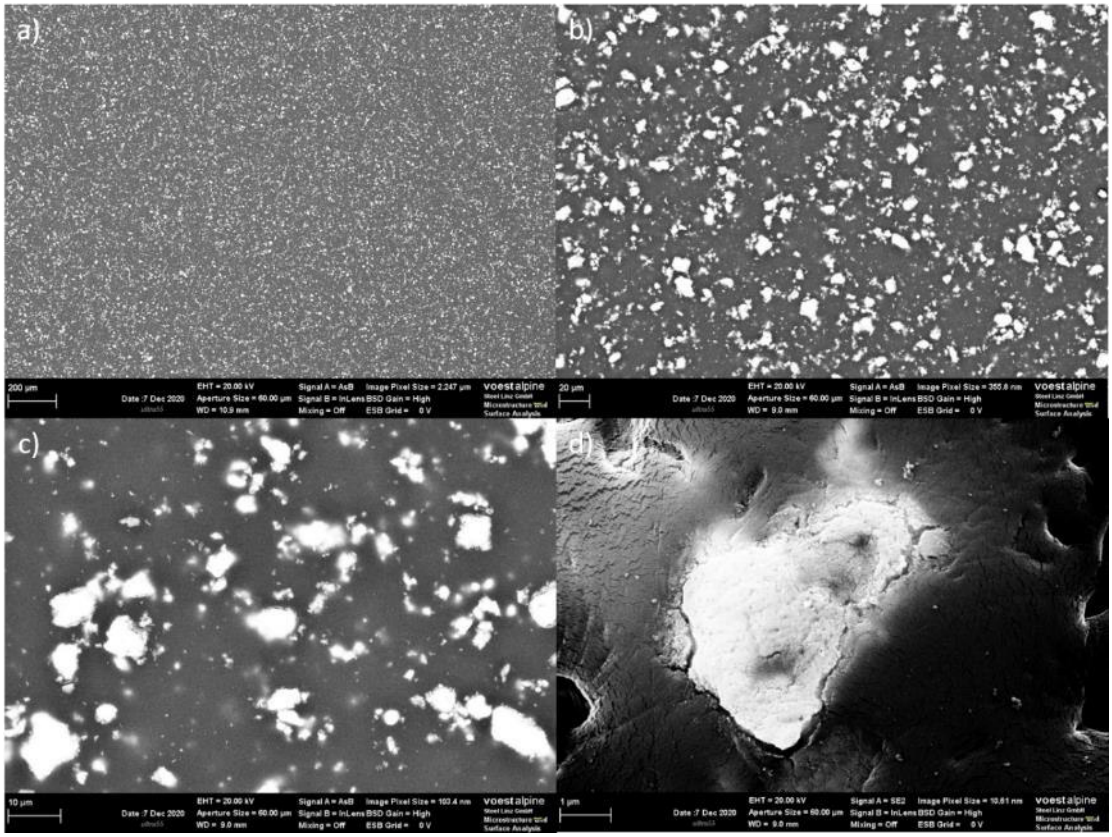

Figure 64: SEM images of Novinox PC01 at different magnifications: a) 50, b) 1,000, c) 3,000, d) 30,000.

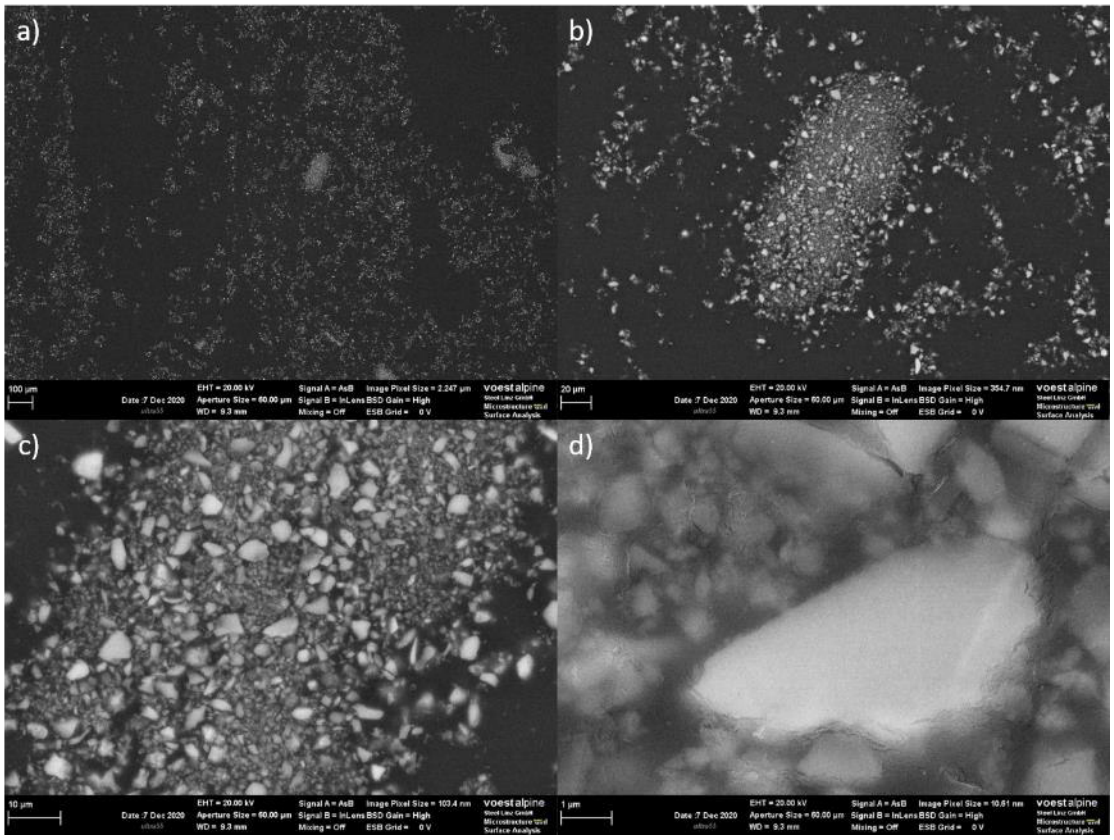

Figure 65: SEM images of Shieldex C303 at different magnifications: a) 50, b) 1,000, c) 3,000, d) 30,000.

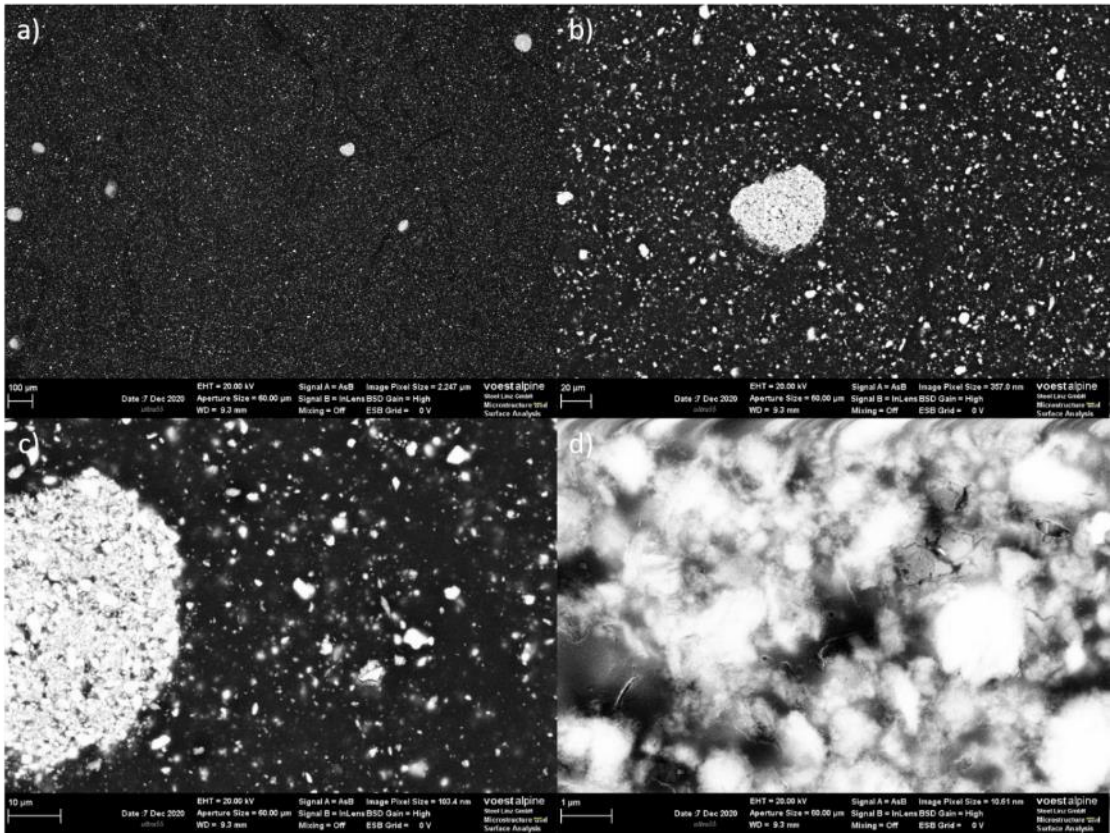

Figure 66: SEM images of Heucophos CMP at different magnifications: a) 50, b) 1,000, c) 3,000, d) 30,000.

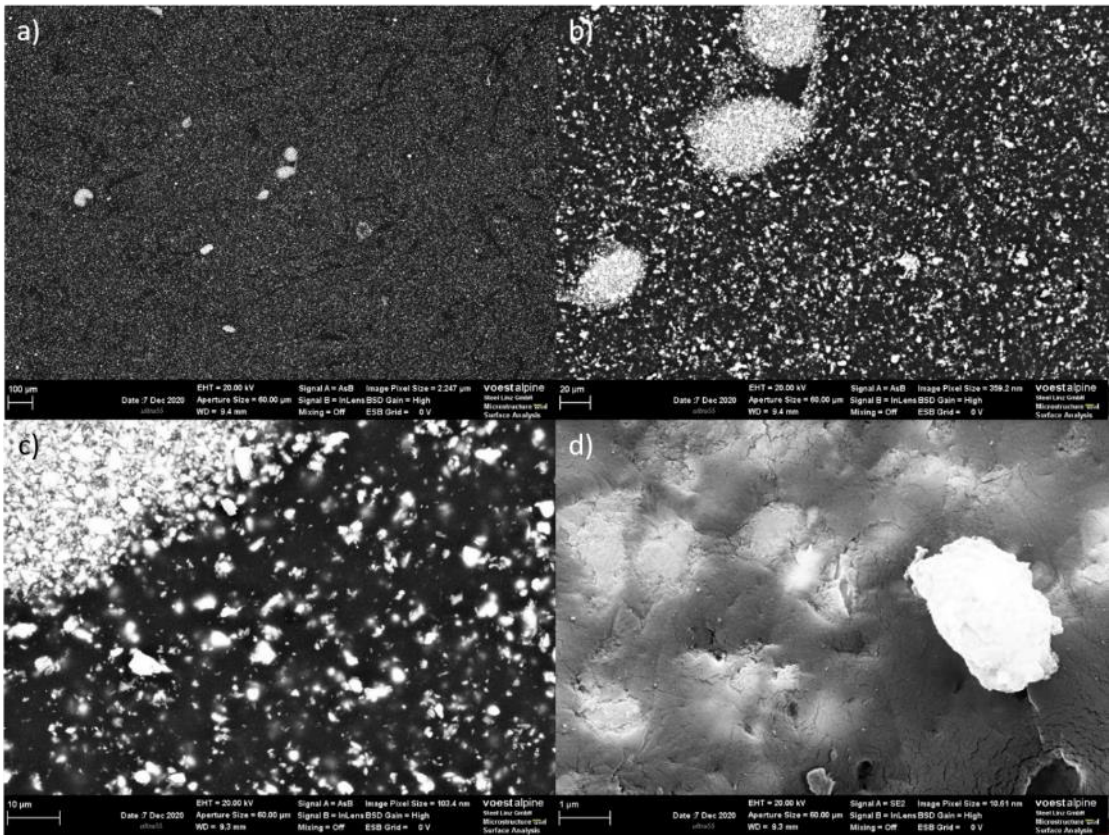

Figure 67: SEM images of Heucophos SRPP at different magnifications: a) 50, b) 1,000, c) 3,000, d) 30,000.

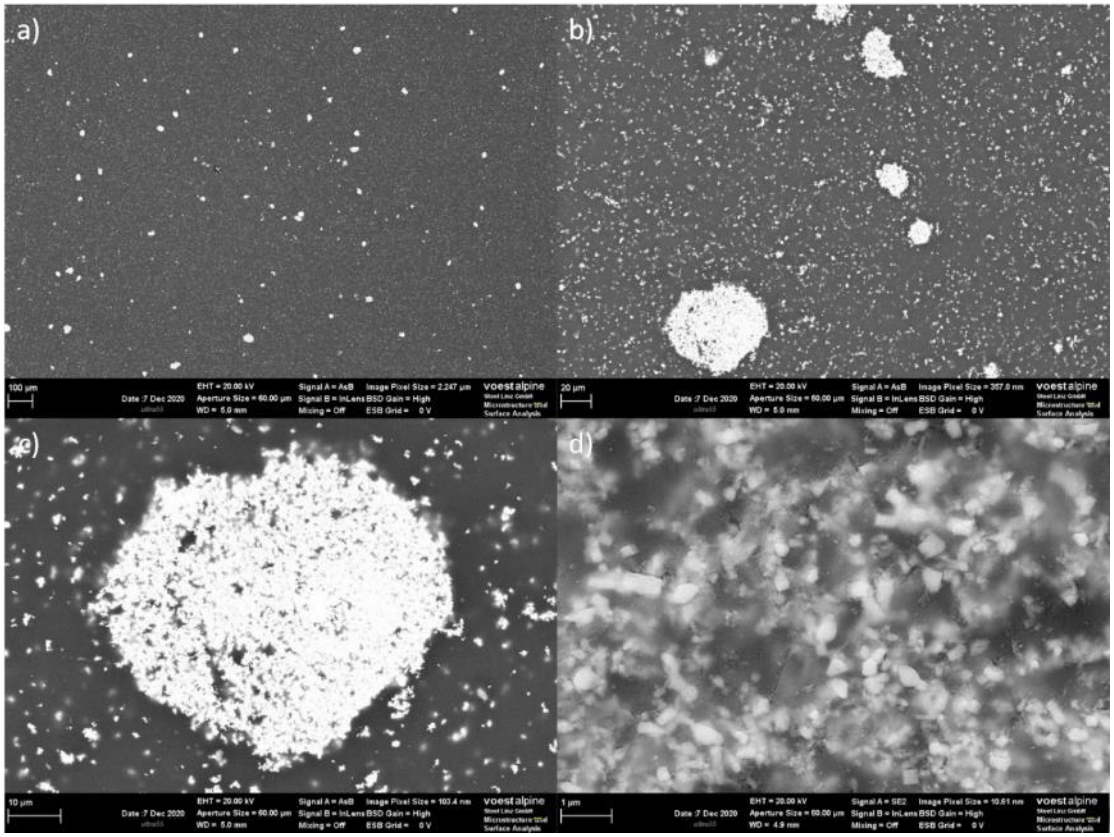

Figure 68: SEM images of zinc white resin seal CF at different magnifications: a) 50, b) 1,000, c) 3,000, d) 30,000.

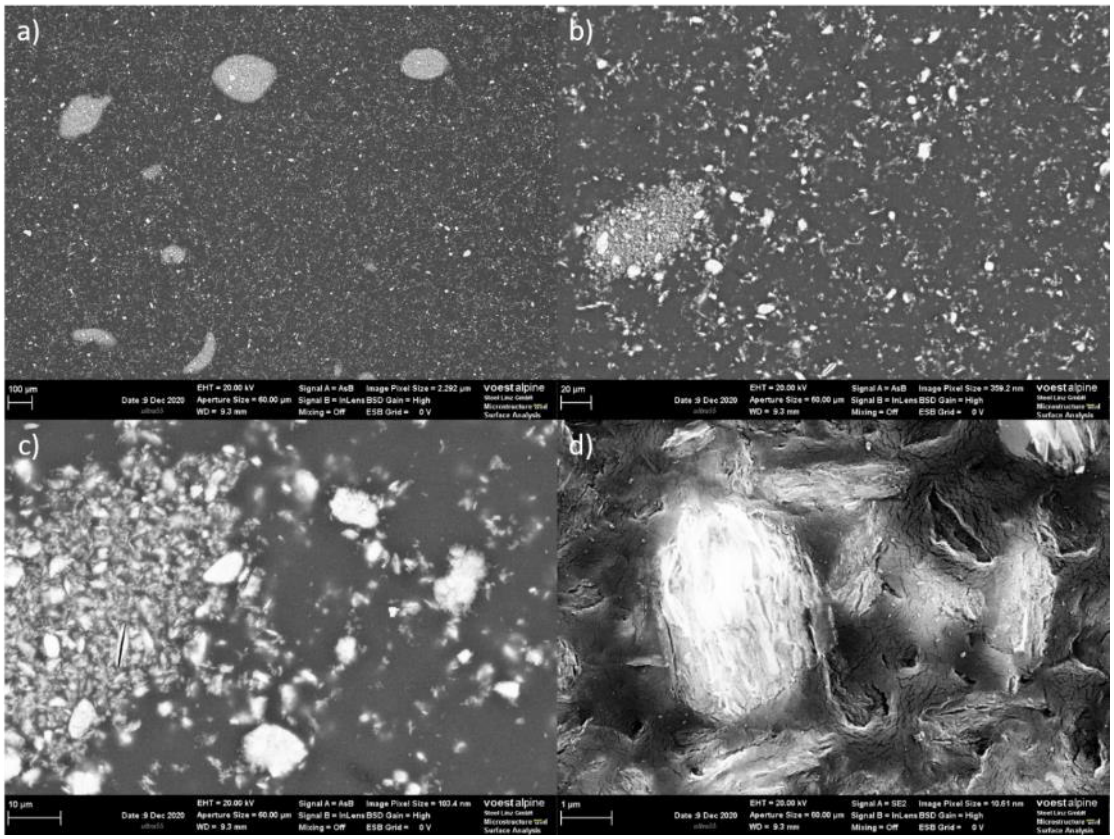

Figure 69: SEM images of ASP 600 at different magnifications: a) 50, b) 1,000, c) 3,000, d) 30,000.

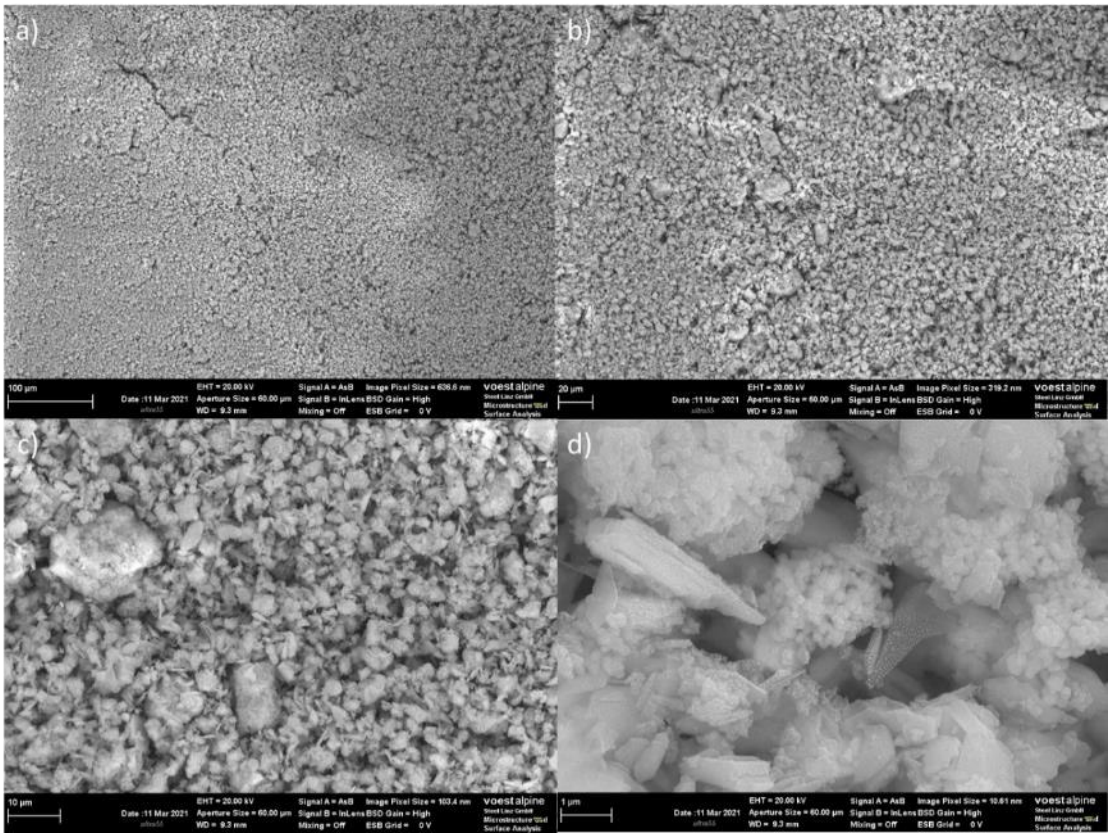

Figure 70: SEM images of K-White G 730 at different magnifications: a) 500, b) 1,000, c) 3,000, d) 30,000.

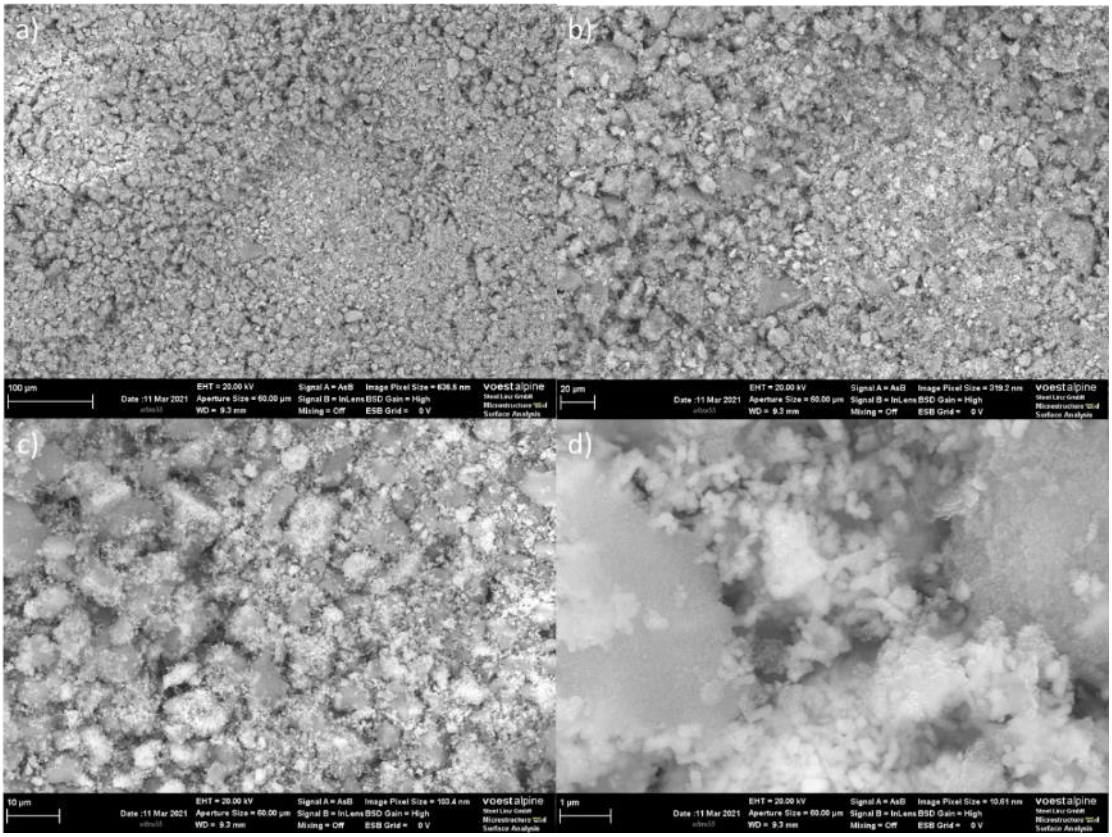

Figure 71: SEM images of K-White TC 720 at different magnifications: a) 500, b) 1,000, c) 3,000, d) 30,000.

8 Appendix 2 – Publication List and Copyright Agreements

1. S. Wiener, B. Strauß, G. Luckeneder, J. Hagler and M. Valtiner, "Thermoset thin film primers: Influence of substrate, layer," Materials and Corrosion, vol. 74, no. 8, p. 1183-1195, 2023.

2. S. Wiener, B. Strauß, G. Luckeneder, J.-F. Hagler and M. Valtiner, "Evaluation of a commercial graphene-additive for boosting the corrosion performance of a thermal curing primer," Materials and Corrosion, vol. 74, no. 10, pp. 1416-142, 2023.

CCC Marketplace

Order Number: 1385228
Order Date: 11 Aug 2023

Payment Information

Simon Wiener
wiener.simon@gmail.com
Payment method: Invoice

Billing Address:
Mr. Simon Wiener
Rainerstraße 23A
Linz
Austria

+43 6706075551
wiener.simon@gmail.com

Customer Location:
Mr. Simon Wiener
Rainerstraße 23A
Linz
Austria

Order Details

1. Materials and corrosion

Billing Status: Open

Article: Thermoset thin film primers: Influence of substrate, layer thickness and wettability of additives in laboratory testing

Order License ID	1385228-1	**Type of Use**	Republish in a thesis/dissertation
Order detail status	Completed		
ISSN	0947-5117	**Publisher**	WILEY - V C H VERLAG GMBH & CO. KGAA
		Portion	Chapter/article

0,00 EUR
Republication Permission

LICENSED CONTENT

Publication Title	Materials and corrosion	**Publication Type**	Journal
Article Title	Thermoset thin film primers: Influence of substrate, layer thickness and wettability of additives in laboratory testing	**Start Page**	1183
		End Page	1195
		Issue	8
		Volume	74
Date	01/01/1995		
Language	English, German		
Country	Germany		
Rightsholder	John Wiley & Sons - Books		

REQUEST DETAILS

Portion Type	Chapter/article	**Rights Requested**	Main product
Page Range(s)	1183-1195	**Distribution**	Worldwide
Total Number of Pages	13	**Translation**	Original language of publication
Format (select all that apply)	Print, Electronic	**Copies for the Disabled?**	Yes
Who Will Republish the Content?	Academic institution	**Minor Editing Privileges?**	Yes
		Incidental Promotional Use?	No
Duration of Use	Life of current and all future editions	**Currency**	EUR
Lifetime Unit Quantity	Up to 499		

NEW WORK DETAILS

Title	Use of Complementary Testing Technology for the Evaluation of the Characteristics of Different Systems	**Institution Name**	TU Wien
		Expected Presentation Date	2023-11-01

Instructor Name	Markus Valtiner

ADDITIONAL DETAILS

The Requesting Person/Organization to Appear on the License	Simon Wiener

REQUESTED CONTENT DETAILS

Title, Description or Numeric Reference of the Portion(s)	Thermoset thin film primers: Influence of substrate, layer thickness and wettability of additives in laboratory testing	**Title of the Article/Chapter the Portion Is From**	Thermoset thin film primers: Influence of substrate, layer thickness and wettability of additives in laboratory testing
Editor of Portion(s)	Wiener, Simon; Strauß, Bernhard; Luckeneder, Gerald; Hagler, Josef; Valtiner, Markus	**Author of Portion(s)**	Wiener, Simon; Strauß, Bernhard; Luckeneder, Gerald; Hagler, Josef; Valtiner, Markus
Volume / Edition	74	**Publication Date of Portion**	2023-08-01
Page or Page Range of Portion	1183-1195		

John Wiley & Sons - Books Terms and Conditions

No right, license or interest to any trademark, trade name, service mark or other branding ("Marks") of WILEY or its licensors is granted hereunder, and you agree that you shall not assert any such right, license or interest with respect thereto. You may not alter, remove or suppress in any manner any copyright, trademark or other notices displayed by the Wiley material. This Agreement will be void if the Type of Use, Format, Circulation, or Requestor Type was misrepresented during the licensing process. In no instance may the total amount of Wiley Materials used in any Main Product, Compilation or Collective work comprise more than 5% (if figures/tables) or 15% (if full articles/chapters) of the (entirety of the) Main Product, Compilation or Collective Work. Some titles may be available under an Open Access license. It is the Licensors' responsibility to identify the type of Open Access license on which the requested material was published, and comply fully with the terms of that license for the type of use specified Further details can be found on Wiley Online Library http://olabout.wiley.com/WileyCDA/Section/id-410895.html.

John Wiley & Sons - Books Special Terms and Conditions

Total Items: 1

Subtotal: 0,00 EUR

Order Total: 0,00 EUR

Marketplace Permissions General Terms and Conditions

The following terms and conditions ("General Terms"), together with any applicable Publisher Terms and Conditions, govern User's use of Works pursuant to the Licenses granted by Copyright Clearance Center, Inc. ("CCC") on behalf of the applicable Rightsholders of such Works through CCC's applicable Marketplace transactional licensing services (each, a "Service").

1) **Definitions.** For purposes of these General Terms, the following definitions apply:

"License" is the licensed use the User obtains via the Marketplace platform in a particular licensing transaction, as set forth in the Order Confirmation.

"Order Confirmation" is the confirmation CCC provides to the User at the conclusion of each Marketplace transaction. "Order Confirmation Terms" are additional terms set forth on specific Order Confirmations not set forth in the General Terms that can include terms applicable to a particular CCC transactional licensing service and/or any Rightsholder-specific terms.

"Rightsholder(s)" are the holders of copyright rights in the Works for which a User obtains licenses via the Marketplace platform, which are displayed on specific Order Confirmations.

"Terms" means the terms and conditions set forth in these General Terms and any additional Order Confirmation Terms collectively.

"User" or "you" is the person or entity making the use granted under the relevant License. Where the person accepting the Terms on behalf of a User is a freelancer or other third party who the User authorized to accept the General Terms on the User's behalf, such person shall be deemed jointly a User for purposes of such Terms.

"Work(s)" are the copyright protected works described in relevant Order Confirmations.

2) **Description of Service.** CCC's Marketplace enables Users to obtain Licenses to use one or more Works in accordance with all relevant Terms. CCC grants Licenses as an agent on behalf of the copyright rightsholder identified in the relevant Order Confirmation.

3) **Applicability of Terms.** The Terms govern User's use of Works in connection with the relevant License. In the event of any conflict between General Terms and Order Confirmation Terms, the latter shall govern. User acknowledges that Rightsholders have complete discretion whether to grant any permission, and whether to place any limitations on any grant, and that CCC has no right to supersede or to modify any such discretionary act by a Rightsholder.

4) **Representations; Acceptance.** By using the Service, User represents and warrants that User has been duly authorized by the User to accept, and hereby does accept, all Terms.

5) **Scope of License; Limitations and Obligations.** All Works and all rights therein, including copyright rights, remain the sole and exclusive property of the Rightsholder. The License provides only those rights expressly set forth in the terms and conveys no other rights in any Works

6) **General Payment Terms.** User may pay at time of checkout by credit card or choose to be invoiced. If the User chooses to be invoiced, the User shall: (i) remit payments in the manner identified on specific invoices, (ii) unless otherwise specifically stated in an Order Confirmation or separate written agreement, Users shall remit payments upon receipt of the relevant invoice from CCC, either by delivery or notification of availability of the invoice via the Marketplace platform, and (iii) if the User does not pay the invoice within 30 days of receipt, the User may incur a service charge of 1.5% per month or the maximum rate allowed by applicable law, whichever is less. While User may exercise the rights in the License immediately upon receiving the Order Confirmation, the License is automatically revoked and is null and void, as if it had never been issued, if CCC does not receive complete payment on a timely basis.

7) **General Limits on Use.** Unless otherwise provided in the Order Confirmation, any grant of rights to User (i) involves only the rights set forth in the Terms and does not include subsequent or additional uses, (ii) is non-exclusive and non-transferable, and (iii) is subject to any and all limitations and restrictions (such as, but not limited to, limitations on duration of use or circulation) included in the Terms. Upon completion of the licensed use as set forth in the Order Confirmation, User shall either secure a new permission for further use of the Work(s) or immediately cease any new use of the Work(s) and shall render inaccessible (such as by deleting or by removing or severing links or other locators) any further copies of the Work. User may only make alterations to the Work if and as expressly set forth in the Order Confirmation. No Work may be used in any way that is unlawful, including without limitation if such use would violate applicable sanctions laws or regulations, would be defamatory, violate the rights of third parties (including such third parties' rights of copyright, privacy, publicity, or other tangible or intangible property), or is otherwise illegal, sexually explicit, or obscene. In addition, User may not conjoin a Work with any other material that may result in damage to the reputation of the Rightsholder. Any unlawful use will render any licenses hereunder null and void. User agrees to inform CCC if it becomes aware of any infringement of any rights in a Work and to cooperate with any reasonable request of CCC or the Rightsholder in connection therewith.

8) **Third Party Materials.** In the event that the material for which a License is sought includes third party materials (such as photographs, illustrations, graphs, inserts and similar materials) that are identified in such material as having been used by permission (or a similar indicator), User is responsible for identifying, and seeking separate licenses (under this Service, if available, or otherwise) for any of such third party materials; without a separate license, User may not use such third party materials via the License.

9) **Copyright Notice.** Use of proper copyright notice for a Work is required as a condition of any License granted under the Service. Unless otherwise provided in the Order Confirmation, a proper copyright notice will read substantially as follows: "Used with permission of [Rightsholder's name], from [Work's title, author, volume, edition number and year of copyright]; permission conveyed through Copyright Clearance Center, Inc." Such notice must be provided in a reasonably legible font size and must be placed either on a cover page or in another location that any person, upon gaining access to the material which is the subject of a permission, shall see, or in the case of republication Licenses, immediately adjacent to the Work as used (for example, as part of a by-line or footnote) or in the place where substantially all other credits or notices for the new work containing the republished Work are located. Failure to include the required notice results in loss to the Rightsholder and CCC, and the User shall be liable to pay liquidated damages for each such failure equal to twice the use fee specified in the Order Confirmation, in addition to the use fee itself and any other fees and charges specified.

10) **Indemnity.** User hereby indemnifies and agrees to defend the Rightsholder and CCC, and their respective employees and directors, against all claims, liability, damages, costs, and expenses, including legal fees and expenses, arising out of any use of a Work beyond the scope of the rights granted herein and in the Order Confirmation, or any use of a Work which has been altered in any unauthorized way by User, including claims of defamation or infringement of rights of copyright, publicity, privacy, or other tangible or intangible property.

11) **Limitation of Liability.** UNDER NO CIRCUMSTANCES WILL CCC OR THE RIGHTSHOLDER BE LIABLE FOR ANY DIRECT, INDIRECT, CONSEQUENTIAL, OR INCIDENTAL DAMAGES (INCLUDING WITHOUT LIMITATION DAMAGES FOR LOSS OF BUSINESS PROFITS OR INFORMATION, OR FOR BUSINESS INTERRUPTION) ARISING OUT OF THE USE OR INABILITY TO USE A WORK, EVEN IF ONE OR BOTH OF THEM HAS BEEN ADVISED OF THE POSSIBILITY OF SUCH DAMAGES. In any event, the total liability of the Rightsholder and CCC (including their respective employees and directors) shall not exceed the total amount actually paid by User for the relevant License. User assumes full liability for the actions and omissions of its principals, employees, agents, affiliates, successors, and assigns.

12) **Limited Warranties.** THE WORK(S) AND RIGHT(S) ARE PROVIDED "AS IS." CCC HAS THE RIGHT TO GRANT TO USER THE RIGHTS GRANTED IN THE ORDER CONFIRMATION DOCUMENT. CCC AND THE RIGHTSHOLDER DISCLAIM ALL OTHER WARRANTIES RELATING TO THE WORK(S) AND RIGHT(S), EITHER EXPRESS OR IMPLIED, INCLUDING WITHOUT LIMITATION IMPLIED WARRANTIES OF MERCHANTABILITY OR FITNESS FOR A PARTICULAR PURPOSE. ADDITIONAL RIGHTS MAY BE REQUIRED TO USE ILLUSTRATIONS, GRAPHS, PHOTOGRAPHS, ABSTRACTS, INSERTS, OR OTHER PORTIONS OF THE WORK (AS OPPOSED TO THE ENTIRE WORK) IN A MANNER CONTEMPLATED BY USER; USER UNDERSTANDS AND AGREES THAT NEITHER CCC NOR THE RIGHTSHOLDER MAY HAVE SUCH ADDITIONAL RIGHTS TO GRANT.

13) **Effect of Breach.** Any failure by User to pay any amount when due, or any use by User of a Work beyond the scope of the License set forth in the Order Confirmation and/or the Terms, shall be a material breach of such License. Any breach not cured within 10 days of written notice thereof shall result in immediate termination of such License without further notice. Any unauthorized (but licensable) use of a Work that is terminated immediately upon notice thereof may be liquidated by payment of the Rightsholder's ordinary license price therefor; any unauthorized (and unlicensable) use that is not terminated immediately for any reason (including, for example, because materials containing the Work cannot reasonably be recalled) will be subject to all remedies available at law or in equity, but in no event to a payment of less than three times the Rightsholder's ordinary license price for the most closely analogous licensable use plus Rightsholder's and/or CCC's costs and expenses incurred in collecting such payment.

14) **Additional Terms for Specific Products and Services.** If a User is making one of the uses described in this Section 14, the additional terms and conditions apply:

a) ***Print Uses of Academic Course Content and Materials (photocopies for academic coursepacks or classroom handouts).*** For photocopies for academic coursepacks or classroom handouts the following additional terms apply:

i) The copies and anthologies created under this License may be made and assembled by faculty members individually or at their request by on-campus bookstores or copy centers, or by off-campus copy shops and other similar entities.

ii) No License granted shall in any way: (i) include any right by User to create a substantively non-identical copy of the Work or to edit or in any other way modify the Work (except by means of deleting material immediately preceding or following the entire portion of the Work copied) (ii) permit "publishing ventures" where any particular anthology would be systematically marketed at multiple institutions.

iii) Subject to any Publisher Terms (and notwithstanding any apparent contradiction in the Order Confirmation arising from data provided by User), any use authorized under the academic pay-per-use service is limited as follows:

A) any License granted shall apply to only one class (bearing a unique identifier as assigned by the institution, and thereby including all sections or other subparts of the class) at one institution;

B) use is limited to not more than 25% of the text of a book or of the items in a published collection of essays, poems or articles;

C) use is limited to no more than the greater of (a) 25% of the text of an issue of a journal or other periodical or (b) two articles from such an issue;

D) no User may sell or distribute any particular anthology, whether photocopied or electronic, at more than one institution of learning;

E) in the case of a photocopy permission, no materials may be entered into electronic memory by User except in order to produce an identical copy of a Work before or during the academic term (or analogous period) as to which any particular permission is granted. In the event that User shall choose to retain materials that are the subject of a photocopy permission in electronic memory for purposes of producing identical copies more than one day after such retention (but still within the scope of any permission granted), User must notify CCC of such fact in the applicable permission request and such retention shall constitute one copy actually sold for purposes of calculating permission fees due; and

F) any permission granted shall expire at the end of the class. No permission granted shall in any way include any right by User to create a substantively non-identical copy of the Work or to edit or in any other way modify the Work (except by means of deleting material immediately preceding or following the entire portion of the Work copied).

iv) Books and Records; Right to Audit. As to each permission granted under the academic pay-per-use Service, User shall maintain for at least four full calendar years books and records sufficient for CCC to determine the numbers of copies made by User under such permission. CCC and any representatives it may designate shall have the right to audit such books and records at any time during User's ordinary business hours, upon two days' prior notice. If any such audit shall determine that User shall have underpaid for, or underreported, any photocopies sold or by three percent (3%) or more, then User shall bear all the costs of any such audit; otherwise, CCC shall bear the costs of any such audit. Any amount determined by such audit to have been underpaid by User shall immediately be paid to CCC by User, together with interest thereon at the rate of 10% per annum from the date such amount was originally due. The provisions of this paragraph shall survive the termination of this License for any reason.

b) ***Digital Pay-Per-Uses of Academic Course Content and Materials (e-coursepacks, electronic reserves, learning management systems, academic institution intranets).*** For uses in e-coursepacks, posts in electronic reserves, posts in learning management systems, or posts on academic institution intranets, the following additional terms apply:

i) The pay-per-uses subject to this Section 14(b) include:

A) **Posting e-reserves, course management systems, e-coursepacks for text-based content,** which grants authorizations to import requested material in electronic format, and allows electronic access to this material to members of a designated college or university class, under the direction of an instructor designated by the college or university, accessible only under appropriate electronic controls (e.g., password);

B) **Posting e-reserves, course management systems, e-coursepacks for material consisting of photographs or other still images not embedded in text,** which grants not only the authorizations described in Section 14(b)(i)(A) above, but also the following authorization: to include the requested material in course materials for use consistent with Section 14(b)(i)(A) above, including any necessary resizing, reformatting or modification of the resolution of such requested material

(provided that such modification does not alter the underlying editorial content or meaning of the requested material, and provided that the resulting modified content is used solely within the scope of, and in a manner consistent with, the particular authorization described in the Order Confirmation and the Terms), but not including any other form of manipulation, alteration or editing of the requested material;

C) **Posting e-reserves, course management systems, e-coursepacks or other academic distribution for audiovisual content,** which grants not only the authorizations described in Section 14(b)(i)(A) above, but also the following authorizations: (i) to include the requested material in course materials for use consistent with Section 14(b)(i)(A) above; (ii) to display and perform the requested material to such members of such class in the physical classroom or remotely by means of streaming media or other video formats; and (iii) to "clip" or reformat the requested material for purposes of time or content management or ease of delivery, provided that such “clipping” or reformatting does not alter the underlying editorial content or meaning of the requested material and that the resulting material is used solely within the scope of, and in a manner consistent with, the particular authorization described in the Order Confirmation and the Terms. Unless expressly set forth in the relevant Order Conformation, the License does not authorize any other form of manipulation, alteration or editing of the requested material.

ii) Unless expressly set forth in the relevant Order Confirmation, no License granted shall in any way: (i) include any right by User to create a substantively non-identical copy of the Work or to edit or in any other way modify the Work (except by means of deleting material immediately preceding or following the entire portion of the Work copied or, in the case of Works subject to Sections 14(b)(1)(B) or (C) above, as described in such Sections) (ii) permit "publishing ventures" where any particular course materials would be systematically marketed at multiple institutions.

iii) Subject to any further limitations determined in the Rightsholder Terms (and notwithstanding any apparent contradiction in the Order Confirmation arising from data provided by User), any use authorized under the electronic course content pay-per-use service is limited as follows:

A) any License granted shall apply to only one class (bearing a unique identifier as assigned by the institution, and thereby including all sections or other subparts of the class) at one institution;

B) use is limited to not more than 25% of the text of a book or of the items in a published collection of essays, poems or articles;

C) use is limited to not more than the greater of (a) 25% of the text of an issue of a journal or other periodical or (b) two articles from such an issue;

D) no User may sell or distribute any particular materials, whether photocopied or electronic, at more than one institution of learning;

E) electronic access to material which is the subject of an electronic-use permission must be limited by means of electronic password, student identification or other control permitting access solely to students and instructors in the class;

F) User must ensure (through use of an electronic cover page or other appropriate means) that any person, upon gaining electronic access to the material, which is the subject of a permission, shall see:

- a proper copyright notice, identifying the Rightsholder in whose name CCC has granted permission,
- a statement to the effect that such copy was made pursuant to permission,
- a statement identifying the class to which the material applies and notifying the reader that the material has been made available electronically solely for use in the class, and
- a statement to the effect that the material may not be further distributed to any person outside the class, whether by copying or by transmission and whether electronically or in paper form, and User must also ensure that such cover page or other means will print out in the event that the person accessing the material chooses to print out the material or any part thereof.

G) any permission granted shall expire at the end of the class and, absent some other form of authorization, User is thereupon required to delete the applicable material from any electronic storage or to block electronic access to the applicable material.

iv) Uses of separate portions of a Work, even if they are to be included in the same course material or the same university or college class, require separate permissions under the electronic course content pay-per-use Service. Unless otherwise provided in the Order Confirmation, any grant of rights to User is limited to use completed no later than the end of the academic term (or analogous period) as to which any particular permission is granted.

v) Books and Records; Right to Audit. As to each permission granted under the electronic course content Service, User shall maintain for at least four full calendar years books and records sufficient for CCC to determine the numbers of copies made by User under such permission. CCC and any representatives it may designate shall have the right to audit such books and records at any time during User's ordinary business hours, upon two days' prior notice. If any such audit shall determine that User shall have underpaid for, or underreported, any electronic copies used by three percent (3%) or more, then User shall bear all the costs of any such audit; otherwise, CCC shall bear the costs of any such audit. Any amount determined by such audit to have been underpaid by User shall immediately be paid to CCC by User, together with interest thereon at the rate of

10% per annum from the date such amount was originally due. The provisions of this paragraph shall survive the termination of this license for any reason.

c) ***Pay-Per-Use Permissions for Certain Reproductions (Academic photocopies for library reserves and interlibrary loan reporting) (Non-academic internal/external business uses and commercial document delivery).*** The License expressly excludes the uses listed in Section (c)(i)-(v) below (which must be subject to separate license from the applicable Rightsholder) for: academic photocopies for library reserves and interlibrary loan reporting; and non-academic internal/external business uses and commercial document delivery.

i) electronic storage of any reproduction (whether in plain-text, PDF, or any other format) other than on a transitory basis;

ii) the input of Works or reproductions thereof into any computerized database;

iii) reproduction of an entire Work (cover-to-cover copying) except where the Work is a single article;

iv) reproduction for resale to anyone other than a specific customer of User;

v) republication in any different form. Please obtain authorizations for these uses through other CCC services or directly from the rightsholder.

Any license granted is further limited as set forth in any restrictions included in the Order Confirmation and/or in these Terms.

d) ***Electronic Reproductions in Online Environments (Non-Academic-email, intranet, internet and extranet).*** For "electronic reproductions", which generally includes e-mail use (including instant messaging or other electronic transmission to a defined group of recipients) or posting on an intranet, extranet or Intranet site (including any display or performance incidental thereto), the following additional terms apply:

i) Unless otherwise set forth in the Order Confirmation, the License is limited to use completed within 30 days for any use on the Internet, 60 days for any use on an intranet or extranet and one year for any other use, all as measured from the "republication date" as identified in the Order Confirmation, if any, and otherwise from the date of the Order Confirmation.

ii) User may not make or permit any alterations to the Work, unless expressly set forth in the Order Confirmation (after request by User and approval by Rightsholder); provided, however, that a Work consisting of photographs or other still images not embedded in text may, if necessary, be resized, reformatted or have its resolution modified without additional express permission, and a Work consisting of audiovisual content may, if necessary, be "clipped" or reformatted for purposes of time or content management or ease of delivery (provided that any such resizing, reformatting, resolution modification or “clipping” does not alter the underlying editorial content or meaning of the Work used, and that the resulting material is used solely within the scope of, and in a manner consistent with, the particular License described in the Order Confirmation and the Terms.

15) **Miscellaneous.**

a) User acknowledges that CCC may, from time to time, make changes or additions to the Service or to the Terms, and that Rightsholder may make changes or additions to the Rightsholder Terms. Such updated Terms will replace the prior terms and conditions in the order workflow and shall be effective as to any subsequent Licenses but shall not apply to Licenses already granted and paid for under a prior set of terms.

b) Use of User-related information collected through the Service is governed by CCC's privacy policy, available online at www.copyright.com/about/privacy-policy/.

c) The License is personal to User. Therefore, User may not assign or transfer to any other person (whether a natural person or an organization of any kind) the License or any rights granted thereunder; provided, however, that, where applicable, User may assign such License in its entirety on written notice to CCC in the event of a transfer of all or substantially all of User's rights in any new material which includes the Work(s) licensed under this Service.

d) No amendment or waiver of any Terms is binding unless set forth in writing and signed by the appropriate parties, including, where applicable, the Rightsholder. The Rightsholder and CCC hereby object to any terms contained in any writing prepared by or on behalf of the User or its principals, employees, agents or affiliates and purporting to govern or otherwise relate to the License described in the Order Confirmation, which terms are in any way inconsistent with any Terms set forth in the Order Confirmation, and/or in CCC's standard operating procedures, whether such writing is prepared prior to, simultaneously with or subsequent to the Order Confirmation, and whether such writing appears on a copy of the Order Confirmation or in a separate instrument.

e) The License described in the Order Confirmation shall be governed by and construed under the law of the State of New York, USA, without regard to the principles thereof of conflicts of law. Any case, controversy, suit, action, or proceeding arising out of, in connection with, or related to such License shall be brought, at CCC's sole discretion, in any federal or state court located in the County of New York, State of New York, USA, or in any federal or state court whose geographical jurisdiction covers the location of the Rightsholder set forth in the Order Confirmation. The parties expressly submit to the personal jurisdiction and venue of each such federal or state court.

Last updated October 2022

CCC Marketplace

Order Number: 1400156
Order Date: 25 Sep 2023

Payment Information

Simon Wiener
wiener.simon@gmail.com
Payment method: Invoice

Billing Address:
Mr. Simon Wiener
Rainerstraße 23A
Linz
Austria

+43 6706075551
wiener.simon@gmail.com

Customer Location:
Mr. Simon Wiener
Rainerstraße 23A
Linz
Austria

Order Details

1. Materials and corrosion

Billing Status: Open

Article: Evaluation of a commercial graphene-additive for boosting the corrosion performance of a thermal curing primer

Order License ID	1400156-1	**Type of Use**	Republish in a thesis/dissertation
Order detail status	Completed		
ISSN	0947-5117	**Publisher**	WILEY - V C H VERLAG GMBH & CO. KGAA
		Portion	Chapter/article

0,00 EUR
Republication Permission

LICENSED CONTENT

Publication Title	Materials and corrosion	**Country**	Germany
Article Title	Evaluation of a commercial graphene-additive for boosting the corrosion performance of a thermal curing primer	**Rightsholder**	John Wiley & Sons - Books
		Publication Type	Journal
Date	01/01/1995		
Language	English, German		

REQUEST DETAILS

Portion Type	Chapter/article	**Rights Requested**	Main product
Page Range(s)	n/a	**Distribution**	Worldwide
Total Number of Pages	13	**Translation**	Original language of publication
Format (select all that apply)	Print, Electronic	**Copies for the Disabled?**	No
Who Will Republish the Content?	Publisher, not-for-profit	**Minor Editing Privileges?**	Yes
		Incidental Promotional Use?	No
Duration of Use	Life of current edition	**Currency**	EUR
Lifetime Unit Quantity	Up to 499		

NEW WORK DETAILS

Title	Use of Complementary Testing Technology for the Evaluation of the Characteristics of Different Systems	**Institution Name**	TU Wien
		Expected Presentation Date	2023-11-27
Instructor Name	Markus Valtiner		

ADDITIONAL DETAILS

The Requesting Person/Organization to Appear on the License	Simon Wiener

REQUESTED CONTENT DETAILS

Title, Description or Numeric Reference of the Portion(s)	Evaluation of a commercial graphene-additive for boosting the corrosion performance of a thermal curing primer	**Title of the Article/Chapter the Portion Is From**	Evaluation of a commercial graphene-additive for boosting the corrosion performance of a thermal curing primer
Editor of Portion(s)	Wiener, Simon; Strauß, Bernhard; Luckeneder, Gerald; Hagler, Josef; Valtiner, Markus	**Author of Portion(s)**	Wiener, Simon; Strauß, Bernhard; Luckeneder, Gerald; Hagler, Josef; Valtiner, Markus
Volume / Edition	n/a	**Publication Date of Portion**	2023-06-12
Page or Page Range of Portion	n/a		

John Wiley & Sons - Books Terms and Conditions

No right, license or interest to any trademark, trade name, service mark or other branding ("Marks") of WILEY or its licensors is granted hereunder, and you agree that you shall not assert any such right, license or interest with respect thereto. You may not alter, remove or suppress in any manner any copyright, trademark or other notices displayed by the Wiley material. This Agreement will be void if the Type of Use, Format, Circulation, or Requestor Type was misrepresented during the licensing process. In no instance may the total amount of Wiley Materials used in any Main Product, Compilation or Collective work comprise more than 5% (if figures/tables) or 15% (if full articles/chapters) of the (entirety of the) Main Product, Compilation or Collective Work. Some titles may be available under an Open Access license. It is the Licensors' responsibility to identify the type of Open Access license on which the requested material was published, and comply fully with the terms of that license for the type of use specified Further details can be found on Wiley Online Library http://olabout.wiley.com/WileyCDA/Section/id-410895.html.

Total Items: 1

Subtotal: 0,00 EUR

Order Total: 0,00 EUR

Marketplace Permissions General Terms and Conditions

The following terms and conditions ("General Terms"), together with any applicable Publisher Terms and Conditions, govern User's use of Works pursuant to the Licenses granted by Copyright Clearance Center, Inc. ("CCC") on behalf of the applicable Rightsholders of such Works through CCC's applicable Marketplace transactional licensing services (each, a "Service").

1) **Definitions.** For purposes of these General Terms, the following definitions apply:

"License" is the licensed use the User obtains via the Marketplace platform in a particular licensing transaction, as set forth in the Order Confirmation.

"Order Confirmation" is the confirmation CCC provides to the User at the conclusion of each Marketplace transaction. "Order Confirmation Terms" are additional terms set forth on specific Order Confirmations not set forth in the General Terms that can include terms applicable to a particular CCC transactional licensing service and/or any Rightsholder-specific terms.

"Rightsholder(s)" are the holders of copyright rights in the Works for which a User obtains licenses via the Marketplace platform, which are displayed on specific Order Confirmations.

"Terms" means the terms and conditions set forth in these General Terms and any additional Order Confirmation Terms collectively.

"User" or "you" is the person or entity making the use granted under the relevant License. Where the person accepting the Terms on behalf of a User is a freelancer or other third party who the User authorized to accept the General Terms on the User's behalf, such person shall be deemed jointly a User for purposes of such Terms.

"Work(s)" are the copyright protected works described in relevant Order Confirmations.

2) **Description of Service.** CCC's Marketplace enables Users to obtain Licenses to use one or more Works in accordance with all relevant Terms. CCC grants Licenses as an agent on behalf of the copyright rightsholder identified in the relevant Order Confirmation.

3) **Applicability of Terms.** The Terms govern User's use of Works in connection with the relevant License. In the event of any conflict between General Terms and Order Confirmation Terms, the latter shall govern. User acknowledges that Rightsholders have complete discretion whether to grant any permission, and whether to place any limitations on any grant, and that CCC has no right to supersede or to modify any such discretionary act by a Rightsholder.

4) **Representations; Acceptance.** By using the Service, User represents and warrants that User has been duly authorized by the User to accept, and hereby does accept, all Terms.

5) **Scope of License; Limitations and Obligations.** All Works and all rights therein, including copyright rights, remain the sole and exclusive property of the Rightsholder. The License provides only those rights expressly set forth in the terms and conveys no other rights in any Works

6) **General Payment Terms.** User may pay at time of checkout by credit card or choose to be invoiced. If the User chooses to be invoiced, the User shall: (i) remit payments in the manner identified on specific invoices, (ii) unless otherwise specifically stated in an Order Confirmation or separate written agreement, Users shall remit payments upon receipt of the relevant invoice from CCC, either by delivery or notification of availability of the invoice via the Marketplace platform, and (iii) if the User does not pay the invoice within 30 days of receipt, the User may incur a service charge of 1.5% per month or the maximum rate allowed by applicable law, whichever is less. While User may exercise the rights in the License immediately upon receiving the Order Confirmation, the License is automatically revoked and is null and void, as if it had never been issued, if CCC does not receive complete payment on a timely basis.

7) **General Limits on Use.** Unless otherwise provided in the Order Confirmation, any grant of rights to User (i) involves only the rights set forth in the Terms and does not include subsequent or additional uses, (ii) is non-exclusive and non-transferable, and (iii) is subject to any and all limitations and restrictions (such as, but not limited to, limitations on duration of use or circulation) included in the Terms. Upon completion of the licensed use as set forth in the Order Confirmation, User shall either secure a new permission for further use of the Work(s) or immediately cease any new use of the Work(s) and shall render inaccessible (such as by deleting or by removing or severing links or other locators) any further copies of the Work. User may only make alterations to the Work if and as expressly set forth in the Order Confirmation. No Work may be used in any way that is unlawful, including without limitation if such use would violate applicable sanctions laws or regulations, would be defamatory, violate the rights of third parties (including such third parties' rights of copyright, privacy, publicity, or other tangible or intangible property), or is otherwise illegal, sexually explicit, or obscene. In addition, User may not conjoin a Work with any other material that may result in damage to the reputation of the Rightsholder. Any unlawful use will render any licenses hereunder null and void. User agrees to inform CCC if it becomes aware of any infringement of any rights in a Work and to cooperate with any reasonable request of CCC or the Rightsholder in connection therewith.

8) **Third Party Materials.** In the event that the material for which a License is sought includes third party materials (such as photographs, illustrations, graphs, inserts and similar materials) that are identified in such material as having been used by permission (or a similar indicator), User is responsible for identifying, and seeking separate licenses (under this Service, if available, or otherwise) for any of such third party materials; without a separate license, User may not use such third party materials via the License.

9) **Copyright Notice.** Use of proper copyright notice for a Work is required as a condition of any License granted under the Service. Unless otherwise provided in the Order Confirmation, a proper copyright notice will read substantially as follows: "Used with permission of [Rightsholder's name], from [Work's title, author, volume, edition number and year of copyright]; permission conveyed through Copyright Clearance Center, Inc." Such notice must be provided in a reasonably legible font size and must be placed either on a cover page or in another location that any person, upon gaining access to the material which is the subject of a permission, shall see, or in the case of republication Licenses, immediately adjacent to the Work as used (for example, as part of a by-line or footnote) or in the place where substantially all other credits or notices for the new work containing the republished Work are located. Failure to include the required notice results in loss to the Rightsholder and CCC, and the User shall be liable to pay liquidated damages for each such failure equal to twice the use fee specified in the Order Confirmation, in addition to the use fee itself and any other fees and charges specified.

10) **Indemnity.** User hereby indemnifies and agrees to defend the Rightsholder and CCC, and their respective employees and directors, against all claims, liability, damages, costs, and expenses, including legal fees and expenses, arising out of any use of a Work beyond the scope of the rights granted herein and in the Order Confirmation, or any use of a Work which has been altered in any unauthorized way by User, including claims of defamation or infringement of rights of copyright, publicity, privacy, or other tangible or intangible property.

11) **Limitation of Liability.** UNDER NO CIRCUMSTANCES WILL CCC OR THE RIGHTSHOLDER BE LIABLE FOR ANY DIRECT, INDIRECT, CONSEQUENTIAL, OR INCIDENTAL DAMAGES (INCLUDING WITHOUT LIMITATION DAMAGES FOR LOSS OF BUSINESS PROFITS OR INFORMATION, OR FOR BUSINESS INTERRUPTION) ARISING OUT OF THE USE OR INABILITY TO USE A WORK, EVEN IF ONE OR BOTH OF THEM HAS BEEN ADVISED OF THE POSSIBILITY OF SUCH DAMAGES. In any event, the total liability of the Rightsholder and CCC (including their respective employees and directors) shall not exceed the total amount actually paid by User for the relevant License. User assumes full liability for the actions and omissions of its principals, employees, agents, affiliates, successors, and assigns.

12) **Limited Warranties.** THE WORK(S) AND RIGHT(S) ARE PROVIDED "AS IS." CCC HAS THE RIGHT TO GRANT TO USER THE RIGHTS GRANTED IN THE ORDER CONFIRMATION DOCUMENT. CCC AND THE RIGHTSHOLDER DISCLAIM ALL OTHER WARRANTIES RELATING TO THE WORK(S) AND RIGHT(S), EITHER EXPRESS OR IMPLIED, INCLUDING WITHOUT LIMITATION IMPLIED WARRANTIES OF MERCHANTABILITY OR FITNESS FOR A PARTICULAR PURPOSE. ADDITIONAL RIGHTS MAY BE REQUIRED TO USE ILLUSTRATIONS, GRAPHS, PHOTOGRAPHS, ABSTRACTS, INSERTS, OR OTHER PORTIONS OF THE WORK (AS OPPOSED TO THE ENTIRE WORK) IN A MANNER CONTEMPLATED BY USER; USER UNDERSTANDS AND AGREES THAT NEITHER CCC NOR THE RIGHTSHOLDER MAY HAVE SUCH ADDITIONAL RIGHTS TO GRANT.

13) **Effect of Breach.** Any failure by User to pay any amount when due, or any use by User of a Work beyond the scope of the License set forth in the Order Confirmation and/or the Terms, shall be a material breach of such License. Any breach not cured within 10 days of written notice thereof shall result in immediate termination of such License without further notice. Any unauthorized (but licensable) use of a Work that is terminated immediately upon notice thereof may be liquidated by payment of the Rightsholder's ordinary license price therefor; any unauthorized (and unlicensable) use that is not terminated immediately for any reason (including, for example, because materials containing the Work cannot reasonably be recalled) will be subject to all remedies available at law or in equity, but in no event to a payment of less than three times the Rightsholder's ordinary license price for the most closely analogous licensable use plus Rightsholder's and/or CCC's costs and expenses incurred in collecting such payment.

14) **Additional Terms for Specific Products and Services.** If a User is making one of the uses described in this Section 14, the additional terms and conditions apply:

a) ***Print Uses of Academic Course Content and Materials (photocopies for academic coursepacks or classroom handouts).*** For photocopies for academic coursepacks or classroom handouts the following additional terms apply:

i) The copies and anthologies created under this License may be made and assembled by faculty members individually or at their request by on-campus bookstores or copy centers, or by off-campus copy shops and other similar entities.

ii) No License granted shall in any way: (i) include any right by User to create a substantively non-identical copy of the Work or to edit or in any other way modify the Work (except by means of deleting material immediately preceding or following the entire portion of the Work copied) (ii) permit "publishing ventures" where any particular anthology would be systematically marketed at multiple institutions.

iii) Subject to any Publisher Terms (and notwithstanding any apparent contradiction in the Order Confirmation arising from data provided by User), any use authorized under the academic pay-per-use service is limited as follows:

A) any License granted shall apply to only one class (bearing a unique identifier as assigned by the institution, and thereby including all sections or other subparts of the class) at one institution;

B) use is limited to not more than 25% of the text of a book or of the items in a published collection of essays, poems or articles;

C) use is limited to no more than the greater of (a) 25% of the text of an issue of a journal or other periodical or (b) two articles from such an issue;

D) no User may sell or distribute any particular anthology, whether photocopied or electronic, at more than one institution of learning;

E) in the case of a photocopy permission, no materials may be entered into electronic memory by User except in order to produce an identical copy of a Work before or during the academic term (or analogous period) as to which any particular permission is granted. In the event that User shall choose to retain materials that are the subject of a photocopy permission in electronic memory for purposes of producing identical copies more than one day after such retention (but still within the scope of any permission granted), User must notify CCC of such fact in the applicable permission request and such retention shall constitute one copy actually sold for purposes of calculating permission fees due; and

F) any permission granted shall expire at the end of the class. No permission granted shall in any way include any right by User to create a substantively non-identical copy of the Work or to edit or in any other way modify the Work (except by means of deleting material immediately preceding or following the entire portion of the Work copied).

iv) Books and Records; Right to Audit. As to each permission granted under the academic pay-per-use Service, User shall maintain for at least four full calendar years books and records sufficient for CCC to determine the numbers of copies made by User under such permission. CCC and any representatives it may designate shall have the right to audit such books and records at any time during User's ordinary business hours, upon two days' prior notice. If any such audit shall determine that User shall have underpaid for, or underreported, any photocopies sold or by three percent (3%) or more, then User shall bear all the costs of any such audit; otherwise, CCC shall bear the costs of any such audit. Any amount determined by such audit to have been underpaid by User shall immediately be paid to CCC by User, together with interest thereon at the rate of 10% per annum from the date such amount was originally due. The provisions of this paragraph shall survive the termination of this License for any reason.

b) ***Digital Pay-Per-Uses of Academic Course Content and Materials (e-coursepacks, electronic reserves, learning management systems, academic institution intranets).*** For uses in e-coursepacks, posts in electronic reserves, posts in learning management systems, or posts on academic institution intranets, the following additional terms apply:

i) The pay-per-uses subject to this Section 14(b) include:

A) **Posting e-reserves, course management systems, e-coursepacks for text-based content,** which grants authorizations to import requested material in electronic format, and allows electronic access to this material to members of a designated college or university class, under the direction of an instructor designated by the college or university, accessible only under appropriate electronic controls (e.g., password);

B) **Posting e-reserves, course management systems, e-coursepacks for material consisting of photographs or other still images not embedded in text,** which grants not only the authorizations described in Section 14(b)(i)(A) above, but also the following authorization: to include the requested material in course materials for use consistent with Section 14(b)(i)(A) above, including any necessary resizing, reformatting or modification of the resolution of such requested material (provided that such modification does not alter the underlying editorial content or meaning of the requested material, and provided that the resulting modified content is used solely within the scope of, and in a manner consistent with, the particular authorization described in the Order Confirmation and the Terms), but not including any other form of manipulation, alteration or editing of the requested material;

C) **Posting e-reserves, course management systems, e-coursepacks or other academic distribution for audiovisual content,** which grants not only the authorizations described in Section 14(b)(i)(A) above, but also the following authorizations: (i) to include the requested material in course materials for use consistent with Section 14(b)(i)(A) above; (ii) to display and perform the requested material to such members of such class in the physical classroom or remotely by

means of streaming media or other video formats; and (iii) to "clip" or reformat the requested material for purposes of time or content management or ease of delivery, provided that such “clipping” or reformatting does not alter the underlying editorial content or meaning of the requested material and that the resulting material is used solely within the scope of, and in a manner consistent with, the particular authorization described in the Order Confirmation and the Terms. Unless expressly set forth in the relevant Order Conformation, the License does not authorize any other form of manipulation, alteration or editing of the requested material.

ii) Unless expressly set forth in the relevant Order Confirmation, no License granted shall in any way: (i) include any right by User to create a substantively non-identical copy of the Work or to edit or in any other way modify the Work (except by means of deleting material immediately preceding or following the entire portion of the Work copied or, in the case of Works subject to Sections 14(b)(1)(B) or (C) above, as described in such Sections) (ii) permit "publishing ventures" where any particular course materials would be systematically marketed at multiple institutions.

iii) Subject to any further limitations determined in the Rightsholder Terms (and notwithstanding any apparent contradiction in the Order Confirmation arising from data provided by User), any use authorized under the electronic course content pay-per-use service is limited as follows:

A) any License granted shall apply to only one class (bearing a unique identifier as assigned by the institution, and thereby including all sections or other subparts of the class) at one institution;

B) use is limited to not more than 25% of the text of a book or of the items in a published collection of essays, poems or articles;

C) use is limited to not more than the greater of (a) 25% of the text of an issue of a journal or other periodical or (b) two articles from such an issue;

D) no User may sell or distribute any particular materials, whether photocopied or electronic, at more than one institution of learning;

E) electronic access to material which is the subject of an electronic-use permission must be limited by means of electronic password, student identification or other control permitting access solely to students and instructors in the class;

F) User must ensure (through use of an electronic cover page or other appropriate means) that any person, upon gaining electronic access to the material, which is the subject of a permission, shall see:

- a proper copyright notice, identifying the Rightsholder in whose name CCC has granted permission,
- a statement to the effect that such copy was made pursuant to permission,
- a statement identifying the class to which the material applies and notifying the reader that the material has been made available electronically solely for use in the class, and
- a statement to the effect that the material may not be further distributed to any person outside the class, whether by copying or by transmission and whether electronically or in paper form, and User must also ensure that such cover page or other means will print out in the event that the person accessing the material chooses to print out the material or any part thereof.

G) any permission granted shall expire at the end of the class and, absent some other form of authorization, User is thereupon required to delete the applicable material from any electronic storage or to block electronic access to the applicable material.

iv) Uses of separate portions of a Work, even if they are to be included in the same course material or the same university or college class, require separate permissions under the electronic course content pay-per-use Service. Unless otherwise provided in the Order Confirmation, any grant of rights to User is limited to use completed no later than the end of the academic term (or analogous period) as to which any particular permission is granted.

v) Books and Records; Right to Audit. As to each permission granted under the electronic course content Service, User shall maintain for at least four full calendar years books and records sufficient for CCC to determine the numbers of copies made by User under such permission. CCC and any representatives it may designate shall have the right to audit such books and records at any time during User's ordinary business hours, upon two days' prior notice. If any such audit shall determine that User shall have underpaid for, or underreported, any electronic copies used by three percent (3%) or more, then User shall bear all the costs of any such audit; otherwise, CCC shall bear the costs of any such audit. Any amount determined by such audit to have been underpaid by User shall immediately be paid to CCC by User, together with interest thereon at the rate of 10% per annum from the date such amount was originally due. The provisions of this paragraph shall survive the termination of this license for any reason.

c) ***Pay-Per-Use Permissions for Certain Reproductions (Academic photocopies for library reserves and interlibrary loan reporting) (Non-academic internal/external business uses and commercial document delivery).*** The License expressly excludes the uses listed in Section (c)(i)-(v) below (which must be subject to separate license from the applicable Rightsholder) for: academic photocopies for library reserves and interlibrary loan reporting; and non-academic internal/external business uses and commercial document delivery.

i) electronic storage of any reproduction (whether in plain-text, PDF, or any other format) other than on a transitory basis;

ii) the input of Works or reproductions thereof into any computerized database;

iii) reproduction of an entire Work (cover-to-cover copying) except where the Work is a single article;

iv) reproduction for resale to anyone other than a specific customer of User;

v) republication in any different form. Please obtain authorizations for these uses through other CCC services or directly from the rightsholder.

Any license granted is further limited as set forth in any restrictions included in the Order Confirmation and/or in these Terms.

d) ***Electronic Reproductions in Online Environments (Non-Academic-email, intranet, internet and extranet).*** For "electronic reproductions", which generally includes e-mail use (including instant messaging or other electronic transmission to a defined group of recipients) or posting on an intranet, extranet or Intranet site (including any display or performance incidental thereto), the following additional terms apply:

i) Unless otherwise set forth in the Order Confirmation, the License is limited to use completed within 30 days for any use on the Internet, 60 days for any use on an intranet or extranet and one year for any other use, all as measured from the "republication date" as identified in the Order Confirmation, if any, and otherwise from the date of the Order Confirmation.

ii) User may not make or permit any alterations to the Work, unless expressly set forth in the Order Confirmation (after request by User and approval by Rightsholder); provided, however, that a Work consisting of photographs or other still images not embedded in text may, if necessary, be resized, reformatted or have its resolution modified without additional express permission, and a Work consisting of audiovisual content may, if necessary, be "clipped" or reformatted for purposes of time or content management or ease of delivery (provided that any such resizing, reformatting, resolution modification or “clipping” does not alter the underlying editorial content or meaning of the Work used, and that the resulting material is used solely within the scope of, and in a manner consistent with, the particular License described in the Order Confirmation and the Terms.

15) **Miscellaneous.**

a) User acknowledges that CCC may, from time to time, make changes or additions to the Service or to the Terms, and that Rightsholder may make changes or additions to the Rightsholder Terms. Such updated Terms will replace the prior terms and conditions in the order workflow and shall be effective as to any subsequent Licenses but shall not apply to Licenses already granted and paid for under a prior set of terms.

b) Use of User-related information collected through the Service is governed by CCC's privacy policy, available online at www.copyright.com/about/privacy-policy/.

c) The License is personal to User. Therefore, User may not assign or transfer to any other person (whether a natural person or an organization of any kind) the License or any rights granted thereunder; provided, however, that, where applicable, User may assign such License in its entirety on written notice to CCC in the event of a transfer of all or substantially all of User's rights in any new material which includes the Work(s) licensed under this Service.

d) No amendment or waiver of any Terms is binding unless set forth in writing and signed by the appropriate parties, including, where applicable, the Rightsholder. The Rightsholder and CCC hereby object to any terms contained in any writing prepared by or on behalf of the User or its principals, employees, agents or affiliates and purporting to govern or otherwise relate to the License described in the Order Confirmation, which terms are in any way inconsistent with any Terms set forth in the Order Confirmation, and/or in CCC's standard operating procedures, whether such writing is prepared prior to, simultaneously with or subsequent to the Order Confirmation, and whether such writing appears on a copy of the Order Confirmation or in a separate instrument.

e) The License described in the Order Confirmation shall be governed by and construed under the law of the State of New York, USA, without regard to the principles thereof of conflicts of law. Any case, controversy, suit, action, or proceeding arising out of, in connection with, or related to such License shall be brought, at CCC's sole discretion, in any federal or state court located in the County of New York, State of New York, USA, or in any federal or state court whose geographical jurisdiction covers the location of the Rightsholder set forth in the Order Confirmation. The parties expressly submit to the personal jurisdiction and venue of each such federal or state court.

Last updated October 2022

CCC Marketplace

Order Number: 1399166
Order Date: 21 Sep 2023

Payment Information

Simon Wiener
wiener.simon@gmail.com
Payment method: Invoice

Billing Address:
Mr. Simon Wiener
Rainerstraße 23A
Linz
Austria

+43 6706075551
wiener.simon@gmail.com

Customer Location:
Mr. Simon Wiener
Rainerstraße 23A
Linz
Austria

Order Details

1. Progress in organic coatings

Billing Status: Open

Article: Evaluation of the cathodic disbondment resistance of pipeline coatings ? A review

Order License ID	1399166-1	**Type of Use**	Republish in a thesis/dissertation
Order detail status	Completed	**Publisher**	ELSEVIER BV
ISSN	0300-9440	**Portion**	Image/photo/illustration

0,00 EUR
Republication Permission

LICENSED CONTENT

Publication Title	Progress in organic coatings	**Rightsholder**	Elsevier Science & Technology Journals
Article Title	Evaluation of the cathodic disbondment resistance of pipeline coatings ? A review	**Publication Type**	Journal
		Start Page	105728
Date	01/01/1972	**Volume**	146
Language	English, French, German		
Country	Netherlands		

REQUEST DETAILS

Portion Type	Image/photo/illustration	**Distribution**	Worldwide
Number of Images / Photos / Illustrations	1	**Translation**	Original language of publication
Format (select all that apply)	Print, Electronic	**Copies for the Disabled?**	No
		Minor Editing Privileges?	Yes
Who Will Republish the Content?	Publisher, not-for-profit	**Incidental Promotional Use?**	No
		Currency	EUR
Duration of Use	Life of current edition		
Lifetime Unit Quantity	Up to 499		
Rights Requested	Main product		

NEW WORK DETAILS

Title	Use of Complementary Testing Technology for the Evaluation of the Characteristics of Different Systems	**Institution Name**	TU Wien
		Expected Presentation Date	2023-11-27
Instructor Name	Markus Valtiner		

ADDITIONAL DETAILS

The Requesting Person/Organization to Appear on the License	Simon Wiener

REQUESTED CONTENT DETAILS

Title, Description or Numeric Reference of the Portion(s)	Fig.1	Title of the Article/Chapter the Portion Is From	Evaluation of the cathodic disbondment resistance of pipeline coatings ? A review
Editor of Portion(s)	Xu, Min; Lam, C.N. Catherine; Wong, Dennis; Asselin, Edouard	Author of Portion(s)	Xu, Min; Lam, C.N. Catherine; Wong, Dennis; Asselin, Edouard
Volume / Edition	146	Publication Date of Portion	2020-09-01
Page or Page Range of Portion	105728		

Elsevier Science & Technology Journals Terms and Conditions

Elsevier publishes Open Access articles in both its Open Access journals and via its Open Access articles option in subscription journals, for which an author selects a user license permitting certain types of reuse without permission. Before proceeding please check if the article is Open Access on http://www.sciencedirect.com and refer to the user license for the individual article. Any reuse not included in the user license terms will require permission. You must always fully and appropriately credit the author and source. If any part of the material to be used (for example, figures) has appeared in the Elsevier publication for which you are seeking permission, with credit or acknowledgement to another source it is the responsibility of the user to ensure their reuse complies with the terms and conditions determined by the rights holder. Please contact permissions@elsevier.com with any queries.

---

2. Chemical communications

Billing Status: Open

Article: Solvent-starved conditions in confinement cause chemical oscillations excited by passage of a cathodic delamination front.

Order License ID	1399166-2	Type of Use	Republish in a thesis/dissertation
Order detail status	Completed		
ISSN	1364-548X	Publisher	ROYAL SOCIETY OF CHEMISTRY
		Portion	Image/photo/illustration
			0,00 EUR Republication Permission

LICENSED CONTENT

Publication Title	Chemical communications	Rightsholder	Royal Society of Chemistry
Article Title	Solvent-starved conditions in confinement cause chemical oscillations excited by passage of a cathodic delamination front.	Publication Type	e-Journal
		Start Page	16041
		End Page	16044
		Issue	89
Author/Editor	Royal Society of Chemistry (Great Britain)	Volume	51
Date	01/01/1996		
Language	English		
Country	United Kingdom of Great Britain and Northern Ireland		

REQUEST DETAILS

Portion Type	Image/photo/illustration	Distribution	Worldwide
Number of Images / Photos / Illustrations	1	Translation	Original language of publication
Format (select all that apply)	Print, Electronic	Copies for the Disabled?	No
		Minor Editing Privileges?	Yes
Who Will Republish the Content?	Publisher, not-for-profit	Incidental Promotional Use?	No
		Currency	EUR
Duration of Use	Life of current edition		
Lifetime Unit Quantity	Up to 499		
Rights Requested	Main product		

NEW WORK DETAILS

Title	Use of Complementary Testing Technology for the Evaluation of the Characteristics of Different Systems	**Institution Name**	TU Wien
		Expected Presentation Date	2023-11-27
Instructor Name	Markus Valtiner		

ADDITIONAL DETAILS

The Requesting Person/Organization to Appear on the License	Simon Wiener

REQUESTED CONTENT DETAILS

Title, Description or Numeric Reference of the Portion(s)	Fig. 4	**Title of the Article/Chapter the Portion Is From**	Solvent-starved conditions in confinement cause chemical oscillations excited by passage of a cathodic delamination front.
Editor of Portion(s)	Iqbal, Danish; Sarfraz, Adnan; Stratmann, Martin; Erbe, Andreas	**Author of Portion(s)**	Iqbal, Danish; Sarfraz, Adnan; Stratmann, Martin; Erbe, Andreas
Volume / Edition	51		
Page or Page Range of Portion	16041-16044	**Issue, if Republishing an Article From a Serial**	89
		Publication Date of Portion	2015-11-18

Total Items: 2

Subtotal: 0,00 EUR

Order Total: 0,00 EUR

Marketplace Permissions General Terms and Conditions

The following terms and conditions ("General Terms"), together with any applicable Publisher Terms and Conditions, govern User's use of Works pursuant to the Licenses granted by Copyright Clearance Center, Inc. ("CCC") on behalf of the applicable Rightsholders of such Works through CCC's applicable Marketplace transactional licensing services (each, a "Service").

1) **Definitions.** For purposes of these General Terms, the following definitions apply:

"License" is the licensed use the User obtains via the Marketplace platform in a particular licensing transaction, as set forth in the Order Confirmation.

"Order Confirmation" is the confirmation CCC provides to the User at the conclusion of each Marketplace transaction. "Order Confirmation Terms" are additional terms set forth on specific Order Confirmations not set forth in the General Terms that can include terms applicable to a particular CCC transactional licensing service and/or any Rightsholder-specific terms.

"Rightsholder(s)" are the holders of copyright rights in the Works for which a User obtains licenses via the Marketplace platform, which are displayed on specific Order Confirmations.

"Terms" means the terms and conditions set forth in these General Terms and any additional Order Confirmation Terms collectively.

"User" or "you" is the person or entity making the use granted under the relevant License. Where the person accepting the Terms on behalf of a User is a freelancer or other third party who the User authorized to accept the General Terms on the User's behalf, such person shall be deemed jointly a User for purposes of such Terms.

"Work(s)" are the copyright protected works described in relevant Order Confirmations.

2) **Description of Service.** CCC's Marketplace enables Users to obtain Licenses to use one or more Works in accordance with all relevant Terms. CCC grants Licenses as an agent on behalf of the copyright rightsholder identified in the relevant Order Confirmation.

3) **Applicability of Terms.** The Terms govern User's use of Works in connection with the relevant License. In the event of any conflict between General Terms and Order Confirmation Terms, the latter shall govern. User acknowledges that Rightsholders have complete discretion whether to grant any permission, and whether to place any limitations on any grant, and that CCC has no right to supersede or to modify any such discretionary act by a Rightsholder.

4) **Representations; Acceptance.** By using the Service, User represents and warrants that User has been duly authorized by the User to accept, and hereby does accept, all Terms.

5) **Scope of License; Limitations and Obligations.** All Works and all rights therein, including copyright rights, remain the sole and exclusive property of the Rightsholder. The License provides only those rights expressly set forth in the terms and conveys no other rights in any Works

6) **General Payment Terms.** User may pay at time of checkout by credit card or choose to be invoiced. If the User chooses to be invoiced, the User shall: (i) remit payments in the manner identified on specific invoices, (ii) unless otherwise specifically stated in an Order Confirmation or separate written agreement, Users shall remit payments upon receipt of the relevant invoice from CCC, either by delivery or notification of availability of the invoice via the Marketplace platform, and (iii) if the User does not pay the invoice within 30 days of receipt, the User may incur a service charge of 1.5% per month or the maximum rate allowed by applicable law, whichever is less. While User may exercise the rights in the License immediately upon receiving the Order Confirmation, the License is automatically revoked and is null and void, as if it had never been issued, if CCC does not receive complete payment on a timely basis.

7) **General Limits on Use.** Unless otherwise provided in the Order Confirmation, any grant of rights to User (i) involves only the rights set forth in the Terms and does not include subsequent or additional uses, (ii) is non-exclusive and non-transferable, and (iii) is subject to any and all limitations and restrictions (such as, but not limited to, limitations on duration of use or circulation) included in the Terms. Upon completion of the licensed use as set forth in the Order Confirmation, User shall either secure a new permission for further use of the Work(s) or immediately cease any new use of the Work(s) and shall render inaccessible (such as by deleting or by removing or severing links or other locators) any further copies of the Work. User may only make alterations to the Work if and as expressly set forth in the Order Confirmation. No Work may be used in any way that is unlawful, including without limitation if such use would violate applicable sanctions laws or regulations, would be defamatory, violate the rights of third parties (including such third parties' rights of copyright, privacy, publicity, or other tangible or intangible property), or is otherwise illegal, sexually explicit, or obscene. In addition, User may not conjoin a Work with any other material that may result in damage to the reputation of the Rightsholder. Any unlawful use will render any licenses hereunder null and void. User agrees to inform CCC if it becomes aware of any infringement of any rights in a Work and to cooperate with any reasonable request of CCC or the Rightsholder in connection therewith.

8) **Third Party Materials.** In the event that the material for which a License is sought includes third party materials (such as photographs, illustrations, graphs, inserts and similar materials) that are identified in such material as having been used by permission (or a similar indicator), User is responsible for identifying, and seeking separate licenses (under this Service, if available, or otherwise) for any of such third party materials; without a separate license, User may not use such third party materials via the License.

9) **Copyright Notice.** Use of proper copyright notice for a Work is required as a condition of any License granted under the Service. Unless otherwise provided in the Order Confirmation, a proper copyright notice will read substantially as follows: "Used with permission of [Rightsholder's name], from [Work's title, author, volume, edition number and year of copyright]; permission conveyed through Copyright Clearance Center, Inc." Such notice must be provided in a reasonably legible font size and must be placed either on a cover page or in another location that any person, upon gaining access to the material which is the subject of a permission, shall see, or in the case of republication Licenses, immediately adjacent to the Work as used (for example, as part of a by-line or footnote) or in the place where substantially all other credits or notices for the new work containing the republished Work are located. Failure to include the required notice results in loss to the Rightsholder and CCC, and the User shall be liable to pay liquidated damages for each such failure equal to twice the use fee specified in the Order Confirmation, in addition to the use fee itself and any other fees and charges specified.

10) **Indemnity.** User hereby indemnifies and agrees to defend the Rightsholder and CCC, and their respective employees and directors, against all claims, liability, damages, costs, and expenses, including legal fees and expenses, arising out of any use of a Work beyond the scope of the rights granted herein and in the Order Confirmation, or any use of a Work which has been altered in any unauthorized way by User, including claims of defamation or infringement of rights of copyright, publicity, privacy, or other tangible or intangible property.

11) **Limitation of Liability.** UNDER NO CIRCUMSTANCES WILL CCC OR THE RIGHTSHOLDER BE LIABLE FOR ANY DIRECT, INDIRECT, CONSEQUENTIAL, OR INCIDENTAL DAMAGES (INCLUDING WITHOUT LIMITATION DAMAGES FOR LOSS OF BUSINESS PROFITS OR INFORMATION, OR FOR BUSINESS INTERRUPTION) ARISING OUT OF THE USE OR INABILITY TO USE A WORK, EVEN IF ONE OR BOTH OF THEM HAS BEEN ADVISED OF THE POSSIBILITY OF SUCH DAMAGES. In any event, the total liability of the Rightsholder and CCC (including their respective employees and directors) shall not exceed the total amount actually paid by User for the relevant License. User assumes full liability for the actions and omissions of its principals, employees, agents, affiliates, successors, and assigns.

12) **Limited Warranties.** THE WORK(S) AND RIGHT(S) ARE PROVIDED "AS IS." CCC HAS THE RIGHT TO GRANT TO USER THE RIGHTS GRANTED IN THE ORDER CONFIRMATION DOCUMENT. CCC AND THE RIGHTSHOLDER DISCLAIM ALL OTHER WARRANTIES RELATING TO THE WORK(S) AND RIGHT(S), EITHER EXPRESS OR IMPLIED, INCLUDING WITHOUT LIMITATION IMPLIED WARRANTIES OF MERCHANTABILITY OR FITNESS FOR A PARTICULAR PURPOSE. ADDITIONAL RIGHTS MAY BE REQUIRED TO USE ILLUSTRATIONS, GRAPHS, PHOTOGRAPHS, ABSTRACTS, INSERTS, OR OTHER PORTIONS OF THE WORK (AS OPPOSED TO THE ENTIRE WORK) IN A MANNER CONTEMPLATED BY USER; USER UNDERSTANDS AND AGREES THAT NEITHER CCC NOR THE RIGHTSHOLDER MAY HAVE SUCH ADDITIONAL RIGHTS TO GRANT.

13) **Effect of Breach.** Any failure by User to pay any amount when due, or any use by User of a Work beyond the scope of the License set forth in the Order Confirmation and/or the Terms, shall be a material breach of such License. Any breach not cured within 10 days of written notice thereof shall result in immediate termination of such License without further notice. Any unauthorized (but licensable) use of a Work that is terminated immediately upon notice thereof may be liquidated by payment of the Rightsholder's ordinary license price therefor; any unauthorized (and unlicensable) use that is not terminated immediately for any reason (including, for example, because materials containing the Work cannot reasonably be recalled) will be subject to all remedies available at law or in equity, but in no event to a payment of less than three times the Rightsholder's ordinary license price for the most closely analogous licensable use plus Rightsholder's and/or CCC's costs and expenses incurred in collecting such payment.

14) **Additional Terms for Specific Products and Services.** If a User is making one of the uses described in this Section 14, the additional terms and conditions apply:

a) ***Print Uses of Academic Course Content and Materials (photocopies for academic coursepacks or classroom handouts).*** For photocopies for academic coursepacks or classroom handouts the following additional terms apply:

i) The copies and anthologies created under this License may be made and assembled by faculty members individually or at their request by on-campus bookstores or copy centers, or by off-campus copy shops and other similar entities.

ii) No License granted shall in any way: (i) include any right by User to create a substantively non-identical copy of the Work or to edit or in any other way modify the Work (except by means of deleting material immediately preceding or following the entire portion of the Work copied) (ii) permit "publishing ventures" where any particular anthology would be systematically marketed at multiple institutions.

iii) Subject to any Publisher Terms (and notwithstanding any apparent contradiction in the Order Confirmation arising from data provided by User), any use authorized under the academic pay-per-use service is limited as follows:

A) any License granted shall apply to only one class (bearing a unique identifier as assigned by the institution, and thereby including all sections or other subparts of the class) at one institution;

B) use is limited to not more than 25% of the text of a book or of the items in a published collection of essays, poems or articles;

C) use is limited to no more than the greater of (a) 25% of the text of an issue of a journal or other periodical or (b) two articles from such an issue;

D) no User may sell or distribute any particular anthology, whether photocopied or electronic, at more than one institution of learning;

E) in the case of a photocopy permission, no materials may be entered into electronic memory by User except in order to produce an identical copy of a Work before or during the academic term (or analogous period) as to which any particular permission is granted. In the event that User shall choose to retain materials that are the subject of a photocopy permission in electronic memory for purposes of producing identical copies more than one day after such retention (but still within the scope of any permission granted), User must notify CCC of such fact in the applicable permission request and such retention shall constitute one copy actually sold for purposes of calculating permission fees due; and

F) any permission granted shall expire at the end of the class. No permission granted shall in any way include any right by User to create a substantively non-identical copy of the Work or to edit or in any other way modify the Work (except by means of deleting material immediately preceding or following the entire portion of the Work copied).

iv) Books and Records; Right to Audit. As to each permission granted under the academic pay-per-use Service, User shall maintain for at least four full calendar years books and records sufficient for CCC to determine the numbers of copies made by User under such permission. CCC and any representatives it may designate shall have the right to audit such books and records at any time during User's ordinary business hours, upon two days' prior notice. If any such audit shall determine that User shall have underpaid for, or underreported, any photocopies sold or by three percent (3%) or more, then User shall bear all the costs of any such audit; otherwise, CCC shall bear the costs of any such audit. Any amount determined by such audit to have been underpaid by User shall immediately be paid to CCC by User, together with interest thereon at the rate of 10% per annum from the date such amount was originally due. The provisions of this paragraph shall survive the termination of this License for any reason.

b) ***Digital Pay-Per-Uses of Academic Course Content and Materials (e-coursepacks, electronic reserves, learning management systems, academic institution intranets).*** For uses in e-coursepacks, posts in electronic reserves, posts in learning management systems, or posts on academic institution intranets, the following additional terms apply:

i) The pay-per-uses subject to this Section 14(b) include:

A) **Posting e-reserves, course management systems, e-coursepacks for text-based content,** which grants authorizations to import requested material in electronic format, and allows electronic access to this material to members of a designated college or university class, under the direction of an instructor designated by the college or university, accessible only under appropriate electronic controls (e.g., password);

B) **Posting e-reserves, course management systems, e-coursepacks for material consisting of photographs or other still images not embedded in text,** which grants not only the authorizations described in Section 14(b)(i)(A) above, but also the following authorization: to include the requested material in course materials for use consistent with Section 14(b)(i)(A) above, including any necessary resizing, reformatting or modification of the resolution of such requested material (provided that such modification does not alter the underlying editorial content or meaning of the requested material, and provided that the resulting modified content is used solely within the scope of, and in a manner consistent with, the particular authorization described in the Order Confirmation and the Terms), but not including any other form of manipulation, alteration or editing of the requested material;

C) **Posting e-reserves, course management systems, e-coursepacks or other academic distribution for audiovisual content,** which grants not only the authorizations described in Section 14(b)(i)(A) above, but also the following authorizations: (i) to include the requested material in course materials for use consistent with Section 14(b)(i)(A) above; (ii) to display and perform the requested material to such members of such class in the physical classroom or remotely by means of streaming media or other video formats; and (iii) to "clip" or reformat the requested material for purposes of time or content management or ease of delivery, provided that such “clipping” or reformatting does not alter the underlying editorial content or meaning of the requested material and that the resulting material is used solely within the scope of, and in a manner consistent with, the particular authorization described in the Order Confirmation and the Terms.

Unless expressly set forth in the relevant Order Conformation, the License does not authorize any other form of manipulation, alteration or editing of the requested material.

ii) Unless expressly set forth in the relevant Order Confirmation, no License granted shall in any way: (i) include any right by User to create a substantively non-identical copy of the Work or to edit or in any other way modify the Work (except by means of deleting material immediately preceding or following the entire portion of the Work copied or, in the case of Works subject to Sections 14(b)(1)(B) or (C) above, as described in such Sections) (ii) permit "publishing ventures" where any particular course materials would be systematically marketed at multiple institutions.

iii) Subject to any further limitations determined in the Rightsholder Terms (and notwithstanding any apparent contradiction in the Order Confirmation arising from data provided by User), any use authorized under the electronic course content pay-per-use service is limited as follows:

A) any License granted shall apply to only one class (bearing a unique identifier as assigned by the institution, and thereby including all sections or other subparts of the class) at one institution;

B) use is limited to not more than 25% of the text of a book or of the items in a published collection of essays, poems or articles;

C) use is limited to not more than the greater of (a) 25% of the text of an issue of a journal or other periodical or (b) two articles from such an issue;

D) no User may sell or distribute any particular materials, whether photocopied or electronic, at more than one institution of learning;

E) electronic access to material which is the subject of an electronic-use permission must be limited by means of electronic password, student identification or other control permitting access solely to students and instructors in the class;

F) User must ensure (through use of an electronic cover page or other appropriate means) that any person, upon gaining electronic access to the material, which is the subject of a permission, shall see:

- a proper copyright notice, identifying the Rightsholder in whose name CCC has granted permission,
- a statement to the effect that such copy was made pursuant to permission,
- a statement identifying the class to which the material applies and notifying the reader that the material has been made available electronically solely for use in the class, and
- a statement to the effect that the material may not be further distributed to any person outside the class, whether by copying or by transmission and whether electronically or in paper form, and User must also ensure that such cover page or other means will print out in the event that the person accessing the material chooses to print out the material or any part thereof.

G) any permission granted shall expire at the end of the class and, absent some other form of authorization, User is thereupon required to delete the applicable material from any electronic storage or to block electronic access to the applicable material.

iv) Uses of separate portions of a Work, even if they are to be included in the same course material or the same university or college class, require separate permissions under the electronic course content pay-per-use Service. Unless otherwise provided in the Order Confirmation, any grant of rights to User is limited to use completed no later than the end of the academic term (or analogous period) as to which any particular permission is granted.

v) Books and Records; Right to Audit. As to each permission granted under the electronic course content Service, User shall maintain for at least four full calendar years books and records sufficient for CCC to determine the numbers of copies made by User under such permission. CCC and any representatives it may designate shall have the right to audit such books and records at any time during User's ordinary business hours, upon two days' prior notice. If any such audit shall determine that User shall have underpaid for, or underreported, any electronic copies used by three percent (3%) or more, then User shall bear all the costs of any such audit; otherwise, CCC shall bear the costs of any such audit. Any amount determined by such audit to have been underpaid by User shall immediately be paid to CCC by User, together with interest thereon at the rate of 10% per annum from the date such amount was originally due. The provisions of this paragraph shall survive the termination of this license for any reason.

c) ***Pay-Per-Use Permissions for Certain Reproductions (Academic photocopies for library reserves and interlibrary loan reporting) (Non-academic internal/external business uses and commercial document delivery).*** The License expressly excludes the uses listed in Section (c)(i)-(v) below (which must be subject to separate license from the applicable Rightsholder) for: academic photocopies for library reserves and interlibrary loan reporting; and non-academic internal/external business uses and commercial document delivery.

i) electronic storage of any reproduction (whether in plain-text, PDF, or any other format) other than on a transitory basis;

ii) the input of Works or reproductions thereof into any computerized database;

iii) reproduction of an entire Work (cover-to-cover copying) except where the Work is a single article;

iv) reproduction for resale to anyone other than a specific customer of User;

v) republication in any different form. Please obtain authorizations for these uses through other CCC services or directly from the rightsholder.

Any license granted is further limited as set forth in any restrictions included in the Order Confirmation and/or in these Terms.

d) ***Electronic Reproductions in Online Environments (Non-Academic-email, intranet, internet and extranet).*** For "electronic reproductions", which generally includes e-mail use (including instant messaging or other electronic transmission to a defined group of recipients) or posting on an intranet, extranet or Intranet site (including any display or performance incidental thereto), the following additional terms apply:

i) Unless otherwise set forth in the Order Confirmation, the License is limited to use completed within 30 days for any use on the Internet, 60 days for any use on an intranet or extranet and one year for any other use, all as measured from the "republication date" as identified in the Order Confirmation, if any, and otherwise from the date of the Order Confirmation.

ii) User may not make or permit any alterations to the Work, unless expressly set forth in the Order Confirmation (after request by User and approval by Rightsholder); provided, however, that a Work consisting of photographs or other still images not embedded in text may, if necessary, be resized, reformatted or have its resolution modified without additional express permission, and a Work consisting of audiovisual content may, if necessary, be "clipped" or reformatted for purposes of time or content management or ease of delivery (provided that any such resizing, reformatting, resolution modification or “clipping” does not alter the underlying editorial content or meaning of the Work used, and that the resulting material is used solely within the scope of, and in a manner consistent with, the particular License described in the Order Confirmation and the Terms.

15) **Miscellaneous.**

a) User acknowledges that CCC may, from time to time, make changes or additions to the Service or to the Terms, and that Rightsholder may make changes or additions to the Rightsholder Terms. Such updated Terms will replace the prior terms and conditions in the order workflow and shall be effective as to any subsequent Licenses but shall not apply to Licenses already granted and paid for under a prior set of terms.

b) Use of User-related information collected through the Service is governed by CCC's privacy policy, available online at www.copyright.com/about/privacy-policy/.

c) The License is personal to User. Therefore, User may not assign or transfer to any other person (whether a natural person or an organization of any kind) the License or any rights granted thereunder; provided, however, that, where applicable, User may assign such License in its entirety on written notice to CCC in the event of a transfer of all or substantially all of User's rights in any new material which includes the Work(s) licensed under this Service.

d) No amendment or waiver of any Terms is binding unless set forth in writing and signed by the appropriate parties, including, where applicable, the Rightsholder. The Rightsholder and CCC hereby object to any terms contained in any writing prepared by or on behalf of the User or its principals, employees, agents or affiliates and purporting to govern or otherwise relate to the License described in the Order Confirmation, which terms are in any way inconsistent with any Terms set forth in the Order Confirmation, and/or in CCC's standard operating procedures, whether such writing is prepared prior to, simultaneously with or subsequent to the Order Confirmation, and whether such writing appears on a copy of the Order Confirmation or in a separate instrument.

e) The License described in the Order Confirmation shall be governed by and construed under the law of the State of New York, USA, without regard to the principles thereof of conflicts of law. Any case, controversy, suit, action, or proceeding arising out of, in connection with, or related to such License shall be brought, at CCC's sole discretion, in any federal or state court located in the County of New York, State of New York, USA, or in any federal or state court whose geographical jurisdiction covers the location of the Rightsholder set forth in the Order Confirmation. The parties expressly submit to the personal jurisdiction and venue of each such federal or state court.

Last updated October 2022